Carderock Division

Naval Surface Warfare Center

Bethesda, MD 20084-5000

CARDEROCKDIV, NSWC-92/L01 May 1992

Systems Department

Research and Development Report

Handbook of Reliability Prediction Procedures for Mechanical Equipment

CARDEROCKDIV, NSWC-92/L01 Reliability Prediction Procedures for Mechanical Equipment

PREFACE

Recognition of reliability and maintainability (R&M) as vital factors in the development, production, operation, and maintenance of today's complex systems has placed greater emphasis on the application of design evaluation techniques to logistics management. An analysis of a design for reliability and maintainability can identify critical failure modes and causes of unreliability and provide an effective tool for predicting equipment behavior and selecting appropriate logistics measures to assure satisfactory performance. Application of design evaluation techniques can provide a sound basis for determining spare parts requirements, required part improvement programs, needed redesign efforts, reallocation of resources and other logistics measures to assure that specified reliability and maintainability requirements will be met.

Many efforts have been applied toward duplicating the data bank approach or developing a new approach for mechanical equipment. The statistical analysis of equipment aging characteristics, regression techniques of equipment operating parameters related to failure rates, and analysis of field failure data have been studied in attempts to develop a methodology that can be used to evaluate a new mechanical design for R&M characteristics.

Many of the attempts to develop R&M prediction methodology have been at a system or subsystem level. The large number of variables at these levels and lack of detailed knowledge regarding operating environment have created a problem in applying the results to the design being evaluated. Attempts to collect failure rate data or develop an R&M prediction methodology at the system or subsystem level produce a wide dispersion of failure rates for apparently similar components because of the basic characteristics of mechanical components.

The Design Evaluation Techniques program was initiated by the Carderock Division of the Naval Surface Warfare Center (NSWC) and is sponsored by the Office of Naval Technology under the Logistics Exploratory Development Program, P.E. 62233N. The methodology for predicting R&M characteristics as part of this development effort does not rely solely on failure rate data. Instead, the design evaluation procedures consider the material properties, operating environment and critical failure modes at the component part level to evaluate a design for R&M. The purpose of this Handbook is to present the proposed methodology for predicting the reliability of mechanical equipment and solicit comments as to the potential utility of a complete handbook of reliability prediction procedures.

The development of this Handbook by the Logistics R & D Division (Code 129) of CARDEROCKDIV, NSWC is being coordinated with the military, industry and academia. Recent sponsors of this effort

include the U. S. Army Armament Research, Development & Engineering Center (SMCAR-QAH-P), Picatinny Arsenal and the Robins AFB, WR-ALC/LVRS. These sponsors have provided valuable technical guidance in the development of the methodology and the Handbook. In addition, the Armament R,D & E Center has coordinated this effort with the RAMCAD (Reliability and Maintainability in Computer Aided Design) program. Also, the Robins AFB has supplied an MC-2A Air Compressor Unit for validation testing purposes. The procedures contained in this Handbook were used to predict the failure modes of the MC-2A and their frequency of occurrence. Reliability tests were then performed with a close correlation between predicted and actual reliability being achieved.

Past sponsors and participants in the program include the Belvoir Research, Development, & Engineering Center; Wrignt-Patterson AFB; Naval Sea Systems Command; Naval Air Test Center and Louisiana Tech University. The contractor for this effort is Support Systems Technology Corp. in Gaithersburg, Maryland. At the conclusion of this development effort NAVAIR (AIR-5165), the Reliability and Maintainability Branch, will assume sponsorship of the Handbook and be its point of contact.

Previous editions of this Handbook were distributed to interested engineering personnel in industry and DoD for comments as to the utility of the methodology in evaluating mechanical designs for reliability. The comments have been extremely useful in improving the prediction methodology and contents of the Handbook. Every effort has been made to validate the equations presented in this Handbook. However, limited funding has prevented the extensive testing and application of prediction procedures to the design/procurement process for full validation of the approach. Therefore, users are cautioned that this Handbook is the result of a research program and not an official DoD document.

Several companies have chosen to produce software packages containing the material in this draft Handbook. The commercial use of preliminary information which is a part of a research project prior to complete evaluation of the methodology is premature. The Navy has not been and is not now in any way connected with the commercial ventures to produce software packages of unproven technology and do not endorse their use. Interested users of the technology presented in this Handbook are urged to contact the Carderock Division of the Naval Surface Warfare Center to obtain the latest available information on mechanical reliability.

Comments and recommended changes to the Handbook should be addressed to:

James C. Chesley
Code 129
Carderock Division
Naval Surface Warfare Center
Bethesda, MD 20084

TABLE OF CONTENTS

TABLE OF CONTENTS
(CONTINUED)

TABLE OF CONTENTS
(CONTINUED)

TABLE OF CONTENTS
(CONTINUED)

TABLE OF CONTENTS
(CONTINUED)

THIS PAGE INTENTIONALLY LEFT BLANK

CHAPTER 1

INTRODUCTION

1.1 CURRENT METHODS OF PREDICTING RELIABILITY

A reliability prediction is performed in the early stages of a development program to support the design process. Performing a reliability prediction provides for visibility of reliability requirements in the early development phase and an awareness of potential degradation of the equipment during its life cycle. As a result of performing a reliability prediction, equipment designs can be improved, costly over-designs prevented and development testing time optimized.

Performance of a reliability prediction for electronic equipment is well supported by standardized documentation in the form of military standards, specifications and handbooks. Such documents as MIL-STD-756 and MIL-HDBK-217 have been developed for predicting the reliability of electronic equipment. Development of these documents was made possible because the standardization and mass production of electronic parts has permitted the creation of valid failure rate data banks for high population electronic devices. Such extensive sources of quality and reliability information can be used directly to predict operational reliability while the electronic design is still on the drawing board.

A commonly accepted method for predicting the reliability of mechanical equipment based on a data bank has not been possible because of the wide dispersion of failure rates which occur for apparently similar components. Inconsistencies in failure rates for mechanical equipment are the result of several basic characteristics of mechanical components:

a. Individual mechanical components such as valves and gearboxes often perform more than one function and failure data for specific applications of nonstandard components are seldom available. A hydraulic valve for example may contain a manual shut-off feature as well as an automatic control mechanism on the same valve structure.

b. Failure rates of mechanical components are not usually described by a constant failure rate distribution because of wear, fatigue and other stress related failure mechanisms resulting in equipment degradation. Data gathering is complicated when the

constant failure rate distribution can not be assumed and individual times to failure must be recorded in addition to total operating hours and total failures.

c. Mechanical equipment reliability is more sensitive to loading, operating mode and utilization rate than electronic equipment reliability. Failure rate data based on operating time alone are usually inadequate for a reliability prediction of mechanical equipment.

d. Definition of failure for mechanical equipment depends upon its application. For example, failure due to excessive noise or leakage can not be universally established. Lack of such information in a failure rate data bank limits its usefulness.

The above deficiencies in a failure rate data base result in problems in applying the failure rates to an actual design analysis. For example, the most commonly used tools for determining the reliability characteristics of a mechanical design result in a listing of component failure modes, system level effects, critical safety related issues, and projected maintenance actions. Estimating the design life of mechanical equipment is a difficult task for the design engineer. Many life-limiting failure modes such as corrosion, erosion, creep, and fatigue operate on the component at the same time and have a synergistic effect on reliability. Also, the loading on the component may be static, cyclic, or dynamic at different points during the life cycle and the severity of loading may also be a variable. Material variability and the inability to establish an effective data base of historical operating conditions such as operating pressure, temperature, and vibration further complicate life estimates.

Although several analytical tools such as the Failure Modes, Effects and Criticality Analysis (FMECA) are available to the engineer, they have been developed primarily for electronic equipment evaluations, and their application to mechanical equipment has had limited success. The FMECA, for example, is a very powerful technique for identifying equipment failure modes, their causes, and the effect each failure mode will have on system performance. Results of the FMECA provide the engineer with a valuable insight as to how the equipment will fail; however, the problem in completing the FMECA for mechanical components is determining the probability of occurrence for each identified failure mode.

The above listed problems associated with acquiring failure rate data for mechanical components demonstrates the need for

reliability prediction models that do not rely solely on existing failure rate data banks. Predicting the reliability of mechanical equipment requires the consideration of its exposure to the environment and subjection to a wide range of stress levels such as impact loading. The approach to predicting reliability of mechanical equipment presented in this Handbook considers the intended operating environment and determines the effect of that environment at the lowest part level where the material properties can also be considered. The combination of these factors permits the use of engineering design parameters to determine the design life of the equipment in its intended operating environment and the rate and pattern of failures during the design life.

1.2 DEVELOPMENT OF THE HANDBOOK

Useful models must provide the capability of predicting the reliability of all types of mechanical equipment by specific failure mode considering the operating environment, the effects of wear and other potential causes of degradation. The models developed for the Handbook are based upon identified failure modes and their causes. The first step in developing the models was the derivation of equations for each failure mode from design information and experimental data as contained in published technical reports and journals. These equations were simplified to retain those variables affecting reliability as indicated from field experience data. The failure rate models utilize the resulting parameters in the equations and modification factors were compiled for each variable to reflect its effect on the failure rate of individual component parts. The total failure rate of the component is the sum of the failure rates for the component parts for a particular time period in question. Failure rate equations for each component part, the methods used to generate the models in terms of failures per hour or failures per cycle and the limitations of the models are presented. The models are being validated to the extent possible with laboratory testing or engineering analysis.

The objective is to provide procedures which can be used for the following elements of a reliability program:

- Evaluate designs for reliability in the early stages of development
- Provide management emphasis on reliability with standardized evaluation procedures
- Provide an early estimate of potential spare parts requirements

- Quantify critical failure modes for initiation of specific stress or design analyses
- Provide a relative indication of reliability for performing trade off studies, selecting an optimum design concept or evaluating a proposed design change
- Determine the degree of degradation with time for a particular component or potential failure mode
- Design accelerated testing procedures for verification of reliability performance.

One of the problems any engineer can have in evaluating a design for reliability is attempting to predict performance at the system level. The problem of predicting the reliability of mechanical equipment is easier at the lower indenture levels where a clearer understanding of design details affecting reliability can be achieved. Predicting the life of a mechanical component, for example, can be accomplished by considering the specific wear, erosion, fatigue and other deteriorating failure mechanism, the lubrication being used, contaminants which may be present, loading between the surfaces in contact, sliding velocity, area of contact, hardness of the surfaces, and material properties. All of these variables would be difficult to record in a failure rate data bank; however, the derivation of such data can be achieved for individual designs and the potential operating environment can be brought down through the system level and the effects of the environmental conditions determined at the part level.

The development of design evaluation procedures for mechanical equipment includes mathematical equations to estimate the design life of mechanical components. These reliability equations consider the design parameters, environmental extremes, and operational stresses to predict the reliability parameters. The equations rely on a base failure rate derived from laboratory test data where the exact stress levels are known and engineering equations are used to modify this failure rate to the appropriate stress/strength and environmental relationships for the equipment application.

As part of the effort to develop a new methodology for predicting the reliability of mechanical components, Figure 1.1 illustrates the method of considering the effects of the environment and the operating stresses at the lowest indenture level. A component such as a valve assembly may consist of seals, springs, fittings, and the valve housing. The design life of the entire mechanical system is accomplished by evaluating the design

at the component and part levels considering the material properties of each part. The operating environment of the system is included in the equations by determining its impact at the part level. Some of the component parts may not have a constant failure rate as a function of time and the total system failure rate of the system can be obtained by adding part failure rates for the time period in question.

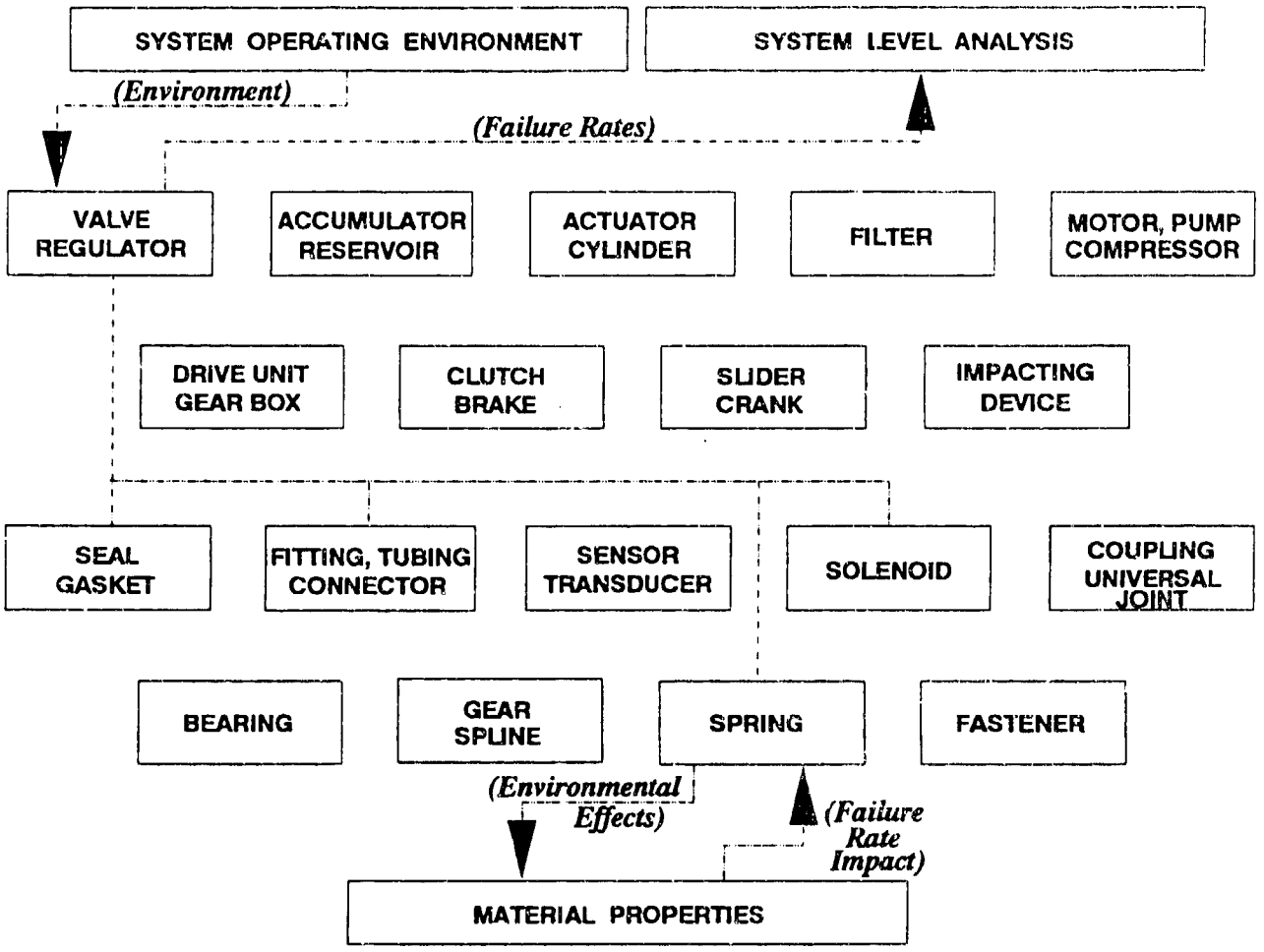

Figure 1.1 Mechanical Components and Parts

Many of the parts are subject to wear and other deteriorating type failure mechanisms and the reliability equations must include the parameters which are readily accessible to the equipment designer. A typical project to develop an engineering model for mechanical wear established the correlation between material

strength and surface wear. This method of predicting wear considers the materials involved, the lubrication properties, the stress imposed on the part and other aspects of the wear process. The relationship between the material properties and the wear rate was used to establish generalized wear life equations for actuator assemblies and other components subject to surface wear.

In another research project, lubricated and unlubricated spline couplings were operated under controlled angular misalignment and loading conditions to provide empirical data to verify spline coupling life prediction models. A special rotating mechanical coupling test machine was developed for use in generating reliability data under controlled operating conditions. This high-speed closed loop testbed was used to establish the relationships between the type and volume of lubricating grease employed in the spline coupling and gear life. Additional tests determined the effects of material hardness, torque, rotational speed and angular misalignment on gear life.

Results of these wear research projects are being used to develop and refine the reliability equations for those components subject to wear.

1.3 EXAMPLE DESIGN EVALUATION PROCEDURE

A hydraulic valve assembly will be used to illustrate the Handbook approach to predicting the reliability of mechanical equipment. Developing reliability equations for all the different types of hydraulic valves would be an impossible task since there are over one hundred different types of valve assemblies available. For example, some valves are named for the function they perform, e.g. check valve, regulator valve and unloader valve. Others are named for a distinguishing design feature, e.g. globe valve, needle valve, solenoid valve. From a reliability standpoint, dropping down one indenture level provides two basic types of valve assemblies: the poppet valve and the sliding action valve.

The example assembly chosen for analysis is a poppet valve which consists of a poppet assembly, spring, seals, and housing.

1.3.1 Poppet Assembly

The functions of the poppet valve would indicate the primary failure mode as incomplete closure of the valve resulting in leakage around the poppet seat. This failure mode can be caused by contaminants being wedged between the poppet and seat, wear of the poppet seat, and corrosion of the poppet/seat combination. External seal leakage, sticking valve stem, and damaged poppet

return spring are other failure modes which must be considered in the design life of the valve.

A new poppet assembly may be expected to have a sufficiently smooth surface for the valve to meet internal leakage specifications. However, after some period of time contaminants will cause wear of the poppet assembly until leakage rate is beyond tolerance. This leakage rate, at which point the valve is considered to have failed, will depend on the application and to what extent leakage can be tolerated.

As derived in Chapter 6 the following equation can be used to determine the failure rate of a poppet assembly:

$$\lambda_P = \lambda_{P,B} \frac{2 \times 10^4 \, D_{MS} \, f^3 \, (P_1^2 - P_2^2)}{Q_f \, \nu_a \, L_W \, (S_s)^{3/2}} K_1$$

Where:
- λ_P = failure rate of the poppet assembly, failures/million cycles
- $\lambda_{P,B}$ = base failure rate for poppet assembly,
- D_{MS} = mean seat diameter, in
- f = mean surface finish of opposing surfaces, in
- P_1 = upstream pressure, lb/in^2
- P_2 = downstream pressure, lb/in^2 failures/million cycles
- Q_f = leakage rate considered to be a valve failure, in^3/min
- ν_a = absolute fluid viscosity, lb-min/in^2
- L_W = radial seat land width, in
- S_s = apparent seat stress, lb/in^2
- K_1 = constant which considers the impact of contaminant size, hardness and quantity of particles

Values used to determine the failure rates for the parts used in this example are listed in Table 1-1. Throughout the Handbook failure rate equations for each component and part are translated into a base failure with a series of multiplying factors to modify the base failure rate to the operating environment being considered. For example, the above equation can be rewritten as follows: (See Equation 6-6 in Chapter 6)

$$\lambda_P = \lambda_{P,B} \cdot C_P \cdot C_Q \cdot C_F \cdot C_V \cdot C_H \cdot C_S \cdot C_{DT} \cdot C_{SW} \cdot C_W$$

Where: C_P = Multiplying factor which considers the effect of fluid pressure on the base failure rate

C_Q = Multiplying factor which considers the effect of allowable leakage on the base failure rate

C_F = Multiplying factor which considers the effect of surface finish on the base failure rate

C_V = Multiplying factor which considers the effect of fluid viscosity on the base failure rate

C_N = Multiplying factor which considers the effect of contaminants on the base failure rate

C_S = Multiplying factor which considers the effect of seat stress on the base failure rate

C_{DI} = Multiplying factor which considers the effect of seat diameter on the base failure rate

C_{SW} = Multiplying factor which considers the effect of seat land width on the base failure rate

C_W = Multiplying factor which considers the effect of fluid flow rate on the base failure rate

The parameters in the failure rate equation can be located on an engineering drawing, by knowledge of design standards or by actual measurement. Other design parameters which have a minor effect on reliability are included in the base failure rate as determined from field performance data.

1.3.2 Spring Assembly

Depending on the application, a spring may be in a static, cyclic, or dynamic operating mode. In the current example of a valve assembly, the spring will be in a cyclic mode. The operating life of a mechanical spring arrangement is dependent upon the susceptibility of the materials to corrosion and stress levels (static, cyclic or dynamic). The most common failure modes for springs include fracture due to fatigue and excessive loss of load due to stress relaxation. Other failure mechanisms and causes may be identified for a specific application. Typical failure rate considerations include: level of loading, operating temperature, cycling rate and corrosiveness of the fluid environment.

The failure rate of a spring depends upon the stress on the spring and the relaxation properties of the material. The load on the spring is equal to the spring rate multiplied by the change in load per unit deflection and calculated as explained in Chapter 4.

$$P_L = K\ (L_1 - L_2) = \frac{G_M\ (D_W)^4\ (L_1 - L_2)}{8\ (D_C)^3\ N_a}$$

Where: P_L = Load, lbs
K = Spring rate, lb/in
L_1 = Initial deflection of spring, in
L_2 = Final deflection of spring, in
G_M = Modulus of rigidity, lb/in^2
D_C = Mean diameter of spring, in
D_W = Mean diameter of wire, in
N_a = Number of active coils

Stress in the spring will be proportional to loading according to the following relationship:

$$S_G = \frac{8\ P_L\ D_C}{\pi\ (D_W)^3}\ K_W$$

Where: S_G = Actual stress, psi
K_W = Wahl stress correction factor

$$= \frac{4C - 1}{4C - 4} + \frac{0.615}{C}$$

and: $C = D_C/D_W$

This equation permits determination of expected life of the spring by plotting the material S-N curve on a modified Goodman diagram. In the example valve application, the spring force and the failure rate remain constant. This projection is valid if the spring does not encounter temperature extremes. The anticipated failure rate as a function of time is shown in Figure 1.2.

Corrosion is a critical factor in spring design because most springs are made of steel which is susceptible to a corrosive environment. In this example the fluid medium is assumed to be non-corrosive and the spring is always surrounded by the fluid, thus a corrosion factor need not be included in this analysis. If the valve were a safety device and subjected intermittently to a steam environment, then a corrosion factor would have to be applied consistent with any corrosion protection in the original spring

design.

1.3.3 Seal Assembly

The primary failure mode of a seal is leakage, and the following equation as derived in Chapter 3 uses a similar approach as developed for evaluating a poppet design:

$$\lambda_{SE} = \lambda_{SE,B} \frac{P_S^2 - P_O^2}{Q_f \nu_a P_O} \cdot \frac{r_2 + r_1}{r_2 - r_1} H^3 K_1$$

Where:
- λ_{SE} = Failure rate of seal, failures/million cycles
- $\lambda_{SE,B}$ = Base failure rate of seal, failures/million cycles
- P_S = System pressure, lb/in^2
- P_O = Standard atmospheric pressure or downstream pressure, lb/in^2
- Q_f = Allowable leakage rate under conditions of usage, in^3/min
- ν_a = Absolute fluid viscosity, $lb\text{-}min/in^2$
- r_1 = Inside radius of circular interface, in
- r_2 = Outside radius of circular interface, in
- H = Conductance parameter (Meyer hardness, M; contact pressure, C; surface finish, f
- K_1 = Multiplying factor considering effects of contaminants, temperature

In the case of an O-ring seal, the failure rate will increase as a function of time because of gradual hardening of the rubber material. A typical failure rate curve for an O-ring is shown in Figure 1.2.

1.3.4 Combination of Failure Rates

The addition of failure rates to determine the total valve failure rate depends on the life of the valve and the maintenance philosophy established. If the valve is to be discarded upon the first failure, a time-to-failure can be calculated for the particular operating environment. If, on the other hand, the valve will be repaired upon failure with the failed part(s) being replaced, then the failure rates must be combined for different time phases throughout the life expectancy until the wear-out phase has been reached. The effect of part replacement and overhaul is

a tendency toward a constant failure rate at the system level and will have to be considered in the prediction for the total system.

After the failure rates are determined for each component part, the rates are summed to determine the failure rate of the total valve assembly. Because some of the parameters in the failure rate equation are time dependent, i.e. the failure rate changes as a function of time, the total failure rate must be determined for particular intervals of time. In the example of the poppet assembly, nickel plating was assumed with an initial surface finish of 35 μ inches. The change in surface finish over a one year time period for non-acidic fluids such as water, mild sodium chloride solutions, and hydraulic fluids will be a deterioration to 90 μ inches. In the case of the O-ring seal, the hardness of the rubber material will change with age. This combination of failure rates is shown in Figure 1.2. The housing will exhibit an insignificant failure rate, usually verified by experience or by finite element analysis. Typical values and assumed for the example equations are listed in Table 1-1.

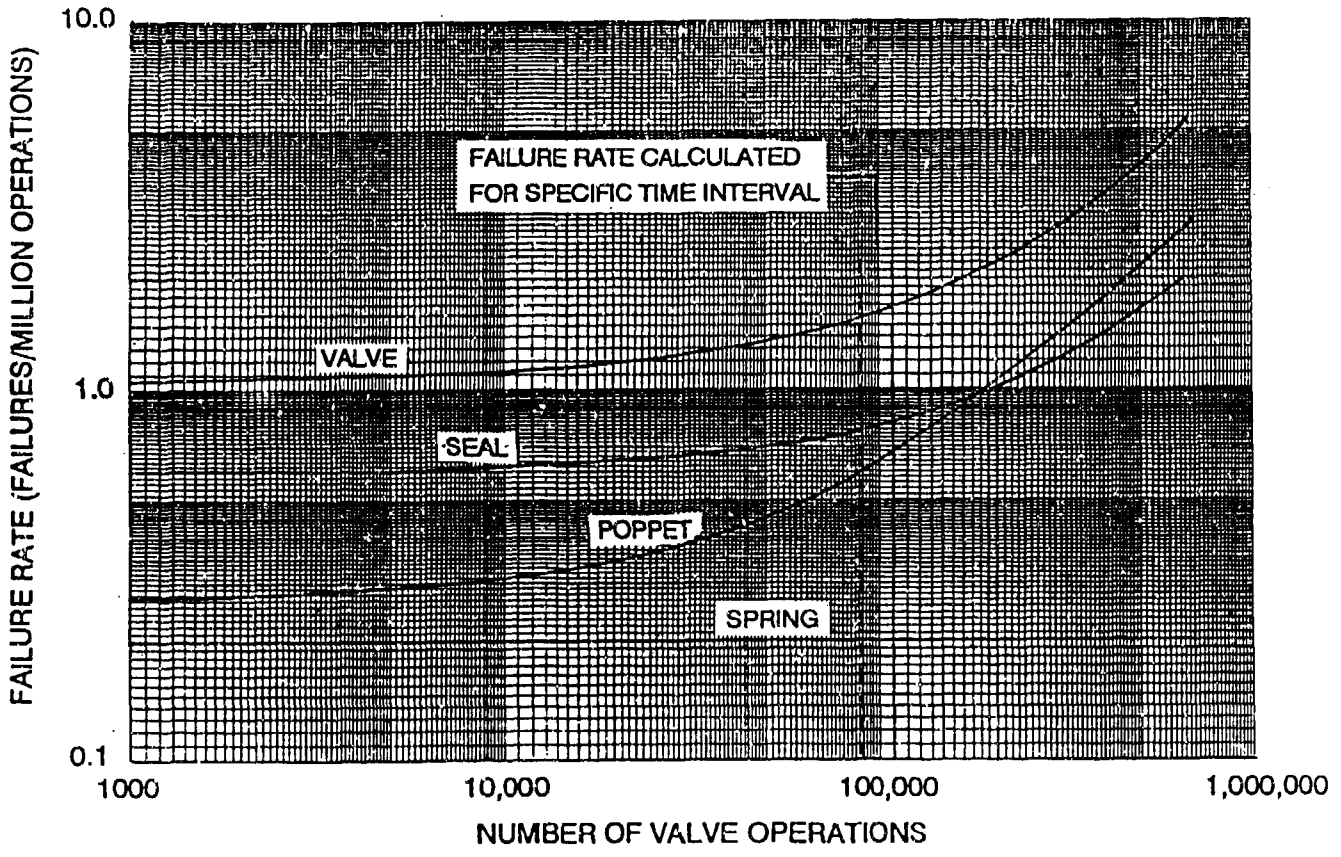

Figure 1.2. Combination of Component Failure Rates

1.4 VALIDATION OF RELIABILITY PREDICTION EQUATIONS

A very limited budget for this project has prevented the procurement of a large number of components to perform the necessary failure rate tests for all of the possible combinations of loading roughness, operational environments, and design parameters to validate the equations. For example, valve assemblies were procured and tested at the Belvoir Research, Development and Engineering Center in Ft. Belvoir, Virginia. The number of failures for each test were predicted using the equations presented in this Handbook. Failure rate tests were performed for several combinations of stress levels and results compared to predictions. Typical results are shown in Table 1-2.

The procedures presented in this Handbook should not be considered as the only methods for a design analysis. An engineer needs many evaluation tools in his toolbox and new methods of performing dynamic modeling, finite element analysis and other stress/strength evaluation methods must be used in combination to arrive at the best possible reliability prediction for mechanical equipment.

The examples included in this introduction are intended to illustrate the point that there are no simplistic approaches to predicting the reliability of mechanical equipment. Accurate predictions of reliability are best achieved by considering the effects of the operating environment of the system at the part level. The failure rates derived from equations as tailored to the individual application then permits an estimation of design life for any mechanical system.

It will be noted upon review of the equations that some of the parameters are very critical in terms of life expectancy. For example, the failure rate equation for the poppet assembly contains the surface finish parameter which deteriorates as a function of time and is raised to the third power. The same problem exists in many of the equations for predicting the reliability of mechanical equipment. Additional research is needed to obtain additional information on some of these cause and effect relationships for use in the equations and continual improvement to the Handbook.

TABLE 1-1
TYPICAL VALUES FOR FAILURE RATE EQUATIONS

POPPET		SPRING		SEAL	
PARAMETER	VALUE	PARAMETER	VALUE	PARAMETER	VALUE
$\lambda_{P,B}$	1.25	L_1	3.50	$\lambda_{SE,B}$	0.85
Q_f	0.055	L_2	2.28	Q_f	0.055
D_{MS}	0.70	G_M	10×10^6	P_S	3000
f *	35×10^{-6}	D_C	0.6	P_0	---
P_1	3000	D_W	0.085	ν_a	2×10^{-8}
P_2	0.0	N_a	14	r_1	0.17
ν_a	2×10^{-8}	T_S	245	r_2	0.35
L_W	0.18	P_L	26.3	M/C **	0.55
S_S	1.2	S_G	75×10^{-3}	f	10
K_1	2.5	$\lambda_{SP,B}$	0.65	K_1	2.5
λ_p	0.26	λ_{SP}	0.21	λ_{SE}	0.57

* Initial value = 35 μin; after 1 year (500,000 operations) surface finish will equal 110 μin (Reference 5)

** Initial value = .55 (hardness, H = 500 psi; contact stress, C = 910 psi); after 1 year H estimated to be 575 psi (M/C = 0.63)

TABLE 1-2
SAMPLE TEST DATA FOR VALIDATION OF
RELIABILITY EQUATIONS FOR VALVE ASSEMBLIES

TEST SERIES	VALVE NUMBER	TEST CYCLES TO FAILURE	ACTUAL FAILURES/ MILLION CYCLES	AVERAGE FAILURES/ MILLION CYCLES	PREDICTED FAILURES/ MILLION CYCLES	FAILURE MODE #
15	11	68,322	14.64	14.64	18.02	3
24	8	257,827				1
24	9	131,126	7.63	10.15	10.82	1
24	10	81,113	12.33			1
24	11	104				2
24	12	110,488	9.05			1
24	13	86,285	11.59			1
25	14	46,879	21.33	19.67	8.45	2
25	15	300				3
25	18	55,545	18.00			1

TEST PARAMETERS:

SYSTEM PRESSURE: 3500 psi

FLUID FLOW: 100% rated

FLUID TEMPERATURE: 90°C

FLUID: Hydraulic, MIL-H-83282

FAILURE MODE:
1 - Spring Fatigue
2 - No Apparent
3 - Accumulated Debris

CHAPTER 2

DEFINITIONS

This report is intended for use by reliability analysts and equipment designers. Accordingly, a review of some basic terms will help to establish a cross reference for these two disciplines. MIL-STD-721 should be referred to for basic reliability definitions.

- Base Failure Rate - A failure rate for a component or part in failures per million hours or failures per million operations depending on the application and derived from a data base where the exact design, operational, and environmental parameters are known. Multiplying factors are then used to adjust the base failure rate to the new operating environment.
- Brake Lining - a frictional material used for stopping or retarding the relative movement of two surfaces.
- Coefficient of Friction - this relationship is the ratio between two measured forces. The denominator is the normal force pressing two surfaces together. The numerator is the frictional force resisting the motion of one surface over other.
- Contamination - foreign matter or particles in a fluid system that are transported during its operation and which may be detrimental to system performance or even cause failure of a component.
- Corrosion - the slow destruction of materials by chemical agents and/or electromechanical reactions.
- Creep - continuous increase in deformation under constant or decreasing stress.
- Dependent failure - failure caused by failure of an associated item or by a common agent.
- Dirt lock - complete impedance of movement caused by stray contaminant particles wedged between moving parts.
- Endurance Limit - the stress level value when plotted as a function of the number of stress cycles at which point a constant stress value is reached.
- External leakage - leakage resulting in loss of fluid to the external environment.
- Failure mode - the indicator or symptom by which a failure is evidenced.

• Failure rate - the probable number of times that a given component will fail during a given period of operation under specified operating conditions. Failure rate may be in terms of time, cycles, revolutions, miles, etc.

• Fatigue - the cracking, fracture or breakage of mechanical material due to the application of repeated, fluctuating or reversed mechanical stress less than the tensile strength of the material.

• Friction Material - a product manufactured to resist sliding contact between itself and another surface in a controlled manner.

• Hardness - a measure of material resistance to permanent or plastic deformation equal to a given load divided by the resulting area of indentation.

• Independent failure - a failure of a device which is not caused by or related to failure of another device.

• Internal leakage - leakage resulting in loss of fluid in the direction of fluid flow past the valving unit.

• Leakage - the flow of fluid through the interconnecting voids formed when the surfaces of two materials are brought into contact.

• Mean cycles between failure - the total number of functioning cycles of a population of parts divided by the total number of failures within the population during the same period of time. This definition is appropriate for the number of hours as well as for cycles.

• Mean cycles to failure - the total number of functioning cycles divided by the total number of failures during the period of time. This definition is appropriate for the number of hours as well as for cycles.

• Modulus of Elasticity - Slope of the initial linear portion of the stress-strain diagram; the larger the value, the larger the stress required to produce a given strain. Also known as Young's Modulus.

• Modulus of Rigidity - the rate of change of unit shear stress with respect to unit shear strain for the condition of pure shear within the proportional limit. Also called Shear Modulus of Elasticity.

• Poisson's Ratio - Ratio of lateral strain to axial strain of a material when subjected to uniaxial loading.

• Random failures - failures that occur before wear out, are not predictable as to the exact time of similar and are not associated with any pattern of similar failures. However, the number of random failures for a given population over a period of time at a constant failure rate can be predicted.

• Silting - an accumulation and settling of particles during component inactivity.

• Stiction - a change in performance characteristics or complete impedance of poppet or spool movement caused by wedging of minute particles between a poppet stem and housing or between spool and sleeve

• Stress - A measure of intensity of force acting on a definite plane passing through a given point, measured in force per unit area.

• Tensile Strength - Value of nominal stress obtained when the maximum (or ultimate) load that the specimen supports is divided by the cross-sectional area of the specimen. See Ultimate Strength

• Ultimate Strength - the maximum stress the material will withstand. See Tensile Strength

• Viscosity - a measure of internal resistance of a fluid which tends to prevent it from flowing.

• Wear out failure - a failure which occurs as a result of mechanical, chemical or electrical degradation.

• Yield strength - The stress that will produce a small amount of permanent deformation, generally a strain equal to 0.1 or 0.2 percent of the length of the specimen.

THIS PAGE INTENTIONALLY LEFT BLANK

CHAPTER 3

SEALS AND GASKETS

3.1 INTRODUCTION

A seal is a device placed between two surfaces to restrict the flow of fluid from one region to another. Seals are required for both static and dynamic applications. Static seals, such as gaskets, are used to prevent leakage through a mechanical joint when there is no relative motion of mating surfaces other than that induced by environmental changes. A dynamic seal is a mechanical device used to control leakage of fluid from one region to another when there is rotating or reciprocating motion between the sealing interface. Some types of seals such as O-rings are used in both static and dynamic applications. An example of static and dynamic seal application is shown in Figure 3.1.

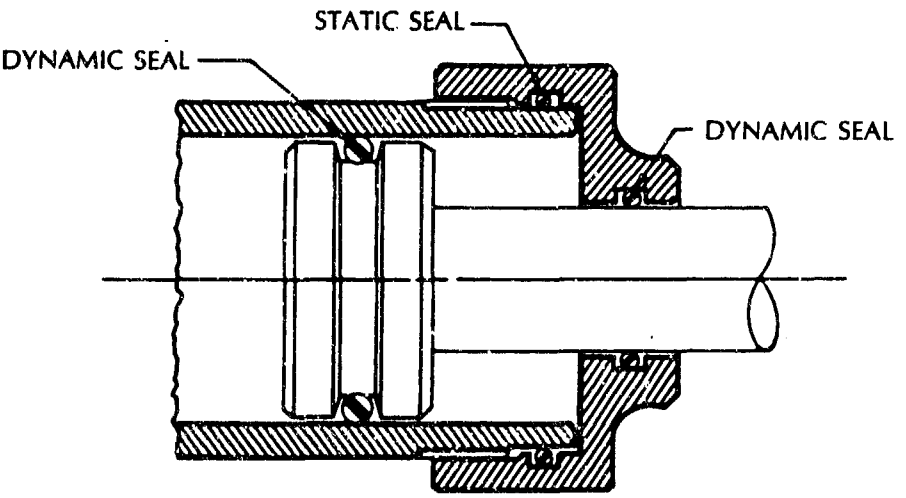

Figure 3.1 Static And Dynamic Seals

The reliability of a seal design is determined by the ability of the seal to restrict the flow of fluid from one region to another for its intended life in a prescribed operating environment. The evaluation of a seal design for reliability must include a definition of the design characteristics and the operating environment in order to determine its intended life. Section 3.2

discusses the reliability of gaskets and static seals. A discussion of dynamic seal reliability is contained in Section 3.3.

3.2 GASKETS AND STATIC SEALS

3.2.1 Failure Modes

The primary failure mode of a gasket or seal is leakage. The integrity of a seal depends upon the compatibility of the components, conditions of the sealing environment, and the applied load during application. Table 3-1 is a list of failure mechanisms and causes of seal leakage. Other failure mechanisms and causes should be identified for the specific product to assure that all considerations of reliability are included in any design evaluation.

Table 3-1. Typical Failure Mechanisms and Causes for Static Seals and Gaskets

FAILURE MODE	FAILURE MECHANISMS	FAILURE CAUSES
Leakage	Wear	Contaminants Misalignment
	Elastic Deformation Gasket/seal distortion	Extreme temperature Misalignment Seal eccentricity Extreme loading/ extrusion
	Surface damage Embrittlement	Inadequate lubrication Contaminants Fluid/seal degradation Thermal degradation Idle periods between component use

3.2.2 Failure Rate Model Considerations

A review of failure rate data suggests the following characteristics be included in the failure rate model for gaskets and seals:

- Static vs. dynamic conditions
- Material characteristics
- Amount of seal compression
- Surface irregularities
- Seal size
- Extent of pressure pulses
- Contamination level
- Fluid/material compatibility
- Leakage requirements
- Fluid viscosity
- Q. C./ Manufacturing process
- Fluid pressure

The failure rate of a seal or gasket material will be proportional to the ratio of actual leakage to that allowable under conditions of usage. This rate can be expressed as follows:

$$\lambda_{SE} \propto \lambda_{SE,B} \left(\frac{Q_a}{Q_f} \right) \tag{3-1}$$

Where:
λ_{SE} = Failure rate of gasket or seal considering operating environment, failures per million cycles
$\lambda_{SE,B}$ = Base failure rate of seal or gasket due to random cuts, installation errors, etc. based on field experience data, failures per million cycles
Q_a = Actual leakage rate, in^3/min
Q_f = Allowable leakage rate under conditions of usage, in^3/min

The allowable leakage, Q_f, is determined from design drawings, specifications or knowledge of component applications. The actual leakage rate, Q_a, for a seal is determined from a standard equation for laminar flow around two curved surfaces (Ref. 5).

$$Q_a = \left(\frac{\pi \ (P_s^2 - P_o^2)}{25 \ \nu_a \ P_c} \right) \left(\frac{r_2 + r_1}{r_2 - r_1} \right) H^3 \tag{3-2}$$

Where: P_s = System pressure, lb/in^2
P_o = Standard atmospheric pressure or downstream pressure, lb/in_2
ν_a = Absolute fluid viscosity, $lb\text{-}min/in^2$
r_1 = Inside radius of circular interface, in
r_2 = Outside radius of circular interface, in
H = Conductance parameter, in (See Equation 3-4)

For flat seals or gaskets the leakage can be determined from the following equation:

$$Q_a = \left(\frac{2\pi\, r_1\, (P_s^2 - P_o^2)}{24 \nu_a\, L\, P_o} \right) H^3 \qquad (3\text{-}3)$$

Where: r_1 = Inside radius, in
L = Contact length, in

The conductance parameter H is dependent upon contact stress, hardness of the softer material and surface finish of the harder material. First, the apparent contact stress (load/area) is calculated and the ratio of contact stress to Meyer hardness of the softer interface material computed. The surface finish of the harder material is then determined. The conductance parameter is computed from the following empirically derived formula:

$$H = \left[\frac{C}{10^{11} M_p} \right]^{\frac{1}{3}} \cdot f^{\frac{3}{2}} \qquad (3\text{-}4)$$

Where: C = Apparent contact stress, psi (See Equation 3-11)
M_p = Meyer hardness (or Young's modulus) for rubber and resilient materials. (See Equation 3-10)
f = Surface finish, in

The surface finish, f, will deteriorate at a rate dependent upon several factors:

- Seal degradation
- Contaminant wear coefficient $(in^3/particle)^2$

- Number of contaminant particles per in^3
- Flow rate, in^3/min
- Ratio of time the seal is subjected to contaminants under pressure
- Temperature of operation, °F

The contaminant wear coefficient is an inherent sensitivity factor for the seal or gasket based upon performance requirements. The number of contaminants includes those produced by wear in components upstream of the seal and after the filter and those ingested by the system. Combining and simplifying terms provides the following equations for the failure rate of a seal.

For circular seals:

$$\lambda_{SE} = \lambda_{SE,B} \left[\frac{K_1 \, (P_s^2 - P_o^2) \, H^3}{Q_f \, \nu_a \, P_o} \right] \cdot \left[\frac{r_2 + r_1}{r_2 - r_1} \right] \qquad (3\text{-}5)$$

or, for flat seals and gaskets:

$$\lambda_{SE} = \lambda_{SE,B} \left[\frac{K_1 \, (P_s^2 - P_o^2) \, r_1 \, H^3}{Q_f \, \nu_a \, L \, P_o} \right] \qquad (3\text{-}6)$$

Where: K_1 is an empirically derived constant.

3.2.3 Failure Rate Model for Gaskets and Static Seals

By normalizing the equation to those values for which historical failure rate data (3-M) are available, the following model can be derived:

$$\lambda_{SE} = \lambda_{SE,B} \cdot C_p \cdot C_Q \cdot C_{DL} \cdot C_H \cdot C_F \cdot C_v \cdot C_T \cdot C_M \qquad (3\text{-}7)$$

Where:
- λ_{SE} = Failure rate of a seal in failures/million cycles
- $\lambda_{SE,B}$ = Base failure rate of seal, 0.85 failures/million operations *
- C_p = Multiplying factor which considers the effect of fluid pressure on the base failure rate (See Table 3-6)

C_Q = Multiplying factor which considers the effect of allowable leakage on the base failure rate (See Table 3-7)

C_{DL} = Multiplying factor which considers the effect of seal size on the base failure rate (See Table 3-8)

C_H = Multiplying factor which considers the effect of contact stress and seal hardness on the base failure rate (See Table 3-9)

C_F = Multiplying factor which considers the effect of seat smoothness on the base failure rate (See Table 3-9)

C_V = Multiplying factor which considers the effect of fluid viscosity on the base failure rate (See Table 3-10)

C_T = Multiplying factor which considers the effect of temperature on the base failure rate (See Table 3-12)

C_N = Multiplying factor which considers the effect of contaminants on the base failure rate (See Table 3-11)

* Base failure rate was established in terms of failures/million hours. It has been converted to failures/million operations to be compatible with other failure rate models in the handbook.

The parameters in the failure rate equation can be located on an engineering drawing, by knowledge of design standards or by actual measurement. Other design parameters which have a minor effect on reliability are included in the base failure rate as determined from field performance data. The following paragraphs provide background information on those parameters included in the model.

3.2.3.1 Fluid Pressure

Table 3-6 contains the fluid pressure modification factors for use in the model. Fluid pressure on a seal will usually be the same as the system pressure.

The fluid pressure at the sealing interface required to achieve good mating depends on the resiliency of the sealing materials and their surface finish. It is the resilience of the seal which insures that adequate sealing stress is maintained while the two

surfaces move in relation to one another with thermal changes, vibration, shock and other changes in the operating environment. The reliability analysis should include a verification that sufficient pressure will be applied to effect a good seal.

At least three checks should be made to assure the prevention of seal leakage:

(1) One surface should remain relatively soft and compliant so that it will readily conform to the irregularities of the harder surface

(2) Sufficient sealing load should be provided to elastically deform the softer of the two sealing surfaces

(3) Sufficient smoothness of both surfaces is maintained so that proper mating can be achieved

3.2.3.2 Allowable Leakage

Table 3-7 contains the allowable leakage multiplying factors for use in the model. Determination of the acceptable amount cf leakage which can be tolerated at a seal interface can usually be obtained from component specifications. The allowable rate is a function of operational requirements and the rate may be different for an internal or external leakage path.

3.2.3.3 Conductance Parameter

Table 3-9 contains the conductance parameters for use in the model. The seal gland is the structure which retains the seal. The surface finish on the gland will usually be about 32 microinches for elastomer seals, 16 microinches for plastic seals and 8 microinches for metals.

Seals deform to mate with rigid surfaces by elastic deformation. Since the deformation of the seal is almost entirely elastic, the initially applied seating load must be maintained. Thus, a load margin must be applied to allow for strain relaxation during the life of the seal yet not to the extent that permanent deformation takes place. An evaluation of cold flow characteristics is required for determining potential seal leakage of soft plastic materials. Although dependent on surface finish, mating of metal-to-metal surfaces generally requires a seating stress of two to three times the yield strength of the softer material.

In addition to average surface finish, the allowable number and magnitude of flaws in the gland must be considered in projecting leakage characteristics. Flaws such as surface cracks, ridges or scratches will have a detrimental effect on seal leakage.

In the case of rubber seals and o-rings, the hardness of rubber is measured either by durometer (ASTM-D-2240-81) or international hardness methods (ASTM-D-1414-78, ASTM-D-1415-81), as outlined in the ASTM Handbook, Volumes 37 and 38.

Both hardness test methods are based on the measurement of the penetration of a rigid ball into a rubber specimen. The scale of hardness is from 0 degrees for elastic modulus of a liquid to 100 degrees for an infinite elastic modulus of a material, such as glass.

One International Rubber Hardness Degree (IRHD) represents approximately the same proportionate difference in Young's Modulus for rubber seals in the usual range of resilience. Readings of IRHD are comparable with those given by durometer (Ref. 18) when testing standard specimens. Well-vulcanized elastic isotropic materials, like rubber seals manufactured from natural rubbers and measured by IRHD methods, have a known relationship to Young's modulus. This relationship is shown in Table 3-4.

The relation between a rigid ball penetration and Young's Modulus for a perfectly elastic isotropic material is:

$$\frac{F_1}{M_p} = 1.9\,(R_p)^2 \left(\frac{P_D}{R_p}\right)^{1.35} \qquad (3\text{-}8)$$

Where:
F_1 = Indenting Force, N
M_p = Young's Modulus, MPA
R_p = Radius of Ball, mm
P_D = Penetration, mm

Standard IRHD testers have a ball radius of 1.19 mm with a total force on the ball of 5.53 N.

Table 3-3 provides the relation between IRHD and penetration difference for the cases involving O-Rings and rubber seals. These values may be assumed to be equal to a durometer reading. A value for Young's Modulus (M_p) in psi can be calculated as follows:

$$M_p = \frac{251}{\left(\frac{P_D}{1.19}\right)^{1.35}} \qquad (3\text{-}9)$$

Where: M_p = Young's modulus, psi
P_D = Penetration from Durometer or IRHD measurement

Since Young's modulus is expressed in psi and calculated in the same manner as Meyer's Hardness for Rigid Material, an expression can be calculated:

$$\text{Meyer's Hardness} = M_p = \frac{4P_F}{\pi (D_{IN})^2} \qquad (3\text{-}10)$$

Where: P_F = Load applied to sample, lbs
D_{IN} = diameter of indentation of sample, in

Then, for rubber materials, Young's modulus and Meyer's hardness can be considered equivalent.

The Contact Stress, C, in psi can be calculated by:

$$C = \frac{F_C}{A_{SC}} \qquad (3\text{-}11)$$

Where: F_C = Force compressing seals, lbs
A_{SC} = Area of seal contact, in^2

Contact pressure for various seal materials are listed in Table 3-5.

For most seals, the maximum allowable force F_C is normally two and one-half times the Young's modulus for the material. A study of gasket and seal joints shows that, for design purposes, the apparent seal contact pressure should be used (Ref. 38). This value can be obtained from Figure 3.2.

Table 3-5 provides the minimum contact pressure required for a seal in pressure applications. From this table and use of the relationship between seal contact stress pressure and apparent contact pressure, a minimum hardness of O-ring material can be deduced. This value of hardness turns out to be an approximate IRHD of 60, which yields a M/C of 0.35. Therefore, materials with M less than 60 should not be considered for a seal. If a softer material is used, the seal material will have insufficient strength to withstand the forces induced by the fluid and will rapidly fail

by seal blowout. This is not considered in the model because the failure would occur during break-in and be caused by poor design and not wear or use induced.

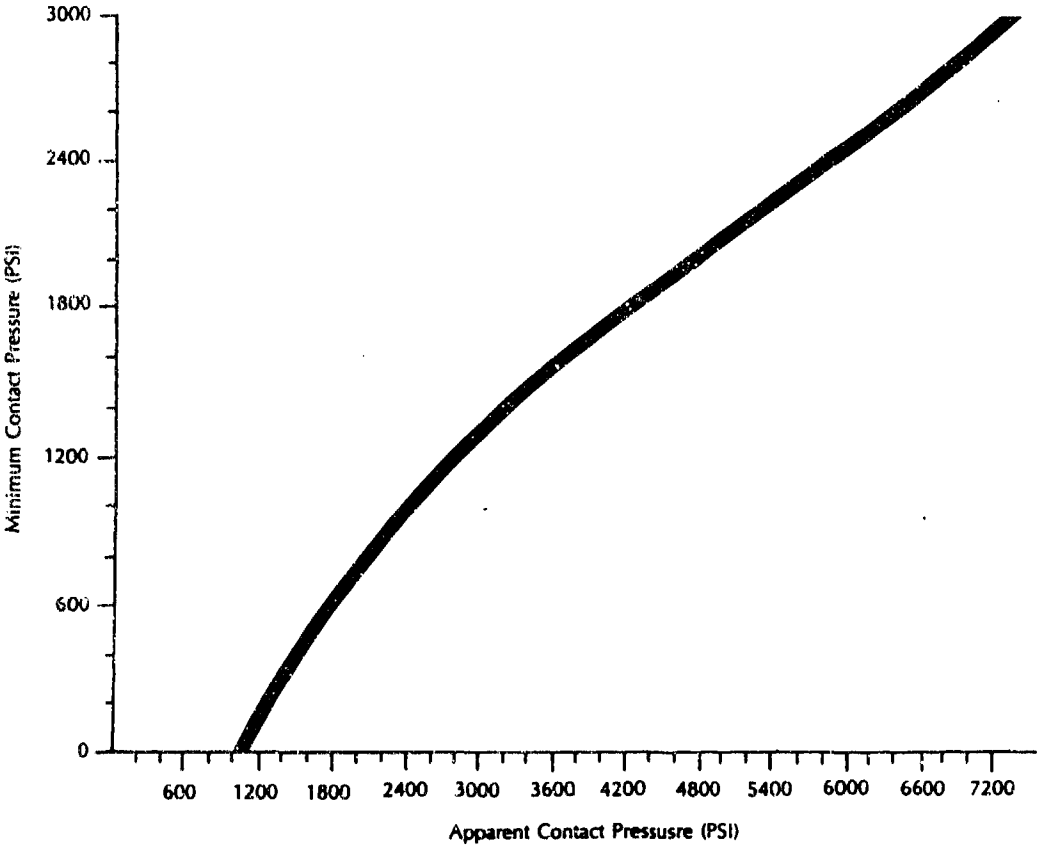

Figure 3.2 Relationship Between Seal Contact Pressure and Apparent Contact Pressure

3.2.3.4 Fluid Viscosity

Fluid viscosities for typical fluids are provided in Table 3-10. Viscosities for other fluids at the operating temperature can be found in referenced sources. Surface irregularities of dynamic seals may be more pronounced than static seals. In dynamic seal applications where the seal mates with a shaft, shaft hardness, smoothness and material are factors which must be considered in the design evaluation process. Maximum seal efficiency and life are obtained with a finely finished gland surface, usually in the 10 to 20 microinch range. The degree to which the finish can be maintained in the operating range must be

considered when determining the surface finish of the gland for use in the model.

3.2.3.5 Fluid Contaminants

The quantities of contaminants likely to be generated by upstream components are listed in Table 3-11. The number of contaminants depends upon the design, the enclosures surrounding the seal, its physical placement within the system, maintenance practices and quality control. The number of contaminants may have to be estimated from experience with similar components.

3.2.3.6 Operating Temperature

The operating temperature has a definite effect on the aging process of elastomer and rubber seals. Elevated temperatures, those temperatures above the normal use temperatures, tend to continue the vulcanization or curing process of the materials, thereby, significantly changing the original characteristics of the seal or gasket. It can cause increased hardening, brittleness, loss of resilience, cracking, and excessive wear. Since a change in these characteristics has a definite effect on the failure rate of the component, a reliability adjustment must be made.

Temperature effects on rubber and other elastomers can be expressed by (Ref. 31):

$$H_F = \frac{1.2 \times 10^5}{\varepsilon_{bT}} (2)^{\frac{(T_R - T_o)}{18}} \qquad (3\text{-}12)$$

Where:

H_F = Hours of use before failure at the operating temperature

ε_{bT} = Elongation stress, tension or compression at the operating temperature, percent of elongation

T_R = Temperature rating of the material, °F

T_0 = Temperature to which the material will be exposed in operation, °F

Manufacturers of rubber seals usually specify the maximum temperature, T_R, for their products. An alternative "life" definition is the time taken to reduce original mechanical properties by 50 percent. Under this definition, temperature limits, T_R, that give a one-year life for common static seal

materials are given in Table 3-13.

For O-Rings, it is standard practice to design the seals for ε_{bT} = 25 percent compression.

$$C_T = \frac{F_o}{F_R} \qquad (3\text{-}13)$$

Where:
- C_T = Temperature factor.
- F_o = Failure rate of operating component in failures per million cycles (See Equation 3-14).
- F_R = Failure rate of components, operating at rated temperature, measured in failures per million cycles.

$$F_o = \frac{10^6}{H_F\, N_{HC}} \qquad (3\text{-}14)$$

Where:
- N_{HC} = Operating cycles per hr.

These expressions are only valid below the temperature at which the seal or gasket begins to melt or char. For the case where all parameters are equal except temperature;

$$C_T = \frac{1}{2^t} \qquad (3\text{-}15)$$

Where:
$$t = \frac{T_R - T_o}{18} \qquad (3\text{-}16)$$

3.2.3.7 Other Considerations

Those failure rate considerations not specifically included in the model but rather included in the base failure rates are as follows:

- Proper selection of seal materials with appropriate coefficients of thermal expansion for the applicable fluid temperature and compatibility with fluid medium.
- Potential corrosion from the gland, seal, fluid interface.
- Possibility of the seal rolling in its groove when system surges are encountered.

- If O-rings can not be installed or replaced easily they are subject to being cut by sharp gland edges.

3.3 DYNAMIC SEALS

3.3.1 Failure Modes

The mechanical seal may be used to seal many different liquids at various speeds, pressures, and temperatures. The sealing surfaces are perpendicular to the shaft with contact between the primary and mating rings to achieve a dynamic seal.

The wear occurs between the primary ring and mating ring. This surface contact is maintained by a spring. There is a film of liquid maintained between the sealing surfaces to eliminate as much friction as possible. For most dynamic seals, the three common points of sealing contact occur between the following points:

1. Mating surfaces between primary and mating rings.
2. Between the rotating component and shaft or sleeve.
3. Between the stationary component and the gland plate.

The various failure mechanisms and causes for mechanical seals are listed in Table 3-2.

3.3.2 Failure Rate Model

The mating ring is usually a separate replaceable part. The static seal and the mating ring are separated from leakage to the gland plate by the O-Ring or static seal. Of greatest importance with dynamic seals is a properly designed seal face. The mating surfaces are usually made from different materials. The proper materials must be matched so that excessive heat isn't generated from the dynamic motion of the seal faces. Too much heat can cause thermal distortions on the face of the seal and cause gaps which can increase the leakage rate. It can also cause material changes that can significantly increase the seal wear rate. Therefore, careful material selection should be included for each surface of the dynamic seal face. Equation (3-17) (Ref. 26) expresses such coefficients of friction, and wear rates. Table 3-14 shows frictional values for various seal face materials.

$$Q_s = C_1 \cdot PV \cdot \mu \cdot a_0 \qquad (3\text{-}17)$$

Where:

Q_s = Heat input from the seal, BTU/n(W)

C_1 = Numerical constant; 0.077 for USCS units and 1.0 for SI

PV = Pressure-velocity coefficient (See Eq. 3-18)

μ = Coefficient of friction (See Table 3-14)
a_0 = Seal face area, in^2 (m^2)

Two important parameters that effect seal wear are seal face pressure and fluid velocity. These parameters multiplied together provide a "PV" factor. The following equation defines the "PV" factor.

$$PV = \left[DP(b-k) + \frac{F_{SP}}{a_o}\right] V_M \qquad (3\text{-}18)$$

Where:
DP = Pressure differential across seal face, psi (N/m^2)
b = Seal balance, the ratio of hydraulic closing area to seal face area.
k = Pressure gradient factor, See Table 3-15
F_{SP} = Seal spring load. Lb (N)
V_M = Fluid velocity at the seal mean face diameter, ft/min (m/s)

The frictional aspects of materials are not only important from a reliability viewpoint, but also from an efficiency aspect. The more resistance a system incurs, the more power is lost and also the lower the efficiency value for the component. Therefore, the extra cost for a component with special wear resistant seals may well pay for itself through savings in powering the component plus the savings involved with lower maintenance costs. There should be special consideration for tradeoffs involved with each type of seal material. For example, solid silicon carbide has excellent abrasion resistance, good corrosion resistance, and moderate thermal shock resistance. This material has better qualities than a carbon-graphite base material but has a PV value of 500,000 lb/in-min while carbon-graphite has a 50,000 lb/in-min PV value. With all other values being the same, the heat generated would be five times greater for solid silicon carbide than for carbon-graphite materials. The required cooling flow to the solid silicon carbide seal would be larger to maintain the film thickness on the dynamic seal faces. If this cooling flow can't be maintained, then an increase in wear would occur due to higher surface temperatures. The analyst should perform tradeoff analysis for each candidate design to maximize reliability.

The PV factor will be incorporated into the seal reliability model. Most of the seal modifying factors will remain the same as the ones previously specified by Equation 3-7. The seal model is modified as shown in Equation 3-19.

$$\lambda_{SE} = \lambda_{SE,B} \cdot C_F \cdot C_V \cdot C_T \cdot C_M \cdot C_H \cdot C_{PV} \cdot C_Q \qquad (3\text{-}19)$$

$\lambda_{SE,B}$ is the base failure rate and the multiplying factors are equal to the ones previously defined in Equation (3-7) with the exception of C_{PV} and C_T. The temperature factor, C_T, and the pressure/velocity factor, C_{PV}, are presently discussed.

C_{PV} is the multiplying factor that multiplies the base failure rate by the ratio of PV value for actual seal operation to design PV value. The values for PV_{DS} and PV_{OP} used in Equation (3-20) will use the PV formulation in Equation (3-18).

$$C_{PV} = PV_{OP} / PV_{DS} \qquad (3\text{-}20)$$

Where: PV_{OP} = PV factor for the original design
PV_{DS} = PV factor for actual seal operation

The temperature factor, C_T is formulated from research showing that the values for PV will decrease by one-half when the operating temperature is doubled. Equation (3-21) represents this relationship.

$$C_T = 1 + \frac{T_o - T_R}{T_R} \qquad (3\text{-}21)$$

Where: T_o = Operating temperature
T_R = Rated temperature

An additional important seal design consideration is seal balance. This performance characteristic measures how effective the seal mating surfaces match. The seal load at the dynamic facing may be too high causing the liquid film to be squeezed out and vaporized - thus causing a high wear rate. The seal surfaces also have structural load limitations that, if breached, may cause premature failures. The dynamic facing pressure can be controlled by manipulating the hydraulic closing area. The fluid pressure from one side of the primary ring causes a certain amount of force

to impinge on the dynamic seal face. This force can be controlled by changing the hydraulic closing area. By increasing the area, the sealing force is increased. The process of manipulating this face area is called seal balancing. The ratio of hydraulic closing area to seal face area is defined as "seal balance" (parameter b in Equation 3-18). This ratio is normally modified by decreasing the hydraulic closing area by a shoulder on a sleeve or by seal hardware.

Table 3-2. Typical Failure Mechanisms and Causes for Dynamic Seals

FAILURE MODE	FAILURE MECHANISMS	FAILURE CAUSES
Leakage	Wear	- Misalignment - Shaft out-of-roundness - Surface finish - Contaminants - Inadequate lubrication
	Dynamic instability	- Misalignment
	Embrittlement	- Contaminants - Fluid/seal incompatibility - Thermal degradation - Idle periods between component use

Table 3-3. Relation Between International Rubber Hardness Degree (IRHD) and Penetration Differences

IRHD	Movement of Plunger, mm	IRHD	Movement of Plunger, mm
28	1.934	66	0.589
30	1.803	68	0.552
32	1.685	70	0.516
34	1.578	72	0.481
36	1.479	74	0.447
38	1.389	76	0.415
40	1.305	78	0.384
42	1.227	80	0.353
44	1.155	82	0.323
46	1.087	84	0.294
48	1.024	86	0.266
50	0.964	88	0.237
52	0.908	90	0.209
54	0.855	92	0.180
56	0.805	94	0.151
58	0.758	96	0.114
60	0.173	98	0.083
62	0.670	100	0.000
64	0.629		

Table 3-4. Hardness Readings vs Young's Modulus

IRHD/Durometer (degrees)	Young's Modulus (psi)
10	43
20	86
30	143
40	222
50	334
60	501
70	776
80	1296
90	2714
95	4739

Table 3-5. Minimum Contact Pressures for Seal Material Used in Pressure Applications

MATERIAL	MINIMUM CONTACT PRESSURE psi
Asbestos and Rubber	800 - 2000
Cellulose and Rubber	1000 - 2000
Cork	500 - 1000
Rubber	400 - 600

Table 3-6. Fluid Pressure Multiplying Factor, C_p

FLUID PRESSURE, psi	C_p
0 - 500	0.01
501 - 1500	0.11
1501 - 2500	0.44
2501 - 3500	1.00
3501 - 4500	1.80
4501 - 5500	2.80
5501 - 6500	4.00
6501 - 7500	5.44
7501 - 8500	7.11

$$C_p = \left(\frac{P_s}{3000}\right)^2$$

Table 3-7. Allowable Leakage Multiplying Factor, C_Q

ALLOWABLE LEAKAGE (Q_F) $INCHES^3/MINUTE$ Max Rated GPM	C_Q
.005 - .009	3.5
.010 - .014	3.2
.015 - .019	2.8
.020 - .024	2.4
.025 - .029	2.0
.030 - .039	1.6
.040 - .049	1.3
.050 - .059	1.0
.060 - .079	0.8
.080 - .100	0.6

For Leakage (Per GPM_R) > 0.03, $C_Q = 0.055/Q_F$

For Leakage (Per GPM_R) ≤ 0.03, $C_Q = 4.1 - (79\ Q_F)$

Table 3-8. Seal Diameter Multiplying Factors

SEAL DIAMETER (inches)	C_{DL}
0.00 - 0.24	0.6
0.25 - 0.39	0.7
0.40 - 0.59	0.8
0.60 - 0.79	1.0
0.80 - 0.99	1.2
1.00 - 1.19	1.5
1.20 - 1.39	1.8
1.40 - 1.59	2.1
1.60 - 1.79	2.3
1.80 - 2.00	2.4

$C_{DL} = 1.1\ D_{SL} + 0.32$

Where: D_{SL} = Inner diameter of seal

Table 3-9. Conductance Parameter Multiplying Factors, C_H & C_F

M/C	C_H	f	C_F
.2 - .3	0.034	0 - 10	0.06
.3 - .4	0.14	10 - 19	0.17
.4 - .5	0.42	20 - 29	0.5
.5 - .6	1.0	30 - 39	1.0
.6 - .7	2.1	40 - 49	1.5
.7 - .8	3.8	50 - 59	2.1
.8 - .9	6.5	60 - 69	2.7
.9 - 1.0	10.5	70 - 79	3.4
1.0 - 1.2	19.7	80 - 89	4.2
1.2 - 1.4	40.4	90 - 100	5.2
1.4 - 1.6	74.8		
1.6 - 1.8	128.0		
1.8 - 2.0	206.6		
2.0 - 2.2	317.7		
2.2 - 2.4	469.8		
2.4 - 2.6	672.3		
2.6 - 2.8	936.1		

M = Meyer Hardness, psi
C = Contact Pressure, psi
f = Surface Finish, μin

$$C_F = \frac{f^{1.65}}{353}$$

$$C_H = \left(\frac{M/C}{0.55}\right)^{4.3}$$

Table 3-10. Fluid Viscosity/Temperature Multiplying Factor, C_υ for Typical Fluids

FLUID	FLUID TEMPERATURE, °F						
	-50	0	50	100	150	200	250
MIL-H-83282	0.6	0.7	0.8	0.9	1.0	2.0	3.0
MIL-H-5606	0.7	0.8	0.85	0.9	1.0	2.0	___
AIRCRAFT PHOSPHATE ESTERS	___	0.8	0.85	1.0	1.0	2.0	___
INDUSTRIAL PHOSPHATE ESTERS	___	___	0.7	0.8	0.85	0.9	___
WATER GLYCOL	___	0.7	0.8	0.8	0.9	___	___
SAE 10 OIL	___	___	0.7	0.8	1.0	1.0	2.0
SAE 60 OIL	___	___	___	0.7	0.8	0.85	1.0

$$C_\upsilon = (\upsilon_0/\upsilon)$$

Where: $\upsilon_0 = 2 \times 10^{-8}$ lb min/in^2

Table 3-11. Contaminant Multiplying Factor, C_N

TYPICAL QUANTITIES OF PARTICLES PRODUCED BY HYDRAULIC COMPONENTS	PARTICLE MATERIAL	NUMBER PARTICLES (mg) UNDER 10 MICRON PER HOUR PER GPM (N_{10})
Piston Pump	steel	1.7
Gear Pump	steel	1.9
Vane Pump	steel	0.6
Cylinder	steel	0.8
Sliding action valve	steel	0.04
Hose	rubber	0.13

$$C_N = \left(\frac{C_o}{C_{10}}\right)^3 N_{10} GPM_R$$

Where: GPM_R = Rated Flow in Gallons/Min
C_{10} = Standard System Filter Size = 10 micron
C_o = System Filter Size (microns)

Table 3-12. Temperature Multiplying Factor, C_T

$T_R - T_O$, °F	C_T
+20	.46
+10	.68
0	1.0
-10	1.47
-20	2.17
-30	3.17
-40	4.67
-50	6.86

$$C_T = \frac{1}{2^I}$$

$$I = \frac{(T_R - T_O)}{18}$$

Table 3-13. T_R Values for Typical Seal Materials (Ref. 27)

SEAL MATERIAL	T_R (°F)
NATURAL RUBBER	162
ETHYLENE PROPYLENE	248
NEOPRENE	48
NITRILE	262
POLYACRYLATE	298
FLUOROSILICONE	385
FLUOROCARBON	471
SILICON	471

Table 3-14. Coefficient of Friction for Various Seal Face Materials

SLIDING MATERIALS		COEFFICIENT OF FRICTION (μ)
ROTATING	STATIONARY	
CARBON-GRAPHITE (RESIN FILLED)	CAST IRON	0.07
	CERAMIC	0.07
	TUNGSTEN CARBIDE	0.07
	SILICON CARBIDE	0.02
	SILICON CARBIDE CONVERTED CARBON	0.015
SILICON CARBIDE	TUNGSTEN CARBIDE	0.02
	SILICON CARBIDE CONVERTED CARBON	0.05
	SILICON CARBIDE	0.02
	TUNGSTEN CARBIDE	0.08

Table 3-15. Pressure Gradient for Various Services

LIQUID SEALED	k
Light-specific-gravity fluids	0.3
Water-base solutions	0.5
Oil-base solutions	0.7

THIS PAGE INTENTIONALLY LEFT BLANK

CHAPTER 4

SPRINGS

4.1 INTRODUCTION

Springs are provided for many different applications such as compression, extension, torsion, power, and constant force. Depending on the application, a spring may be in a static, cyclic or dynamic operating mode. A spring is usually considered to be static if a change in deflection or load occurs only a few times, such as less than 10,000 cycles during the expected life of the spring. A static spring may remain loaded for very long periods of time. Cyclic springs are flexed repeatedly and can be expected to exhibit a higher failure rate due to fatigue. Dynamic loading refers to those occurrences of a load surge inducing higher than normal stresses on the spring.

4.2 FAILURE MODES

The operating life of a mechanical spring arrangement is dependent upon the susceptibility of the materials to corrosion and stress levels (static, cyclic or dynamic). The most common failure modes for springs are fracture due to fatigue and excessive loss of load due to stress relaxation. Table 4-1 is a list of failure mechanisms and causes of spring failure. Other failure mechanisms and causes may be identified for a specific application to assure that all considerations of reliability are included in the prediction. Typical failure rate considerations include: level of loading, operating temperature, cycling rate and corrosive environment.

If an S_{10} value for the spring can be obtained, this value should be used in conjunction with the environmental multiplying factors contained in this section. The procedure for estimating spring failure rates contained herein is intended to be used in the absence of specific data.

4.3 FAILURE RATE MODEL

The failure rate of a spring depends upon the stress on the spring and the relaxation provided by the material. The load on the spring is equal to the spring rate multiplied by the change in load per unit deflection and calculated as follows (Ref. 14):

$$P_L = \frac{G_M (D_W)^4 (L_1 - L_2)}{8 (D_C)^3 N_a} \quad (4\text{-}1)$$

Where:
- P_L = Load, lbs
- G_M = Modulus of rigidity, lbs/in^2
- D_W = Wire diameter, in
- L_1 = Free length of spring, in
- L_2 = Final deflection of spring, in
- D_C = Mean diameter of spring, in
- N_a = Number of active coils (See Section 4.3.5)

Stress in the spring will be proportional to loading according to the following relationship:

$$S_G = \frac{8 P_L D_C}{\pi (D_W)^3} K_W \quad (4\text{-}2)$$

Where:
- S_G = Spring stress
- K_W = Wahl factor

The Wahl factor, K_W, is a function of the spring index.

$$K_W = \frac{4r - 1}{4r - 4} + \frac{0.615}{r} \quad (4\text{-}3)$$

Where: r = Spring index = D_C/D_W

P_L in Equation 4-1 can be substituted into Equation 4-2. The ratio of spring stress to the tensile strength of the spring material will determine the reliability of the spring. A generalized equation that adjusts the base failure rate of a spring considering anticipated operating conditions can be established:

$$\lambda_{SP} = \lambda_{SP,B} \cdot C_G \cdot C_{DW} \cdot C_{DC} \cdot C_M \cdot C_Y \cdot C_L \cdot C_K \cdot C_{CS} \quad (4\text{-}4)$$

Where:

λ_{SP} = Failure rate of spring, failures/million cycles

$\lambda_{SP,B}$ = Base failure rate for spring, failures/million cycles, 0.65 failures/million cycles

C_G = Multiplying factor which considers the effect of the material rigidity modulus on the base failure rate. See Table 4-2

C_{DW} = Multiplying factor which considers the effect of the wire diameter on the base failure rate. See Table 4-3

C_{DC} = Multiplying factor which considers the effect of coil diameter on the base failure rate. See Table 4-3

C_N = Multiplying factor which considers the effect of the number of active coils on the base failure rate. See Table 4-3

C_Y = Multiplying factor which considers the effect of material tensile strength on the base failure rate. See Table 4-4

C_L = Multiplying factor which considers the effect of spring deflection on the base failure rate. See Table 4-5

C_K = Multiplying factor which includes the spring concentration factor and the Wahl factor. See below and Table 4-6

C_{CS} = Multiplying factor which considers the effect of spring cycle rate on the base failure rate. See below.

C_K, the spring stress concentration factor, is a function of the Wahl factor, K_w which is a function of the spring index. Values for C_K are provided in Table 4-6 in terms of the spring index.

C_{CS}, the spring cycle rate factor, has been initially derived from data given by (Ref.12). If the cycle rate is less than 300 cycles per minute, C_{CS} is 1.0. If the cycle rate is between 300 and 360 cycles per minute, C_{CS} is 6.0. For rates above 360 cycles per minute, C_{CS} is estimated to be 12.0.

The parameters in the failure rate equation can be located on an engineering drawing by knowledge of design standards or by actual measurement. Other manufacturing, quality, and maintenance contributions to failure rate are included in the base failure rate as determined from field performance data. The following paragraphs provide background information on those parameters included in Equation (4-4).

4.3.1 Static Springs

Static springs can be used in constant deflection or constant load applications. A constant deflection spring is cycled through a specified deflection range, the loads on the spring causing some set or relaxation which in turn lowers the applied stress. The spring may relax with time and reduce the applied load. Under constant load conditions, the load applied to the spring does not change during operation. Constant load springs may set or creep, but the applied stress is constant. The constant stress may result in fatigue lives shorter than those found in constant deflection applications. The failure rate model included in this section was derived for cyclic springs. The base failure rate can be used as an approximate value for static springs.

4.3.2 Cyclic Springs

Cyclic springs can be classified as being unidirectional or reverse loaded. In one case, the stress is always applied in the same direction, while in the other, stress is applied first in one direction then in the opposite direction.

4.3.3 Modulus of Rigidity

The modulus of rigidity provides a measure of elasticity in shear for the spring material. Values are provided in Table 4-2.

4.3.4 Spring Index

Spring index (r) is the ratio of mean coil diameter to wire diameter. A spring with a high index will tend to tangle or buckle. Modification factors for spring coil diameter and wire diameter are provided in Table 4-3.

4.3.5 Number of Active Coils

The number of active coils is usually two less than the total number of coils. There is some activity in the end coils, but during deflection, some active material comes in contact with the end coils and becomes inactive. Therefore, the total number of coils minus two is a good approximation for the number of active coils. Modification factors for the number of coils are provided in Table 4-3.

4.3.6 Tensile Strength

The tensile strength provides a measure of spring material deformation or set as a function of stress. Values of tensile strength are included in Table 4-4.

4.3.7 Shaped Springs

If the spring has a variable diameter such as occurs for conical, barrel and hourglass springs, the spring can be divided analytically into smaller increments and the failure rate calculated for each. The failure rate for the total spring is computed by adding the rates for the increments.

4.3.8 Corrosion

The reliability of a spring in terms of fatigue life and load-carrying ability will be affected by corrosion, the quantitative effect being very hard to predict. Springs are almost always in contact with other metal parts. If a spring is to be subjected to a corrosive environment, the use of inert materials provides the best defense against corrosion. Protective coatings can also be applied. The spring material is normally more noble (chemically resistant to corrosion) than the structural components in contact with it because the lesser noble alloy will be attacked by the electrolyte. The effects of corrosion on spring reliability are included in the base failure rate. This rate may have to be adjusted based on experience data considering the extent of a corrosive environment.

4.3.9 Other Reliability Considerations for Springs

The most common failure modes of springs include fracture due to fatigue and excessive loss of load. A reliability analysis should include a review of the following items to assure maximum, possible life.

- Sharp corners and similar stress risers should be minimized.
- The hardness of the spring material can be sensitive to plating and baking operations. Quality control procedures for these operations should be reviewed.
- When a spring is loaded or unloaded, a surge wave may transmit torsional stress to the point of restraint. The impact velocity should be determined to assure that the maximum load rating of the spring is not exceeded.
- Operating temperature should be determined. Both high and low temperature conditions may require consideration of specialized materials.
- Exposure to electrical fields which may magnetize the spring material.

Table 4-1. Failure Rate Considerations for a Spring

APPLICATION	FAILURE MODES	FAILURE MECHANISMS	FAILURE CAUSES
- Static (constant deflection or constant load)	- Load loss - Creep - Set	- Stress relaxation - Fracture	- Parameter change - Hydrogen embrittlement
- Cyclic * (unidirectional or reverse stress)	- Fracture	- Fatigue	- Material flaws - Hydrogen embrittlement - Stress concentration due to tooling marks and rough finishes - Corrosion - Misalignment

* 10,000 cycles or more during life of spring

Table 4-2. Modulus of Rigidity Multiplying Factor, C_G

MATERIAL	MODULUS OF RIGIDITY, psi x 10^6 (G_M)	C_G
Carbon Steel	11.5	1.00
Alloy Steel	11.5	1.00
Stainless Steel	10.0 - 11.0	0.78
Copper Base Alloy	5.7 - 7.0	0.17
Nickel Base Alloy	9.7 - 11.5	0.73

$$C_G = \left(\frac{G_M}{11.5}\right)^3$$

Table 4-3. Multiplying Factor for Wire Diameter, Coil Diameter and Number of Coils

Wire Dia. D_w, in	C_{DW}	Coil Dia. D_C, in	C_{DC}	# Active Coils N_a	C_M
.046 - .049	0.20	.30 - .39	20.70	6	12.70
.050 - .059	0.27	.50 - .64	1.00	8	5.36
.060 - .069	0.45	.65 - .79	0.27	10	2.74
.070 - .079	0.69	.80 - .99	0.07	12	1.59
.080 - .089	1.00			14	1.00
.090 - .099	1.40			18	0.47
.110 - .119	2.48			20	0.34
.120 - .129	3.18			22	0.26
.130 - .139	4.00				
.140 - .150	5.00				

$$C_{DW} = \left(\frac{D_w}{0.085}\right)^3 \qquad C_{DC} = \left(\frac{0.58}{D_c}\right)^6 \qquad C_M = \left(\frac{14}{N_a}\right)^3$$

Table 4-4. Material Tensile Strength Modification Factor, C_y

MATERIAL	TENSILE STRENGTH (T_s), 10^3 psi	C_y
Brass	90	9.40
Phosphor Bronze	100	6.86
Monel 400	100	6.86
Inconel 600	150	2.03
Monel K500	175	1.28
Copper-Beryllium	190	1.00
Stainless Steel 301, 302	190	1.00
17-7 PH RH 950	210	0.90
Spring Temper Steel	245	0.47

$$C_y = \left(\frac{190}{T_s}\right)^3$$

Table 4-5. Spring Deflection Modification Factor, C_L

$L_1 - L_2$, in	C_L
0.30 - 0.39	0.03
0.40 - 0.54	0.08
0.55 - 0.69	0.19
0.70 - 0.89	0.42
0.90 - 1.09	0.82
1.10 - 1.34	1.00
1.35 - 1.49	2.34
1.60 - 1.89	4.37
1.90 - 2.19	7.03

$$C_L = \left(\frac{D_L}{1.07}\right)^3$$

Table 4-6. Stress Concentration Modification Factor, C_K

r	K_w	C_K
4	1.40	1.527
5	1.31	1.242
6	1.25	1.095
7	1.21	0.985
8	1.18	0.916
9	1.16	0.866
10	1.14	0.828
11	1.13	0.798
12	1.12	0.774
13	1.11	0.755
14	1.10	0.738
15	1.09	0.724
16	1.09	0.719

$$C_K = \left(\frac{K_w}{1.219}\right)^3$$, where K_w is defined in Equation (4-3)

CHAPTER 5

SOLENOIDS

5.1 INTRODUCTION

The primary failure modes of a solenoid coil assembly include one or more winding shorts or an open coil usually caused by overheating. The maximum specified cycling rate of the solenoid should be determined and compared with the potential operating rate to make sure the coil will not be overheated in its operating environment.

Clearance between the coil assembly and the armature assembly must be maintained for proper operation and the design should be evaluated for reliability considering the operating environment.

The failure rate of the solenoid assembly is more dependent upon manufacturing defects associated with the assembly of the coil in relation to the armature than it is upon operating environment. Therefore, a base failure rate based on field experience data can be used as an estimate of the failure rate for a solenoid in its operating environment:

$$\lambda_{SO} = \lambda_{SO,B} \qquad (5\text{-}1)$$

Where: λ_{SO} = Failure rate of a solenoid in failures/million cycles

$\lambda_{SO,B}$ = Base failure rate of solenoid, 3.00 failures/million cycles

THIS PAGE INTENTIONALLY LEFT BLANK

CHAPTER 6

VALVE ASSEMBLIES

6.1 INTRODUCTION

This section contains failure rate models for fluid valve assemblies which can be used to support the development of mechanical equipment and provide a reliability estimate for a new design or a proposed design modification. The models are intended to focus attention on further design analyses which should be accomplished to assure the allocated reliability of the valve in its intended operating environment.

Failure rate models included in this section are based upon identified failure modes of the individual parts. A listing of failure modes and their failure causes and effects is provided in Table 6-1.

A typical valve assembly is shown in Figure 6-1. After the failure rates are determined for each component part, the results are summed to determine the failure rate of the total valve assembly:

$$\lambda_{VA} = \lambda_{PO} + \lambda_{SE} + \lambda_{SP} + \lambda_{SO} + \lambda_{HO} \qquad (6\text{-}1)$$

for a poppet type valve, or

$$\lambda_{VA} = \lambda_{SV} + \lambda_{SE} + \lambda_{SP} + \lambda_{SO} + \lambda_{HO} \qquad (6\text{-}2)$$

for a sliding-action valve.

Where:

λ_{VA} = Failure rate of total valve assembly in failures/million operations

λ_{PO} = Failure rate of poppet assembly in failures/million operations as derived from Section 6.3

λ_{SV} = Failure rate of sliding action valve assembly in failures/million operations as derived from Section 6.4

λ_{SE} = Failure rate of the seals in failures/million operations as derived from Chapter 3

λ_{SP} = Failure rate of spring(s) in failures/million operations as derived from Chapter 4

λ_{SO} = Failure rate of solenoid in failures/million operations as derived from Chapter 5

λ_{HO} = Failure rate of valve housing as derived from Section 6.5

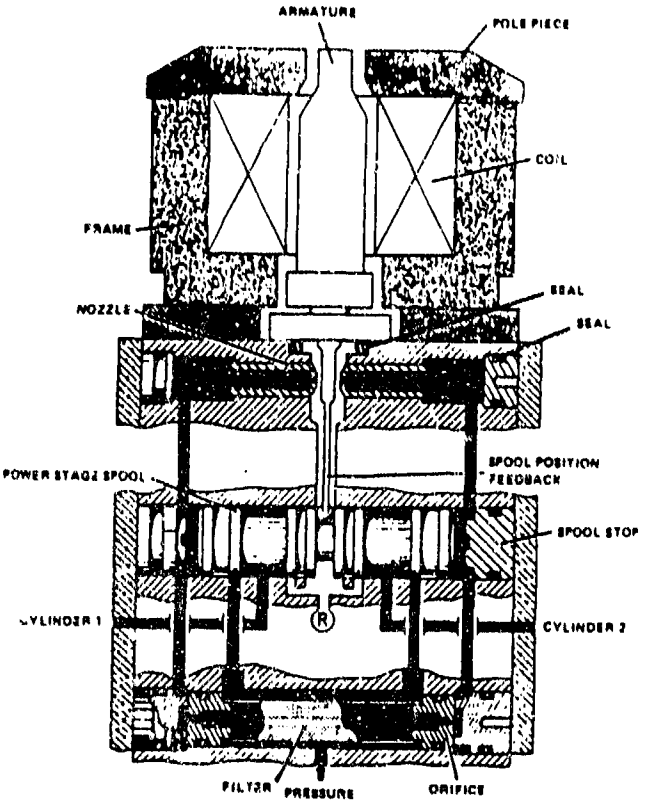

Figure 6-1. Typical Valve Configuration

6.2 FAILURE MODES OF VALVE ASSEMBLIES

Failure rate models included in this section are based upon the identification of failure modes. Appropriate models to predict the rate of occurrence for each component part are used as applicable and then the failure rates of all component parts are added together to determine the component failure rate. The models can also be used to determine the probability of occurrence of a particular failure mode. Many valve assemblies are uniquely designed for special applications and a more detailed analysis is often required for those failure modes identified as critical or where results of the analysis indicate that an additional investigation is warranted.

Typical failure modes for a valve assembly are listed in Table 6-1. It should be noted that the failure modes, failure causes and failure effects may be interchanged depending upon the type of analysis being performed. For example, a functional analysis will tend to identify those entries in Table 6-1 under local effects as the failure mode while a very detailed hardware analysis would result in the identification of those entries under failure cause as the failure mode.

Table 6-1. Failure Modes of a Valve Assembly

Failure Mode	Failure Cause	Local Effect
Seal leakage	Embrittlement, installation damage, wear, surface damage, distortion, dynamic instability	Internal or external valve leakage
Worn or damaged poppet seat	Wear of poppet/seat assembly, contaminants	Poppet not seating properly causing internal leakage and low/erratic pressure drop.
Worn or damaged spool	Contaminants, misalignment	Internal leakage
Sticking valve piston in main valve body	Contaminants, loss of lubrication, air entrapment; excessively high temperature; structural interference	Low/erratic pressure drop;slow operating response, valve immobile
Broken spring or damaged spring ends	Fatigue	Unable to adjust/maintain pressure
Inoperative solenoid assembly	Open coil winding, misalignment of solenoid with respect to spool or poppet stem	Valve fails to open or close
External leakage	Poppet Stem Wear	Contaminants
Cracked connector/housing	Fatigue, external shock, vibration	External leakage

6.3 FAILURE RATE MODEL FOR POPPET ASSEMBLY

The term poppet refers to those valves in which the valve element travels perpendicular to a plane through the seating surface. The poppet valve element is used in flow control, pressure control and directional control valves. In a poppet valve, a relatively large flow area is provided with short travel of the poppet. This characteristic simplifies the actuator requirements and permits the use of solenoids and diaphragms, which are characteristically short stroke devices.

Figure 6.2 illustrates the operation of a simple poppet valve. The valve consists primarily of a movable poppet which closes against a valve seat. In the closed position, fluid pressure on the inlet side tends to hold the valve tightly closed. A force applied to the top of the valve stem opens the poppet and allows fluid to flow through the valve.

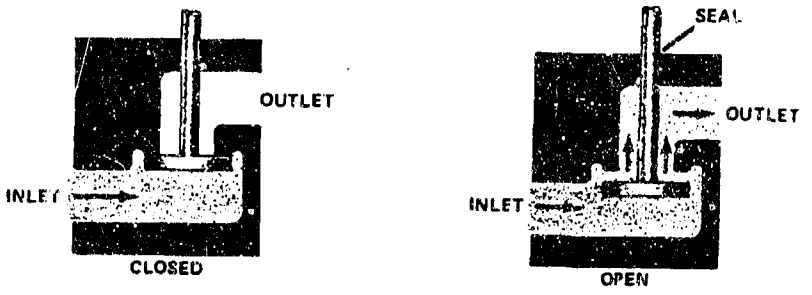

Figure 6-2. Poppet Valve Assembly

The poppet fits into the center bore of the seat. The seating surfaces of the poppet and the seat are lapped or closely machined so that the center bore will be sealed when the poppet is seated. An O-ring is usually installed on the stem of the poppet to prevent leakage past this portion of the poppet assembly.

Table 6-2 is a list of typical failure modes, mechanisms and causes for a poppet assembly. A review of failure rate data suggests the following characteristics be included in the failure rate model for poppet assemblies:

- Leakage requirement
- Material hardness
- Surface irregularities

- Fluid viscosity
- Fluid/material compatibility
- Fluid pressure
- Physical size of poppet/seat
- Q.C./manufacturing processes
- Contamination level
- Utilization rate

Table 6-2. Failure Rate Considerations for Poppet Assembly

FAILURE MODE	FAILURE MECHANISMS	FAILURE CAUSES
- Internal Leakage	- Worn poppet/seat	- Contaminants
- Poor Response	- Sticking/jammed poppet assembly	- Side Loading - Incorrect spring pressure - Contaminants
- External Leakage	- Wear of poppet stem	- Contaminants

A new poppet assembly may be expected to have a sufficiently smooth surface finish for the valve to meet internal leakage specifications. However, after some period of time contaminants will cause wear of the poppet/seat assembly until leakage rate is beyond tolerance. This leakage rate at which point the valve is considered to have failed will depend upon the application.

A failure rate equation for a poppet assembly is dependent upon the ratio of actual leakage rate to that allowable under conditions of usage. This rate can be expressed as follows:

$$\lambda_{PO} = \lambda_{PO,B} \frac{Q_a}{Q_f} \qquad (6\text{-}3)$$

Where: λ_{PO} = Failure rate of the poppet assembly, failures/million operations
$\lambda_{PO,B}$ = Base failure rate for poppet assembly, failure/million operations
Q_a = Leakage rate, in^3/min
Q_f = Leakage rate considered to be valve failure, in^3/min

The allowable leakage, Q_f, is determined from design drawings, specifications or knowledge of component applications. The actual leakage rate, Q_a, is determined from the following equation (Ref.5):

$$Q_a = \frac{2 \times 10^4 \, D_{MS} \, f^3 \, (P_1^2 - P_2^2)}{\nu_a \, L_W \, (S_s)^{3/2}} \qquad (6\text{-}4)$$

Where:
- Q_a = Actual fluid leakage, in^3/min
- D_{MS} = Mean seat diameter, in
- f = Mean surface finish of opposing surfaces, min
- P_1 = Upstream pressure, lb/in^2
- P_2 = Downstream pressure, lb/in^2
- ν_a = Absolute fluid viscosity, $lb\text{-}min/in^2$
- L_W = Radial seat land width, in.
- S_s = Apparent seat stress, lb/in^2

Failure rate of the poppet assembly will be dependent upon leakage rate and those factors which influence the deterioration of surface finish such as rate of cycling, material properties and contaminants. Deterioration of the poppet and seat by contaminants is dependent upon material properties and the number of contaminants.

A contamination factor can be derived from the following equation:

$$Z = f(\alpha, n, Q, d, T) \qquad (6\text{-}5)$$

Where:
- Z = Poppet/seat degradation
- α = Contaminant wear coefficient $(in^3/particle)^2$
- n = number of contaminant particles/in^3
- Q = Flow rate, in^3/min
- d = Ratio of time the poppet is open and subject to contaminants under pressure
- T = Temperature of Operation, °F

Table 6-8 provides typical quantities of contaminants for use in establishing a multiplying factor. By normalizing the equation to those values for which historical failure rate data are available the following model can be derived:

$$\lambda_{PO} = \lambda_{PO,B} \cdot C_P \cdot C_Q \cdot C_F \cdot C_v \cdot C_N \cdot C_S \cdot C_{DT} \cdot C_{SW} \cdot C_W \quad (6\text{-}6)$$

Where:
- λ_{PO} = Failure rate of poppet assembly in failures/million operations
- $\lambda_{PO,B}$ = Base failure rate of poppet assembly, 1.40 failures/million operations
- C_P = Multiplying factor which considers the effect of fluid pressure on the base failure rate (See Table 6-4)
- C_Q = Multiplying factor which considers the effect of allowable leakage on the base failure rate (See Table 6-5)
- C_F = Multiplying factor which considers the effect of surface finish on the base failure rate (See Table 6-6)
- C_v = Multiplying factor which considers the effect of fluid viscosity/temperature on the base failure rate (See Table 6-7)
- C_N = Multiplying factor which considers the effect of contaminants on the base failure rate (See Table 6-8)
- C_S = Multiplying factor which considers the effect of the apparent seat stress on the base failure rate (See Table 6-9)
- C_{DT} = Multiplying factor which considers the effect of the seat diameter on the base failure rate (See Table 6-10)
- C_{SW} = Multiplying factor which considers the effect of the seat land width on the base failure rate (See Table 6-10)
- C_W = Multiplying factor which considers the effect of flow rate on the base failure rate (See Equation 6-7)

$$C_W = 1 + \left[\frac{F_L}{100}\right]^2 \quad (6\text{-}7)$$

Where:
- F_L = Ratio of actual flow rate to manufacturer's rating

The following paragraphs provide background information on those parameters included in the model.

6.3.1 Fluid Pressure

Table 6-4 contains the fluid pressure multiplying factors for use in the model. Valves having high response characteristics and consequently a high poppet velocity will incur large seat stresses which tend to reduce the life expectancy of the valve. As with any piece of mechanical equipment, the higher the structural loads the shorter the life. Pressure forces arise from any net pressure unbalance acting on the valve element. Depending upon the functional design of the valve, the pressure force may increase, decrease, or virtually have no effect on the actuation force. In an unbalanced valve design such as a conventional poppet, upstream pressure normally acts in a direction to seat the valve so that an increasing upstream pressure will tend to force the valve element tighter against its seat. The use of pressure unbalance to aid in sealing requires a higher actuation force to open the valve. When the size of the valve and the magnitude of pressure demand excessively large actuation forces, a balanced design and/or piloting is often utilized. In most cases the pressure on the poppet, P_s, can be assumed to be the system upstream pressure, P_1, minus the downstream pressure, P_2.

6.3.2 Allowable Leakage

Table 6-5 contains the allowable leakage multiplying factor for use in the model. Allowable internal leakage of a poppet design can be obtained from valve specifications. Leakage requirements vary from molecular flow for certain shutoff valves at one extreme to several cubic feet per minute in some inexpensive valves which control water or other inexpensive fluid. Allowable leakage must be evaluated with respect to total mission and operational requirements.

6.3.3 Contamination Sensitivity

Cleanliness of the system and of the fluid medium has a direct effect upon the operation and life of a poppet valve. Contaminants can clog or jam the poppet and cause excessive leakage in metal-to-metal seated valves. Particulate matter in gaseous media, especially in the lighter gases such as helium, can be extremely destructive to internal parts, particularly seats, because of the very high velocity that can be attained under sonic conditions.

The analysis of particle sizes includes the determination of

upstream filter size, the filter maintenance schedule, the number of upstream components between the valve and filter, and the number of particles likely to be encountered at the poppet/seat assembly. Table 6-8 lists typical quantities of contaminants for use in determining the multiplying factor.

6.3.4 Surface Finish

Evaluation of surface finish involves both poppet and seat assemblies. Surface finishes will usually be specified on assembly drawings in terms of microinches or by manufacturing process. Typical surface finishes for manufacturing processes are provided in Table 6-6. These values are for a finish as initially manufactured and a new valve can be expected to have a sufficiently smooth surface finish to meet internal leakage specifications. However, after some period of time contaminants will cause wear of the poppet/seat assembly until leakage rate is beyond tolerance. This deterioration of surface finish will be influenced by operating temperature and pressure, rate of cycling, loads and material properties.

6.3.5 Fluid Viscosity

Fluid viscosities for typical fluids are provided in Table 6-7. Viscosities for other fluids at the operating temperature can be found in reference sources.

6.3.6 Apparent Seat Stress

The apparent seat stress is found by actual measurement or design specifications. The apparent seat stress can be calculated by:

$$A_{ST} = \frac{\pi (D_s)^2}{4} \qquad (6\text{-}8)$$

Where: A_{ST} = Seat Area, in^2
D_s = Diameter of seat exposed to fluid pressure P_s, in

Therefore, the force on the seat holding it closed is:

$$F_s = \frac{\pi P_s D_s^2}{4} \qquad (6\text{-}9)$$

The seat area acting as a seal when the valve is closed is calculated by:

$$A_{SL} = \pi D_M \cdot L_W \qquad (6\text{-}10)$$

Where: A_{SL} = Seat land area, in^2
L_W = Land area width, in
D_M = Mean land width diameter, in

Then the expression for the apparent seat stress S_s becomes:

$$S_s = \frac{\text{Force on Seat}}{\text{Seat Land Area}} = \frac{F_s}{A_{SL}} \qquad (6\text{-}11)$$

Therefore:

$$S_s = \frac{P_s D_s^2}{4 D_M L_W} \qquad (6\text{-}12)$$

The minimum contact stress to prevent leakage for most materials is approximately three times the fluid pressure.

Therefore, Minimum Contact Pressure = $S_c = 3P_s$ (6-13)

A ratio of minimum contact pressure and the apparent seat stress can be used as an expression for the stress on a valve to cause leakage:

$$\text{Stress Ratio} = S_c/S_s = S_R \qquad (6\text{-}14)$$

In Equation (6-4), leakage varies with the seat stress as:

$$\left(\frac{1}{S}\right)^{3/2}$$

Therefore, a multiplying factor for the effect of seat stress on the valve base failure rate can be expressed:

$$C_s = \frac{1}{S_R^{1.5}} \qquad (6\text{-}15)$$

Where:

$$S_R = \frac{12\pi D_M L_w}{D_s^2} \qquad (6\text{-}16)$$

Table 6-9 lists the multiplying factors for different values of seat stress.

6.3.7 Poppet Size

The seat diameter, D_s, is approximately equal to the inside diameter of the connecting pipe or tubing and this dimension as well as the land width of the seat, L_w, can be obtained or estimated from engineering drawings. Table 6-10 lists the multiplying factors for seat diameter and land width.

6.3.8 Operating Temperature

The duty cycle of a poppet valve can vary from several on-off cycles to many hundreds of cycles per hour. Multiple cycling under high pressure or operating temperature decreases the life of the valve. The rate of cycling may be important if the temperature rise, as a result of the operation, becomes significant. The effects of fluid temperature on failure rate are included in the fluid viscosity multiplying factor, C_v.

6.3.9 Other Considerations

Several failure rate considerations are not specifically included in the model but rather included in the base failure rate. The base failure rate is an average value which reflects field performance data. The following items can be used as a check list to assure that the potential failure mechanisms have been considered:

- Fluid medium considerations which are important in valve designs include the physical properties of the fluid and the compatibility of the fluid with poppet/seat materials. Corrosive

fluids will rapidly change the surface finish. The state and physical properties of the fluid become particularly important in determining pressure drop and flow capacity.

• In considering maintenance, requirements for special tasks must be identified. Valve seats should be accessible and easily replaced, preferably without removing the valve from its circuit. When it is necessary to service a valve in the field, care must be exercised to insure that contamination from the work area is not introduced into the valve or system. Requirements for lubrication and adjustments should be minimized to provide high reliability in service use.

• While critical design features are usually based upon one primary fluid, consideration must also be given to secondary fluids with which the valving unit will be required to operate during cleaning and testing operations.

6.4 FAILURE RATE MODEL FOR SLIDING ACTION VALVES

Sliding action valves consist of a movable spool (a piston with more than one land) within a cylinder. Sliding action valves are usually designed such that the spool slides longitudinally to block and uncover ports in the housing. A rotary spool is sometimes used. Fluid under pressure which enters the inlet port acts equally on both piston areas regardless of the position of the spool. Sealing is accomplished by a very closely machined fit between the spool and the valve body. In sleeve valves the solid piston or spool is replaced by a hollow cylinder with either the inner or outer cylinder serving as the valve element. A typical sliding action valve is shown in Figure 6-3.

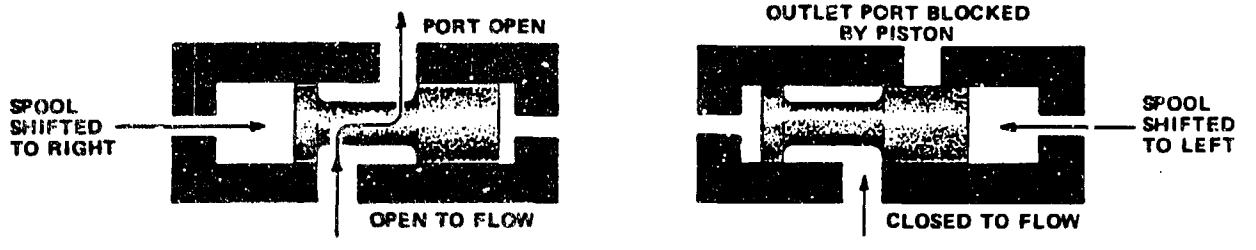

Figure 6-3. Sliding Action Valve Assembly

The great majority of sliding action valves utilize axial motion of the valving element, although some designs for special applications use rotating pistons or sleeves. A primary advantage

of sliding action valves is the feasibility of obtaining a pressure-balanced design, especially with sleeve or spool configurations. An inherent disadvantage of sliding action valves is leakage, a problem which can only be controlled by close machining or reliable dynamic sealing techniques. Spool valves, for example, are widely used in fluid power applications where perfect internal sealing is not required.

Diametrical spool clearances of approximately 50 microinches are common and surface finishes of 4 to 6 microinches rms are standard requirements for spools and sleeves. Therefore, contamination tolerance and dirt sensitivity are critical factors in the design and use of sliding action valves, and reliability will be directly affected by dirt particles. Force balances, flow rate and general mechanical operation can be influenced by the presence of contaminants within the valve. Contamination problems include wear of the spool and sleeve until the leakage rate is beyond tolerance. The steps to investigating internal leakage are the same as for the poppet type valve. Table 6-3 is a list of failure modes, mechanisms and causes for spool assemblies. Other failure modes should be identified for the specific application and evaluated to determine the applicability of the failure rate model to the analysis being performed.

Table 6-3. Failure Rate Considerations For Sliding Action Valve

FAILURE MODE	FAILURE MECHANISMS	FAILURE CAUSES
- Internal leakage	- Worn spool/sleeve	- Contaminant side loading
- Poor response	- Sticking sleeve assembly	- Incorrect spring pressure/contaminants
- Fails to open	- Jammed sleeve assembly	- Excessive side loading/contaminants

An equation similar to that for poppet valves can be used to predict the reliability of a sliding action valve:

$$\lambda_{SV} = \frac{\lambda_{SV,B}\, B^2\, D_{SP}\, (P_1^2 - P_2^2)^{1/2}\, \mu\, \alpha\, n}{Q_f\, \nu_a} \qquad (6\text{-}17)$$

Where:
- λ_{SV} = Failure rate of sliding action valve assembly in failures/million operations
- $\lambda_{SV,B}$ = Base failure rate = 1.25 failures/million operations
- B = Spool clearance, in
- D_{SP} = Spool diameter, in
- P_1 = Upstream pressure, lb/in^2
- P_2 = Downstream pressure, lb/in^2
- ν_a = Absolute fluid viscosity, lb-min/in^2
- Q_f = Leakage rate considered to be device failure, in^3/min
- μ = Friction coefficient
- α = Contaminant wear coefficient, in^3/particle
- n = Number of contaminant particles/in^3

By normalizing the characteristic equation to those values for which historical failure rate data are available, the following model can be derived:

$$\lambda_{SV} = \lambda_{SV,B} \cdot C_P \cdot C_Q \cdot C_\nu \cdot C_N \cdot C_B \cdot C_{DS} \cdot C_\mu \cdot C_W \qquad (6\text{-}18)$$

Where:
- C_P = Multiplying factor which considers the effect of fluid pressure on the base failure rate. See Table 6-4
- C_Q = Multiplying factor which considers the effect of allowable leakage on the base failure rate. See Table 6-5
- C_ν = Multiplying factor which considers the effect of fluid viscosity/temperature on the base failure rate. See Table 6-7
- C_N = Multiplying factor which considers the effect of fluid contaminants on the base failure rate. See Table 6-8.
- C_B = Multiplying factor which considers the effect of spool clearance on the base failure rate. See Table 6-11

C_{DS} = Multiplying factor which considers the effect of spool diameter on the base failure rate. See Table 6-11

C_{μ} = Multiplying factor which considers the effect of friction coefficient on the base failure rate. See Table 6-12

C_{W} = Multiplying factor which considers the effect of flow rate on the base failure rate. See Equation (6-7)

6.4.1 Fluid Pressure

In most sliding action valves the applied fluid pressure is the upstream pressure minus the downstream pressure. Table 6-4 provides the multiplying factors for fluid pressure. Other factors in evaluating the effects of fluid pressure on valve reliability include the following:

Size - Structural strength becomes an increasingly important consideration with increasing valve size because pressure loads are a function of the square of the valve size.

Balance - If the valve is inherently pressure-balanced, the influence of pressure upon such parameters as size and actuation forces will be far less than in the case of an inherently unbalanced unit.

Pressure Induced Strain - Binding of certain close-tolerance sliding action valves can result with excessive pressure load on a port.

Conditions of Pressure - Circumstances under which the valve unit is subjected to high pressure must be considered. A drain valve, for example, may be required to seal against high pressure, but never be required to open until after the pressure has been relieved.

6.4.2 Allowable Leakage

Allowable internal leakage of the sliding action valve can be obtained from valve specifications usually in terms of quiescent flow or leakage flow. Quiescent flow is the internal valve flow or leakage from supply-to-return with no flow in the load ports. Allowable leakage will vary considerably according to the operational requirements. Table 6-5 provides the multiplying

factors for allowable leakage.

6.4.3 Contamination Sensitivity

Cleanliness of the fluid medium and surrounding medium has a direct effect upon the occurrence of stiction, weldment and general operation of sliding valve assemblies. No fluid system is completely free of particulate contamination and sensitivity of a valve to contamination is an important consideration in reliability.

In sliding action valves there is a tradeoff between contamination sensitivity and leakage based on clearances between the spool and sleeve. If leakage is minimized by reducing the clearance between the valving element and its housing, a larger number of contaminant particles can become lodged, causing valve failure. The clearance values should be checked at both of the temperature extremes to which the valve will be subjected, in order to ensure adequate design for the largest size of contamination particle anticipated.

The analysis of particle sizes includes the determination of upstream filter sizes, the filter maintenance schedule, the number of upstream components between the valve and filter, and the number of particles likely to be encountered at the spool assembly. Table 6-8 provides typical quantities of contaminants for use in the failure rate equation.

6.4.4 Fluid Viscosity

Viscosities for typical fluids are provided in Table 6-7. Multiplying factors for other fluids are determined from the table by a knowledge of viscosity at the applicable fluid temperature. Viscosity for a specific fluid is obtainable from many reference sources.

6.4.5 Spool-to-Sleeve Clearance

Highly polished and uniform surface finishes of 4-6 microinches can usually be assumed for a valve spool. The model assumes that the spool is environmentally protected. If this is not the case, a separate analysis will be required to determine the effects of aging and deterioration of the surfaces on the spool to sleeve clearance. A diametrical spool clearance of 50 microinches is typical for sliding action valves. The exact value is taken from assembly drawings. Table 6-11 provides the multiplying factors for spool diameter and the spool-to-sleeve clearance.

6.4.6 Friction Coefficient

A sticking valve spool is usually caused by contaminants. Particles can accumulate between the spool and sleeve as part of the silting process until the build-up is sufficient to cause stiction. Results include valve hunting, erratic regulation and eventual locking. The silting process can be aggravated by inactivity of the valve. Another failure mechanism to be considered is reduced clearance between the spool and sleeve caused by soft metal particles being wedged and burnished on the surfaces. Table 6-12 contains friction coefficients for typical materials used in valve designs. The actual friction coefficient is used in the model. Friction coefficients can be located in text books and other reference material.

6.5 FAILURE RATE ESTIMATE FOR HOUSING ASSEMBLY

There are many factors which could be considered in determining the potential rate of fatigue failure of a valve housing including connectors. For critical safety related applications, a review of the stress analysis is warranted. Normally, the probability of a cracked housing is minimal and the failure rate is best determined from field experience data.

$$\lambda_{HO} = \lambda_{HO,B} \qquad (6\text{-}19)$$

Where: λ_{HO} = Failure rate of valve housing, failures/million operating hours

$\lambda_{HO,B}$ = Base failure rate of housing, 0.10 failures/million operations

Table 6-4. Fluid Pressure Multiplying Factor

FLUID PRESSURE, psi	C_p
0 - 500	0.01
501 - 1500	0.11
1501 - 2500	0.44
2501 - 3500	1.00
3501 - 4500	1.80
4501 - 5500	2.80
5501 - 6500	4.00
6501 - 7500	5.44
7501 - 8500	7.11

$$C_p = \left(\frac{P_1 - P_2}{3000}\right)^2$$

Table 6-5. Allowable Leakage Multiplying Factor

ALLOWABLE LEAKAGE (Q_f) $INCHES^3/MINUTE$ per Max Rated GPM	C_Q
.005 - .009	3.5
.010 - .014	3.2
.015 - .019	2.8
.020 - .024	2.4
.025 - .029	2.0
.030 - .039	1.6
.040 - .049	1.3
.050 - .059	1.0
.060 - .079	0.8
.080 - .100	0.6

For Leakage (Per GPM_R) > 0.03, $C_Q = 0.055/Q_f$

For Leakage (Per GPM_R) $\leq$ 0.03, $C_Q = 4.1 - (79\ Q_f)$

Table 6-6. Surface Finish Multiplying Factor, C_F

SURFACE FINISH, f, μin	C_F
0 - 10	0.06
10 - 19	0.17
20 - 29	0.05
30 - 39	1.0
40 - 49	1.5
50 - 59	2.1
60 - 69	2.7
70 - 79	3.4
80 - 89	4.2
90 - 99	5.2

$$C_F = \frac{f^{1.65}}{353}$$

Table 6-7. Fluid Viscosity, Temperature Multiplying Factor

FLUID	FLUID TEMPERATURE, °F						
	-50	0	50	100	150	200	250
MIL-H-83282	0.6	0.7	0.8	0.9	1.0	2.0	3.0
MIL-H-5606	0.7	0.8	0.85	0.9	1.0	2.0	___
AIRCRAFT PHOSPHATE ESTERS	___	0.8	0.85	1.0	1.0	2.0	___
INDUSTRIAL PHOSPHATE ESTERS	___	___	0.7	0.8	0.85	0.9	___
WATER GLYCOL	___	0.7	0.8	0.8	0.9	___	___
SAE 10 OIL	___	___	0.7	0.8	1.0	1.0	2.0
SAE 60 OIL	___	___	___	0.7	0.8	0.85	1.0

$$C_\nu = \left(\frac{\nu_o}{\nu}\right)$$

Where: $\nu_0 = 2 \times 10^{-8}$ lb min/in^2

Table 6-8. Contaminant Multiplying Factor, C_N

HYDRAULIC COMPONENT PRODUCING PARTICLES	PARTICLE MATERIAL	NUMBER PARTICLES UNDER 10 MICRON PER HOUR PER GPM (N_{10})
Piston Pump	steel	1.7
Gear Pump	steel	1.9
Vane Pump	steel	0.6
Cylinder	steel	0.8
Sliding action valve	steel	0.04
Hose	rubber	0.13

$$C_N = \left(\frac{C_o}{C_{10}}\right)^3 N_{10}\, GPM_R$$

Where: GPM_R = Rated Flow in gallons/min
C_{10} = Standard System Filter Size = 10 micron
C_o = System Filter Size in microns

Table 6-9. Seat Stress Multiplying Factor, C_S

Seat Stress Ratio S_R	C_S
< 0.10	33.7
0.10 - 0.19	11.1
0.20 - 0.29	6.3
0.30 - 0.49	5.1
0.50 - 0.69	2.0
0.70 - 0.89	1.3
0.90 - 1.19	0.9
1.20 - 1.50	0.5

$$C_S = \frac{1}{S_R^{3/2}}$$

Table 6-10. Seat Diameter and Land Width Multiplying Factors

DIAMETER OF SEAT, inches D_S	C_{DT}	LAND WIDTH OF POPPET SEAT, inches L_W	C_{SW}
0.01 - 0.24	0.6	.01 - .05	2.52
0.25 - 0.39	0.7	.06 - .09	2.05
0.40 - 0.59	0.8	.10 - .12	1.60
0.60 - 0.79	1.0	.13 - .15	1.31
0.80 - 0.99	1.2	.16 - .18	1.09
1.00 - 1.19	1.5	.19 - .21	0.89
1.20 - 1.39	1.8	.22 - .24	0.73
1.40 - 1.59	2.1	.25 - .27	0.59
1.60 - 1.79	2.3	.28 - .31	0.44
1.80 - 2.00	2.4	.32 - .38	0.24

$C_{DT} = 1.1\ D_S + 0.32$

$C_{SW} = 3.55 - 24.52L_W + 72.99\ L_W^2 - 85.75L_W^3$
for $L_W < 6$)

Table 6-11 Spool Clearance and Diameter Multiplying Factors

SPOOL TO SLEEVE CLEARANCE, μin (B)	C_B	SPOOL DIAMETER, in (D_{SP})	C_{DS}
400 - 540	0.6	<1.00 inch	0.6
550 - 690	0.7	1.00 - 1.39	0.8
700 - 840	0.8	1.40 - 1.79	1.0
850 - 990	1.2	1.80 - 2.19	1.2
1000 - 1090	1.6	2.20 - 2.39	1.4
1100 - 1190	1.9	2.40 - 2.79	1.6
1200 - 1290	2.3	2.80 - 3.19	1.8
1300 - 1390	2.7	3.20 - 3.39	2.0
1400 - 1490	3.1		
1500 - 1590	3.6		

$C_B = B/750$ for $B < 600$ μin

$C_B = B^2/600{,}000$ for $B \geq 600$ μin

$C_{DS} = 0.615\ D_{SP}$

Table 6-12. Friction Coefficient Multiplying Factor, C_μ
(Use actual friction coefficient)

MATERIAL	C_μ DRY	C_μ LUBRICATED
Steel on Steel	0.8	0.5
Aluminum on Steel	0.6	0.5
Copper on Steel	0.5	0.4
Brass on Steel	0.5	0.4
Cast Iron on Steel	0.4	
Brass on Nylon	0.3	
Steel on Nylon	0.3	
Teflon on Teflon	0.05	0.04
Hard Carbon on Carbon	0.2	0.1
Copper on Copper	1.3	0.8
Aluminum on Aluminum	1.1	
Nickel on Nickel	0.7	0.3
Brass on Brass	0.9	0.6

CHAPTER 7

BEARINGS

7.1 INTRODUCTION

Bearings are among the few components that are designed for a finite life. Bearing life is generally expressed as a B_{10} life, which is the number of hours at a given load that 90 percent of a set of apparently identical bearings will complete or exceed. There are a number of other factors that can be applied to the B_{10} life so that it more accurately correlates with the intended operating environment. These factors include the use of newer high performance materials and manufacturing processing techniques, and the application of the bearing including actual lubrication film thickness, misalignment, velocity, load stresses and subjection to contaminants.

There are many different types of bearings in use making it extremely difficult to establish base failure rates for bearings based on field performance data. Bearing analysis is also extremely difficult due to the large number of engineering parameters associated with bearing design. The procedures for estimating bearing reliability presented in this chapter utilize the manufacturer's published B_{10} life with multiplying factors to relate the B_{10} value to intended operating conditions. An outline of the basic types of bearings to be discussed is shown in Figure 7.1.

7.1.1 Bearing Types

Ball Bearings - Ball bearings are generally used where there is likely to be excessive misalignment or shaft deflection. They are also used, especially in duplex arrangements, where accurate axial positioning is required in the presence of thrust load, such as with bevel gear shafts. Ball bearings are not as common in the main drive train of more recent designs because of advancements made with tapered roller bearings. Ball bearings are, however, often used on lightly loaded accessory shafts. Higher bearing life is easily achieved in these applications due to the very small loads and installation is simplified, since a ball bearing is nonseparable and requires no special setup procedures.

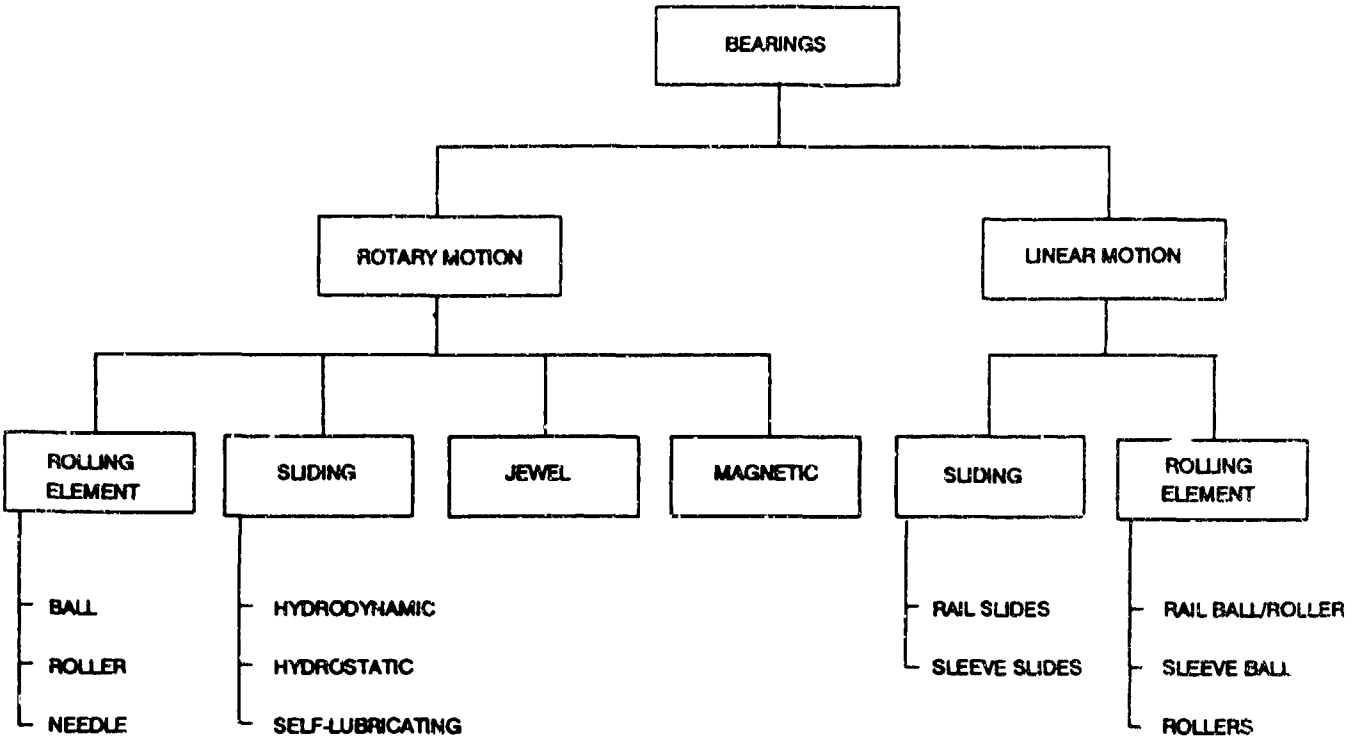

Figure 7.1 Outline of Bearing Types

Cylindrical Roller Bearings - Cylindrical roller bearings are used to support pure radial loads. They are often used at one end of a highly loaded gear shaft with either tapered roller bearings or multiple-row matched ball bearings at the other end. Roller bearing life is drastically reduced by excessive misalignment or deflection; hence, when using roller bearings, the stack-up of tolerances contributing to misalignment and the shaft or housing deflections should be carefully considered. To compensate for some degree of misalignment or deflection and to carry heavy radial loads, roller bearings are crowned to prevent the phenomenon known as end loading. End loading invariably leads to a drastic reduction in bearing life. The crowning process distributes the load away from the roller ends and prevents excessive stress that could cause fatigue at the roller bearing ends. The amount of crown to be used should be based on maximum continuous power. At lower power, the crown will not significantly change bearing life, while any higher power will be transients that load the bearing for short durations only.

Tapered Roller Bearings - Tapered roller bearings are being used increasingly in modern drive systems, since they can react to both thrust and radial loads and can offer the greatest load-carrying capacity in the smallest possible envelope. Although early tapered roller bearings were speed limited, these restrictions have been removed by utilizing bearings with special lubrication features. However, on very high-speed shafts, the use of tapered roller bearings may be precluded due to their inability to operate for required time intervals under survivability (oil-off) conditions. Tapered roller bearings, unlike single-row ball and cylindrical roller bearings, require spacers or shims to give these bearings the proper amount of preload or end play for proper operation. Usually it is desirable to have a light preload although a small amount of end play is often acceptable. As with internal clearance, extremes in end play or preload should be scrupulously avoided.

Sleeve Bearings - Although sleeve bearings are relatively inexpensive, they can cause costly equipment shutdowns if not properly integrated into the design. Short bearing life can be caused by misalignment, a bent shaft, a rotating part rubbing on a stationary part, a rotor out of balance causing vibration, excessive thrust caused by mechanical failure of other parts, excessive temperature caused by lack of lubrication, dirt or other contaminant and corrosion from water in the bearing housing. These problems can be classified in the following failure modes: fatigue, wiping, overheating, corrosion, and wear. Descriptions of these modes are as follows:

Fatigue occurs due to cyclic loads normal to the bearing surface. Wiping occurs from surface to surface contact due to loss of sufficient lubrication film thickness. This malfunction can occur from under-rotation or from system fluid losses. Overheating is indicated by babbit cracking or surface discoloration. Corrosion is frequently caused by the chemical reaction between the acids in the lubricants and the base metals in the babbit. Lead based babbits tend to show a higher rate of corrosion failures.

Severe performance requirements may affect the reliability of the bearings if there is a path of heat conduction from the machine or any friction creating components within it to the bearings (for example, brakes or clutches). This condition may cause a decrease in the bearing lubricant's operating viscosity and, consequently, a reduction in bearing life. A lubricant with a higher temperature rating should prevent leakage or excessive wear.

7.1.2 Design Considerations

Internal Clearance - Internal clearance is an important consideration in the design of ball and roller bearings, since improperly mounted internal clearance can drastically shorten the life of a bearing. Too little internal clearance limits the amount of misalignment that can be tolerated and can lead to heavily preloaded bearings, particularly at low temperatures. Excessive internal clearance will cause the load to be carried by too few rolling elements. The best practice is to ensure that under all conditions there will be a small positive internal clearance. Usually, the most significant factors to consider when determining mounted internal clearance of the bearing are the reduction of internal clearance due to shaft or housing fits and the effect of temperature on the housing/outer race interface diameters.

Bearing Race Creep - The creeping or spinning of bearing inner races on gearshafts is a fairly common, although not usually serious, problem in most drive systems. Lundberg and Palmgren developed fairly simple parametric calculations for the minimum fit to prevent creep with solid shafts, but there has been little if anything published on minimum press fits for hollow shafts, such types as used in helicopter drive systems. Since an accurate mathematical solution to such a problem would be extremely difficult, the best approach at this time seems to be a reliance on past experience. Sometimes it may not be possible to achieve the necessary press fit to prevent creep without introducing excessively high hoop stress in the bearing race. A common practice in this case is to use separate antirotation devices with a slotted bearing race. Although this practice is fairly effective with stationary races, it is seldom effective with rotating races.

Bearing Material - By far the greatest advance in bearing technology has been the development of extremely clean bearing steels resulting from vacuum-melt processing. Vacuum-melt 52100 bearings, for example, offer one and one-half to two times the life of vacuum-degassed 52100 bearings. Bearings of such advanced materials as M-50 steel can offer even further improvement. Just because these materials are available, however, does not mean that all bearings have to be made of vacuum-melt material. Depending on the bearing, vacuum-melt bearings can be from 2 to 5 times more costly than vacuum-degassed bearings, as well as requiring longer lead times to procure. Hence, bearings for high-speed primary

power train applications should be fabricated of M-50 (or in the case of tapered roller bearings, carburized CVM steel) for the sake of improved survivability following loss of lubrication. All other bearings should be fabricated of vacuum-degassed material unless there is a problem with low life, in which case the more expensive vacuum-melt materials should be used.

Inspection Requirements - Proper inspection of bearings can significantly reduce their mortality rate. Besides the obvious dimensional inspection requirements, two additional inspections should be specified for all high performance drive system bearings:

- Magnetic particle
- Nital etch

Magnetic particle inspection can detect the presence of relatively large surface or near-surface anomalies, such as inclusions, which are often the cause of bearing spalls. Nital etch inspection can detect the presence of grinding burns, which locally change the hardness of the material and cause premature bearing failure.

Bearing Installation/Removal - The installation of bearings should be carefully considered during design not only to prevent assembly errors, but also to permit easy removal of the bearing without damaging it. Lead chamfers should be provided at all bearing journals to facilitate installation. When specifying the breakout on the bearing corners, the shaft drawing should be checked to ensure that the maximum radius at the shaft shoulder will be cleared by the bearing. The height of the shaft shoulder should, if possible, be consistent with that recommended by bearing manufacturers. Where necessary, flats should be machined on the shaft shoulder so that a bearing puller can remove the bearing by contacting the inner race. Many bearings have been damaged in the past where the bearing puller could grab only the cage or rollers of the bearing. Where duplex bearings are used, the bearings should be marked so that the installer can readily determine the proper way for the bearings to be installed. Incorrectly installed duplex bearings will not properly react to the design loads. All bearings that can be separated should have the serial number clearly shown on all of the separable components. This will prevent the inadvertent mixing of components. Every assembly drawing that contains bearings should clearly explain in the drawing notes how the bearing should be installed. It is imperative that the mechanics building up this assembly have this

information available.

7.2 BEARING FAILURE MODES

The common bearing failure modes, mechanisms and causes are listed in Table 7-1. The most prevalent mode of bearing failure is spalling, which is defined as chipping or breaking of the bearing surface. The failure is usually caused by poor lubrication (premature failure) or by fatigue or wearout due to the repeated stress and strain of a lifetime of usage. Another mode of bearing failure is creeping or spin, caused by an improper fit between the bearing and the shaft or outer surface of the bearing. This allows movement of the race in relation to the housing or shaft. The surfaces then wear or score, thereby damaging the surfaces and preventing a firm, fixed contact.

Table 7-1. Typical Modes of Bearing Failure

FAILURE MODES	FAILURE MECHANISMS	FAILURE CAUSES
Fatigue Damage	Ball/Roller-raceway spalling, brinnelling	Heavy, prolonged load; Excess speed; Shock load
Noisy or Overheated Bearing	Glazing, microspalling of stressed surfaces	Loss of lubricant; Housing bore out of round; Corrosive agents; Distorted bearing seals
Excessive Equipment Vibration	Scuffing, fretting, pitted surfaces	Misalignment; Housing bore out of round; Unbalanced load; Inadequate housing support
Bearing Seizure	Crack formation on rings and balls/rollers, skidding	Inadequate heat removal capability; Loss of lubricant; High environmental temperature; Excessive speed

Roller and tapered bearings have an additional failure mode defined as hard lines or scuffing of the bearing surfaces. This failure mode is usually caused by bearing exposure to an excessive load for an extensive period of time. The surfaces of the moving parts are scored or scratched, increasing the roughness of the surfaces, setting up stress concentrations and increasing friction. The scoring also interferes with the normal lubricant film and increases the metal-to-metal contact during use.

7.3 BEARING FAILURE RATE PREDICTION

Bearing life is usually calculated using the Lundberg-Palmgren method (Ref. 53). This method is a statistical technique based on the sub-surface initiation of fatigue cracks through hardened air-melt bearing material. Most mechanical systems are not utilized precisely as the bearing manufacturer envisioned; therefore, some adjustment factors must be used to approximate the failure rate of the bearings under specific conditions.

Experience has shown that the service life of a bearing is usually limited by either excessive wear or fatigue. Excessive wear occurs when the bearings are improperly installed or exposed to hostile operating environments. Inadequate lubrication, misalignment, contamination, shock, vibration, or extreme temperature all cause bearings to wear out prior to their estimated design life. In contrast, a bearing can be expected to perform adequately for the duration of its rated life, given proper operating conditions, until failure occurs due to fatigue.

All bearings ultimately fail due to fatigue because the load carrying balls, raceways, rollers, etc. are subjected to cyclical contact stresses. Under laboratory conditions the fatigue characteristics of bearings can be quantified in terms of stress magnitude and number of stress cycles, which in turn relates to the bearing load and number of revolutions. A heavily loaded bearing, for example, has a much shorter fatigue life than a lightly loaded one when both are operated at the same low speed. Conversely, a bearing operated under a light load and low speed provides a service life several times greater than the rated life. In this latter case service will generally be terminated by wear.

Attempting to estimate the fatigue life of an individual bearing is not very practical because of the large number of design parameters to consider in relation to the sensitivity of the operating environment. Instead, statistical methods are used to rate bearings based on the results of large groups of the same type of bearing tested to failure under controlled laboratory conditions

to establish a fatigue life rating. This rating is universally defined as the number of hours that 90% of the bearings operating at their rated load and speed, can be expected to complete or exceed before exhibiting the first evidence of fatigue.

Standard equations have been developed to extend the B_{10} rating to determine the statistical rated life for any given set of conditions. These equations are based on an exponential relationship of load to life.

$$\frac{\lambda_{BE}}{\lambda_{BE,B}} = \left(\frac{C}{P}\right)^{k} \qquad (7\text{-}1)$$

Where:
λ_{BE} = Failure rate, failures/10^6 revolutions
$\lambda_{BE,B}$ = Base failure rate from B_{10} life
C = Basic dynamic load rating, lb
P = Equivalent radial load, lb
k = Constant, 3 for ball bearings, 10/3 for roller bearings

The basic dynamic load rating, C, is provided in manufacturer's catalogs or engineering drawings and determined through tests based upon a B_{10} life of 500 hours at 33.3 rpm.

The equivalent radial load parameter, P, is the equivalent radial load determined from applied loads. All bearing loads are converted to an equivalent radial load. If only pure radial loads are involved, then the value for P is simply the radial load.

Except for the special case of pure thrust bearings, bearing ratings shown in manufacturers' catalogs are for radial loads. When thrust is present, an equivalent radial load must be determined before estimating reliability. The equivalent radial load is defined as the radial load producing the same theoretical fatigue life as the combined radial and thrust loads. Most bearing manufacturers provide methods of combining thrust and radial loads in accordance with ANSI standards to obtain an equivalent load. This relationship can be written as follows:

$$RE = RF_{th} \qquad (7\text{-}2)$$

Where:
RE = Equivalent radial load
R = Radial load
F_{th} = Thrust factor

A bearing catalog will display separate tables of values to cover single-row, double-row, and angular-contact variations.

An inspection of both B_{10} expressions shows that the expected life decreases rapidly with increased loads. For example, when the load is doubled, ball bearing life drops to about 1/8 the life expectancy under the lower load. Moreover, a reduction of only 20% increases the predicted bearing life by approximately 100%.

Substantial improvements in materials processing and manufacturing techniques have been made since the original development of the B_{10} concept for predicting bearing life. For instance, high-purity steels that are vacuum degassed or vacuum melted are now widely used for bearings. Also, bearing components are manufactured to tighter tolerances on geometry and ball/raceways have finer finishes, which help to improve lubricating films. For reasons such as these, bearing manufacturers have modified their B_{10} ratings with certain adjustment factors. Therefore, the B_{10} life provides the latest and best estimate for the base failure rate. To evaluate a manufacturer's bearing for reliability, it is best to utilize the published B_{10} life and modify it according to the particular application.

$$\lambda_{BE} = \lambda_{BE,B} \left(\frac{L_A}{L_S}\right)^y \left(\frac{\nu_o}{\nu_L}\right)^{0.54} \left(\frac{C_{AL}}{60}\right)^{2/3} \cdot C_{CW} \qquad (7\text{-}3)$$

Where:

y = 3.33 for Roller Bearing; 3.0 for Ball Bearings
L_A = Equivalent radial load, lbs
L_S = Specification radial load, lbs
ν_o = Specification lubricant viscosity, lb-min/in^2
ν_L = Operating lubricant viscosity, lb-min/in^2
C_{AL} = Actual contamination level, micrograms/meter^3
C_{CW} = Water contamination factor

Multiplying factors for the following parameters will be added in future editions of the Handbook:

C_{PV} = Load/velocity factor
C_T = Temperature factor
C_V = Vibration factor

All of the base parameters can be obtained from manufacturer's drawings or specifications. The environmental parameters can either be measured at an operating site or estimated from a knowledge of the operating conditions.

Less than 10 percent of all ball bearings last long enough to fail due to normal fatigue (Ref. 8). Most bearings will fail due to static overload, wear, corrosion, lubricant failure, contamination, or overheating. The effects of water contamination, for example, is shown in terms of fatigue life reduction by Table 7-2 (Ref. 4).

Table 7-2. Reduction of Rolling Contact Life Due To Water In Lubricating Oil

WATER CONTENT OF WET OIL, PERCENT	REDUCTION IN FATIGUE LIFE, PERCENT
0.002	48
0.014	54
3.0	78
6.0	83

Base Oil Description: Base mineral oil dried over sodium
Test Equipment and Hertzian Stress: Rolling 4-ball bearing, 8.60 GPa (1.25×10^4 psi)

The values in Table 7-2 can be represented by a water contamination multiplication factor which accounts for the reduction in fatigue life due to the leakage of water into the oil lubrication. This factor is represented as C_{CW} and is represented by the following equations derived from data in Ref. 19.

$$\text{For } X < 0.002,\ C_{CW} = 1 + 460X \qquad (7\text{-}4)$$

$$\text{For } X \geq 0.002,\ C_{CW} = 2.036 + 1.029X - 0.0647X^2 \qquad (7\text{-}5)$$

Where: X = Percentage of water in the lubricant.

The C_{CW} multiplication factor will modify the base failure rate as shown in Equation (7-3). The value for L_A will vary with the bearing type and is given in Equation (7-6). Table 7-3 shows the

equations that represent the load capacity for the various types of ball and roller bearings.

Table 7-4 gives values for f_c used to determine L_A in Equation (7-6) for the various types of bearing configurations. The value of f_c is used in the L_S equation(s) of Table 7-3. This is the value in the denominator of the bearing load factor in Equation 7-4. L_A is determined using the following equation:

$$L_A = XF_r + YF_a \qquad (7\text{-}6)$$

where X and Y are listed in Table 7-5 for the various bearing types and designs. The value for L_S is obtained from Tables 7-3 and 7-4 and then used in Equation (7-3) along with the value from Equation (7-6) to find the expected bearing reliability.

Table 7-3. Dynamic Load Capacity Calculations for Ball and Roller Bearings (Ref. 44)

For radial ball bearings having a ball diameter D_W of 25.4 mm or less

$$L_S = f_c(i \cos\alpha)^{0.7} Z^{2/3}(D_W)^{1.8}$$

For radial ball bearings with ball diameter greater than 25.4 mm

$$L_S = 3.647\, f_c\, (i \cos\alpha)^{0.7} Z^{2/3}(D_W)^{1.4}$$

For ball thrust bearings with contact angle α of 90 deg.

$$L_S = f_c\, Z^{2/3}(D_W)^{1.8} \text{ for balls of 25.4 mm or less}$$

$$L_S = 3.647\, f_c\, Z^{2/3}(D_W)^{1.4} \text{ for balls larger than 25.4 mm}$$

For balls thrust bearings with contact angle α other than 90 deg.

$$L_S = f_c\, (\cos\alpha)^{0.7} \tan\alpha\, Z^{2/3}(D_W)^{1.8} \text{ for balls of 25.4 mm or less}$$

$$L_S = 3.647\, f_c\, (\cos\alpha)^{0.7} \tan\alpha\, Z^{2/3}(D_W)^{1.4} \text{ for balls 25.4 mm}$$

For radial roller bearings

$$L_S = f_c(i\, l_{eff} \cos\alpha)^{7/9} Z^{3/4}(D_W)^{29/27}$$

For thrust roller bearings

$$L_S = f_{c6}(l_{eff})^{7/9} Z^{3/4}(D_W)^{29/27} \text{ for a contact angle of 90 deg.}$$

$$L_S = f_c\, (l_{eff} \cos\alpha)^{7/9} \tan\alpha\, Z^{3/4}(D_W)^{29/27} \text{ for contact angle other than 90 deg.}$$

Where:

- d_m = bearing pitch diameter (mm)
- D = bearing outer diameter (mm)
- D_W = diameter of balls or rollers in bearing (mm)
- e = equivalent load function
- f_c = bearing load capacity factor for N and mm units
- F_a = thrust load (N)
- F_r = radial load (N)
- i = number of rows of balls or rollers in bearing (dimensionless)
- l_{eff} = effective contact length of rollers in bearing (mm)
- L_S = bearing load capacity for 10^6 revolutions rated life (N)
- X = radial load factor (dimensionless)
- Y = thrust load factor (dimensionless)
- Z = number of ball or rollers per row in bearing (dimensionless)
- α = bearing contact angle between ball or roller load line and plane perpendicular to axis (degrees)

Table 7-4(a). f_c Values for Roller Bearing Dynamic Capacity Calculation (Ref. 44)

RADIAL AND ANGULAR CONTACT BALL BEARINGS

$\frac{D_W \cos\alpha}{d_m}$	Single Row Radial Contact: Single and Double Row Angular Contact Groove Type (1) f_c	Double Row Radiall Contact Groove Type f_c
	Metric (2)	Metric(2)
0.05	46.7	44.2
0.06	49.1	46.5
0.07	51.1	48.4
0.08	52.8	50.0
0.09	54.3	51.4
0.10	55.5	52.6
0.12	57.5	54.5
0.14	58.8	55.7
0.16	59.6	56.5
0.18	59.9	56.8
0.20	59.9	56.8
0.22	59.6	56.5
0.24	59.0	55.9
0.26	58.2	55.1
0.28	57.1	54.1
0.30	56.0	53.0
0.32	54.6	51.8
0.34	53.2	50.4
0.36	51.7	48.9
0.38	50.0	47.4
0.40	48.4	45.8

(1) a. When calculating the basic load rating for a unit consisting of two similar, single row, radial contact ball bearings, in a duplex mounting, the pair is considered as one, double row, radial contact ball bearing.

b. When calculating the basic load rating for a unit consisting of two, similar, single row, angular contact ball bearings in a duplex mounting. "Face-to-Face" or "Back-to-Back," the pair is considered as one, double row, angular contact ball bearing.

c. When calculating the basic load rating for a unit consisting of two or more similar, single angular contact ball bearings mounted "in Tandem," properly manufactured and mounted for equal load distribution, the rating of the combination is the number of bearings to the 0.7 power times the rating of a single row ball bearing. If the unit may be treated as a number of individual interchangeable single row bearings, this footnote 1c does not apply.

(2) Use to obtain L_A in N when D is in mm.

Table 7-4(b). f_c Values for Roller Bearing Dynamic Capacity Calculation (Ref. 44)

THRUST BALL BEARINGS
(Use to obtain L_s in Newtons when D_w is in mm)

$\frac{D_w}{d_m}$	$\alpha = 90°$	$\alpha = 45°$	$\alpha = 60°$	$\alpha = 75°$
0.01	36.7	42.1	39.2	37.3
0.02	45.2	51.7	48.1	45.9
0.03	51.1	58.2	54.2	51.7
0.04	55.7	63.3	58.9	56.1
0.05	59.5	67.3	62.6	59.7
0.06	62.9	70.7	65.8	62.7
0.07	65.8	73.5	68.4	65.2
0.08	68.5	75.9	70.7	67.3
0.09	71.0	78.0	72.6	69.2
0.10	73.3	79.7	74.2	70.7
0.12	77.4	82.3	76.6	
0.14	81.1	84.1	78.3	
0.16	84.4	85.1	79.2	
0.18	87.4	85.5	79.6	
0.20	90.2	85.4	79.5	
0.22	92.8	84.9		
0.24	95.3	84.0		
0.26	97.6	82.8		
0.28	99.8	81.3		
0.30	101.9	79.6		
0.32	103.9			
0.34	105.8			

Table 7-4(c). f_c Values for Roller Bearing Dynamic Capacity Calculation (Pef. 44)

RADIAL ROLLER BEARINGS
(Use to obtain L_S when I_{eff} and D_w are in mm)

$\frac{D_w \cos\alpha}{d_m}$	f_c	$\frac{D_w \cos\alpha}{d_m}$	f_c
0.01	52.1	0.26	86.4
0.02	60.8	0.27	85.8
0.03	66.5	0.28	85.2
0.04	70.7	0.29	84.5
0.05	74.1	0.30	83.8
0.06	76.9	0.31	83.0
0.07	79.2	0.32	82.2
0.08	81.2	0.33	81.3
0.09	82.8	0.34	80.4
0.10	84.2	0.35	79.5
0.11	85.4	0.36	78.6
0.12	86.4	0.37	77.6
0.13	87.1	0.38	76.7
0.14	87.7	0.39	75.7
0.15	88.2	0.40	74.6
0.16	88.5	0.41	73.6
0.17	88.7	0.42	72.5
0.18	88.8	0.43	71.4
0.19	88.8	0.44	70.3
0.20	88.7	0.45	69.2
0.21	88.5	0.46	68.1
0.22	88.2	0.47	67.0
0.23	87.9	0.48	65.8
0.24	87.5	0.49	64.6
0.25	87.0	0.50	63.5

Table 7-4(d). f_c Values for Roller Bearing Dynamic Capacity Calculations (Ref. 44)

THRUST ROLLER BEARINGS
(Use to obtain L_s when I_{eff} and D_w are in mm)

$\frac{D_w \cos\alpha}{d_m}$	$45 < \alpha < 60°$	$60° < \alpha < 75°$	$75° < \alpha < 90°$	$\frac{D_w}{d_m}$	$\alpha = 90°$
0.01	109.7	107.1	105.6	0.01	105.4
0.02	127.8	124.1	123.0	0.02	122.9
0.03	139.5	136.2	134.3	0.03	134.5
0.04	148.3	144.7	142.8	0.04	143.4
0.05	155.2	151.1	149.4	0.05	150.7
0.06	160.9	157.0	154.9	0.06	156.9
0.07	165.6	161.6	159.4	0.07	162.4
0.08	169.5	165.5	163.2	0.08	167.2
0.09	172.8	168.7	166.4	0.09	171.7
0.10	175.5	171.4	169.0	0.10	175.7
0.12	179.7	175.4	173.0	0.12	183.0
0.14	182.3	177.9	175.5	0.14	189.4
0.16	183.7	179.3	0.16	195.1	
0.18	184.1	179.7	0.18	200.3	
0.20	183.7	179.3	0.20	205.0	
0.22	182.6	0.22	209.4		
0.24	180.9	0.24	213.5		
0.26	178.7	0.26	217.3		
0.28	0.28	220.9			
0.30	0.30	224.3			

Table 7-5(a). Values of Combined Load Factors X and Y (Ref. 44)

(1) Two similar, single row, angular contact ball bearings mounted "Face-to-Face" or "Back-to-Back" are considered as one, double row, angular contact bearing.

(2) Values of X, Y and e for a load or contact angle other than shown in Table 7-5 are obtained by linear interpolation.

(3) Values of X, Y and e shown in Table 7-5 do not apply to filling slot bearings for applications in which ball-raceway contact areas project substantially into the filling slot under load.

(4) For single row bearings when $\frac{Fa}{Fr} \leq e$, use X = 1, Y = 0.

Radial Ball Bearing Type			Single Row Bearings		Double Row Bearings				e
			$\frac{Fa}{Fr} > e$		$\frac{Fa}{Fr} \leq e$		$\frac{Fa}{Fr} > e$		
			X	Y	X	Y	X	Y	
Radial Contact Groove Ball Bearings	$\frac{Fa}{C_S}$	$F_a/iZ(D_w)^2$ Units Newtons, mm							
	0.014	0.172		2.30				2.30	0.19
	0.028	0.345		1.99				1.99	0.22
	0.058	0.689		1.71				1.71	0.26
	0.084	1.03	0.56	1.56	1	0	0.56	1.55	0.28
	0.11	1.38		1.45				1.45	0.30
	0.17	2.07		1.31				1.31	0.34
	0.28	3.45		1.15				1.15	0.38
	0.42	5.17		1.04				1.04	0.42
	0.56	6.89		1.00				1.00	0.44
Angular Contact Groove Ball Bearing with Contact Angle 5°	$\frac{iFa}{C_S}$	$F_a/iZ(D_w)^2$ Units Newtons, mm	For this type use the X, Y, e values applicable to single row radical contact bearings						
	0.014	0.172				2.78		3.74	0.23
	0.028	0.345				2.40		3.23	0.26
	0.056	0.689			1	2.07		2.78	0.30
	0.085	1.03				1.87	0.78	2.52	0.34
	0.11	1.38				1.75		2.36	0.36
	0.17	2.07				1.58		2.13	0.40
	0.28	3.45				1.39		1.87	0.45
	0.42	5.17				1.26		1.69	0.50
	0.56	6.89				1.21		1.63	0.52
10°	0.014	0.172		1.88		2.18		3.06	0.29
	0.029	0.345		1.71		1.98		2.78	0.32
	0.057	0.689		1.52		1.76		2.47	0.36
	0.086	1.03		1.41		1.63		2.20	0.38
	0.11	1.38	0.46	1.34	1	1.58	0.75	2.18	0.40
	0.17	2.07		1.23		1.42		2.00	0.44
	0.29	3.45		1.10		1.27		1.79	0.49
	0.43	5.17		1.01		1.17		1.64	0.54
	0.57	6.89		1.00		1.16		1.63	0.54
15°	0.015	0.172		1.47		1.65		2.39	0.38
	0.029	0.345		1.40		1.57		2.28	0.40
	0.058	0.689		1.30		1.46		2.11	0.43
	0.087	1.03	0.44	1.23	1	1.38	0.72	2.00	0.46
	0.12	1.38		1.19		1.34		1.93	0.47
	0.17	2.07		1.12		1.26		1.82	0.50
	0.29	3.45		1.01		1.14		1.66	0.55
	0.44	5.17		1.00		1.12		1.63	0.56
	0.58	6.89		1.00		1.12		1.63	0.56
20°			0.43	1.00	1	1.09	0.70	1.63	0.57
25°			0.41	0.87	1	0.92	0.67	1.41	0.68
30°			0.39	0.76	1	0.78	0.63	1.24	0.80
35°			0.37	0.66	1	0.66	0.60	1.07	0.95
40°			0.35	0.57	1	0.55	0.57	0.98	1.14

Table 7-5(b). Values of Combined Load Factors X and Y (Ref. 44)

Ball Thrust Bearing Type	Single Direction Bearings		Double Direction Bearings				e
	$\frac{Fa}{Fr} > e$		$\frac{Fa}{Fr} \leq e$		$\frac{Fa}{Fr} > e$		
	X	Y	X	Y	X	Y	
Thrust Ball (1) Bearings with Contact Angle							
$\alpha = 45^0$	0.66	1	1.18	0.59	0.66	1	1.25
$\alpha = 65^0$	0.92	1	1.90	0.54	0.92	1	2.17
$\alpha = 75^0$	1.66	1	3.89	0.52	1.66	1	4.67

(1) For $\alpha = 90^0$: $F_r = 0$ and $X = 1$

Table 7-5(c). Values of Combined Load Factors X and Y (Ref. 44)

Radial Roller Bearing Type	$\frac{Fa}{Fr} \leq e$		$\frac{Fa}{Fr} > e$		e
Self-aligning and Tapered Roller Bearings $\alpha \neq 0^0$ (1)	X	Y	X	Y	
	Single Row Bearings				
	1	0	0.4	0.4 cot α	1.5 tanα
	Double Row Bearings				
	1	0.45 cotα	0.67	0.57cotα	1.5 tan

Note: (1) For $\alpha = 0^0$: $F_a = 0$ and $X = 1$

Table 7-5(d). Values of Combined Load Factors x and Y (Ref. 44)

Roller Thrust Bearings Type	Single Direction Bearings		Double Direction Bearings				e
	$\frac{Fa}{Fr} > e$		$\frac{Fa}{Fr} \leq e$		$\frac{Fa}{Fr} > e$		
	X	Y	X	Y	X	Y	
Self-aligning and Tapered Thrust Roller	tan α	1	1.5tanα	0.67	tanα	1	1.5 tanα

For $\alpha = 90^0$: $F_r = 0$ and $Y = 1$

CHAPTER 8

GEARS AND SPLINES

8.1 INTRODUCTION

The reliability of gear or drive components is perhaps one of the most important considerations when designing a system. Some general design constraints and requirements should be given special attention because of their potential impact on the long-term reliability of the total system. The first of these is the operating power spectrum. The key point with regard to this design parameter is to anticipate potential requirements for growth. The second is that changing requirements may cause a configuration change where alignments are altered. This can be critical if the misalignment could cause vibration that could set up stresses and lead to fatigue failure. When a lubrication system is included, care should be taken to assure that the capacity, filter and transferring components are adequate. If superfine filters should be introduced, larger traps would be required to accommodate the increase in particles trapped in the element. The lubricant flow should be designed so that the particles within the system are removed prior to reentry into the gear box area.

Noise and vibration can affect reliability, not only the drive system itself, but also associated components of the complete system. Hence, every effort should be made to select a gearbox that is as quiet and as vibration-free as possible. When selecting gear candidates, consideration should be given to helical or high contact spur gears instead of conventional spur gears. Also, one should make certain that critical speeds and gear clash resonance frequencies, which may reinforce each other, are avoided.

In most gearbox applications, especially in Airborne Systems, weight is usually a constraining and, in some cases, the controlling factor. In general, overdesign means higher reliability, but in weight critical systems, overdesign in one area requires underdesign elsewhere; thereby, defeating the purpose of the overdesign. For example, bearing life should never be sacrificed in the design because bearings are likely to be the main drivers in the establishment of the failure rates of the gear system.

When a gearbox is exposed to overstress, several conditions

occur that greatly affect the failure rate. Bolted gear flanges will be subject to fretting, high loads will cause bevel gears to shift patterns, making tooth breakage a likely occurrence. Spur gears develop hard lines or scuffing as loads are increased. The use of a gear system in a design that exceeds the specification load should be done only after detailed analysis of the impact on each part or component has been made.

8.2 FAILURE MODES

8.2.1 Spur and Helical Gears

Spur gears are commonly used in all types of gearing situations, both for parallel-axis speed reduction and in coaxial planetary designs. In general, the reliability of drive train spur gears is extremely high due to present design standards. There are, however, some considerations that should be addressed because they are frequently overlooked in spur gear design or selection for specific purposes.

Generally, the initial design of a spur gear mesh is one of standard proportions and equal tooth thickness for both pinion and gear. This is, however, rarely the optimum configuration for a spur gear mesh, because this type of design does not have two very desirable characteristics: recess action and a balanced bending stress in pinion and gear. A recess-action gear mesh has a long addendum pinion and short addendum gear. A recess-action mesh is quieter and smoother running than standard mesh and has a much lower tendency to score due to better lubrication within the mesh.

Although the advantage of having balanced bending stresses on a pinion and gear is primarily lower weight, it does have an indirect effect on reliability. As stated earlier, whenever there is an inefficient use of weight, reliability is compromised somewhat. For example, even a fraction of a pound wasted to non-optimization of a spur gear mesh could be applied to a bearing where the life could perhaps be doubled. While overemphasis of weight reduction can be detrimental to reliability, the carrying of excess weight can have a far-reaching effect; therefore, a balanced gear system must be the goal for efficient and reliable systems. Fortunately, it is usually a simple task to achieve recess-action and balanced bonding stress in most spur gear designs. This is accomplished by experimentally shifting the length of contact up the line of action toward the driver gear, while increasing the circular tooth thickness of the pinion and decreasing that of the gear.

There are four design criteria that are used to evaluate the adequacy of spur or helical design: Bending stress, hertz or vibrational stress, flash temperature index and/or lubrication film thickness (EHD). The first three have long been used in gear design and methods of calculation are well documented in many publications. EHD (Elastrohydrodynamic) film thickness is a newer technique and has not yet been completely standardized. Some gear specialists have advanced EHD film thickness as a check on scoring probability. It is obvious that if an oil film of a greater thickness than the contact surface asperities can be maintained scoring will not occur, since a metal-to-metal contact must be experienced to allow scoring to occur.

An important parameter to evaluate lubrication effectiveness is the lubricant film thickness. The equation below is a non-dimensional expression for lubricant film thickness:

$$H_L = \frac{2.65\ G^{0.54}\ U^{0.7}}{W^{0.13}} \qquad (8\text{-}1)$$

Where: H_L = Dimensionless film thickness
G = Viscosity and material parameter
U = Speed parameter
W = Load parameter

Since it is often difficult to obtain these parameters directly, this expression will only be used for a qualitative evaluation. The major impact of the formula is to establish the dependence of lubricant film thickness (H) from the various parameters. It should be noted that a change in lubricant viscosity and gear system velocity have a major impact on h, whereas a change in load has a weaker influence. These trends can be used when adjustment factors are developed later in the text.

Allowable tooth stress is the subject of much uncertainty and most gear manufacturers have a proprietary method for establishing this criteria. Therefore, it is usually a stated parameter from the manufacturer that is used. The use of allowable stress published by AGMA will usually result in satisfactory gear performance.

To ensure smooth operation of the gear mesh under load, it is generally the practice to modify the involute profile, usually with tip relief, to correct for the deflection of the gear tooth under load. The deflection can be accurately calculated; therefore, the

correct deflection profile should be used. Too little relief will result in the gear teeth going into mesh early and going out of mesh late. This results in higher dynamic loads with the accompanying stress, vibration, noise and possible non-involute contact that can lead to hard-lines, scuffing or scoring of gear teeth. Too much tip relief lowers the contact ratio of the gear set and again can result in less than optimum performance with respect to stress, vibration, and noise.

Crowning is generally applied to spur gears to ensure full contact across the face of the gear without end loading. With insufficient crowning, end loading will occur and result in higher than predicted vibrational stresses. The methods used to calculate the amount of crowning is similar to the methods used for calculating crowning on roller bearings.

Helix correction must be used if the bearing mountings of the spur gear are not of equal stiffness. This causes the gear to cock and concentrate the load at one end of the gear tooth. Analytical prediction is not usually practical and strain gaging the gear rim is the better method to determine helix corrections. This process involves iterative grinding and testing until an equal reading is obtained across the gear face. Edge break is advisable for all gear teeth, including spiral bevel and helical teeth. This will prevent chipping of the gear teeth at the corners, which carburization has made quite brittle.

Helical gears are usually quieter and have a greater load-carrying capacity per inch of face than spur gears. The major disadvantage is that a thrust load is introduced along the gear shaft, thereby requiring larger and stronger bearings. Analysis of helical gears is very similar to that used for spur gears. The stress analysis is performed using an equivalent spur tooth. AGMA standard procedures have been developed for strength analysis of spur and helical gears.

8.2.2 Spiral Bevel Gears

The geometry of spiral bevel gears is considerably more complex than the spur or helical gear; therefore spiral bevel gears are probably the most difficult type gear to design and analyze. The hand of spiral gears should be chosen, if possible, so that axial forces tend to push both the pinion and gear out of mesh. If this is impossible, then the hand is chosen so the pinion is forced out of mesh. The face contact ratio of the mesh should be as high as possible to ensure quiet running. The face width of the spiral bevel gear should never exceed one-third of the outer cone distance

to prevent load concentration on the toe of the gear and possible tooth breakage.

8.2.3 Planetary Gears

Planetary gear units are used in many designs, because they offer relatively large speed reduction in a compact package. The load shared among the pinions and the face width of the planetary gear is much less than that which would be required for a single mesh reduction. From a design point of view, it is desirable to use as many pinions as possible. It is normally desired to refrain from equally spaced planets meshing in unison with a sun or ring gear. The most common problem with this design is thrust washer wear. The excessive wear generally results from an inadequate supply of lubricant to the thrust washer area. The spherical bearing type support is generally preferred from a reliability point of view, since there are fewer parts and the thrust washer problem is eliminated. The spherical bearings also allow the pinions to maintain alignment with the sun and ring gears despite the deflection of the pinion posts. Despite the advantage of this design, it may be impossible to provide adequate support for cantilevered pinions in high torque situations, thereby requiring a two-plate design.

8.2.4 Involute Splines

Involute splines are used to transfer torque between shafts and flanges, gears and shafts, and shafts and shafts. The most common problem associated with splines is wear due to fretting; particularly, with loose splines. Strict attention must be given to the maintenance of bearing stress below the allowable limit. Tight splines should have an adequate length pilot to react with bending loads. Lubrication is a particular factor in the reliability of loose splines and, if at all possible, should remain flooded with oil at all times. Crowning is usually required to prevent excessive wear.

8.3 GEAR RELIABILITY PREDICTION

The previous paragraphs have provided an insight into the specific characteristics and failure modes of the more common gear types. Gears, fortunately, are designed to a specification and through the standardization of the American Gear Manufacturer's Association (AGMA), gears of various manufacturers and designs can be compared. The best approach for the calculation of failure rates for a gear system is to use the manufacturer's specification

for each gear as the base failure rate, and adjust the failure rate for any difference in the actual usage from that purpose for which the gear was designed. This gear failure rate can be expressed as:

$$\lambda_{GE} = \lambda_{GE,B} \cdot C_{GS} \cdot C_{GP} \cdot C_{GA} \cdot C_{GL} \cdot C_{GN} \cdot C_{GT} \cdot C_{GV} \qquad (8\text{-}2)$$

Where:
- λ_{GE} = Failure Rate of Gear under specific operation, failures/million revolutions
- $\lambda_{GE,B}$ = Base Failure of Gear specified by manufacturer, failures/million revolutions
- C_{GS} = Multiplying factor considering speed deviation with respect to design
- C_{GP} = Multiplying factor considering torque deviation with respect to design
- C_{GA} = Multiplying factor considering misalignment
- C_{GL} = Multiplying factor considering lubrication deviation with respect to design
- C_{GN} = Multiplying factor considering contamination environment
- C_{GT} = Multiplying factor considering temperature
- C_{GV} = Multiplying factor considering vibration and shock

$\lambda_{GE,B}$ can usually be obtained from the manufacturer and it will be expressed in failures/operating hour at a specified speed, load, lubricant, and temperature. Also, a service factor will usually be provided to adjust the normal usage factor for certain specific conditions found in typical industries. These factors include such things as vibration, shock, contamination, temperature and usage rate.

C_{GS} can be calculated by using the information provided by Equation (8-1) noting that the lubrication film thickness varies with speed to the 0.7 power. Therefore:

$$C_{GS} = \left(\frac{\text{Operating Speed}}{\text{Design Speed}}\right)^{0.7} \qquad (8\text{-}3)$$

C_{GP} or load factor has a lubricant and a fatigue impact. From previous expressions of EHD, the impact of load or torque can be expressed as:

From Equation (8-1):

$$\text{Change in Expected Life} = \frac{1}{W^{0.13}} = \frac{1}{\left(\frac{L_D}{L_O}\right)^{0.13}} \quad \text{(Lubricant Impact)} \quad (8\text{-}4)$$

Where: L_O = Operating Load
L_D = Design Load

and the expression for torque or load on the fatigue rate of the component is:

$$\text{Change in Expected Life} = \left(\frac{L_O}{L_D}\right)^{4.56} \quad \text{(Fatigue Impact)} \quad (8\text{-}5)$$

Therefore:

$$C_{GP} = \left(\frac{L_O}{L_D}\right)^{4.69} \quad (8\text{-}6)$$

The alignment of gears, bearings and shafts can be critical in the operation of a system. C_{GA}, the misalignment factor, can be expressed as:

$$C_{GA} = \left(\frac{A_E}{0.006}\right)^{2.36} \quad (8\text{-}7)$$

Where: A_E = Misalignment angle in radians.

The lubricant factor C_{GL} is a function of the viscosity of the lubricant used in a gear system. C_{GL} can be expressed as:

$$C_{GL} = \left(\frac{\nu_O}{\nu_L}\right)^{0.54} \quad (8\text{-}8)$$

Where: ν_O = viscosity of specification lubricant

ν_L = viscosity of lubricant used

The contamination factor for dust or corrosion is usually a function of concentration of contaminants and normally varies with concentration. Therefore:

$$C_{GN} = \left(\frac{\text{Contaminant Concentration}}{\text{Standard Contaminant Concentration}}\right)^{2/3} \quad (8\text{-}9)$$

Temperature conditions of the gear system have an impact on other parameters such as C_{GL} and C_{GP}. As the temperature increases, the lubricant viscosity decreases and the dimensions of the gears, shafts and bearings increase. This change normally causes a closer tolerance between operating units and an increase in the frictional losses in the system. The multiplying factor for temperature C_{GT} can be expressed as:

$$C_{GT} = \left(\frac{\text{Operating Temp } °R}{\text{Specification Temp } °R}\right)^3 \quad (8\text{-}10)$$

The American Gear Manufacturers Association (AGMA) has developed service factors for most industrial applications of gears, bearings, and gearbox designs whereby the expected extent of usage in vibration and shock environments can be taken into account when a gear system is selected for use. This service factor can be used as a multiplying factor for determining the inherent reliability or expected failure rate (C_{GV}) for a specific gearbox or bearing in a particular environment. Most manufacturers provide service factor data for each of their products.

$$C_{GV} = \text{AGMA Service Factor} \quad (8\text{-}11)$$

8.4 SPLINE RELIABILITY PREDICTION

The failure rate in failures per million revolutions of spline gears (λ_{GS}) can be calculated by:

$$\lambda_{GS} = \lambda_{GS,B} \cdot C_{GM} \cdot C_{GL} \cdot C_{GT} \cdot C_{GV} \cdot C_{GS} \quad (8\text{-}12)$$

Where: $$\lambda_{GS,B} = \frac{10^6}{\theta} \quad (8\text{-}13)$$

and: θ = Life of spline gear in revolutions

An analytical expression for the spline gear life, θ, has been devised by Canterbury and Lowther (Ref. 11). This equation is expressed as:

$$\theta = 7.08 \cdot 10^{-10} \left(\frac{\phi G_L}{G_D} \right)^{4.56} (A_E)^{-2.36} \qquad (8\text{-}14)$$

Where: G_L = Spline Length
G_D = Spline Diameter

$$\phi = \text{Load Factor} = \frac{1422\, G_B\, (G_D)^2}{G_T}$$

G_T = Torque, in Lbs.
G_B = Tooth Hardness (Brinnell), Kg/mm2
A_E = Misalignment angle, Radians

Substituting the expression for the spline gear base failure rate into Equation (8-12) yields:

$$\lambda_{GS} = \frac{5.93\,(A_E)^{2.36}}{\left(\frac{G_L\, G_B\, G_D}{G_T} \right)^{4.56}} \cdot C_{GN} \cdot C_{GL} \cdot C_{GT} \cdot C_{GV} \cdot C_{GS} \qquad (8\text{-}15)$$

Where: C_{CS}, C_{GL}, C_{GN}, C_{GT}, and G_{GV} are calculated by Equations (8-3), (8-8), (8-9), (8-10), and (8-11) respectively.

THIS PAGE INTENTIONALLY LEFT BLANK

CHAPTER 9

ACTUATORS

9.1 INTRODUCTION

Actuators provide the means to apply mechanical power to systems when and where it is needed. In general, actuators take energy from pumped fluid and convert it to useful work. This conversion is accomplished by using the pumped fluids to generate a differential pressure across a piston, which results in a force and motion being generated. This chapter will identify some of the more common failure modes and failure causes of actuators, and will develop and discuss a failure rate model for actuators.

In general, there are two types of output motions generated by actuators: linear and rotary. Within these two classifications there are many different types of actuator assemblies.

Linear Motion Actuators - Linear motion actuators are usually a derivative of one of the following four types:

1. Single acting
2. Double acting
3. Ram
4. Telescoping

Single acting actuators are the simplest type of the four. Pressurized fluid acts only on one side of the piston so the single acting actuator is capable of generating motion and power only in one direction and requires an external force to move the piston in the opposite direction.

Double acting actuators have fluid chambers on both sides of the piston, which allows pressurized fluid to both extend and retract the piston/rod and provide a faster response. Double acting actuators may have rods extending from either or both ends of the cylinders. Those with rods extending from both ends are balanced; that is, the piston moves at the same rate and delivers equal forces in each direction.

Ram cylinders are a variation on the single acting design, but in this case, the piston rod is the same diameter as the piston. This design is useful where column loads are extremely high or when

the rod hanging in a horizontally mounted cylinder has a tendency to cause sagging.

Telescoping cylinders generate long stroke motions from a short body length. Force output varies with rod extension: highest at the beginning, when the pressurized fluid acts on all of the multiple piston faces; and lowest at the end of the stroke, when the pressurized fluid acts only on the last extension's piston area. Telescoping cylinders may be either single or double acting.

Rotary Motion Actuators - Rotary actuators produce oscillating power by rotating an output shaft through a fixed arc. Rotary actuators are primarily one of two types:

1. Linear motion piston/cylinder with rotary output transmission
2. Rotary motion piston/cylinder coupled directly to output shaft

The first of the two rotary actuator types generally uses one or two linearly moving pistons to drive a transmission to convert the linear motion produced by the piston to a rotary output motion. These rotary actuators generally use crankshafts, gear rack-and-pinions, helical grooves, chains and sprockets, or scotch-yoke mechanisms as transmissions to convert the piston's linear output to rotary output. The piston/cylinder design may be single or double acting.

The second of the two rotary actuator types uses a piston designed to oscillate through a fixed arc to directly drive the output shaft. This design is simpler than the other type of rotary actuator as no transmission is required, but the unusual piston shapes required may create sealing problems.

9.2 COMMON ACTUATOR FAILURE MODES

The primary failure mode of an actuator is a reduction in output force or stroke. This reduction in actuator output power can be caused by excessive wear of the piston/cylinder contact surfaces, which results in an increase in fluid leakage past the piston. Reduction in actuator output power can also be caused by external leakage, such as leakage through the piston rod/rod seal interface. Deterioration of the piston rod seal also permits ingestion of contaminants to the gap between the piston and cylinder increasing the rate of wear and probability of problems associated with corrosion.

Another common failure mode for actuators is jamming of the piston caused by stiction or misalignment. This failure can occur if excessive contaminants are ingested or if excessive side loads are encountered. Misalignment also increases the rate of piston/cylinder wear contributing to early failure.

Temperature extremes may effect the viscosity characteristics of the pressurized fluid and increased seal wear will result from the resultant change in film lubrication.

9.3 FAILURE RATE MODEL FOR ACTUATOR

The reliability of an actuator is primarily influenced by its load environment which can be subdivided into external loads and internal loads. External loads are forces acting on the actuator from outside sources due to its operating environment. Conditions of storage, transportation and ground servicing as well as impact loads during operation have an effect on the rate of failure. Internal loads are caused by forces acting inside the actuator as a result of pressure variations, pressure differentials, friction forces, temperature-related expansion and contraction, and by forces developed and transmitted by the impact of external loads.

Valves often form a part of an actuator assembly and are used for primary movement control of the actuator and also for deceleration of the piston/rod assembly at the ends of their stroke. Failure rate models for valve assemblies are presented in another chapter of this handbook.

9.3.1 Piston/Cylinder

The primary failure effect of internal and external loads on an actuator is wear of the piston and cylinder which results in an increase in leakage past the piston. A criteria of actuator failure would then be a leakage rate resulting from wear which exceeds a maximum allowable leakage rate specified by the user.

Wear of the cylinder and piston will occur in two phases according to the Bayer-Ku sliding wear theory (Ref. 6). The first or constant wear phase is characterized by the shearing of the surface asperities due to the sliding action of the piston within the cylinder. During this period the wear rate is practically linear as a function of the number of actuator cycles and the wear depth at the end of the constant wear phase is one half the original surface finish. During the second or severe wear phase, wear debris becomes trapped between the two sliding surfaces and gouging of the surfaces takes place. The wear rate begins to increase very rapidly and failure of the actuator is eminent.

The number of cycles to complete the constant wear phase can be predicted analytically by a semi-empirical modification of Palmgren's equation (Ref. 6) resulting in the formula:

$$N_o = 2000 (\gamma F_Y / S_c)^9 \qquad (9\text{-}1)$$

Where:
γ = Wear factor
F_y = Yield strength of softer material, psi
S_c = Compressive stress between the surfaces, psi

The wear factor, γ, will be equal to 0.20 for materials that have a high susceptibility to adhesive wear, in which the wear process involves a transfer of material from one surface to the other. The wear factor will be equal to 0.54 for materials that have little tendency to transfer material in which the material is subject to micro-gouging of the surfaces by the asperities on the material surface.

The maximum compressive stress caused by the cylinder acting on the piston is computed assuming a linear distribution of stress level along the contact area. Reference 38 provides the following equation for compressive stress:

$$S_c = 0.8 \left(\frac{\frac{W}{L} \cdot \frac{D_1 - D_2}{D_1 D_2}}{\frac{1 - \eta_1^2}{E_1} + \frac{1 - \eta_2^2}{E_2}} \right)^{1/2} \qquad (9\text{-}2)$$

Where:
W = Side load on the actuator, lb
L = Total linear contact between piston and cylinder, in
D_1 = Diameter of cylinder, in
D_2 = Diameter of piston, in
η = Poisson's ratio
E = Modulus of elasticity

Substituting Equation (9-2) into Equation (9-1) and adding a constant for lubrication provides an equation for the number of cycles for an actuator during Phase I wear until the severe wear period begins.

$$N_o = k \left[\frac{\gamma F_y}{\left(\frac{\frac{W}{L} \cdot \frac{D_1 - D_2}{D_1 D_2}}{\frac{1 - \eta_1^2}{E_1} + \frac{1 - \eta_2^2}{E_2}} \right)^{1/2}} \right]^9 \qquad (9\text{-}3)$$

Where k includes a lubrication factor.

During the second or severe wear phase, the following equation can be used to determine the rate of wear (Ref. 45):

$$V = \frac{K W d}{H} (N - N_o) \qquad (9\text{-}4)$$

Where:

- V = Volume of material removed by wear during the second phase, in^3
- K = Wear coefficient (See Table 9-3)
- W = Applied load, lb
- d = Sliding distance, in
- H = Penetration hardness, psi
- N = Number of cycles in the second wear phase
- N_0 = Number of cycles at the end of the initial wear phase

Solving for N results in the equation:

$$N = \frac{V H}{K W d} + N_o \qquad (9\text{-}5)$$

This second phase of wear is characterized by rapid wear until failure of the actuator occurs usually as a result of poor response due to excessive leakage. The leakage rate past the piston within the cylinder may be modeled as laminar flow between parallel plates (Ref. 5).

$$Q = \frac{\pi D_2 a^3 \Delta p}{12 \nu L} \qquad (9\text{-}6)$$

Where: Q = Leakage rate past piston, in^3/sec
D_2 = Piston diameter, in
a = Gap between piston and cylinder, in
Δp = Pressure differential across piston, psi
ν = Fluid viscosity, $lbf\text{-}sec/in^2$
L = Piston length, in

The gap between the piston and cylinder, a, is a dynamic term being a function of wear.

$$a = (D_1 - D_2) + h \tag{9-7}$$

Where: D_1 = Cylinder diameter, in
h = Depth of wear scar, in

The wear scar depth will be equal to the volume of material lost due to wear, V, divided by the contact surface area, A:

$$h = \frac{V}{A} \tag{9-8}$$

Substituting Equations (9-7) and (9-8) for wear gap into Equation (9-6) results in the following equation for leakage rate between the piston and cylinder:

$$Q = \frac{\pi D_2 \left[(D_1 - D_2) + V/A\right]^3 \Delta p}{12 \nu L} \tag{9-9}$$

Solving Equation (9-9) for V and substituting V in Equation (9-5) results in an equation for the number of cycles to failure.

$$N = \frac{A H}{K W d}\left[\left(\frac{12 Q \nu L}{\pi D_2 \Delta p}\right)^{1/3} + (D_2 - D_1)\right] + N_o \tag{9-10}$$

Combining Equations (9-10) and (9-3) provides the following solution for actuator wear life:

$$N = \frac{AH}{KWd}\left[\left(\frac{12Q\nu L}{\pi D_2 \Delta p}\right)^{\frac{1}{3}} + (D_2 - D_1)\right] + k\left[\frac{\gamma F_y}{\left(\frac{W}{L}\cdot\frac{D_1 - D_2}{D_1 D_2}\right)^{\frac{1}{2}}}\right]^9 \qquad (9\text{-}11)$$

$$\left(\frac{1-\eta_1^2}{E_1} + \frac{1-\eta_2^2}{E_2}\right)$$

A typical plot of wear as a function of the number of cycles is shown in Figure 9.1.

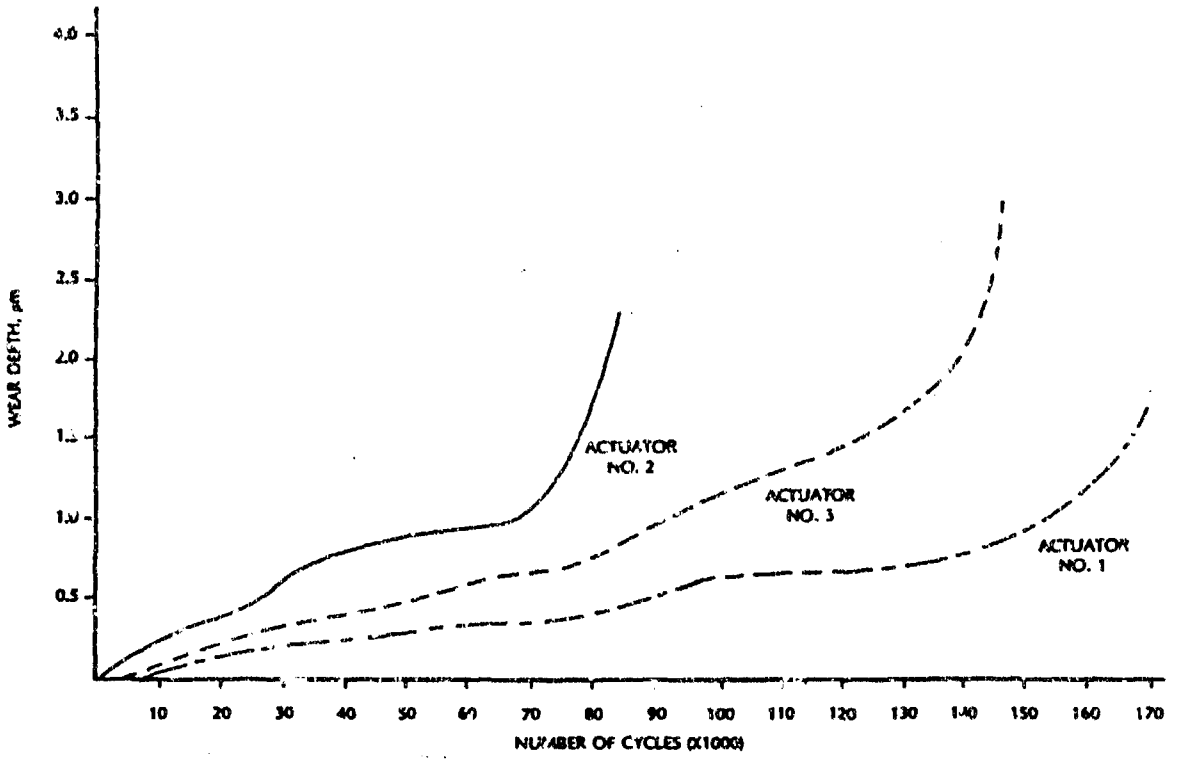

Figure 9.1 Failure Rate as a Function of Cycles for a Typical Actuator under Different Side Loads

Since the first phase of wear is fairly linear as a function of the number of cycles and failure will occur soon after phase one wear, the base failure rate of the actuator can be approximated as follows:

$$\lambda_{AC,B} = 10^6/N_0 \qquad (9\text{-}12)$$

Where: $\lambda_{AC,B}$ = Base failure rate of actuator, failures/million cycles

The complete failure rate model for the piston/cylinder actuator incorporates modifiers for contamination and temperature effects. The complete model can be expressed as follows:

$$\lambda_{AC} = \lambda_{AC,B} \bullet C_{CP} \bullet C_T \qquad (9\text{-}13)$$

Where:
- λ_{AC} = Failure rate of actuator, failures/million cycles
- C_{CP} = Contaminant particle coefficient, see Section 9.3.2
- C_T = Temperature factor, see Section 9.3.3

9.3.2 Effect of contaminants (C_{CP})

During the time that the actuator is at rest, particles can work their way between the piston and cylinder. Then, when the actuator is put into motion, increased forces are needed to move the piston. This stiction phenomena causes a loss of actuator response and in some severe cases, a completely jammed component.

Three types of wear need to be considered in determining the effects of contaminants on actuator reliability:

Erosion - Particles carried in a fluid stream impact against the piston and cylinder surfaces. If the kinetic energy released upon actuator response is large compared to forces binding the piston/cylinder walls, surface fatigue will occur. Hard particles may also cut away surface material.

Abrasive Wear - A hard particle entering the gap between the piston and cylinder surfaces can cut away material of the softer surface on a single actuator engagement. The rate of wear will be proportional to the number of particles in contact with the surfaces and the particle hardness. If the hardness of the piston is significantly less than that of the cylinder, a hard particle, absorbed by the softer material causes severe abrasive wear of the harder actuator surface.

Surface Fatigue - Particulate contaminants interacting with the piston and cylinder surfaces can dent a surface producing plastic deformation. Large numbers of dislocations will increase the

surface roughness and deteriorate the surface material. The result is an accelerated rate of wear and a higher probability of leakage between the surfaces.

The deteriorating effects of contaminant particles on the reliability of an actuator must be equated along with the probability of the contaminants entering the gap between the actuator surfaces. The probability of contaminants entering this area will depend on the operating environment, the types and numbers of particles expected to be encountered, and the filtering system to prevent the entrance of particles. The typical actuator contains a bushing to wipe the piston on the return stroke. The life expectancy and reliability of this device must be determined as part of the overall reliability estimate of the actuator.

If the piston surface slides over a hard contaminant particle in the lubricant, the surface may be subject to pitting. The abrasive particle has edges with a characteristic radius, denoted by r. When the depth of penetration of the abrasive particle (d) reaches a certain critical value, the scratching produces additional wear particles by pitting. This elastic/plastic deformation process occurs when the maximum shear stress in the complex stress distribution beneath the contact exceeds the elastic limit. This maximum shear stress occurs beneath the contact at a depth equal to one half the contact radius. The value of this critical depth is given by (Ref. 49).

$$d_{crit} = \frac{r}{2} = \frac{r\,(1 - 2 f_{s,max})}{F_{sy}} \qquad (9\text{-}14)$$

Where: $f_{s,max}$ = Maximum shear stress
r = Characteristic radius of particle
F_{sy} = Yield strength of material

If this type of wear should occur, it is so severe that actuator performance would be immediately effected and failure would occur. Actuators are designed to prevent particles of sufficient size to cause this type of failure and the probability of failure from this type of pitting is extremely low. The failure mode is presented here as a design evaluation check on the sealing technique for the piston assembly.

Fatigue wear on the microscopic wear due to contaminants is similar to that for pitting just described except that it is

associated with individual asperity contacts rather than with a single large region. The additional material lost due to contaminant wear process can be estimated in the same way as the adhesive wear process was explained earlier in this chapter, the volume δV removed on an individual piston stroke proportional to a^3 where a is the radius of the individual area of contact. Similarly, the sliding distance δL is proportional to A.

$$\frac{\delta V}{\delta L} \propto \frac{\delta A}{3} \tag{9-15}$$

Where: A = Area of contact

Summing for all contacts provides the following equation:

$$\frac{V}{L_1 N} = \frac{1}{3} K_1 A = \frac{1}{3} K_1 \frac{W}{H_v} \tag{9-16}$$

Where:
- V = Volume of material lost due to contaminant wear
- L_1 = Sliding distance of the piston
- N = Number of actuations
- K_1 = Wear coefficient
- W = Transverse load on the actuator
- H_v = Vickers Hardness of the piston

This expression can be rewritten in the form to include a contaminant particle coefficient, C_{CP}:

$$V = \frac{C_{CP} W L_1 N}{H_v} \tag{9-17}$$

The effect of the additional wear due to contaminant particles may be expressed as an additive term in the basic wear relationship. It will be noted from the derivation of equations for the effect of contaminant particles on actuator surface wear and the possibility of stiction problems that a probability of damaging particles entering the gap between the piston and cylinder must be estimated. The contaminant factors involved are as

follows:

Hardness - The wear rate will increase with the ratio of particle hardness to actuator surface hardness. It will normally be the hardness of the piston that will be of concern. If the ratio is less than 1, negligible wear can be expected.

Number of particles - The wear rate will increase with a concentration of suspended particles of sufficient hardness.

Size - For wear of the piston or cylinder to occur, the particle must be able to enter the gap between the two surfaces. The particle must also be equal to or greater than the lubrication film thickness. With decreasing film thickness, a greater proportion of contaminant particles entering the gap will bridge the lubrication film, producing increased surface damage.

Shape - Rough edged and sharp thin particles will cause more damage to the actuator surfaces than rounded particles. As the particles remain in the gap, they will become more rounded and produce less wear. It is the more recent particles being introduced into the gap that cause the damage.

C_{CP} can be estimated by considering these variables and their interrelationship. The following factors can be used to estimate a value for C_{CP}:

$$C_{CP} = C_H \cdot C_S \cdot C_N$$

Where:

C_H = Factor considering ratio of particle to piston hardness, See Table 9-1.

C_S = Factor considering ratio of particle size to gap size between piston and cylinder (use filter size/10 micron

C_N = Factor considering the number of particles meeting hardness, size and shape parameters entering the gap, See Table 9-2

9.3.3 Effect of Temperature (C_T)

The effect of the temperature of the surface on the wear rate is a complicated phenomena, because the corrosion of the wear debris at different temperatures produces different oxidation products. Chemical interactions with the metal surfaces result in different wear rates as the temperature of the surface is changed (Ref. 51). For example, the formation of Fe_3O_4 is likely to predominate when steel is subject to wear in the temperature range between 570 °F

and 930 °F (300 °C to 500 °C).

Wear of metals has been related to the heat of absorption of molecules of debris (Ref. 52). The basic relationship in this treatment is:

$$V = \frac{K_1 WS}{H_v} C_o e^{\frac{\theta}{T}} \qquad (9\text{-}18)$$

Where: C_0 = Arrhenius constant
θ = Activation energy constant, °K
T = absolute temperature, °K

Values for the parameter θ are in the range between 1200 °K and 6000 °K (2,160 °R to 10,800 °R).

The effect of variation of temperature may be determined by eliminating the Arrhenius constant in terms of the value of the exponential at ambienc temperature T. Making this substitution into Equation (9-18), the following is obtained:

$$V = \frac{C_T K_1 W L_1 (N - N_o)}{H_v} \qquad (9\text{-}19)$$

Where C_T, the temperature factor, is given by (Ref. 45):

$$C_T = \exp(\theta/Ta)(1 - (T_a/T) \qquad (9\text{-}20)$$

Where: T_a = ambient temperature, 298.2 °K or 536.7 °R
T = operating temperature, °K or °R

It is noted that the ratio θ/T is in the range between 4.0 and 20.0.

Table 9-1. Material Hardness
(Use ratio of hardest particle/cylinder hardness for C_H)

MATERIAL	HARDNESS (H_V)
Plain Carbon Steels	
Low strength steel	140
High strength steel	220
Low-alloy Steels	
4320	640
4340	560
Stainless Steels	
303	170
304	160
631 (17-7 PH hardened)	520
631 (17-7 PH annealed)	170
Austenitic AISI 201 (annealed)	210
Martensitic 440C (hardened)	635
630 (17-4 PH hardened)	470
Nickel Alloys	
201	100
Nickel-copper Alloys	
Monel (annealed)	120
Monel K-500 (annealed)	162
Ni-Cr-Mo-Fe Alloys	
Inconnel 625	140
Hastelloy	200
Aluminum	
AISI 1100 (annealed)	25
AISI 1100 (cold worked)	45
AISI 2024 (annealed)	50
AISI 2024 T4 (heat treated)	125
AISI 6061 (annealed)	32
AISI 6061 T6 (heat treated)	100

Table 9-2. Typical Component Generation Rates

COMPONENT	EXPECTED RATE OF CONTAMINANT GENERATION	C_N
Gear Pump	7.5 g/gpm rated flow	*
Vane Pump	25.0 " " "	
Piston Pump	6.8 " " "	
Directional Valve	0.008 " " "	
Cylinder	3.2 g/in^2 swept area	

* Add total grams of contaminants expected per hour/100 to determine C_N

Table 9-3. Values of Wear Coefficient (K) In The Severe-Wear Region (Ref. 45)

MATERIAL	K
4130 Alloy Steel (piston)	0.0218
4130 Alloy Steel (cylinder)	0.0221
17-4 PH Stainless Steel (piston)	0.0262
4130 Alloy Steel (cylinder)	0.0305
9310 Alloy Steel (piston)	0.0272
4130 Alloy Steel (cylinder)	0.0251

CHAPTER 10

PUMPS

10.1 INTRODUCTION

Pumps are the most common type of mechanical component used by today's society, exceeded only by electric motors. Not surprisingly, there are in existence today, an almost endless number of pump types that function in systems with dissimilar operating and environmental characteristics. Since there are so many different pump types, one tries to organize and classify them. It is possible to organize these components by their use, the materials used to construct them, or even by the type of fluid they move. However, these categories tend to overlap for many pump types. Therefore, a system to differentiate between all types of pumps is necessary. This system uses the way or means by which energy is added to the fluid being pumped, and is unrelated to application, material type, or outside considerations involving the pump. As seen by Figure 10.1, the pump is classified into two general classes; Dynamic and Displacement. These classes represent

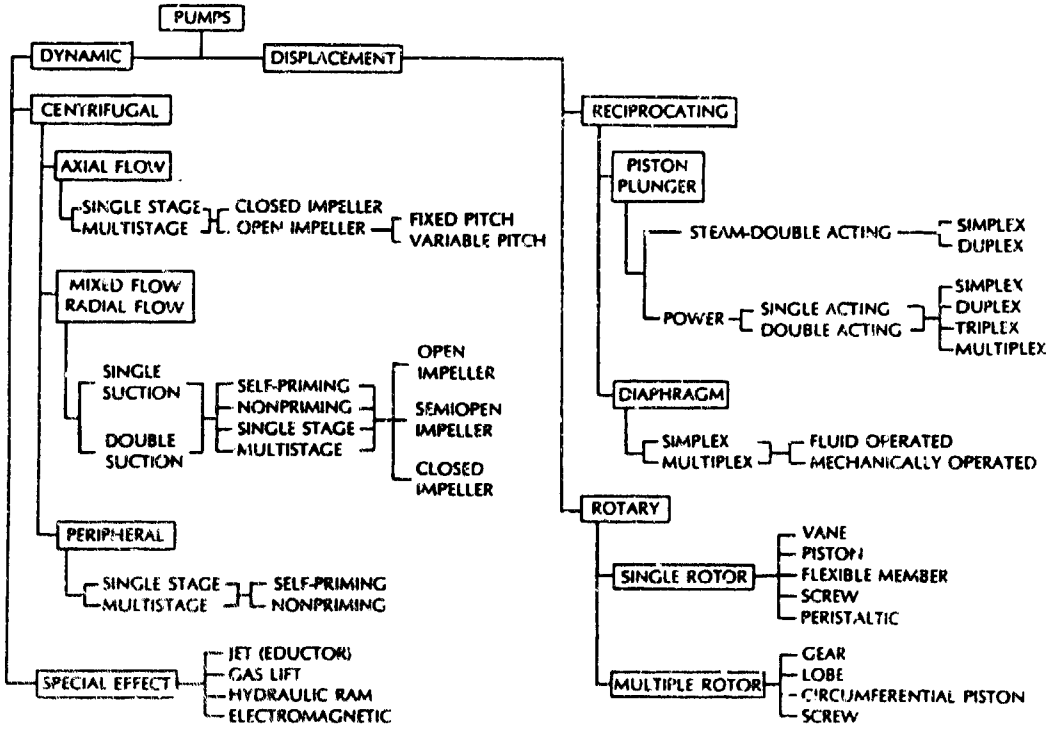

Figure 10.1 Pump Configurations (Ref. 26)

the two ways in which energy is added to the fluid. With dynamic pumps, the energy is added continuously by increasing the fluid velocity with a rotating impeller while reducing the flow area. This arrangement causes an increase in pressure along with the corresponding movement of the fluid. Displacement pumps, on the other hand, have energy added to the fluid periodically by the movement of control boundaries with fluid volumes being displaced causing an increase in pressure.

The dynamic pump can be subdivided further into the centrifugal and special effect categories while displacement pumps can be subdivided into the reciprocating and rotary types. These category breakdowns can then be addressed individually. The reliability models will be developed to address the difference between pump types.

Due to the physical design differences between dynamic and displacement pumps, some pump types have advantages over others. Figure 10.2 shows the basic advantages and disadvantages between the pump types. For example, the centrifugal pumps are limited by pressure but can supply almost any amount of capacity as desired. Some custom designed centrifugal pumps have been known to reach almost 3,000,000 GPM in capacity.

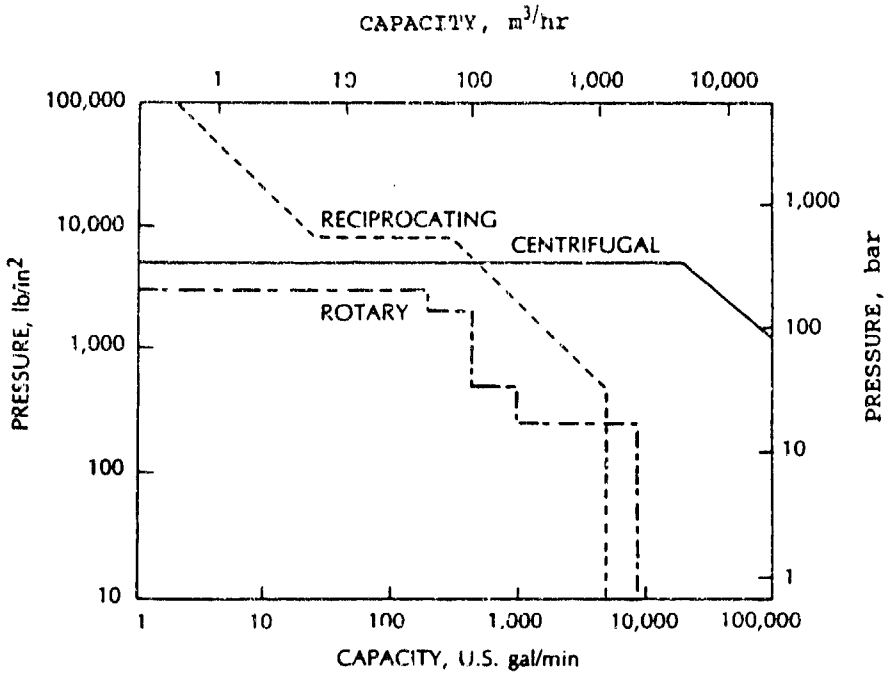

Figure 10.2 Approximate Upper Limit of Pressure and Capacity by Pump Class (Ref. 26)

Displacement pumps, however, lose capacity as the pressure increases. It is well known that as the pump pressure increases, there is a corresponding increase in slip. The amount of slip can vary from pump to pump depending on the actual manufactured clearances in the pump chamber. The slip can also increase with time as wear increases.

Equation (10.1) shows that since slip "S" increases as the pressure requirements increase, the value of capacity "Q" is thus decreased:

$$Q = (0.00433\ DN) - S \qquad (10\text{-}1)$$

Where:
- Q = Capacity, GPM
- D = Net fluid transferred or displaced by one cycle, ft^3
- N = Rotation speed (revolutions/minute)
- S = Slip, ft^3/min (The quantity of fluid that escapes the full rotor cycle through clearances or other "leak paths"

Therefore, high pressure designs are somewhat limited to the amount of capacity, although slip can be reduced. For example, the slip can only be reduced by decreasing the tolerances to the extent that the interference will not occur between moving parts. Interference can be a cause of extremely rapid failures.

10.2 FAILURE MODES

Due to the large number of pump types and applications, some failure modes are more prevalent than others. For example, with displacement pumps there is a much greater chance for cyclic fatigue to have an effect on the system than with centrifugal pumps. This is due to the inherent difference in designs. The displacement pumps have pressure transients which cause temporary unbalanced forces to be applied to the pump and its system. The displacement pump and driver shafting can experience much higher stresses during operation due to the uneven torque loading caused by this natural imbalance. On the other hand, the centrifugal pumps are more balanced and aren't as susceptible to large stress variations.

Cavitation: The formation of bubbles and then the later collapse of these vapor bubbles due to the pumps's dynamic motion is the basic definition of cavitation. In order for cavitation to occur, the local pressure must be at or below the vapor pressure of

the liquid. When a fluid flows over a surface having a curvature, there is a tendency for the pressure near the surface to be lowered. There is a separation of fluid flow lines where there are different velocity regions. Between these fluid regions, turbulence can form which may cause bubbles to occur if the pressure is low enough. The collapsing of these bubbles can cause noise and vibrations. Sometimes, these pressure changes can be very dramatic and cause extensive damage to impellers, casings or shafts. If exposed for a sufficiently long time, pitting or severe erosion can occur. In some instances impeller vanes have experienced 3/8 inch of material loss. This type of damage can cause catastrophic failures.

Cavitation generally occurs in the first stage of a multistage centrifugal pump, although second stages have also been found to be effected when the suction head is substantially reduced. With displacement pumps like the rotary screw, cavitation can also occur. For these pumps it is important to understand the characteristics of entrained and dissolved air with respect to the vapor pressure of the fluid medium. The rotary screw pump shows a greater tendency for cavitation when the total available pressure at the pump inlet is below atmospheric pressure. With both displacement and centrifugal pumps, cavitation can be identified and easily remedied. Many times the inlet piping arrangement can be modified which will cause flow patterns that alleviate the problem.

Interference: For rotary displacement pumps, the interference problem must be seriously addressed since very small distortions of rotors will decrease the clearance causing rubbing or direct impact between the moving parts of the rotary displacement pump. Thermal expansion can also pose a threat if there is no care taken in the proper selection of materials. Improper installation can also lead to interference problems. With centrifugal pumps, cavitation significantly increases the interference problem because cavitation causes vibration and imbalance. Interference can be avoided by designing the parts from the right elastic and thermal properties so that excessive load or temperature won't significantly deflect internal parts. Tolerances should be carefully adhered to.

Corrosion: Consideration must be made for other possible failure modes such as erosion corrosion and intergranular corrosion. Erosion corrosion is dependent on the rate of liquid flow through the pump and also angle of attack to which the fluid impinges on the material. Much of the knowledge for this type of corrosion is documented. Generally, the way in which materials

should be selected is to first determine whether there are abrasive solids in the fluid. If there are, then the base material should be selected for abrasive wear resistance; if not, then design for velocity/corrosion resistance. Intergranular corrosion is the corrosion of the grain boundaries of the material. For austenitic stainless steels, intergranular corrosion can be limited by keeping the carbon content below 0.03 percent.

Material Fatigue: This failure mode, which cycles the material with unequal loadings over time, can be countered by good material selection. Material fatigue occurs with all types of pumps, but may have more of an effect on displacement pumps, which have higher fluctuating stresses.

Pump Bearing Failure Modes: The shutdown of essential equipment can be an expensive undertaking. Although bearings are relatively inexpensive, they can cause costly shutdowns of important systems. Short bearing life for centrifugal pumps, for example, can be caused by a number of troubles including the following: misalignment, a bent shaft, a rotating part rubbing on a stationary part, a rotor out of balance causing vibration, excessive thrust caused by mechanical failure inside the pump, excessive bearing temperature caused by lack of lubrication, dirt or other contaminant in the fluid, excessive grease or oil in an anti-friction bearing housing, and rusting of bearings from water in housing. Most of these problems can be classified by the following failure modes: fatigue, wiping, overheating, corrosion, and wear.

Fatigue occurs due to cyclic loads normal to the bearing surface. Wiping occurs from surface to surface contact from loss of sufficient lubrication film thickness. This can occur from under-rotation or from system fluid losses. Overheating is shown by babbitt cracking or surface discoloration. Corrosion is frequently caused by the chemical reaction between the acids in the lubricants and the base metals in the babbitt. Lead based babbitts tend to show a higher rate of corrosion failures.

10.3 MODEL DEVELOPMENT

The impellers, rotors, shafts, and casings are the pump components which should generally have the longer lives when compared to bearings and seals. With good designs and proper material selection, the reliability of impellers, rotors, and shafts should remain very high. In order to properly determine total pump reliability, failure rate models have been developed for each pump component.

Pumps, just like the other mechanical components, are comprised

of many component parts including: Seals, Shaft, Bearing, Casing, and Fluid Mover.

The fluid movers will be further broken down into the various types common to pumps. These fluid movers can include the following two general categories for centrifugal pumps: impellers; and for displacement pumps, it will be broken down into two further subcategories: reciprocating and rotary. For reciprocating pumps the fluid drivers can be classified as piston/plunger type or diaphragm type. For rotary pumps the fluid drive is a vane type for single rotors and for multiple rotors it is common to find a gear, lobe, or screw type of fluid mover. Equation (10-2) describes the general equation for the failure rate of a pump. The total pump failure rate is a combination of the failure rates of the individual subcomponent parts:

$$\lambda_P = \lambda_{SE} + \lambda_{SH} + \lambda_{BE} + \lambda_{CA} + \lambda_{FM} \qquad (10\text{-}2)$$

Where: λ_{SE} = Total failure rate for all pump seals, failures/million cycles (See Chapter 3)

λ_{SH} = Total failure rate for the pump shaft, failures/million cycles (See Section 10.4)

λ_{BE} = Total failure rate for all pump bearings, failures/million cycles (See Chapter 7)

λ_{CA} = Total failure rate for the pump casing, failure/million cycles (See Section 10.5)

λ_{FM} = Total failure rate for the pump fluid driver, failures/million cycles (See Section 10.6)

The order of failure rankings for typical pump subcomponents which vary from high to low are as follows: seals, bearings, shafts, casings and fluid drivers. The casings and drivers tend to be replaced very infrequently. Because of this fact, emphasis will be placed on the seals, bearings and shafts.

10.4 FAILURE RATE MODEL FOR PUMP SHAFTS

The reliability of the pump shaft itself is generally very high when compared to other components. Studies have shown (Ref. 26) that the average MTBF for the shaft itself is over eight times greater than mechanical seals and over three times that of the ball bearings. The possibility that the shaft itself will fracture, or become inoperable is very unlikely when compared to the more common pump failure modes. Usually the seals or bearings will cause problems first. The effects the shaft has on the reliability of

the other components is of greater importance than the reliability of the shaft itself.

The pump shaft reliability model is shown by Equation (10-3):

$$\lambda_{SH} = \lambda_{SH,B} \cdot C_{ASF} \cdot C_{DSF} \cdot C_{SE} \cdot C_{CON} \cdot C_{D} \qquad (10\text{-}3)$$

Where: $\lambda_{SH,B}$ = The pump shaft base failure rate, failures/million cycles
C_{ASF} = Shaft surface finish factor
C_{DSF} = Material temperature factor
C_{SE} = Material endurance limit factor
C_{CON} = Contamination factor
C_{D} = Pump displacement factor

The multiplying factors account for environmental conditions that vary from the normal operation. The base failure rate represents values that can be expected if all conditions during normal operation are what was originally designed for by the manufacturer. The following discussion explains the values for each multiplication factor.

Shaft Surface Finish Factor: C_{ASF} is the shaft surface finish factor that adjusts the reliability value by an amount depending on the type of manufactured finish. If the normal design calls for particular finish, then a variation from this finish will alter the life expectancy of the shaft. Table 10-1 shows the values and equations for the various finishes versus material tensile strength.

Table 10-1. Pump Shaft Surface Finish Factor

FINISH	C_{ASF}
Polished	1.0
Ground	0.89
Hot Rolled	$C_{ASF} = 0.9381 - 0.0046TS + 8.37 \times 10^{-6} (TS)^2$
Machined or Cold Drawn	$C_{ASF} = 1.073 - 0.00514TS + 2.21 \times 10^{-5} (TS)^2 - 3.57 \times 10^{-8} (TS)^3$
As Forged	$C_{ASF} = 0.746 - 4.06 \times 10^{-3} + 7.58 \times 10^{-6} (TS)^2$

Note: TS = Tensile Strength of Material in kpsi

Material temperature factor: The temperature factor C_{DSF}, represented by Equation (10-4), is applicable for steels at temperatures greater than 160 °F. However, for temperatures below 160 °F unity is used.

$$C_{DSF} = \frac{\frac{1}{460 + T_{AT}}}{\frac{1}{460 + T_{OD}}} \qquad T > 160°F \qquad \textbf{(10-4)}$$

Where: T_{OD} = Design operating temperature, °F
T_{AT} = Actual operating temperature, °F

Material endurance limit factor: The material endurance factor will be approximated by the factor C_{SE}, which is the ratio of endurance limits between what the original design specified and what was actually installed and used. This factor, as described by Equation (10-5), shows the relationship between the design endurance limit, S_{ED}, and the actual endurance limit, S_{EA}.

$$C_{SE} = \frac{S_{ED}}{S_{EA}} \qquad \textbf{(10-5)}$$

The endurance limits for some common steels and alloys are shown in Table 10-2. These values may be used as inputs for Equation (10-5).

Contamination factor: The contamination factor, C_{CON}, was developed from research performed for the Naval Air Warfare Center in Warminster, Pennsylvania on the effect of contamination and filtration level on pump wear and performance. The contamination factor equation is shown below:

$$C_{CON} = \frac{C_{PAC}}{C_{PDS}}$$

Where: $C_{PAC} = 0.5607 + 0.5321F_{AC}$
$C_{PDS} = 0.5607 + 0.5321F_{DS}$
F_{AC} = Actual filtration level, (MABS)

F_{DS} = Design filtration level, (MABS)

Table 10-2. Average Values of Endurance Limits (Ref. 39)

MATERIAL *	TENSILE STRENGTH		ENDURANCE LIMIT (S_{ED})	
	MPa	kpsi	MPa	kpsi
G43400 Steel	965	140	489	71
	1310	190	586	85
	1580	230	620	90
	1790	260	668	97
G43500	2070	300	689	100
R50001 Titanium Alloy	1000	145	579	84
A97076 Aluminum Alloy	524	76	186	27
C63000 Aluminum Bronze	806	117	331	48
C17200 Beryllium Copper	1210	175	248	36

* Alloys are heat treated, hot worked; specimens are smooth, subjected to long life rotating beam tests

Pump displacement factor: The pump displacement factor, C_D, will vary with the amount of load the shaft will see. This factor will be equated to a casing thrust load factor, C_{TLF} (Equation 10-9) multiplied by the normal shaft displacement factor, C_{DY} (Equation 10-8).

$$C_D = C_{DY} \cdot C_{TLF} \qquad (10\text{-}7)$$

Shaft misalignment or excessive deflection seems to have a great influence on the life of the pump bearings and seals. Equation (10-8) (Ref. 8) expresses the shaft displacement factor, C_{DY}. Figure 10.3 shows the dimensions specified in Equation (10-8). The casing thrust load factor C_{TLF}, will be dependent upon the casing type and normal pump capacity percentage. The pump capacity percentage is the actual operating flow divided by the maximum pump specification flow, in GPM.

$$C_{DY} = \frac{F}{3E}\left[\frac{N^3}{I^N} + \frac{M^3 - N^3}{I^M} + \frac{L^3 - M^3}{I^L} + \frac{L^2 X}{I^X}\right] \qquad (10\text{-}8)$$

Where: F = Hydraulic radial unbalance force
E = Modulus of elasticity of shaft material, psi
N, M, L, X, DX, DM, DN, and DL are shown in Figure 10-3
I = Moment of Inertia, in^4

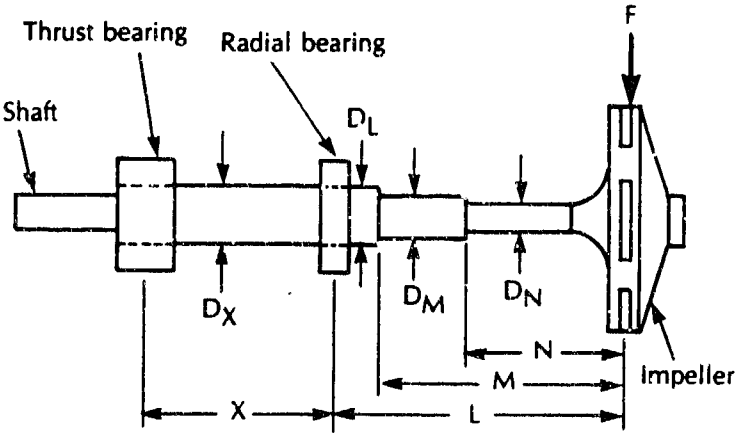

Figure 10-3. Shaft Deflection Depends on Various Dimensions (Ref. 8)

Because operational and maintenance costs tend to rise with increasing shaft deflection, new pump designs try to decrease possible shaft deflection. For centrifugal pumps, there is a large difference in deflection between the type of pump casing design. In a single volute casing, there are varying amounts of fluid pressure distributed about the casing causing unequal distributions of forces on the pump shaft. This imbalance causes shaft deflection and greater seal and bearing wear.

The amount of radial thrust will vary depending on the casing design and on the amount of the operating flow. The thrust load will increase from normal operation for any type of casing design when the pump is not run at its optimum flow rate speed. When the pump is not operating at its optimum rate, then the type of casing design will have a significant effect on the radial load.

The single volute type shows the greatest pressure imbalance and

hence, the greatest deflection. Pump designers have learned to decrease this imbalance through different casing designs. The modified concentric casing and the double volute casing both have lower relative radial thrust because they cause a more even pressure distribution across the face of the impeller. The double volute is the most balanced and the design with the least amount of radial thrust. The maximum deflection now recommended for a shaft design is approximately 0.001 inches when operating at a capacity between 0.25 and 1.25 of it's optimum points.

$$C_{TLF} = \frac{[(Tr / Trmax)\ actual]}{[(Tr / Trmax)\ design]} \qquad (10\text{-}9)$$

For Ordinary Volute Casings:

For $0 < Q/Qr < 100$:

$$\frac{Tr}{Trmax} = 99.38 - 0.09\left(\frac{Q}{Qr}\right) - 0.10\left(\frac{Q}{Qr}\right)^2 + 1.77 \times 10^{-5}\left(\frac{Q}{Qr}\right)^3 \qquad (10\text{-}10)$$

and for $100 < Q/Qr < 180$:

$$Tr/Trmax = -247.26 + 3.26\ (Q/Qr) + 3.26\ +(Q/Qr)^2 - 0.0084\ (Q/Qr)^3 \qquad (10\text{-}11)$$

For Modified Concentric Casings:

For $0 < Q/Qr < 180$:

$$Tr/Trmax = 53.05 - 0.055\ (Q/Qr) - 0.012\ (Q/Qr)^2 + 1.26 \times 10^{-4}\ (Q/Qr)^3 - 4.63 \times 10\text{-}7\ (Q/Qr)^4 + 6.77 \times 10^{-10}\ (Q/Qr)^5 \qquad (10\text{-}12)$$

For Double Volute:

For $0 < Q/Qr < 40$:

$$Tr/Trmax = 10.72 - 4.785\ (Q/Qr) \qquad (10\text{-}13)$$

and for $40 < Q/Qr < 180$:

$$Tr/Trmax = 14.292 - 0.297\ (Q/Qr) + 4.11 \times 10^3\ (Q/Qr)^2 \quad (10\text{-}14)$$

Where: Q = Actual operating flow, gpm
Qr = Maximum pump specification flow, gpm

10.5 FAILURE RATE MODEL FOR IMPELLERS, CASINGS, AND ROTORS

The pump casing is a very reliable component. Defined as λ_{CA}, the case will have a greater effect on total pump reliability from the standpoint of how it effects other less reliable components. For instance, for an ANSI pump, the casing may have an average life expectancy of 10 years where a seal or bearing may have only one or two years. However, the type of casing used in the pump can have a large effect on the lifetime of the bearings and seals. This is due to differing loads placed on the pump shaft by the fluid flow pattern. The fluid flow patterns are a function of the casing design. As shown in the following equations, the thrust will vary with the type of casing design and the pump flow rate. The value for reliability of the pump casings (λ_{CA}) themselves will be presently equated to .0001 failures/million cycles.

10.6 FAILURE RATE ESTIMATES FOR FLUID MOVERS

All pumps require some vehicle to move the fluid from the intakes and expel it through the volutes to the exhaust opening. The means by which pumps do this is what differentiates most of today's numerous types of pumps. The reliability of these fluid movers will vary from pump to pump. Impellers will wear out long after the seals. Pump gears for rotary gear pumps will have a lower reliability than impellers due to the nature of the contact between gears and the speed they attain.

Piston-plunger displacement pumps will generally have larger wear rates for the piston walls and rings than for the impellers of centrifugal pumps. The following average failure rates have been determined from data base information developed from the Navy.

The equations that describe the "fluid driver" wear rate may vary drastically since the "fluid driver" varies greatly in design and application. See Table 10-3 for the general categories for the fluid driver.

Since there are many types of fluid drivers, many reliability models are required to be developed. However since little data is available for each model, a base failure rate can be used to quantify these variations until fully developed models are established. Failure of the fluid drivers themselves are much less likely than failures of the other subcomponent pump parts.

Table 10-3 Failure Rates for Pump Fluid Drivers (λ_{FM})
(Ref. 26)

PUMP TYPE	FLUID DRIVER MODE	MODEL TYPE	BASE RATE*
Centrifugal	Axial Flow Impeller	Closed/Open Impellers	0.1 - 0.3
	Mixed Flow/Radial Flow Impeller	Open/Semi-Open/Closed Impellers	0.1 - 0.14
	Peripheral	Single Stage/Multi-Stage	0.1 - 0.3
Displacement	Reciprocating	Piston/Plunger	1.0 - 1.35
	Reciprocating	Diaphragm	0.4 - 0.75
	Rotary (Single Rotor)	Vane	0.2 - 0.6
	Rotary (Single Rotor)	Piston	0.9 - 1.2
	Rotary (Multiple Rotor)	Gear	0.6 - 0.9
	Rotary (Multiple Rotor)	Lobe	0.4 - 0.5
	Rotary (Multiple Rotor)	Screw	0.2 - 0.95

* Failures/million hours of operation

THIS PAGE INTENTIONALLY LEFT BLANK

CHAPTER 11

FILTERS

11.1 INTRODUCTION

Fluid filtration equipment is unique in that the reliability of this equipment is more concerned with the effects of the filter on associated equipment than on the lifetime of the filter itself. This is due to severe wear of fluid system components which can occur when these components are operated with poorly filtered fluid. This chapter will review the conditions which can lead to degradation or failure of the filter. The effects of contamination on the wear of various components is also discussed. A basic failure rate model with correction factors will also be developed.

11.2 FILTRATION MECHANISMS

Filters are constructed of a porous filter media through which fluid is passed. The filter media is typically corrugated to increase the amount of filtration area in the filter volume. Filtration of gases is accomplished by absorption and direct interception of the suspended particles. Filtration of liquids is primarily accomplished by direct interception of the suspended particles.

11.3 SERVICE LIFE

The porous structure of a filter media presents a resistance to fluid flow which causes a pressure drop across the filter. This filter differential pressure increases as captured particles or contaminants are collected and plug the porous media. Every system has a maximum differential pressure at which the filter must be cleaned or replaced. The filter service life is the time it takes the filter to reach the maximum allowable differential pressure. Use of the filter beyond its service life could result in catastrophic failure of the filter due to the high differential pressure or it could result in unfiltered fluid bypassing the filter (Ref. 33)

11.4 FILTER FAILURE

A filter is considered to have failed when it releases previously captured contaminants, when it allows unfiltered fluid

to pass throughout the filter media, or when the filter collapses and contaminates the fluid with filter media. Plugging of the filter with contaminants, with a resulting increase in filter differential pressure, is a normal consequence of operation and is not considered a failure even if it occurs prematurely. Failure of the filter can be caused by operating conditions such as high differential pressures, cyclic flow, vibration, system startups when cold, and even the fluid being filtered, if the fluid is incompatible with the filter.

11.5 FILTER FAILURE MODES

Channelling: Excessively high differential pressures can cause filter media pores to enlarge, allowing large amounts of unfiltered fluid to bypass the filter media. Enlargement of the media pores also allows previously captured contaminants to be released. Channelling can also be the result of media fatigue caused by cyclic flow conditions.

Fatigue Cracks: Cyclic flow conditions in the fluid system can cause fatigue cracks in the filter media. Such cracks may occur at the roots of pleats in corrugated filters or within the volume of loose packed media. The cracks will allow the release of contaminants from the filter and will allow some of the fluid to bypass the filter. Media fatigue can result from cyclic flow conditions such as varying system flow requirements, pump ripple, or cold system startups.

Media Migration: Improper bonding of the media fibers or deterioration of the bonding can result in the down stream release of media fibers. This downstream release of the filter media is termed media migration. Media migration during vibration of the filter may result from an improper fit of the filter in the filter housing or may result from the filter media abrading against the filter casing. Media migration can also occur in conjunction with fatigue cracks in the media, as caused by cyclic flow conditions. Media migration can also occur during cold temperature start-ups due to potential large differential pressure generated as a consequence of increased fluid viscosity.

Filter Disintegration: Complete disintegration of the filter can occur as a result of extremely high differential pressures. Disintegration can also be the result of embrittlement of the filter media from exposure to incompatible fluids or cold temperatures.

Plugging: Plugging of the filter media can be either a normal consequence of operation or failure, depending upon when plugging

occurs. Failure due to premature plugging can be attributed to several causes other than just the accumulation of wear debris. As an example, Hudgens and Feldhaus (Ref. 24) have found that lubrication oil filters in diesel engines can plug by any one of six mechanisms. While some of these are particular to internal combustion engines, the mechanisms may be applicable to any oil-based fluid system. The six mechanisms can be summarized as follows:

1. Absorption of water in the oil from condensed moisture and/or coolant leakage can cause insoluble contaminants, normally dispersed into the lubricating oil, to dump out of suspension. This condition can also arise when there is a combination of moderate soot load, low pH and a high level of oxidation produced in the oil. A filter plugged under these circumstances will be marked by a sticky, shiny, adherent sludge with wavy pleats and the filter will have accumulated from 1/3 to 1/2 of its total contaminant capacity.

2. Saturation of the oil with excessive amounts of combustion contaminants, due to engine problems or overextended oil drain internals, can also cause filter plugging. The filter will appear to have a thick, loosely-held sludge. The filter will have accumulated from 1/3 to 1/2 of its total contaminant capacity typically but it can accumulate up to 100 percent in extreme cases.

3. Absorption of oxidation products such as degraded fuel and oil will also cause the filter to plug and the filter will have accumulated 40 percent to 50 percent of its contaminant capacity. The filter does not appear to have sludge buildup but it does appear to have a brown tint and to be covered by blown snow. The problem occurs most often with API CC spec lubricating oils where overheating or fuel dilution is a problem.

4. Moisture condensation or coolant leakage into the oil reservoir can cause filters to plug as a result of oil additive precipitation. Plugging of the filter can occur at 8 percent to 30 percent of the filter's contaminant capability. The filter will have a gray coloration but no sludge build up.

5. Coolant or moisture can also combine with oil additives to form thick, filter-plugging gels. The filter media in such circumstances will be wavy with a sticky feel but will usually look clean. Filters plugged due to gel formation usually reach only 3 percent to 6 percent of their contaminant capacity before plugging.

6. Accumulation of wear debris also causes filters to plug. In this failure mechanism, the filter plugs by retention of 100 percent or more of its full contaminant capacity. The filter will

appear to have a buildup of visible wear particles on the filter media.

A summation of typical filter failure modes and causes is given in Table 11-1. A summary of the characteristics of the filter-plugging mechanisms, along with more specific information, is provided in Table 11-2.

Table 11-1. Failure Modes of Filters

FAILURE MODE	FAILURE CAUSE	RESULTS OF FAILURE
Channeling	High differential pressures Cyclic flow	Release of contaminants Circulation of unfiltered fluid
Fatigue Cracks	Cyclic flow	Circulation of unfiltered fluid Release of filter media
Media Migration	Vibration Cyclic flow Cold starts	Release of filter media
Filter disintegration	Embrittlement Cold starts High differential pressures	Substantial contamination of fluid with filter media

11.6 FLUID CONTAMINATION EFFECTS

Fluid system component failures related to particulate contamination of the operating fluid are usually either catastrophic or deterioration failures. Catastrophic failures occur when the system components are operated under intolerable conditions. Catastrophic failures may also be the result of wear occurring over a long period of operation. Failures due to component deterioration typically involve a fairly rapid change in component performance, falling below a satisfactory level after a period of normal operation.

Contamination of the operating fluid with hard particles can cause progressive performance deterioration through an abrasive

Table 11-2. Characteristics of Filter Plugging Mechanisms

PLUGGING MECHANISM	APPEARANCE			RETAINED SOLIDS (PERCENT CAPACITY)	MOISTURE CONTENT (PERCENT)	ASH CONTENT (PERCENT)	OIL CONTAMINANTS PERCENT CPI*
	SLUDGE	WAVY PLEATS	OTHER				
Impaired Dispercancy	Yes	Yes	Adherent sticky sludge	42-50	0.2	2-5	2-5
Excessive Contamination	Yes	No	Sludge loosely held	42-50 100 extremes	0.5	3	5
Oxidation	No	No	Brown tint or coloration	42-50	0.2	2-5	0.5-3
Additive Precipation	No	Yes	Grey coloration	8-33	0.2	10-20	3
Gel Formation	No	Yes	Clean appearance sticky feel	3-6	0.2-3	3	
Wear Debris	No	No	Wear metals noticeable	p	0.2	5-25	

*CPI = Coagulated Pentane Insolubles

wear mechanism. This type of wear is characterized by a particle penetrating a softer surface and cutting away material. The rate of wear and thus the rate of performance degradation is dependent on the number of particles and the particle hardness. Particle contamination can also cause cumulative performance degradation where a rapid decline in performance follows an extended period of apparently normal operations. This type of degradation failure is caused by the creation of surface defects during operation. These surface defects may be caused by abrasion, surface fatigue or adhesion wear processes.

Fluid systems requiring filtration typically include components such as pumps, gears, control valves, ball bearings, roller bearings, journal bearings, and seals.

Pumps: In displacement-type piston pumps, the piston face can be damaged by cavitation or corrosion. Contaminant particles can enter the lubricant film between the piston and cylinder and plough the surface several times before being ejected. In swashplate controlled devices, such as variable displacement pumps and hydraulic motors, the piston shoes can cause abrasion-wear-type degradation failures as the shoes are highly loaded and are in sliding contact with the swashplate. Similar abrasive-wear-type degradation failures can occur to the sliding contact surfaces of the rotating cylinder block and the mating valve pressure plates (Ref. 7)

Gears: Gear failures are primarily failures of the gear tooth surface. This surface is damaged by rubbing wear, scoring, pitting, and plastic flow. Rubbing wear occurs when the lubricant film is insufficient to separate the tooth surfaces and is generated by both adhesive and abrasive wear mechanisms. Scoring of the tooth surface is generated by the adhesive wear type mechanisms under intense local frictional heating. Pitting and plastic flow both occur as a result of tooth surface fatigue wear (Ref. 7)

Valves: Particle contamination can cause increased leakage in control valves by severe cutting or by milder abrasive wear mechanisms. Synthetic phosphate ester fluids have been found to cause servo valve erosion by a streaming-potential corrosion process. A brittle corrosion layer is formed on the valve and is abraded by fluid-borne particles, adding additional particulates to the fluid and exposing base metal, allowing further corrosion. Deterioration failures of relief valves can occur from particle contamination caused by erosion. Contamination of hydraulic fluid

by water has been shown to cause rust inhibitor additive to attach to servo valve spools and prevent movement of the valve spool within its housing (Ref. 7).

Bearings: Hard particle contamination of ball and roller bearing lubricants is the cause of two types of abrasive wear of the rolling surfaces. Hard particle contamination causes rolling surface damage that dominates the fatigue life of ball bearings under typical operating conditions. In severe circumstances, hard particle contamination causes indentations and pits which cause rapid failure of the rolling surfaces. Abrasive wear, increasing with particle concentration and hardness, can remove material from the sliding edges of a tapered rolling bearing, reducing the bearing width and allowing increased misalignment. Wear of this type does not stop until the contaminant size is reduced to less than the lubricant film thickness.

The performance of new journal bearings improves with use initially due to better surface conformity caused by wear during boundary lubrication conditions. As wear in the contact region progresses, the performance begins to gradually deteriorate. Wear of the journal bearings is caused by both abrasive and adhesive wear due to the sliding motion in the contact region. Contamination of the lubricant with water can cause the formation of a metal oxide boundary layer on the bearing which can inhibit adhesive wear. However, abrasion of this film can cause bearing failure due to rapid increases in wear, bearing corrosion, and the number of abrasive oxide particles. Maximum bearing life can be achieved by selecting a filter to filter out all particles larger than the minimum lubricating film thickness. (Ref. 7).

Seals: Seal failures are typically caused by fatigue-like surface embrittlement, abrasive removal of material, and corrosion. Elastomeric seals are more sensitive to thermal deterioration than to mechanical wear. However, hard particles can become embedded in soft elastomeric materials and sliding contact metal surfaces, causing leakage by abrasive wear of the harder mating surfaces. Abrasive particles can also plug lubricant passages which causes seal failure from the lack of lubricant. Seal failures can be reduced by reducing the amount of contamination through filtration and concern for the operating environment (Ref. 7).

11.7 RELIABILITY MODEL

A basic filter reliability model can be developed by modeling the fluid system incorporating the filter. By modeling the flow of

particulates through the system, an expression for the rate of retention of particulates by the filter may be developed. This expression, a function of the system and filter parameters, can then be integrated to a form which can be used to calculate the mass of particulates stored within the filter at time T. The amount of stored mass at time T can be compared with the filter capacity, typically a known parameter, to determine the filter reliability.

In order to simplify the development of an initial filter model, the following assumptions were made:

1. The rate of generation of contaminate particulates by system components and the rate of ingestion of environmental contaminates do not vary with time and the particulates are evenly mixed within the system fluid. Furthermore, the rates of generation of contaminant particulates by system components may be modeled using Table 3-11.

2. The system fluid volume and flow rates do not change with time.

3. The system fluid volume may be represented as one lumped sum so that the individual components and lines need not be modeled.

4. The filter will not plug or become unusually restricted prior to reaching its maximum capacity.

A typical hydraulic system consists of a reservoir, pump, filter, one or more control valves, and one or more fluid motors. Such a system can be simplified using the above assumptions to resemble the diagram in Figure 11.1.

Using a diagram similar to that of Figure 11.1, Hubert, Beckand Johnson (Ref. 23) developed an expression for the concentration of contaminant particulates upstream of the system filter at any time, t, as a function of system fluid volume, flow rate, filter efficiency and total contaminant ingestion rates. This is:

$$C_u(t) = C_o - \left(\frac{M_{ci}}{\varepsilon Q}\right) e^{-\frac{[\varepsilon Q]}{V} t} + \left(\frac{M_{ci}}{\varepsilon Q}\right) \qquad \text{(11-1)}$$

Where: $C_u(t)$ = Concentration of contaminant particulates upstream of the system filter at any time t (mg/ml)

M_{ci} = Generation rate of contaminant particulates from all sources and of all sizes (mg/ml)

ϵ = Overall filter efficiency
Q = Volumetric fluid flow rate through filter, (ml/mm)
V = Volume of fluid
C_0 = Initial concentration of contaminant particulates

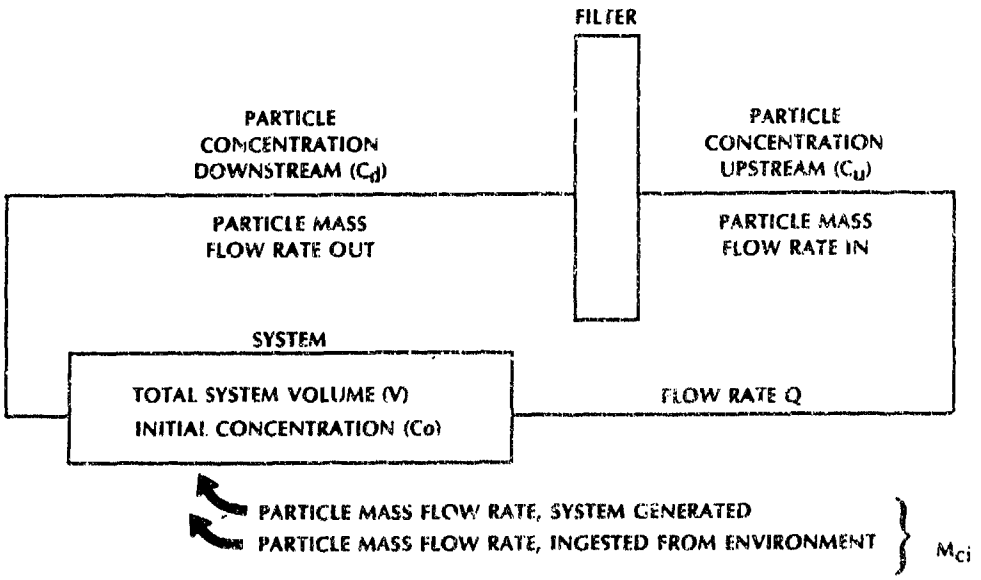

Figure 11.1 Simplified Fluid System with Filter

The concentration of contaminant particulates downstream of the filter can be calculated knowing the filter efficiency and the concentration upstream:

$$C_d = (1 - \epsilon)\, C_u(t) \qquad (11\text{-}2)$$

The mass of contaminate particles retained by the filter is then:

$$M_{filter} = \int_0^t [(C_u(t) - C_d(t)]\, Q dt \qquad (11\text{-}3)$$

Substituting Equation (11-2) into Equation (11-3) yields:

$$M_{filter} = \int_0^t \varepsilon\, C_u(t)\, Q dt \qquad (11\text{-}4)$$

and substitution of Equation (11-1) into Equation (11-4) yields:

$$M_{filter} = \int_0^t \left[(\varepsilon\, Q\, C_o - M_{ci})\, e^{\frac{-\varepsilon Q T}{V}} + M_{ci} \right] dt \qquad (11\text{-}5)$$

This is then integrated to yield the following expression of the retained mass as a function of time:

$$M_{filter} = (\varepsilon Q C_o - M_{ci})\, (e^{\frac{-\varepsilon Q t}{V}} - 1) + M_{ci} t \qquad (11\text{-}6)$$

Knowing the system parameters and the filter contaminant capacity, the filter lifetime can be calculated on a trail-and-error basis using (note the presence of the variable t on both sides of the equation):

$$t = -\frac{V}{\varepsilon Q} \ln \left[\frac{FCC + \varepsilon q c_o - M_{ci}(1-t)}{\varepsilon Q C_o - M_{ci}} \right] \qquad (11\text{-}7)$$

Where: FCC = Contaminate capacity of the filter (mg)
t = Lifetime in minutes

Solution of Equation (11-7) for t yields a base service life t which can be used to calculate the base failure rate for the filter:

$$\lambda_{F,B} = \frac{(6.0 \times 10^7)}{t} \qquad (11\text{-}8)$$

Where: $\lambda_{F,B}$ = Base failure rate of a filter in normal operation (failures/million hours)

The complete filter failure rate model should use adjustments, or correction factors, to modify the base failure and to account for potentially degrading effects of off-design operating conditions. Considering the causes of failures as earlier discussed, the failure rate model is:

$$\lambda_F = \lambda_{F,B} \cdot C_{DP} \cdot C_{CF} \cdot C_V \cdot C_{CS} \cdot C_E \cdot C_T \qquad (11\text{-}9)$$

Where: λ_F = Failure rate of the filter in failures/million hours

$\lambda_{F,B}$ = Base failure rate of the filter in failures/million hours

C_{DP} = Multiplying factor which considers the effects of the filter differential pressure on the base failure rate

C_{CF} = Multiplying factor which considers the effects of cyclic flow on the base failure rate

C_V = Multiplying factor which considers the effects of vibration on the base failure rate

C_{CS} = Multiplying factor which considers the effects of cold start-up conditions on the base failure rate

C_E = Multiplying factor which considers the effects of incompatible fluids and materials on the base failure rate

C_T = Multiplying factor which considers the effects of temperature on the base failure rate

Assuming that the filter may be modeled as a thick-walled cylinder, the correction factor for filter differential pressure (C_{DP}) may be developed from the following equation for radial stress (Ref.39).

$$\sigma_r = \frac{P_i a^2 - P_o b^2 + \dfrac{a^2 b^2 (P_o - P_i)}{r^2}}{b^2 - a^2} \qquad (11\text{-}10)$$

Where: σ_r = Radial stress
a = Inside radius
b = Outside radius
P_i = Inside pressure, design
P_o = Outside pressure, design
r = Radius corresponding to maximum stress

For most filters, the equation for radial stress can be used to model the effects of high differential pressure on the filter media by developing a ratio of off design stresses to design stresses. By indicating the off design inside and outside pressures by P_i' and P_o', and by dividing the corresponding off design stress by the design stress, the following equation for C_{DP} can be derived:

$$C_{DP} = \frac{P_i' a^2 - P_o' b^2 + \frac{a^2 b^2 (P_o' - P_i')}{r^2}}{P_i a^2 - P_o b^2 + \frac{a^2 b^2 (P_o - P_i)}{r^2}} \qquad (11\text{-}11)$$

Where: P_i' = off design inside pressure
P_o' = off design outside pressure

In most filter installations, the flow of fluid through the filter is from the outside to the inside. In this case, the maximum stress will be found at the outer radius, i.e., r = b. Substitution of this into Equation (11-11) results in:

$$C_{DP} = \frac{P_o'}{P_o} \qquad (11\text{-}12)$$

Cyclic flow, pressure surges, and pump ripple have been shown as having significant effects on filter lifetimes. The multiplying factor for the effects of cyclic flow on filters with outside to inside flow is:

$$C_{CF} = \frac{1.7a_2(2P_{i\,max} - 0.3P_{i\,min}) - 0.7P_{o\,max}(a^2+b^2) - 0.3P_{o\,min}(a^2+b^2)}{1.4\ S_T\ (b^2 - a^2)} \qquad (11\text{-}13)$$

Where: $P_{i\ max}$ = Maximum inside pressure
$P_{i\ min}$ = Minimum inside pressure
$P_{o\ max}$ = Maximum outside pressure
$P_{o\ min}$ = Minimum inside pressure
S_T = Tensile strength of filter media

Most filters are tested for media migration caused by vibration. A typical test is performed with the filter immersed in the system fluid and the filter is exposed to low amplitude, high frequency vibrations for about 100,000 cycles. As a result, most filters will not degrade due to vibration. However, in aircraft environments, failure of the filter housing and seals due to vibration accounts for 80 percent of the total filter failure rate (Ref. 15). Thus it appears that in most systems vibration is not a problem, but in aircraft systems excessive vibration can cause filter failure. As a result:

$C_V = 1.25$ for aircraft and mobile systems
$C_V = 1.00$ for all other systems

The normal operating temperature of the system fluid can also influence the filter reliability by affecting the differential pressure across the filter. The correction factor, developed from a curve for flow vs. differential pressure at various temperatures (Ref. 24) is:

$$C_T = \left(\frac{T}{200}\right)^{-4.97} \quad \text{For } 150\ ^\circ F < T < 250\ ^\circ F \qquad (11\text{-}14)$$

The correction factor for cold start degradation can be calculated using a ratio of the cold start fluid viscosity to the normal operating fluid viscosity. This is:

$$C_{CS} = \left(\frac{\nu_{cold\ start}}{\nu_{normal}}\right)^x \qquad (11\text{-}15)$$

Where: $\nu_{cold\ start}$ = Kinematic viscosity at cold start temperature, stokes

ν_{normal} = Kinematic viscosity at normal operating conditions, stokes

x = Exponent which varies with types of fluid

Values for ν and x may be obtained from Table 11-3.

The correction factor for the effect of incompatible fluids and materials increases the failure rate to compensate for the possibility of failure due to premature plugging. This factor is given in Table 11-4 for various system fluids and contaminants.

Table 11-3. Cold Start Data

FLUID	EXPONENT x	VISCOSITY, ν
SAE 10W-30	0.2	$17.4 - 0.5T + 0.00597T^2 - 0.0000359T^3 + 1.07E\text{-}07T^4 - 1.25E\text{-}10T^5$
KEROSENE	0.46	$0.0374 - 3.86E\text{-}04T + 1.796E\text{-}06T^2 - 3.036E\text{-}09T^3$

Table 11-4. Correction Factors for Contaminants

SYSTEM FLUID	CONTAMINANTS	C_g
Kerosene	Water	1.0 + 0.61 (percent water vol)
Hydraulic Oil	Water	1.0 + 2.64 (percent water vol)

CHAPTER 12

BRAKES AND CLUTCHES

12.1 INTRODUCTION

The principal function of a brake or clutch assembly is to convert kinetic energy to heat and then either to absorb or dissipate heat while simultaneously (through energy transfer) reducing the relative movement between the friction material and the part to which it is engaged. Reliability models for brakes and clutches are presented together in this Handbook because of similar design and operational characteristics; and because one of the most important functional parts of each of these components is the friction material. Section 12.2 addresses the brake model, which includes actuators, springs, friction linings, bearings, seals and housings. An analysis of the energy transfer materials which are common to both brakes and clutches is included in the brake model. Section 12.3 outlines and describes the reliability model for clutches, which includes the following subcomponents: actuators, bearings, friction linings, seals and springs.

12.2 BRAKES

12.2.1 Brake Assemblies

The reliability of a brake system is dependent on the reliability of its parts, which may include: actuators, bearings, friction linings, housings, seals, and springs. With the exception of friction linings, all these component parts are addressed in earlier sections of this handbook. The characteristics of these parts that are peculiar to the braking environment will be discussed in this section. Because friction materials are unique to brake and clutch components, an in depth analysis of these mechanical parts is presented in this section of the handbook.

In brake systems the rubbing elements include the friction material and a countersurface. The friction material is the sacrificial element, although the essence of good brake design is to minimize wear. The countersurface is usually metallic, to provide structure and to dissipate the frictional heat. Most countersurfaces are a grey cast iron drum or disc. In a few applications, steel rubbing surfaces are used. The countersurface

is also nominally a non-wearing surface. Countersurfaces typically wear from 1 to 20 percent of the total volume worn from the friction interface (Ref. 16).

Brakes are called upon to convert large amounts of kinetic energy to thermal energy in a very short time. The life of currently used brake lining materials is determined by wear, which in turn is strongly dependent on the temperature experienced by these materials during sliding. This temperature dependence is due largely to softening of the metal binder (usually copper or iron) present in brake lining composite materials.

Some of the systems which use brakes include passenger cars, light trucks, tractors, buses, agricultural equipment, construction equipment, industrial equipment, railroad trains and aircraft. Brake lining materials used in passenger cars and light trucks fall into two categories: drum brake segments, which are less than 3/4" thick, and disk brake pads.

Brake systems used by trucks, truck tractors, and trailer combinations are air assisted hydraulic (air brake) systems. The braking systems used by buses are similar to the conventional air brake system used by large trucks. Brake linings are almost entirely brake blocks used by the drum brake system. Conventional linings create excessive drum wear.

Agricultural, construction and industrial equipment each have different brake requirements. Agricultural equipment includes all equipment used in farming and forestry, such as tractors, harvesters, and log skidders. Construction equipment is used for the construction of roads, homes and buildings and includes wheeled tractors, rollers, scrapers, dozers, power truck cranes, hoists and shovel loaders. Industrial equipment encompasses all equipment used in fixed facility or buildings such as overhead cranes or hoists.

Hydraulic brake systems used in agricultural and construction equipment are of either the dry or the wet brake type. Dry brakes are the conventional types of drum or disk system. Wet brakes use drum and disk brake assemblies but the friction material is in a fluid environment. This type of brake exhibits decreased heat build up and subsequently less fade, reduced lining and drum or rotor wear and improved reliability.

Industrial equipment normally uses the conventional drum brake systems with organic binder/asbestos linings. In industrial equipment, such as cranes and hoists, wet brake systems are not used. As a result, an improved friction material with longer wear is needed in such systems. One of the major costs for overhead

cranes in industrial use is lining maintenance. Lining replacement is required every three to four weeks.

Most railroad trains rely on two braking systems - a dynamic brake and a friction brake. Most self-propelled rail cars have a dynamic brake, which is used either independently or together with the trains friction braking system down to about 5-10 mph, using complete friction braking for the last distance to a complete stop.

The use of organic friction materials in aircraft brakes is currently limited primarily to small general aviation aircraft. The trend in larger aircraft brake materials has been toward higher energy absorption per unit mass of brake materials. On larger aircraft organic friction materials have been replaced by more expensive copper and iron-based metallics. Disk brakes, with one brake for each of the main landing gears is common.

12.2.2 Brake Varieties

There are numerous brake system types, each with its own parts and reliability characteristics:

A. Band Brakes - Simpler and less expensive than most other braking devices. Component parts include friction band element and the actuation levers. Characterized by uneven lining wear and poor heat dissipation.

B. Externally and Internally Pivoted Drum Brakes - Simple design requiring relatively little maintenance. May become self-locking with extreme wear if not properly designed. Component parts include friction materials, springs, actuators, housings, seals, and bearings. Internal types offer more protection from foreign material.

C. Linearly Acting External and Internal Drum Brakes - These brakes are fitted with shoes that, when activated, approach the drum by moving parallel to a radius through the center of the shoe. Springs between the friction materials may separate both shoes when the brake is released. Lining wear is more uniform in comparison with internal drum brakes. Component parts include friction materials, springs, actuators, seals, housings, and bearings.

D. Dry and Wet Disk Brakes - Disk brakes have two main advantages over drum brakes: better heat dissipation and more uniform braking action. However, disk brakes require a larger actuation force due to the absence of either a friction moment or servo action. Both annular and pad type disk brakes are modeled here, and include friction materials, springs, actuators, housings, seals, and bearings. Wet disk brakes may operate in an oil bath.

Thus these brakes are isolated from dirt and water, and the circulation of the oil through a heat exchanger usually provides greater heat dissipation than direct air cooling. A reliability model for wet brakes is not included at this time.

E. Cone Brakes - Cone brakes have no general applications, and will not be modeled in this draft of the handbook.

F. Magnetic Particle, Hysteresis, and Eddy-Current Brakes - In all three of these brake types the braking torque is developed from electromagnetic reactions rather than mechanical friction, and therefore requires a source of electrical power.

The various types of brake systems and methods of actuation are listed in Table 12-1. There are numerous brake lining materials, manufacturing processes, brake types and systems in use today. For example, there are at least six basic methods of making brake linings: Dry process, extruded process, wet board process, sheeter process, sintered metal process and woven process. An analysis of typical linings indicate many common constituents. Chrysotile asbestos is found in most linings at roughly 50 percent (by weight). Rubber, resin, or a combination of both are used as lining binders. Brake lining fillers and friction modifiers include many metals, metallic compounds, graphite, coal rubber and resins. The specific choice of such materials results from controlled test type experimentation in the development of a friction material to meet specific performance goals. In addition to actual vehicle testing of a brake lining material, the industry uses several dynamometer laboratory test machines to characterize friction materials (Ref. 43).

1. Friction Material Test Machine - This apparatus attempts to record the brake lining performance by subjecting it to controlled conditions of pressure and temperature.

2. Friction Assessment Screening Test Machine - The rate of energy dissipation is controlled on a disk while temperature gradually increases.

3. Single End Inertial Dynamometer - An actual brake mechanism is incorporated.

4. Dual End Inertial Dynamometer - This uses the same instrumentation as the single end, but it is operated with one front and one rear brake assembly.

Table 12-1. Methods Of Actuation
(Ref. 32)

TYPE	ADVANTAGES	DISADVANTAGES	POINTS TO WATCH
Mechanical	Robust, simple operation gives good control	Large leverage needed	Frictional losses at pins and pivots
Pneumatic	Large forces available	Compressed air supply needed. Brake chambers may be bulky	Length of stroke (particularly if diaphragm type)
Hydraulic	Compact. Large forces available. Quick response and good control	Special fluid needed. Temperatures must not be high enough to vaporize fluid	Seals
Electrical	Suitable for automatic control, quick response	On off operations	Air gap

12.2.3 Failure Modes of Brake Assemblies

A list of failure modes for a typical brake system is shown in Table 12-2. The brake system friction materials are sacrificial replacements, and they account for most of the "failures". Because friction linings are designed to wear out before the life of the vehicle, service life may be a better measure of their durability than failure rate. For the purpose of compatibility with the other models developed for mechanical components, the lining life will be converted to a rate of failure. Use of the brake system beyond the life of the friction material results in catastrophic failure of the brake system caused by a loss of braking force due to a drastic reduction in coefficient of friction. A description of the countersurface failure characteristics are in Table 12-3.

Table 12-2. Mechanical Brake System Failure Modes (Ref. 9)

COMPONENT	FAILURE MODE	FAILURE CAUSE	FAILURE EFFECT
Piston	Sticking	Contamination	Low output pressure
Cylinder	Leaking	Contamination	Low output pressure
Spring	Broken/weak	Fatigue activation	Unable to adjust pressure
Bleeder Valve	Sticking	Contamination	Inadequate dissipation of air
Lining	Deterioration	Aged/Heat	Exposure metal-on-metal contact reduces arresting capability
Bearing	Worn out	Lack of lubrication	Low rotary motion
Seals	Worn out	Aged	External leakage
Housing	Cracked	Vibration, fatigue	External leakage

Table 12-3. Metal Countersurface Failures
(Ref. 32)

FAILURE	CHARACTERISTICS	CAUSES
Heat Spotting	Often cracks are formed in these regions owing to structural changes in the metal	Friction material not sufficiently conformable to the metal member
Crazing	Randomly oriented cracks	Overheating and repeated stress cycling
Scoring	Scratches in the line of movement	Metal too soft for friction material. Abrasive debris embedded in the lining material

12.2.4 Brake Model Development

The brake system will be reduced to its component parts. Brake systems will contain many of the following components:

- Actuators
- Springs
- Brake friction linings
- Bearings
- Seals
- Housings

Components like brake shoes, which are primarily structural, should be modelled using Finite Element Analysis Techniques.

The total brake system failure rate is the sum of the failure rates of each of the above subcomponent parts in the system:

$$\lambda_{BR} = \lambda_{AC} + \lambda_{SP} + \lambda_{FR} + \lambda_{BE} + \lambda_{SE} + \lambda_{HO} \qquad (12\text{-}1)$$

Where: λ_{BR} = Total failure rate for the broke system, failures/million hours

λ_{AC} = Total failure rate for actuators, failures/million hours

λ_{SP} = Total failure rate for springs, failures/million hours

λ_{FR} = Total failure rate for brake friction materials, failures/million hours

λ_{BE} = Total failure rate for bearings, failures/million hours

λ_{SE} = Total failure rate for seals, failure/million hours

λ_{HO} = Total failure rate for brake housing, 3.0 failures/million hours, from Navy Maintenance and Material Management Information System

In the hydraulic drives of brake systems, seals are used to prevent leakage of brake fluid. The hardness and swelling of the seals, when exposed to brake fluid, must remain within limits such that the seals will give reliable operation. The reliability of springs associated with brake systems is generally very high when compared to other components.

Severe performance requirements may affect the reliability of the bearings if there is a path of heat conduction from the friction surface to the bearings. This conduction may cause a decrease in the bearing lubricants operating viscosity and, consequently, a reduction in bearing life. A lubricant with a higher temperature rating should prevent leakage or excessive wear.

The reliability of brake actuators normally is very high. Under severe brake performance, conditions of increased temperature and excessive vibration may decrease the reliability of these components. Refer to the appropriate sections of this Handbook for the reliability models for individual parts comprising the brake assembly. In some cases the result in failure/million cycles will have to be converted to failures/million hours by multiplying by the number of cycles per hour.

12.2.5 Friction Materials

As stated in the introduction, the major functional components of brake equipment and clutch equipment are the friction materials. The reliability of brakes and clutches is concerned with the wear of these friction materials. For brake assemblies, the friction lining provides the friction necessary to slow down or stop a vehicle. Friction materials used in clutches are placed in the power-transmission system to couple it together so it rotates as one unit.

Friction materials that are used in brake and clutch linings have severe performance requirements. The necessary energy conversion must be accomplished with a minimum of wear on the contacting parts. For a particular type of brake or clutch, the amount of heat and friction generated varies according to 5 conditions: (1) the amount of pressure applied between the sliding surfaces, (2) the operating environment, (3) the roughness of the surfaces, (4) the material from which the surfaces are made, and (5) the frequency of application.

The reliability of these high energy components is important for a variety of reasons: Economy, operational readiness and, most important, safety. In today's modern machinery and equipment, a vast number of friction materials have become available to fulfill the very diverse requirements of this equipment group. However, a material which is exceptional in all areas of friction material criteria does not yet exist.

In design it is necessary to have equations for the prediction of the wear life of clutches and brakes. Lining wear properties are generally considered in terms of system life under several different conditions of use severity. Consequently, lining life is often the last performance character to be quantified. Thus a knowledge of lining wear behavior from laboratory testing can be of great value.

Friction modifier additives, such as cashew resin, graphite, etc. have been used for many years in order to control friction properties in brake and clutch composites. Friction composites are composed of a balanced mixture of resin plus additives and generally contain over a dozen ingredients in order to achieve desired characteristics.

In the past, materials such as wood, leather and felt were used, but it was found that the usable temperature range was inadequate to cope with the ever increasing demands made upon them by the industrial world. Today, friction materials can be divided into five main groups:

1) Woven cotton
2) Solid-woven asbestos
3) Rigid molded asbestos, Semi-flexible molded asbestos, Flexible molded asbestos
4) Sintered metal
5) Cermets

Refer to Table 12-4 for a summary of friction material types and applications.

Table 12-4. Friction Material Types And Applications (Ref. 32)

TYPE	MANFACTURE	USES
Woven cotton	Closely woven belt of fabric is impregnated with resins which are then polymerized	Industrial drum brakes, mine-winding equipment, cranes, lifts
Woven asbestos	Open woven belt of fabric is impregnated with resins which are then polymerized. May contain wire to scour the surface	Industrial band and drum brakes, cranes, lifts, excavators, winches, concrete mixers, Mine equipment
Moulded flexible semi-flexible rigid	Asbestos fiber and friction modifiers mixed with thermo-setting polymer and mixture heated under pressure	Industrial drum brakes Heavy-duty brakes-excavators, tractors, presses
Sintered metal	Iron and/or copper powders mixed with friction modifiers and the whole sintered	Heavy-duty brakes and clutches, press brakes, earthmoving equipment
Cermets	Similar to sintered metal pads, but large portion of ceramic material present	As above

Friction material manufacturers are usually very reluctant to disclose the composition or formulation of their products. Some basic information is, however, necessary to properly analyze and carefully select the friction material for a given application. Formulation of a lining is defined as a specified mixture of materials from which the lining is made and the corresponding sequence of production processing which together determine the characteristics of the lining.

Organic linings are generally comprised of six basic ingredients:

a) Asbestos for heat resistance and high coefficient of friction
b) Friction modifiers such as the oil of cashew nutshell to give desired friction qualities
c) Fillers such as rubber chips for controlling noise
d) Curing agents to produce the required chemical reactions in the ingredients
e) Materials such as powdered lead, brass chips, and aluminum powders for improving the overall braking performance
f) Binders such as phenolic resins for holding the ingredients together

Organic linings designed for heavy-duty use generally have higher inorganic contents to improve their high temperature wear resistance and fade resistance. Abrasives are generally added to achieve a higher friction coefficient.

Friction materials containing conventional organic binding agents exhibit poor frictional stability under varying temperature conditions. The thermal degradation of such binders results in inferior frictional characteristics, giving rise to fade and often resulting in increased wear. Furthermore, organic materials, particularly resins, tend to have a short shelf life, and are not always easy to reproduce.

In an attempt to overcome the deleterious effects of poor thermal resistance in a friction material having an organic binder, various sintered metal and ceramic materials, in which the sintering effects the bonding, have been developed. In comparison with friction materials produced with organic, resinous binding agents, sintered friction materials have the primary advantage of being able to withstand considerably higher thermal stresses. They are produced from an intimate mixture of powdered metals and nonmetals by pressing and sintering.

These friction materials commonly consist of sintered lead bronzes and iron powders with additions of dry lubricants and so-called friction reinforcers. Graphite and molybdenum sulfide, for example, are suitable as dry lubricants; on the other hand, ceramic additives and minerals, such as quartz and corundum, may be used to increase the coefficient of friction. By appropriate variation in the additives it is possible to make adaptations for all applications, particularly as regards the coefficient of friction.

Semi-metallics rely heavily on iron, steel, and graphite substitutions for the organic and asbestos materials. Some organic components are, however, used to obtain desirable properties. The use of abrasives must be minimized to maintain acceptable mating surface compatibility. Semi-metallics have distinct advantages over conventional organics such as:

a) Improved frictional stability and fade resistance
b) Excellent compatibility with rotors and high temperature wear resistance
c) High performance with minimal noise

Raw material mix cost represents the major factor in the premium prices of semi-metallics, and as such, widespread use of semi-metallics is not yet found. Metallic linings withstand more severe loads, higher temperatures, and have less tendency to fade. Sintered metallic-ceramic friction materials have successfully been used for specialized applications such as jet aircraft. See Table 12-5 for a summary of the brake friction material surface failures.

12.2.6 Brake Friction Material Reliability Model

The accumulated energy of a vehicle while in use may be expressed by the sum of the difference between the square of the brake application speed and the square of the brake release speed, multiplied by one-half times the mass. Thus the energy dissipated by the brakes is given by Equation (12-2) (Ref. 29)

$$E_B = \frac{m}{2} \sum_{i=1}^{n} (VA_i^2 - VR_i^2) \qquad (12\text{-}2)$$

Where:
E_B = Accumulated energy (ft-lbf)
VA = Brake application speed (ft/s)
VR = Brake release speed (ft/s)

i = Number of brake applications
(i = 1,2,. . . . n)

Table 12-5. Brake Friction Material Failure Modes (Ref. 32)

Problem	Characteristics	Causes
Heat Spotting:	Heavy gouging resulting in rapid lining wear	Material rubbing against a heat-spotted metal member
Crazing:	Randomly oriented cracks on the friction material, resulting in a high wear rate	Overheating of the braking surface
Scoring:	Grooves formed on the friction material resulting in a reduction of life	Metal member needs regrinding
Fade:	Material degrades or flows at the friction surface, resulting in a temporary loss of performance	Overheating caused by excessive braking
Metal Pick-Up:	Metal from the mating member embedded in the lining	Unsuitable combination of materials
Grab:	Lining contacting at ends only giving high servo effect and erratic performance. The brake is often noisy	Incorrect radiusing of lining
Strip Braking:	Braking over a small strip of the rubbing path giving localized heating and preferential wear at those areas	Distortion of the brake path
Neglect:	Material completely worn off the shoe giving a reduced performance	Failure to provide any maintenance
Misalignment	Excessive grooving and wear at preferential areas of lining surface	Lining not fitted correctly to the shoe platform

The heat equilibrium of the brake rotor in non-braking periods is shown by Equation 12-3 (Ref. 29).

$$\frac{\delta(\theta - \theta_o)}{\delta_t} + \frac{h A (\theta - \theta_o)}{W_b C} = \frac{T V}{j W_b C R} \qquad (12\text{-}3)$$

Where:
- θ = Brake rotor temperature, °F
- θ_o = Ambient temperature, °F
- t = time, seconds
- h = Heat transfer coefficient (at rotor surface), Kcal/ft^2 °F
- A = Cooling area of the rotor, ft^2
- W_b = Weight of rotor, lbf
- C = Specific heat of the rotor, kcal/lbm °F
- j = Mechanical equivalent of heat
- T = Residual torque, ft-lbf
- V = Vehicle speed, ft/s
- R = Rolling radius of the tire, ft

Applying the calculation method developed by Newcomb (Ref. 34), it is assumed that the pad wear rate is proportional to the absorbed energy and to the specific wear rate of the friction material. This expression is given by Equation (12-4):

$$W_p = \left(\frac{10^4 W_b}{2 A_p}\right) \left(\frac{Wt\ \Delta V^2\ N_b\ Y_b}{4g}\right) \qquad (12\text{-}4)$$

Where:
- W_p = Pad wear per 10,000 miles, inches
- W_b = Specific wear rate of friction material, in^3/ft-lbf
- A_p = Lining area, in^2
- ΔV = Average change in velocity per brake action, ft/s
- Wt = Weight of the vehicle, lbf
- N_b = Frequency of brake applications per mile
- y_b = Proportion of total braking effort transmitted through the lining
- g = Acceleration due to gravity, 32.2 ft/s^2

Therefore, if the effective thickness is d (inches), pad life is commonly given by Equation 12-5:

$$\text{Life} = \frac{d}{W_p} \qquad (12\text{-}5)$$

Where: Life = Total distance before friction material is completely worn, in units of 10,000 miles

By normalizing Equation (12-5) to those values for which historical failure rate data is available, the following failure rate model can be derived:

$$\lambda_{FR} = \lambda_{FR,B} \cdot C_{BT} \cdot C_{RD} \cdot C_{SR} \cdot C_T \qquad (12\text{-}6)$$

Where:
- λ_{FR} = Failure rate of the brake friction material in failures/million hours
- $\lambda_{FR,B}$ = Base failure rate of the brake friction material, failures/million hours
- C_{BT} = Multiplying factor which considers the effect of brake type on the base failure rate
- C_{RD} = Multiplying factor which considers the effect of dust contaminants on the base failure rate
- C_{SR} = Multiplying factor which considers the effect of countersurface surface roughness on the base failure rate
- C_T = Multiplying factor which considers the effect of ambient temperature on the base failure rate

The brake friction material base failure rate, $\lambda_{FR,B}$, may be provided by the lining manufacturer. If not, then the base rate can be calculated from the expression devised by Minegishi, et al. (Ref. 29). This expression is given in Equation (12-7).

$$\lambda_{FR,B} = \frac{3X10^{-3} W_b \text{ Wt } \Delta V^2 N_b \text{ MPY Yb}}{d \text{ Ap}} \qquad (12\text{-}7)$$

Where: W_b = Specific wear rate of the friction material, $in^3/ft\text{-}lbf$

Wt = Weight of the vehicle or aircraft, lbf
ΔV = Average change in velocity per brake action, ft/s
N_b = Number of brake applications per mile
MPY = The number of miles travelled per year
Yb = Proportion of weight carried by lining during braking action. For a four wheel vehicle, each front brake will typically carry 3/10 of the braking load
d = Lining thickness, in
Ap = Lining area, in^2

Most brake tests involve either disk or drum brakes. A typical disk brake will wear better than a drum type due to the disk brakes ability to dissipate heat more quickly. Several types of disk brakes are used in the development of this model (Ref. 20). The friction material for the annular brake is in the shape of an annulus and is bonded to both sides of the rotor disk. The slotted annular brake is nearly the same as the annular brake described above. The only exception is the presence of slots cut through the friction material on both sides of the rotor. The purpose of the slots is to decrease surface temperature and wear rate during braking. The pad brake configuration employs pads of friction material on the brake stators. As a result:

C_{BT} = 1.25 for drum type brakes
C_{BT} = 1.25 for slotted annular disk type brakes
C_{BT} = 1.00 for pad disk type brakes
C_{BT} = 0.90 for annulus disk type brakes

Operating conditions with high amounts of dust contaminants effects lining wear depending on the binder resin used in formulating the friction material. The correction factor for dust conditions is (Ref. 42):

Binder Resin	C_{BD}
Phenolic	3.5
Oil-modified phenolic	1.15
Rubber phenolic	1.1
Cashew	1.1
Oil-phenolic	1.05

The surface roughness of the countersurface can be critical in the wear of the friction material. C_{SR} can be expressed as (Ref. 37):

$$C_{SR} = \frac{\mu^2 + 600}{3000} \qquad (12\text{-}8)$$

Where: μ = Surface roughness of the countersurface, μ in

Wear of the friction material will be influenced by the ambient temperature in which the vehicle is operating. The correction factor for temperature is: (Ref. 3)

$C_T = 1.42 - 1.54E\text{-}3X + 1.38E\text{-}6X^2$
for sintered metallic linings

$C_T = 2.79 - 1.09E\text{-}2X + 1.24E\text{-}5X^2$
for resin-asbestos linings used in light duty automotive and moderate duty industrial brakes

$C_T = 3.80 - 7.59E\text{-}3X + 5.07E\text{-}6X^2$
for carbon-carbon linings

$C_T = 17.59 - 6.03E\text{-}2X + 5.34E\text{-}5X^2$
for resin-asbestos truck linings

Where: $X = 590 + T$
T = Ambient temperature, °F

12.3 CLUTCHES

12.3.1 Introduction

The reliability of a clutch system is generally very high and is the result of the low failure rate of its parts, which may include actuators, bearings, clutch friction linings, seals and springs. With the exception of clutch friction linings, these component parts are addressed earlier in this handbook. The general characteristics of friction materials are also addressed in the first part of this section. Those characteristics of friction materials peculiar to clutches will be discussed in the following paragraphs.

The principal function of friction clutches is to convert kinetic energy to heat and then either to absorb or otherwise

dissipate the heat while simultaneously, through friction, reducing the relative movement between the friction material and the part to which it is engaged. In order to achieve these objectives the necessary energy conversion must be accomplished with a minimum of wear on the contacting parts.

12.3.2 Clutch Varieties

Clutches are made up of two basic components - the pressure plate and disc. The pressure plate supplies sufficient force or pressure to the disc so enough friction is developed to transmit torque to the driveline.

Friction clutches, although available in many different forms tend to be of the axial or rim type. Axial clutches operate where the movement is parallel to the axis of the shaft. Rim types operate where the movement is radial. Examples of the former are the plate and cone clutches. Examples of the latter include coil or wrap spring and chain clutches.

Plate clutches divide into two designs - single and multiplate. The single plate design is the type favored by automotive designers for transmission and light to medium power applications. The single plate is normally provided with a friction lining on each side of the disc. Multiplate designs employ a number of discs lined on both sides which serve to distribute the load over a large area. These types are used for high torque and high load applications. They required only moderate clamping pressures, and are suitable for high speed operation because their relatively small size generates lower centrifugal forces.

Cone clutches are used for smaller, medium power, low speed transmission systems which may be subjected to rough usage. These devices cope well with such treatment because of their simple robust construction, and due to the fact that heat is dissipated more readily than with plate clutches.

Rim and block clutches employ various means of engaging the stationary half of the assembly through radial movement against the rim of the driving member. The action is similar to that of an internally expanding brake shoe.

Centrifugal clutches are often used with squirrel cage motors. The fabric facing may be fitted to shoes or blocks mounted to a spider which is keyed onto the driving shaft. The shoes or blocks are thrown outward by centrifugal force, engagement being automatic when a predetermined speed is reached from starting.

Coil or wrap spring clutches operate on the principle of a spring mounted on a drum being tightened. The action is much like

that of a rope tightening around a revolving capstan. The design is compact, simple in construction and is used where high torques are required from low power. For this reason the clutches have found applications in small equipment such as plain paper copiers and, in their larger versions, for haulage gears and rolling mills and presses.

Chain clutches employ inner and outer friction rings in an oil filled housing actuated by cams bearing on chain toggles which force the rings together.

Sprag clutches consist of a number of specially shaped steel springs or wedges which jam inner and outer races in one direction only. This action leads to their use for applications in over-running (where the clutch acts as a free-wheel) and back-stopping. This design is particularly useful for intermittent rotary motion involving, for example, indexing or inching (Ref. 34)

Materials classification divides the friction materials into organic and metallic groups. The organic group includes all materials composed of both asbestos and non-asbestos fibers and bound by some resin binder. The metallic group consists of all friction materials containing iron, copper, ceramic bronze, graphite, carbon or other metallic material such as the base material.

12.3.3 Clutch Model Development

The clutch system reliability model will contain the following component parts:

- Actuators
- Bearings
- Clutch friction linings
- Seals
- Springs

The total clutch system failure rate is the sum of the failure rates of each of the above subcomponent parts in the system:

$$\lambda_{CL} = \lambda_{AC} + \lambda_{BE} + \lambda_{CF} + \lambda_{SE} + \lambda_{SP} \qquad (12\text{-}9)$$

Where: λ_{CL} = Total failure rate for the clutch system, failures/million hours

λ_{AC} = Total failure rate for actuators, failures/million hours

λ_{BE} = Total failure rate for bearings, failures/million hours
λ_{CF} = Total failure rate for clutch friction materials, failures/million hours
λ_{SE} = Total failure rate for seals, failures/million hours
λ_{SP} = Total failure rate for springs, failures/million hours

Refer to Chapter 3 of this Handbook for a description of the seal reliability model. Note that the failure rate obtained must be converted from failures/million cycles to failures/million hours by multiplying by the number of cycles per hour. Failure rate models for springs, bearings, and actuators are given in Chapters 4, 7, and 9 respectively. Again, note that the results from these sections must be converted to failures/million hours. The failure rate model for clutch friction materials is presented in the following paragraphs.

12.3.4 Clutch Friction Material Reliability Model

A list of failure modes for a clutch friction materials is shown in Table 12-6. Use of the clutch system beyond the life of the friction material results in catastrophic failure of the clutch caused by a drastic reduction in coefficient of friction.

Under normal operating conditions, the friction materials used in clutches are reliable mechanical components. Like brake friction materials, the wear of clutch materials is dependent on the amount of accumulated energy dissipated by the mechanical component. The rating of the clutch friction material, R, is given in Equation (12-11) per Ref 16.

$$R = \frac{E_c}{550\, t\, A_c} \qquad (12\text{-}11)$$

Where:
R = Rating of friction materials, h.p./in^2
E_c = Average energy dissipated per application, ft-blf.
t = Slipping time, sec.
A_c = Area of clutch friction material, in^2

The life of the friction material, L, is given by Equation (12-12): (Ref. 12)

$$L = \frac{3600\, d\, WV}{R\, t\, n} \qquad (12\text{-}12)$$

Where:
- L = Life of clutch friction material, hours
- d = Effective thickness of lining, inches
- WV = Average wear value of the material, h.p.-hr/in^3
- n = Number of applications per hours.

The average wear valve, WV, should be supplied by the friction material manufacturer for each material type. Combining Equation (12-11) with Equation (12-12) yields:

$$L = \frac{2X10^6\, d\, WV\, A_c}{E_c\, n} \qquad (12\text{-}13)$$

The clutch friction material base failure rate, $\lambda_{CF,B}$, may be supplied by the clutch lining manufacturer. The base failure rate can also be calculated from Equation (12-13) as:

$$\lambda_{CF,B} = \frac{E_c\, n}{2\, d\, WV\, A_c} \qquad (12\text{-}14)$$

Where: $\lambda_{CF,B}$ = Base failure rate of the clutch friction material in failures/million hours.

By normalizing Equation (12-14) to those values for which historical failure rate data is available, the following failure rate model can be derived:

$$\lambda_{CF} = \lambda_{CF,B} \bullet C_{NP} \bullet C_T \qquad (12\text{-}15)$$

Where: C_{NP} = Multiplying factor which considers

Where: C_{NP} = Multiplying factor which considers the effect of multiple plates on the base failure rate

C_T = Multiplying factor which considers the effect of ambient temperature on the base failure rate

As noted earlier, clutches can be divided into two design groups: single and multiple. Multiplate designs use a number of discs which distribute the load, and will therefore increase the reliability of the system. The correction factor for the number of plates is given by Equation (12-16):

C_{NP} = Number of disks in the clutch

Because the temperature of the friction material effects the wear of the material, the ambient temperature which the clutch is exposed to will effect the wear of the friction lining (Ref.3). As a result:

$C_T = 1.417 - 1.54E\text{-}3X + 1.38E\text{-}6X^2$
for sintered metallic linings

$C_T = 2.789 - 1.09E\text{-}2X + 1.24E\text{-}5X^2$
for resin-asbestos linings used in light duty automotive and moderate duty industrial brakes

$C_T = 3.80 - 7.59E\text{-}3X + 5.07E\text{-}6X^2$
for carbon-carbon linings

$C_T = 17.59 - 6.03E\text{-}2X + 5.34E\text{-}5X^2$
for resin-asbestos truck linings

Where: $X = 590 + T$

T = Ambient temperature, °F

Table 12-6. Clutch Friction Surface Failure Modes (Ref. 32)

PROBLEM	CHARACTERISTICS	CAUSES
Dishing	Clutch plates distorted into a conical shape	Lack of conformability. The temp. of the outer region of the plate is higher than the inner region
Waviness or Buckling	Clutch plates become buckled into a wavy platter	Lack of conformability. The inner area is hotter than the outer area
Banding Crushing	Loss of friction material at the ends of a band	Crushing and excessive wear of the friction material
Material Transfer	Friction material adhering to opposing plate, often giving rise to excessive wear	Overheating and unsuitable friction material
Bond Failure	Material parting at the bond to the core plate causing loss of performance	Poor bonding or overheating, the high temperature affecting bonding agent
Burst Failure	Material splitting and removed from the spinner plate	High stresses on a facing when working at high speeds
Grooving	Grooving of the facing material on the line of movement	Material transfer to opposing plate
Reduced Performance	Decrease in coefficient of friction giving a permanent loss in performance	Excess oil or grease on friction material or on the opposing surface
Distortion	Facings out of flatness after high operating temperature	Unsuitable friction material

THIS PAGE INTENTIONALLY LEFT BLANK

CHAPTER 13

COMPRESSORS

13.1 INTRODUCTION

The compression of a gas by mechanical means, and the raising of it to some desired pressure above that of the atmosphere, is effected, usually, by an approximate adiabatic change of state. Industrial and commercial uses of compressed air are exceedingly numerous. Ideal adiabatic compression of air, relating pressure and volume can be given by:

$$pv^{1.4} = C \qquad (13\text{-}1)$$

A compression of this nature could heat the air to temperatures which would interfere with the reliable action of an air compressor and introduce lubrication difficulties, if there were no provisions for cooling the walls of the compression chamber. The extraction of heat from a compression cycle modifies the conditions of compression from the ideal to some change more nearly represented by:

$$pv^{n} = C \qquad (13\text{-}2)$$

Where the value of n is usually between 1.35 and 1.60.

If the heat of compression is removed by cooling as rapidly as it is formed, an isothermal compression will result. Less work is needed for compression of a pound of gas to the same discharge pressure. Although isothermal compression is desirable, it is not possible to achieve in fast-moving compressors. As a result, finned or jacketed cylinder compression is more nearly adiabatic than isothermal.

Compressors can be classified, in their broadest sense, in two categories: (1) positive-displacement and (2) dynamic machines. The positive-displacement classification can generally be described as "volume reducing" types. In essence, an increase in gas pressure can be achieved by simultaneously reducing the volume enclosing the gas. The dynamic classification refers to centrifugal velocity increases. These machines impart energy to

the gas, then stationary diffusors convert the velocity head into pressure. The classification tree in Figure 13-1 further defines the subcategories of compressors.

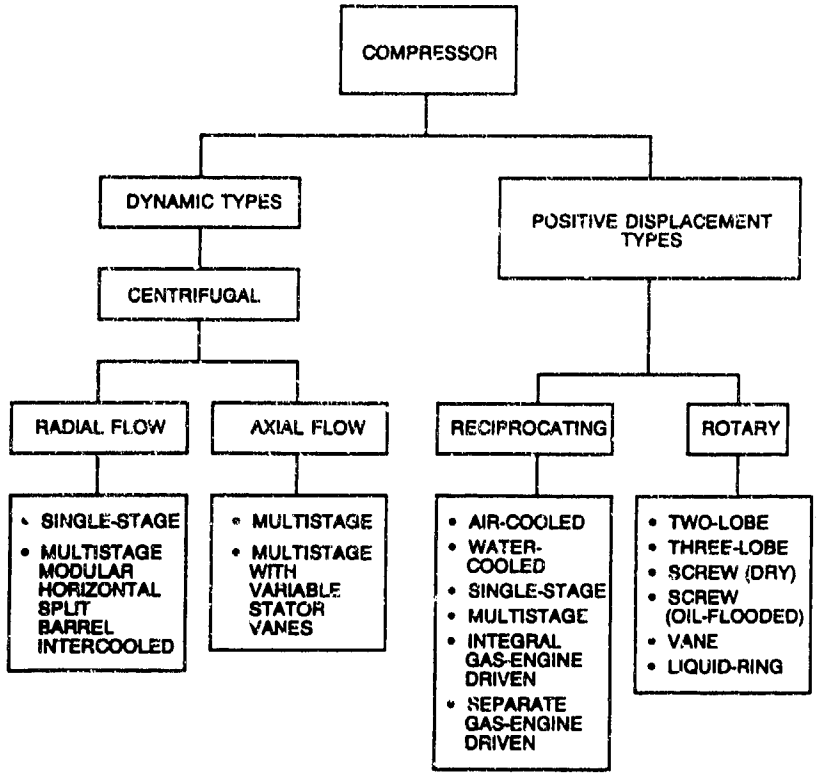

Figure 13-1. Most Common Classifications for Compressors

The positive-displacement (volume reducing) machines can be further defined by two subclassifications; rotary and reciprocating. Both types generally feature steep characteristic curves of performance. A nearly-constant capacity coupled with varying discharge pressure is typical, reflecting a machine capable of slight variations in flow over a wide pressure range.

Reciprocating machines can be modeled as adiabatic pressure generating devices. Systems requiring higher pressures and lower volumetric flow rates usually employ these machines. Typical operating ranges for this type of machine are presented in Figure 13-2. In compression to high pressures, the temperature rise may be too great to permit the compression to be carried to completion in one cylinder, even though it is cooled. In such cases, the compression is carried out in stages, with a partial increase of pressure in each stage, and cooling of the gas between stages. Two

and three-stage compression is very common where pressures of 300-1000 psi are needed. In determining the number of stages (pistons) within a reciprocating compressor, the change in temperature across a stage, the frame or rod loading, and the change in pressure across a stage are among the parameters taken into consideration. The ratio of the temperature before and after compression can be expressed from a form of the Ideal Gas Law:

$$\left[\frac{T_2}{T_1}\right] = \left[\frac{V_2}{V_1}\right]^{n-1} = \left[\frac{P_2}{P_1}\right]^{\frac{(n-1)}{n}} \qquad (13\text{-}3)$$

Where T_1 and T_2 are expressed in °R.

Rotary positive displacement machines incorporate some type of rotating element that displaces a fixed volume during each machine revolution. The characteristics performance curve is basically the same as a reciprocating machine. Typical operating ranges for this type of machine are presented in Figure 13-2.

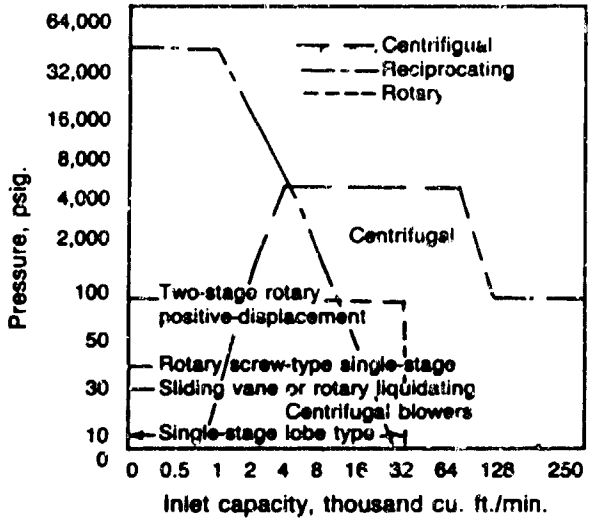

Figure 13-2. Operating Range of the Most Widely Used Compressors for Process Use (Boundaries are not absolute)

The rotary lobe compressor is typically constructed with two or three figure eight-shaped rotors, meshed together, and driven through timing gears attached to each shaft. It is a relatively

low pressure machine (5 to 7 psig, and up to 25 psig for special types) and is well suited for applications with vacuum pressures. Its performance is notable for a greater throughput capability, with little or no flow pulsation.

The rotary screw compressor yields considerably higher pressures and speed. Again, its performance is characteristic of a greater throughput capability with little or no pulsation.

The sliding vane rotary compressor has a rotor construction which is offset, containing slots for vanes to slide in and out during each revolution. These vanes gradually reduce the volume of a trapped gas, raising its pressure. This machine is used for relatively low pressure operations (up to 50 psig per stage).

A liquid ring (or piston) rotary is constructed of circular vanes, turning inside a casing sealed with a liquid. Centrifugal forces cause the liquid to form a ring around the periphery of the casing interior, while forcing the gas inward toward the center of the vaned rotor. The gradual decrease in volume increases the pressure of the gas. Any liquid entrained in the gas is separated out. This type of machine is characteristically used in low pressure and vacuum applications.

Centrifugal compressors can be divided into two subcategories based on the direction of flow of the product gas: radial flow and axial flow machines. The characteristic curves of these machines offer a wide range in flow with a corresponding small change in head. Flow is smooth and pulsation-free beyond the surge point on the performance curve. The lack of rubbing parts in the compressed gas stream is a particularly desirable feature of these machines from a designer's standpoint.

In radial compressors, velocity is imparted to a gas stream through centrifugal forces acting in a radial direction to the shaft. The simplest style of radial centrifugal compressor is the single-stage overhung design. The conventional closed or shrouded impeller is used for adiabatic heads to about 12,000 ft-lb/lb. The open, radial-bladed impeller develops more head for the same diameter and speed.

In axial flow machines, the gas flow remains parallel to the shaft, without a direction change. These machines are typically used for higher capacities than radial flow machines, but generate much lower head per stage. As a result, these machines are usually built with many stages. The characteristic performance curve is steeper than the radial flow machines, with a more narrow stability range.

13.2 COMPRESSOR FAILURE MODES

Some failure modes are more prevalent than others as a direct result of the variety of compressor types and differing environmental conditions of operation. Certain compressor parts will fail more frequently than others. An analysis of various failure modes for compressors and certain compressor parts is presented in Table 13-1.

Table 13-1. Compressor Failure Modes

COMPONENT	FAILURE MODE	FAILURE CAUSE	FAILURE EFFECT
Rotary Displacement Compressor	Reduction of Internal Clearances	Distortion of Rotor due to Cyclic Loading	Rubbing, Increased Wear
	Reduction of Internal Clearances	Improper Mat'l Selection for Thermal Expansion	Rubbing, Increased Wear
	Increased Vibration	High Fluctuating Stresses	Material Fatigue
Reciprocating Compressor	Increased Friction and Wear	Contaminants	Decreased Performance, Increased Vibration
	Valve Sticking	Over Lubrication, Moisture in Oil	Overheating, Increased Wear
Centrifugal Compressor	Low Flow Pulsation	Thrust Reversal, Vibration	Bearing Failure, Overheating
Diaphragm Compressor	Corrosion or Cracking of Diaphragm	Contaminants	Decreased Performance
	Accelerated Curing, Embrittlement of Diaphragm	Extreme High or Low Temperature	Decreased Performance

13.3 MODEL DEVELOPMENT

Any compressor, taken as a complete operating system, can be reduced to the following series of models of each of its subcomponent parts. Each of these parts will sum to the total compressor failure rate:

$$\lambda_C = \lambda_{SH} + \lambda_{BE} + \lambda_{CA} + \lambda_{VA} + \lambda_{SE} + \lambda_{DC} \qquad (13\text{-}4)$$

Where:

λ_C = Total failure rate of compressor, failures/million cycles

λ_{SH} = Total failure rate for the compressor shaft(s), failures/million cycles, see Chapter 10

λ_{BE} = Total failure rate for all compressor bearings, failures/million cycles, see Chapter 7

λ_{CA} = Total failure rate for the compressor casing, failures/million cycles, see Section 13-4

λ_{VA} = Total failure rate for any valve assembly, failures/million cycles, see Chapter 6

λ_{SE} = Total failure rate for all compressor seals, failures/million cycles, see Chapter 3

λ_{DC} = Total failure rate due to design configuration, failures/million cycles, see Section 13-5

The failure rate, λ, for each part listed above must be known or calculated before the entire system failure rate, λ_C, can be determined. Values of each part λ will incorporate expected operational and environmental factors that exist during normal compressor operation.

13.4 FAILURE RATE MODEL FOR CASING

The compressor casing, normally a very reliable component, can have a large effect on the life of other components in the compressor assembly (especially seals and bearings). The value of reliability of compressor casings, through the experience of many different manufacturers, can generally be equated to as high a value as 10^{-4} failures/million cycles.

13.5 FAILURE RATE MODEL FOR COMPRESSOR DESIGN CONFIGURATION

Various reliabilities are inherent in specific designs (types) of compressors. For example, it is expected that reliability due to wear will be different in a rotary screw compressor compared to a centrifugal compressor due to the nature of metal-to-metal contact and rotor speeds.

In its broadest sense, the parameter λ_{DC}, can be approximated by data presented in Table 10-3 for various types of fluid drivers, developed from information collected by the U.S. Navy. This data will suffice in the absence of a complete development of each specific type of compressor presented in Figure 13-1. As new, more specific models are added λ_{DC} can be replaced with the individual model. For Example:

$$\lambda_{DC} = \lambda_{DI}$$

Where: λ_{DI} = Total failure rate of the configuration diaphragm compressor

13-6 FAILURE RATE MODEL FOR COMPRESSOR DIAPHRAGMS

The configuration diaphragm compressor failure rate model can be described by:

$$\lambda_{DI} = \lambda_{BFD} \cdot C_p \cdot C_{AC} \cdot C_{LC} \cdot C_{SF} \cdot C_T \qquad (13\text{-}5)$$

Where:
- λ_{BFD} = Compressor diaphragm base failure rate, 0.40 to 0.75 failures/million hrs.
- C_p = Factor for effects of load variation (performance), see Section 13.6.1
- C_{AC} = Factor for effects of atmospheric contaminants, see Section 13.6.2
- C_{LC} = Factor for effects of liquid contaminants, see Section 13.6.3
- C_{SF} = Factor effects of surface finish or coatings, see Section 13.6.4
- C_T = Factor for effects of temperature, see Section 13.6.5

Diaphragms, in general, are round flexible plates which undergo an elastic deflection when subjected to an axial loading. In the application of compressors, this axial loading and elastic deflection creates a reduction in volume of the space adjacent to the diaphragm. The gas is compressed and a pressure builds. The

diaphragm can be designed in many different ways. The designer can change materials, size, shape, etc. The model developed for a compressor diaphragm is shown in Figure 13-3. It has a passive area in the center which is rigid. This area transmits a force from the push rod to the diaphragm. To be effective, the thickness of the rigid center should be at least 6 times the thickness of the diaphragm.

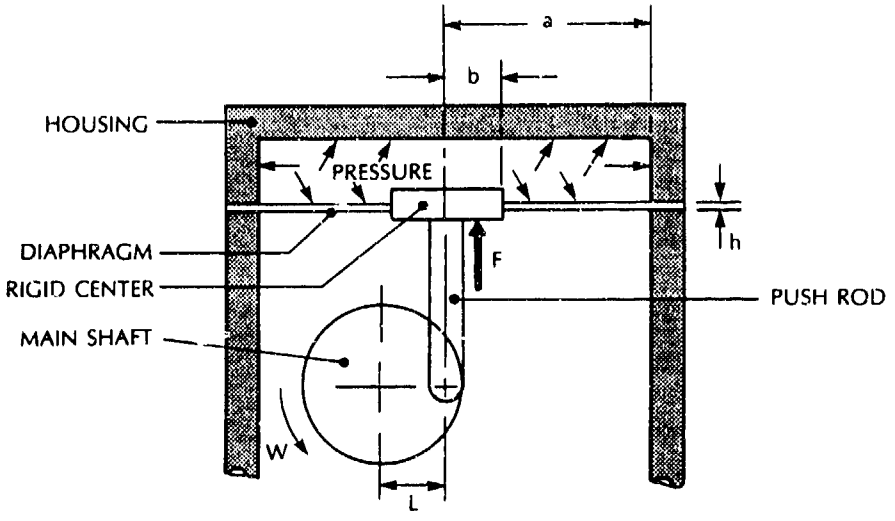

Figure 13-3. Compressor Diaphragm Model

The characteristic equations describing the compressor diaphragm are given in Equations 13-6 through 13-11 and are based on the following restrictive assumptions:

1. Diaphragm is flat and of uniform thickness.
2. Diaphragm material is isotropic and homogeneous.
3. All forces, loads, and reactions are applied normally to the plane of the plate.
4. Diaphragm thickness not greater than 20% of its diameter.
5. The effects of shearing stresses and pressures on planes parallel to the surface of the diaphragm have not been taken into account. They are considered insignificant in diaphragms with thickness to radius ratios (h/a) of less than 0.15.
6. The stresses created in a diaphragm due to bending and tensile loading may be combined by summing their values (method of superposition).

The characteristic equation of a rigid center diaphragm loaded by a force for any magnitude of deflection is given by Equation (13-6). It is applicable for (b/a) ratios greater than 0.05.

$$F = \frac{\pi E}{a^2}\left[\frac{h^3 y_o}{K_P} + h\, y_o^3\, B\right] \qquad (13\text{-}6)$$

Where:

F = Force applied to rigid disk of diaphragm, lbs.

E = Modulus of elasticity, psi

a = Radius of diaphragm, in

h = Diaphragm thickness, in

y_0 = Vertical deflection at center of diaphragm, in

K_P = Modified Stiffness Coefficient based on diaphragm bending loads,

$$= 3(1-\mu^2)\left[\frac{c^2-1}{4c^2} - \frac{\ln^2 c}{c^2-1}\right] \qquad (13\text{-}7)$$

B = Stiffness coefficient based on diaphragm tensile loading, as follows:

$$= \frac{\frac{7-\mu}{3}\left(\frac{1+b^2}{a^2} + \frac{b^4}{a^4}\right) + \frac{[(3-\mu)^2]\, b^2}{[1+\mu]\, a^2}}{(1-\mu)\left(1-\frac{b^4}{a^4}\right)\left(1-\frac{b^2}{a^2}\right)^2} \qquad (13\text{-}8)$$

μ = Poisson's ratio

c = Ratio of radii (diaphragm-to-disk), a/b, in/in

b = Radius of rigid center plate of diaphragm, in

The maximum radial stress for a force-loaded diaphragm with rigid center occurs at the inner perimeter of the diaphragm (b).

$$F = \frac{\sigma_r\, h^{2\pi}}{K_P\, B_P} \qquad (13\text{-}9)$$

Where: B_p = Modified Stiffness Coefficient,

$$= \frac{2}{1-\mu^2} \frac{c^2(2c^2 \ln c - c^2 + 1}{(c^2-1)^2 - 4c^2 \ln^2 c} \quad (13\text{-}10)$$

13.6.1 Factor for Increased Performance

At equilibrium, where the force transmitted by the push rod in Figure 13.3 generates a maximum pressure in the chamber above the diaphragm (i.e., the rod has completed its stroke), a balance of forces in the vertical direction is established.

If the increased performance of a compressor is to be evaluated and the change in shaft power requirements are known, the following equation, in combination with Equation (13-9), will yield the maximum induced stress in the diaphragm:

$$F = \frac{396{,}000\,hp}{2\pi L\omega} \quad (13\text{-}11)$$

Where: hp = Shaft output horsepower
L = Offset of eccentric shaft, in
ω = Output shaft speed, rpm

The maximum stress is calculated from Equation (13-9) for the compressor rated condition. Then maximum stress for the actual operating condition is calculated in the same manner.

Empirical studies show that for moderate to high strains, a mechanical tearing of rubber, referred to as "mechano- oxidative cut growth", can be the mechanism of failure for rubber diaphragms. The cut growth may greatly increase in the presence of oxygen. For this mode of failure, the fatigue life is inversely proportional to a power of the strain energy of the rubber. The strain energy is a characteristic of each type of rubber, and in turn, inversely proportional to the strain experienced by rubber under cyclic stressing. Figure 13.4 shows the stress-strain relationship for natural rubber compounds. Unlike many other engineering materials, rubber can be manufactured with a wide range of elastic moduli. Stiffness variations can be attained with no dimensional changes by varying the incorporation of fillers (reinforcing carbon blacks). This "hardness" variable is essentially a measurement of reversible elastic penetration (International Rubber Hardness degrees or IRHD).

The stress developed in a rubber diaphragm can be calculated from Equation (13-9). Although rubber is flexible, (i.e., has low elastic and shear moduli), it is highly incompressible in bulk and its Poisson's ratio (μ) can be approximated as 0.5. This will facilitate the use of these equations. From the stress calculated, Figure 13.5 will give a corresponding strain.

Using Figure 13.5 and this strain value to determine the number of cycles to failure (fatigue life), Equation (13-12) will yield the performance (C_p) factor for rubber.

The C factor for performance is thus defined as:

$$C_p = \frac{N_o}{N} \qquad (13\text{-}12)$$

Where: N_0 = Number of cycles to failure for rated condition (from Figure 13.5).

N = Number of cycles to failure for actual operating condition (from Figure 13.5).

Note: The value for strain obtained from Figure 13.4 must exceed 75%. Below this strain, the mechano-oxidative cut growth mode of failure does not apply, and the C_p factor becomes 1. Also, the value for N_0 (Equation 13-12) taken from Figure 13.5 may also be substituted as a base failure rate λ_{DI}, in Equation (13-5) at the user's discretion.

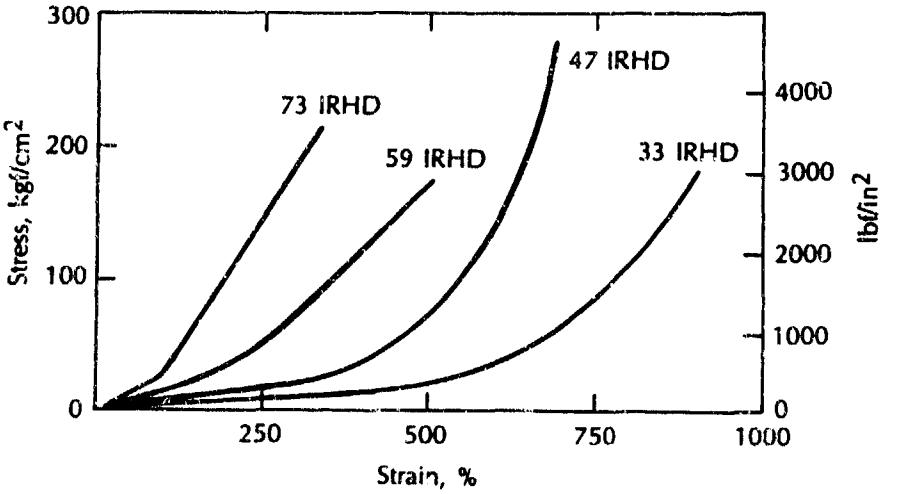

Figure 13.4. Tensile Stress-Strain Curves for Four Natural Rubber Compounds of Different Hardness (Ref. 81)

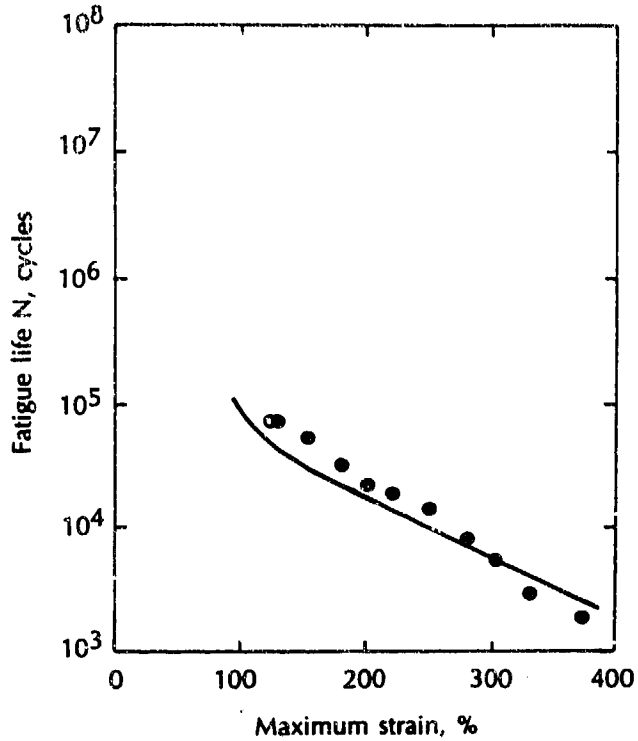

Figure 13.5. Variation in Fatigue Life With Mechano-Oxidative Strain for Natural Rubber (Ref. 81)

13.6.2 C Factor for Atmospheric Contaminants C_{AC}

The very small concentration of ozone in the atmosphere, normally a few parts per hundred million at ground level, may cause cracking in strained rubber components. Under cyclic conditions of strain below about 75%, ozone cut growth is the major factor in determining fatigue life.

Experimental data presented in Figure 13.6 illustrates that fatigue life is proportional to the concentration of ozone. The stress developed in a rubber diaphragm can be calculated from Equation (13-9). Poisson's ratio (μ) can be equated to 0.5. Use Table 13-2 to determine the strain by dividing Young's modulus into the value of stress obtained from Equation (13-9). Using Figure 13-6 and this strain value to determine the number of cycles to failure (fatigue life), Equation (13-12) will yield the contaminant air performance C factor for rubber (C_{ACP}).

Alternately, the C factor for varying concentrations of ozone (C_{ACO}) is given by:

$$C_{ACO} = \frac{N_S}{N_H} \qquad (13\text{-}15)$$

Where: N_H = Fatigue life at actual operating concentrations of ozone, cycles to failure

N_S = Fatigue life at standard atmospheric concentrations of ozone, cycles to failure

NOTE: Both of the N variables in Equation (13-15) must be chosen for the same value of strain from Figure 13.6.

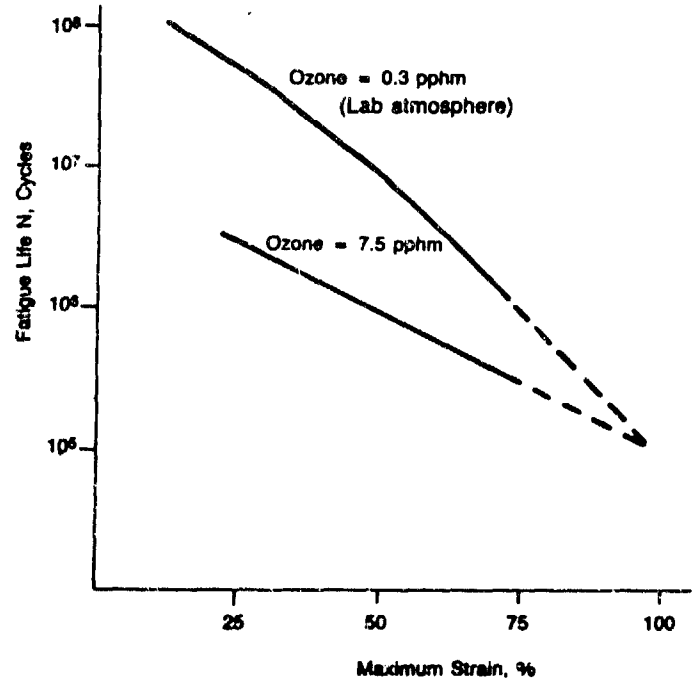

Figure 13.6. Variation of Fatigue Life with Maximum Ozone Cut Growth Strain and Atmospheric Ozone Concentration for Natural Rubber

Table 13-2. Hardness and Elastic Moduli (Ref. 81)

HARDNESS, IRHD	YOUNG'S MODULUS E_0	
	lbf/in^2	kgf/cm^2
30	130	9.2
35	168	11.8
40	213	15.0
45	256	18.0
50	310	22.0
55	460	32.5
60	630	44.5
65	830	58.5
70	1040	73.5
75	1340	94.0

Adjustment of C Factor for use of Coatings

In ozone-dominant failure potentials, the use of chemical antiozonant (coating) on the surface of the rubber diaphragm can reduce crack growth by a factor of 3. If a coating is used, the C factor obtained from Equation (13-12) or (13-15) should be multiplied by 1/3.

13.6.3 C Factor for Liquid Contaminants

Water absorption does not usually cause any significant deterioration of rubber, but the absorption of oil and solvents cause rubber to swell with a consequent deterioration in certain properties. Thin components can be expected to fail rapidly if the major surfaces are exposed to oil. Thick components are effectively protected by their bulk. Such components can last many years in an oily environment. Diffusion theory predicts that the mass of liquid absorbed per unit area of rubber (in the early stages of swelling) is proportional to the square root of the time taken for the absorption.

The rate of movement of the boundary between swollen and unswollen rubber is calculated from (Ref. 81):

$$PR = \frac{L}{\sqrt{t}} \qquad (13\text{-}16)$$

Where: PR = Penetration rate, cm/sec
L = Depth of the swollen layer, cm
t = Time that a given mass of liquid is absorbed by a given surface, sec

Figure 13.7 reveals that the penetration rate into natural rubber decreases as the viscosity of the swelling liquid increases. The base failure rate for a rubber diaphragm, λ_{DI}, in the presence of liquid contaminants can be computed by estimating the viscosity of the liquid in contact with it. The penetration rate is then defined as shown in Figure 13.7. Using this rate and the nomograph in Figure 13.8, the time to total equilibrium swelling (failure) of the rubber component can be predicted.

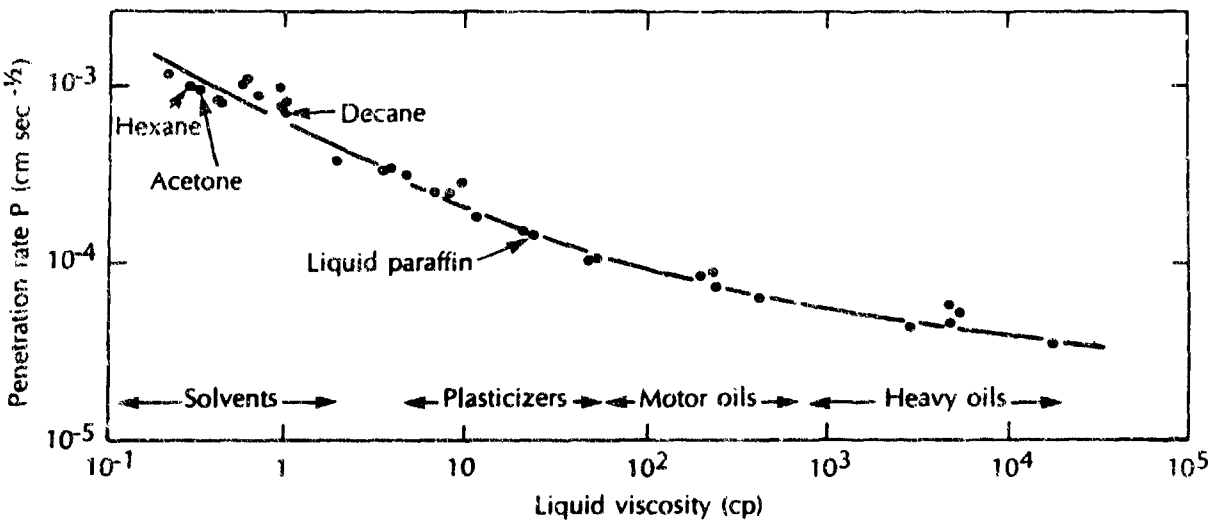

Figure 13.7. Effect of Liquid Viscosity on the Penetration Rate of Liquids into Natural Rubber (Ref. 81)

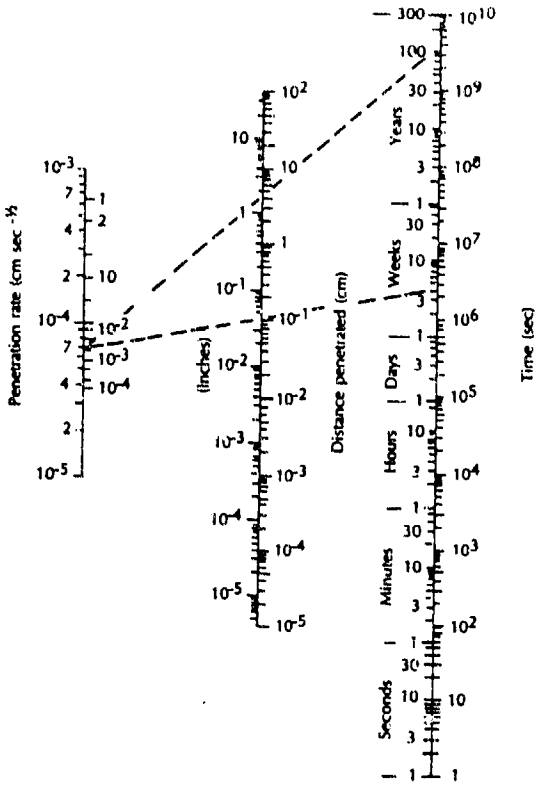

Figure 13.8. Nomogram for the Penetration of Liquids into Natural Rubber (Ref. 81)

It has been found empirically that the apparent equilibrium time obtained from the nomogram should be increased by a factor of about three to obtain the true value. For example, the time taken for a sheet 1 mm thick to reach equilibrium in a liquid having a penetration rate of 1 x 10^{-10} cm $sec^{-1/2}$ is calculated as follows. The nomograph gives a time of three days to penetrate 0.5 mm (half-sheet thickness used since liquid is absorbed from both sides of sheet) but the actual time to reach full equilibrium swelling is nine days.

An adjustment for various types of rubbers can be made using the C factors presented in Table 13-3. These factors should be multiplied by the penetration rate obtained from Figure 13.7 prior to using the nomograph.

Table 13-3. C Factors for Various Rubbers (Ref. 81)

RUBBER	C_{LC}
Natural	1.0
Cis polybutadiene	1.3
Butyl	0.7
SBR	0.7
Neoprene WRT	0.4
Nitrile (38% Acrylonitrile)	0.1

It is necessary to compute the base failure rate given by Figure 13.8 in order to compare it with λ_{DI} obtained by other means. If the base failure rate given by Figure 13.8 is extremely low by comparison, contribution by liquid contamination can be ignored.

The variations in ambient temperature commonly occurring in practice are unlikely to greatly affect fatigue behavior. Experiments (Ref. 81) over a range from -32 to 212 °F show very slight effects of temperature on the fatigue life of crystallizing natural rubber. In general, rubbers become weaker as the temperature is raised. There is a steady fall in strength up to a critical temperature at which an abrupt drop occurs. For natural rubber, this temperature is about 212 °F.

A "C" factor can be developed as follows:

For: $-32°F<T>212°F$, $C_T = 1.0$

$212°F<T$, $C_T = 6.7$

THIS PAGE INTENTIONALLY LEFT BLANK

CHAPTER 14

ELECTRIC MOTORS

14.1 INTRODUCTION

Electric motors play a very important part in supplying power for all types of domestic and industrial applications. Their versatility, dependability, and economy of operation cannot be equaled by any other type of a power unit. It is estimated that over 90 percent of industrial motive power applications utilize electric motors (Ref. 80). Many types are available, therefore motors are classified in various ways. There are general purpose, special purpose, and definite purpose types of motors. They are also classified according to the type of electricity they require; a motor may operate on direct current (DC) or alternating current (AC). If AC, it may be single or polyphase.

This section contains failure rate models that apply to all electric motors which can be used to support the development of mechanical equipment and provide a reliability estimate for a new design, proposed design modification, or application other than verified specification parameters. The models are intended to focus attention on further design analysis which should be accomplished to assure the allocated reliability of the motor in its intended operational environment.

14.2 CHARACTERISTICS OF ELECTRICAL MOTORS

14.2.1 Types of DC Motors

DC motors are classified as either series-wound, shunt-wound, or compound-wound. In the series-wound motor, field windings which are fixed to the stator frame, and the armature windings which are placed around the rotor, are connected in series so that all current that passes through the field windings also passes through the armature windings. In the shunt-wound motor, the armature and field are both connected across the main power supply (in parallel) so that the armature and field currents are separate. The compound-wound motor has both the series and shunt field windings. These may be connected so that the currents are flowing the same direction in both windings, called "cumulative compounding", or so that the currents are flowing in opposite directions, called

"differential compounding".

14.2.2 Types of Polyphase AC Motors

The most extensively used polyphase motors are the induction type. The "squirrel cage" induction motor has a wound stator connected to an external source of AC power and a laminated steel core rotor with heavy aluminum or copper conductors set into the core around its periphery while being parallel to its axis. These conductors are connected together at each end of the rotor by a heavy ring, providing closed paths for currents induced in the rotor to circulate. The rotor windings are not connected to the power supply.

The wound-rotor type of induction motor has a squirrel cage and a series of coils set into the rotor which are connected through slip-rings to external variable resistors. By varying the resistance of the wound-rotor circuits, the amount of current flowing in the circuits, and therefore the speed of the motor, can be controlled. Induction motors are manufactured with a wide range of speed and torque characteristics.

The synchronous motor is the other type of polyphase AC motor. Unlike the induction motor, the rotor of the synchronous motor is connected to a DC supply which provides a field that rotates in step with the AC field in the stator. The synchronous motor operates at a constant speed throughout its entire load range, after having been brought up to this synchronous speed. This speed is governed by the frequency of the power supply and the number of poles in the rotor.

14.2.3 Types of Single-Phase AC Motors

Most of the single-phase AC motors are induction motors distinguished by different arrangements for starting. Single-phase motors are used in sizes up to about 7 1/2 horsepower for heavy starting duty chiefly in home and commercial appliances for which polyphase power is not available.

The series wound single-phase motor has a rotor winding in series with the stator winding as in the series-wound DC motor. Since this motor may also be operated on direct-current, it is called a "universal motor". The series wound motor has a high starting torque and is used in vacuum cleaners, sewing machines, and portable tools. In the capacitor- start single-phase motor, an auxiliary winding in the stator is connected in series with a capacitor and a centrifugal switch. During the starting and accelerating period the motor operates as a two-phase induction

motor. At about two- thirds full-load speed, the auxiliary circuit is disconnected by the switch and the motor then runs as a single phase induction motor. In the capacitor-start, capacitor-run motor, the auxiliary circuit is arranged to provide high effective capacity for high starting torque and to remain connected to the line, but with reduced capacity during the running period. In the single-value capacitor or capacitor split-phase motor, a relatively small continuously-rated capacitor is permanently connected in one of the two stator windings and the motor both starts and runs like a two-phase motor.

In the repulsion-start single-phase motor, a drum-wound rotor circuit is connected to a commutator with a pair of short-circuited brushes set so that the magnetic axis of the rotor winding is inclined to the magnetic axis of the stator winding. The current flowing in this rotor circuit reacts with the field to produce a starting and accelerating torque. At about two-thirds full load speed the brushes are lifted, the commutator is short circuited and the motor runs as a single-phase squirrel-cage motor. The repulsion motor employs a repulsion winding on the rotor for both starting and running. The repulsion-induction motor has an outer winding on the rotor acting as a repulsion winding and an inner squirrel cage winding. As the motor comes up to speed, the induced rotor current partially shifts from the repulsion winding to the squirrel cage winding and the motor runs partly as an induction motor.

In the split-phase motor, an auxiliary winding in the stator is used for starting with either a resistance connected in series with the auxiliary winding (resistance-start) or a reactor in series with the main winding (reactor-start). The split-phase motor is used in refrigerators, air conditioners, freezers, and other compressors involving high starting load.

14.3 FAILURE MODES

Failure rate models included in this section are based upon identified failure modes of the individual parts. Typical failure modes and their failure causes and effects are listed in Table 14-1. Failure rate models or estimates for the following component parts are discussed or referenced in this section:

1. Bearings
2. Windings
3. Brushes
4. Armature (shaft)
5. Stator Housing (casing)

Table 14-1. Electric Motor Failure Modes

ELECTRIC MOTOR FAILURE MODES			
COMPONENT	**FAILURE MODE**	**FAILURE CAUSE**	**FAILURE EFFECT**
BALL OR ROLLER BEARING	WORN OUT a) SPALLING b) CREEPING OR SPIN	POOR LUBRICATION; CONTAMINATION; OVERLOADING; OR HIGH TEMPERATURE	NOISY; HEAT BUILD-UP; ARMATURE RUBBING STATOR; SEIZED
ELECTRICAL WINDINGS (ROTOR OR STATOR)	a) OPEN b) SHORT	EXCESSIVE HIGH TEMPERATURE	MOTOR WON'T RUN SPARKING AT BRUSHES
HOUSING	a) CRACKED	FATIGUE; EXTERNAL SHOCK; VIBRATION	LEAKAGE OR DUST INTO MOTOR; SHORTED OR SEIZED
ARMATURE	a) SHEARED SHAFT b) CRACKED ROTOR LAMINATIONS	FATIGUE; MISALIGNMENT; OR BEARING FAILURE	SEIZED; ARMATURE RUBBING STATOR
BRUSHES	WORN OUT	IMPROPER MAINTENANCE; CONTAMINATION; HIGH TEMPERATURE; LOW ATMOSPHERIC HUMIDITY; IMPROPER CONTACT PRESSURE	EXCESSIVE SPARKING; CHATTER OR HISSING NOISE; MOTOR RUNS TOO FAST OR TOO SLOW UNDER LOAD
SLEEVE BEARING	WORN OUT	EXCESSIVE LOAD (BELT TENSION); TOO FREQUENT STARTS AND STOPS UNDER HEAVY LOADS; POOR LUBRICATION	SEIZED; NOISY; HEAT BUILD-UP; ARMATURE RUBBING STATOR

The models developed in this chapter will be based on an AC fractional horsepower (FHP) type motor, although it will be general enough to be applied to most motors. Therefore, a specific motor being analyzed may not need to include all the failure rates due to its lack of certain parts (e.g., brushes).

14.4 MODEL DEVELOPMENT

The model developed is based on a fractional or integral horsepower AC type motor, although it will be general enough to be applied to most motors.

The reliability of an electric motor is dependent upon the reliability of its parts, which may include: bearings, electrical windings, armature/shaft, housing, and brushes. Failure mechanisms resulting in part degradation and failure rate distribution (as a function of time) are considered to be independent in each failure rate model. The total motor system failure rate is the sum of the failure rates of each of the parts in the system:

$$\lambda_M = \lambda_{BE} + \lambda_{WI} + \lambda_{BS} + \lambda_{AS} + \lambda_{ST} + \lambda_{GE} \qquad (14\text{-}1)$$

Where:

λ_M = Total failure rate for the motor system, failures/million hours

λ_{BE} = Total failure rate for bearings, failures/million hours

λ_{WI} = Total failure rate for electric motor windings, failures/million hours

λ_{BS} = Total failure rate for brushes, failures/million hours

λ_{AS} = Total failure for the armature shaft, failures/million hours

λ_{ST} = Total failure for the stator housing, failures/million hours

λ_{GE} = Total failure for gears, failures/million hours

The failure rates for all the parts in the motor system must be summed before the system failure rate can be found. Failure rate models for shafts, housing (casings), gears, and bearings can be found in Chapters 10, 8, and 7, respectively. A failure rate model for brushes is under development.

14.5 FAILURE RATE MODELS FOR MOTOR WINDINGS

The electric motor windings failure rate, λ_{WI}, is derived by Equation (14-2):

$$\lambda_{WI} = \lambda_{WI,B} \cdot C_T \cdot C_V \cdot C_f \cdot C_{alt} \qquad (14\text{-}2)$$

Where:

$\lambda_{WI,B}$ = Base failure rate of the electric motor windings, failures/million hours

C_T = Multiplying factor which considers the effects of ambient temperature on the base failure rate

C_V = Multiplying factor which considers the effects of electrical source voltage variations

C_f = Multiplying factor which considers the effects of electrical source frequency variations

C_{alt} = Multiplying factor which considers the effects of operation at extreme elevationss

$\lambda_{WI,B}$ is the base failure rate of the specific motor as supplied by the motor manufacturer. For fractional horsepower motors, it can be estimated from Equation (14-9). The C factors are described in the following paragraphs.

14.5.1 Temperature

Heat is the primary limiting factor of motor windings. Heat causes the windings to age and deteriorate, so after time they break down and lose their insulation quality. When this happens the related electrical components "short" and the motor burns out or blows a fuse.

Under normal operating conditions, the insulation material used in the windings of electric motors is generally reliable, thereby making the windings themselves a reliable component.

The life of any given insulation material depends on the degree of heat to which it is exposed. Equations (14-3) through (14-6) reflect the temperature C factors for four insulation classes. It should be noted that the insulation life increases beyond normal life expectancy as temperature is dropped below the rated temperature. Also, these factors were developed from NEMA standards for drip-proof and totally enclosed fan-cooled, integral horsepower motors with 1.0 Service Factor.

- Class A Insulation, normalized at 105 °C

$$C_T = (5.7 \times 10^{-5})\, e^{0.093(T+65)} \qquad (14\text{-}3)$$

- Class B Insulation, normalized at 130 °C

$$C_T = (1.4 \times 10^{-5})\, e^{0.086(T+90)} \qquad (14\text{-}4)$$

- Class F Insulation, normalized at 155 °C

$$C_T = (1.5 \times 10^{-4})\, e^{0.059(T+115)} \qquad (14\text{-}5)$$

- Class H Insulation, normalized at 180 °C

$$C_T = (9.8 \times 10^{-5})\, e^{0.051(T+140)} \qquad (14\text{-}6)$$

Where: T = Ambient temperature during full load operation, °C

The winding temperature is determined by measuring both the ambient and the hot temperature resistances of the windings. The resistance measurement gives an average temperature which is more representative than spot measurements with a thermometer. This method has become standard because of the dimensional restrictions of so many motor designs, which prevent the use of thermometers. Since variation in ambient temperatures during operation is more convenient to estimate, Equations (14-3) through (14-6) above have been adjusted for the maximum allowable temperature rise by resistance and windings "hot spot" temperature for each insulation class. The equations emphasize the importance of avoiding motor overloads in order to maximize insulation life. However, short peak loads involve such a short time that their effect on insulation life is negligible.

The correction factor for the windings of a fractional horsepower motor for varying ambient temperatures is given by:

$$C_T = 10^{2357}\left[\frac{1}{T_o + 273} - \frac{1}{T + 273}\right] \qquad (14\text{-}7)$$

Where: T = Ambient temperature during operation, °C
T_0 = Ambient temperature rating of windings, °C

14.5.2 Temperature Cycling

In many instances, a motor is not run in a steady state temperature environment. Many MIL-STD testing procedures specify cyclic ambient temperature profiles (i.e., MIL-STD-810D). One such example of an elevated ambient cyclic temperature profile is shown in Figure 14.1. A "C" factor for the windings of a fractional horsepower motor, given a temperature profile, can be developed by computing an "equivalent" winding characteristic life, then comparing this value to the value normalized at the windings rated temperature.

$$C_T = \frac{10^{\left[\frac{2357}{T_o+273} - 1.83\right]}\left[\frac{t_1}{L_1} + \frac{t_2}{L_2} + \frac{t_3}{L_3} + \cdots \frac{t_i}{L_i}\right]}{t_1 + t_2 + t_3 + \cdots t_i} \qquad (14\text{-}8)$$

Where: T_0 = Ambient temperature rating of windings, °C
t_i = Time at each temperature interval, i, representing the number of intervals, hours (See Figure 14-1 for example)
L_i = Characteristic winding life at each temperature interval, as represented by Equation 14-9 (i representing the number of intervals), hours

The winding Weibull Characteristic Life for cyclic temperatures can be computed from:

$$L_i = 10^{\left(\frac{3357}{T_i+273} - 1.83\right)} \qquad (14\text{-}9)$$

Where: T_i = Temperature at each cyclic interval, i, representing the number of intervals, °C (See Figure 14.1 for example)

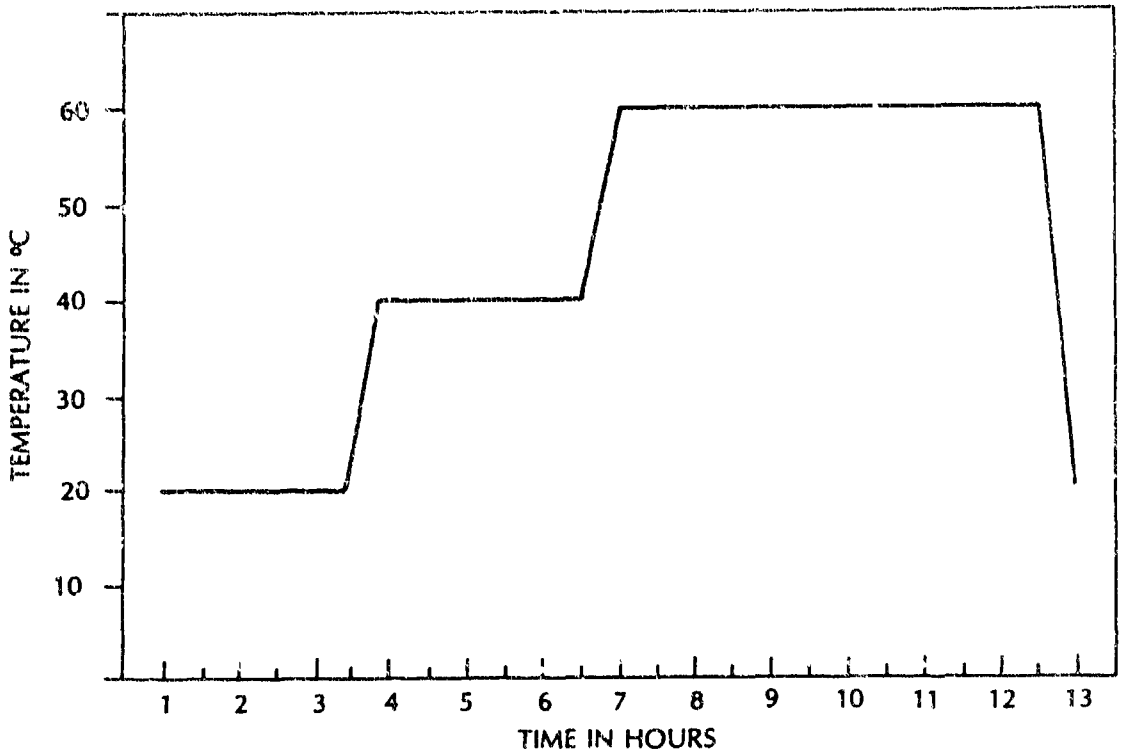

Figure 14.1 Typical Ambient Cyclic Temperature Profile

14.5.3 Voltage and Frequency Variation

The motor horsepower rating on the nameplate may not necessarily indicate the motor's maximum capacity. The motor is often designed with extra capacity built in to allow for variations. Voltage and frequency are two of these variations. A standard motor may operate successfully with the following variations, but not necessarily in accordance with standards established for operation at normal voltage and frequency.

A standard motor will operate successfully when the variation in frequency does not exceed ±5% of normal, or when the voltage does not exceed ±10% of normal. A failure rate multiplying factor can be established for frequency and voltage variations outside these limits:

For $V_L > V_R$:

$$C_V = 0.01\left(100 - \left(\frac{\frac{V_A - V_R}{V_R} \times 100}{2}\right)\right) \quad \textbf{(14-10)}$$

Where: V_R = Rated Voltage
V_A = Actual Voltage

For $V_A < V_R$:

$$C_V = 0.01\left(100 + \left(\frac{\frac{V_R - V_A}{V_R} \times 100}{2}\right)\right) \quad \textbf{(14-11)}$$

For $F_A > F_R$:

$$C_V = 0.01\left(100 - \left(\frac{\frac{F_A - F_R}{F_R} \times 100}{2}\right)\right) \quad \textbf{(14-12)}$$

Where: F_R = Rated Frequency
F_A = Actual Frequency

For $F_A < F_R$:

$$C_V = 0.01\left(100 + \left(\frac{\frac{F_R - F_A}{F_R} \times 100}{2}\right)\right) \quad \textbf{(14-13)}$$

14.5.4 Altitude

The influence of altitude on the life of a fan-cooled motor may be tabulated based on a 50% reduction in life for every 10°C increase in temperature. Table 14-2 is a tabulation of failure rate multipliers for altitude/temperature conditions applicable to fan-cooled motors which are not enclosed. For totally enclosed motors, altitudes to 60,000 feet will not influence life as

compared to sea level.

Table 14-2. Multiplying Factor, C_{alt}, for the Influence of Altitude on Motor Life for Fan-Cooled Motors

ALTITUDE (ft x 1000)	SEA LEVEL MOTOR TEMPERATURE RISE 20°C	30°C	40°C	50°C	60°C
S.L.	1.0	1.0	1.0	1.0	1.0
25	1.0	1.0	1.0	1.0	1.0
30	1.0	1.0	1.0	1.0	2.0
40	1.0	1.0	4.0	8.0	16.0
50	1.0	8.0	---	---	---
60	16.0	---	---	---	---

THIS PAGE INTENTIONALLY LEFT BLANK

CHAPTER 15

ACCUMULATORS, RESERVOIRS AND PRESSURE VESSELS

15.1 INTRODUCTION

An accumulator is a device used to store energy. Accumulators are used for:

- fluid supply
- pump delivery pulsation damping
- system pressure surge damping
- leakage and thermal expansion compensation
- emergency and standby power source

In a hydraulic system the energy is stored as a fluid under pressure and often used to smooth out the delivery flow of pumps. A reservoir is a device for collecting and storing a fluid under ambient conditions. This chapter includes a discussion of the reliability of these and other vessels which may include boiler assemblies, gas pipes, gun tubes and other containers subject to environmental stress.

Typical accumulator designs are shown in Figure 15.1. A dead load accumulator is comprised of a single acting vertical cylinder which raises a heavy load or weight. A dead load accumulator can be designed for large volumes but correspondingly heavy weights are needed resulting in a large physical size. The advantage of this type of accumulator design is the constant discharge pressure, whereas all other types exhibit a variation in pressure with respect to volume of fluid stored.

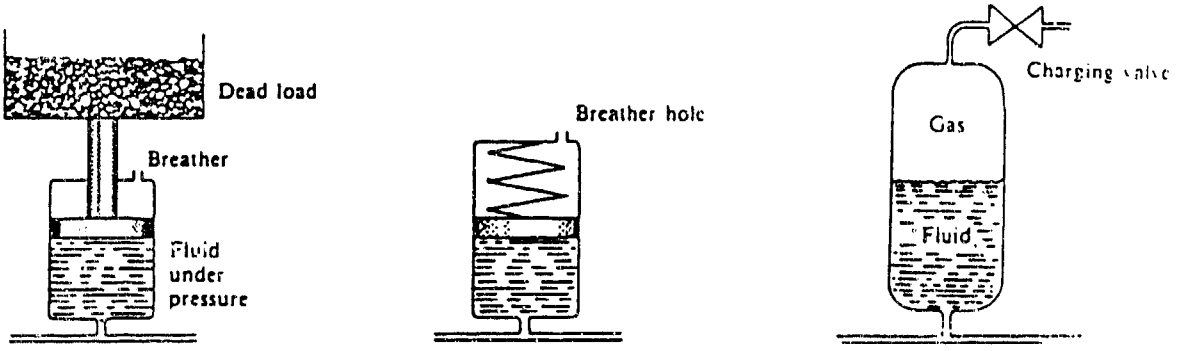

Figure 15.1 Typical Accumulator Designs

A spring loaded accumulator contains a spring which moves within a cylinder. As the volume of fluid in the accumulator is increased, the spring is compressed and the spring force is increased. The minimum pressure in the accumulator depends on the designed spring preload. The advantage of this design is its simplicity. The piston stroke and, therefore, the volume of fluid which can be stored is limited by the physical characteristics of the spring.

A gas loaded accumulator is designed to utilize a compressed gas such as nitrogen or air to pressurize the stored fluid. A piston or bag is used to separate the fluid and gas. Gas loaded accumulators can be very large. As discussed in the next section, accumulators are usually designed to be operated in the vertical position. The fluid pressure as a function of fluid volume in a gas loaded accumulator depends upon many factors such as the gas being used, the temperature of the gas and its pressure - volume characteristics.

15.2 FAILURE MODES

In any type of accumulator utilizing a piston the cylinder bore has to be machined, and wear will occur between the piston and cylinder body. Seals are built into the piston and these are subject to wear and leakage. Depending on the accumulator application, response time may be a factor. The response of the dead load accumulator will be somewhat slow due to the high inertia of the load and piston. The response of spring loaded accumulators will depend on the age of the spring and its modulus of rigidity. A response of a piston type accumulator will be adversely affected by the inertia of the piston and the effect of seal stiction.

Although a piston type accumulator can be used inclined to the vertical, the rate of wear will be increased due to the additional side load. Failure of a piston type accumulator tends to be gradual caused by deterioration of piston seals and wear in the cylinder bore. Failure of a bag type gas loaded accumulator will be more sudden caused by the rupturing of the bag or diaphragm. The failure rate of a bag type accumulator may also depend on its physical characteristics, a tall narrow unit subject to sudden discharge could cause the poppet valve to lock closed a partially discharged unit.

A spring loaded accumulator must be evaluated closely for reliability to verify compatibility between the spring material and the surrounding medium. Any leakage past the seal could have a deteriorating effect on the spring material and its compression

properties or fatigue failure.

Table 15.1 Failure Modes of Accumulators

FAILURE MODE	FAILURE CAUSE	LOCAL EFFECT
Seal leakage	Embrittlement, wear, distortion, incompatibility with medium,	Leakage past piston, internal leakage at valve, external leakage
Worn cylinder bore or piston surface	Contaminants, interaction with fluid medium	Poor response, leakage, loss of pressure
Loss of spring tension	Corrosion Fracture	Incompatibility with fluid medium. Material flaws, stress concentration due to tooling marks
Poor response	Piston stiction	Spring misalignment, surface wear, corrosion
Loss of pressure	Ruptured gas bag External leakage	Improper operating position; loss of fluid causing movement of bag. Seal leakage
Leakage of charge gas into fluid system	Leakage past piston or bag; sudden discharge of fluid from accumulator	Wear; PV characteristics of gas; operational procedures
Inoperative accumulator	Jammed output valve	Refer to chapter on valve assemblies

One of the main applications of an accumulator is the damping of fluid system pulsations or surges. The system effects of these pulsations must be evaluated as part of any reliability analysis. In some applications the pulsations are unimportant as they are partially smoothed by pipes upstream of the pump. A critical element of the reliability analysis is the effect of an accumulator on the probability of failure of other system components. For example, a failed valve assembly within the accumulator which

prevents fluid discharge may not be immediately detected and damage to other components may occur due to pressure transients. Shock waves produced as a result of the sudden closing of a downstream valve, for example, travels through the system fluid to the far end of the system and a decompression wave is formed which travels back to the valve. These waves travel back and forth until the energy is expended. The more rapid the valve closure, the more severe the pressure transient generated. Without detection of an accumulator failure, severe degradation and damage to system components could be occurring without operator or maintainer knowledge.

15.3 FAILURE RATE CONSIDERATIONS

15.3.1 Seals

Specific failure modes of seals and procedures to determine their failure rates under different operating environments are discussed in Chapter 3. Of particular interest in the design evaluation of accumulators and other pressure vessels is the compatibility of the fluid medium and the seal material. The position of the accumulator in the fluid system must also be known to determine the side load on the piston and corresponding stress on the seal.

15.3.2 Springs

Specific failure modes of springs and procedures to determine their failure rates under different operating environments are discussed in Chapter 3. For most accumulators the failure rate equations for static springs can be assumed. The reliability of a spring is very sensitive to corrosion and the compatibility of the fluid and spring material must be considered.

15.3.3 Piston/cylinder

The wear rate of the piston surface and cylinder bore will be sensitive to the position of the accumulator in its operating environment. Tilting of the accumulator from its vertical position will alter the side load of the piston. This parameter and others effecting the reliability of the piston/cylinder are included in the reliability equations contained in Chapter 9.

15.3.4 Valves

The reliability of valve assemblies which may be contained within the accumulator is determined using the equations contained in Chapter 6. One particular failure mode to be considered in the

design evaluation is the possibility of a sudden discharge of fluid causing the output valve to operate without fluid and creating an air lock.

15.3.5 Structural Considerations

The fluid contained within an accumulator under pressure creates stresses in the walls as shown in Figure 15.2. The state of stress is triaxial. A longitudinal or meridional stress acts parallel to the meridian; a circumferential, or hoop, stress acts parallel to the circumference; and a radial stress acts outward at the surface. If the walls of the accumulator are relatively thin (thickness t is less than one-tenth the radius r) and of uniform shape, longitudinal and circumferential stresses will be uniform throughout the thickness of the wall and the radial stress, although varying from zero at the outside surface to a value equal to the internal pressure at the inside surface can be considered negligible. Reference 38 provides equations for determining the stress levels of thin walled pressure vessels. The shell thickness is designed to keep the maximum stresses below the yield strength of the material. The design thickness is the minimum required thickness computed by code formula plus an allowance for corrosion.

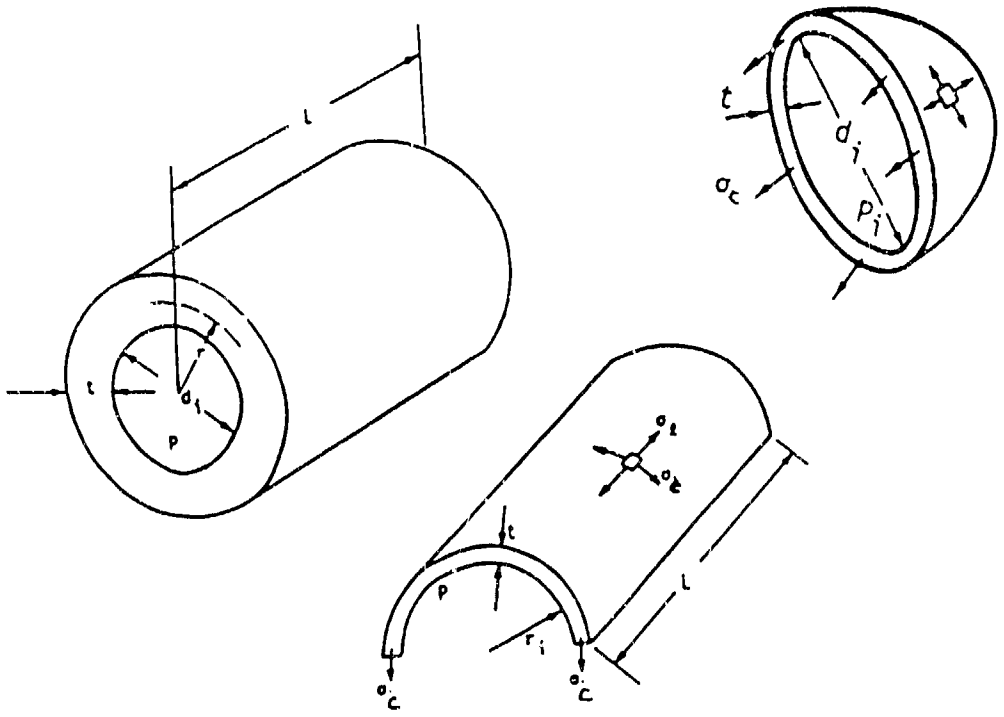

Figure 15.2 Stresses created in walls of accumulator

The bursting effect of internal fluid pressure creates a circumferential pressure in the wall of the accumulator. Total force acting on a half cylinder as shown in Figure 15.1 is:

$$F_c = 2Pr_iL \qquad (15\text{-}1)$$

Where: P = Internal pressure
r_i = Internal radius
L = Cylinder length

The resistive force due to circumferential stress, σ_c acting on the cylinder wall to achieve equilibrium must equal force F_c.

$$F_c = 2\sigma tL \qquad (15\text{-}2)$$

Substituting F_c in equation 15-1 for equation 15-2 provides the following relation:

$$\sigma_c = Pr_i/t \qquad (15\text{-}3)$$

This equation provides the maximum circumferential stress in the vessel wall on the assumption that end closures provide no support, such as is the case for long cylinders or tubes. The equilibrium of forces in the longitudinal direction gives:

$$F_l = \pi Pr^2 \qquad (15\text{-}4)$$

and the corresponding longitudinal stress is:

$$\sigma_l = Pr_i/2t \qquad (15\text{-}5)$$

The effects of end plates and joints on the accumulator is a reduction in strength of the accumulator due to riveted joints, welding and other fabrication techniques. This reduction is accounted for by including a joint efficiency parameter, η_l in the circumferential stress equation and η_c in the equation for longitudinal stress.

$$\eta = \frac{\text{minimum strength of joint}}{\text{strength of solid material}}$$

This addition provides the following equations:

$$\sigma_c = Pr_i/t\eta_l \quad (15\text{-}6)$$

and:

$$\sigma_l = Pr_i/2t\eta_c \quad (15\text{-}7)$$

The relative strength (efficiency) of a joint depends upon its design and type of joint. Table 15-2 provides efficiencies that may be expected in the various types of joints if they are well designed.

TABLE 15-2 APPROXIMATE EFFICIENCIES OF JOINTS
(References 57 and 58)

TYPE OF JOINT	DESIGN	INSPECTION	EFFICIENCY
Riveted Lap Joint	Single Double Triple	Sample-Full	50 - 60% 60 - 70% 70 - 80%
Riveted Butt Joint	Single Double Triple Quadruple	Sample-Full	60 - 70% 75 - 83% 80 - 89% 85 - 94%
Welded Butt Joint	Single Double	Not radiographed to Fully radiographed	65 - 90% 70 - 100%

The actual value for the efficiency parameter from Table 15-2 will depend on the confidence level in manufacturing techniques and quality control.

The ends of the accumulator are often hemispheres. The internal pressure in a thin spherical shell will create two mutually perpendicular circumferential stresses of equal magnitude and a radial stress. Again a thickness/radius ratio of less than 1/10 provides a minimal value of radial stress. The force on the hemisphere due to internal pressure P is:

$$F_c = \pi r_i P/2 \quad (15\text{-}8)$$

and the resistive force due to circumferential stress is:

$$F_c = 2\pi rt\sigma_c \quad (15\text{-}9)$$

Substituting F_c in equation 15-8 for equation 15-9 provides an equation for maximum stress at the hemispherical ends.

$$\sigma_c = Pr_i/2t\eta \qquad (15\text{-}10)$$

It will be noted that for the same wall thickness, the spherical ends of the accumulator provide twice the strength. The hemispherical ends, therefore, are sometimes thinner than the cylindrical section. Equations for various shapes of accumulators can be found in standard textbooks.

If the wall thickness of the pressure vessel is more than one-tenth the radius, the circumferential and longitudinal stresses cannot be considered uniform throughout the thickness of the wall and the radial stress cannot be considered negligible. Again Reference 38 provides the equations for different shapes of thick walled containers. The Lamé theory for determination of stresses in the walls of thick cylindrical shells considers a mutually perpendicular, triaxial, principal-stress system consisting of the longitudinal, circumferential and radial stresses acting at any element in the wall. The Lamé equations provide the following solutions to calculating thick walled accumulator stresses (ref 57):

$$\sigma_l = \frac{pr_i^2}{r_o^2 - r_i^2} \qquad (15\text{-}11)$$

$$\sigma_c = \frac{r_i^2 p_i - r_o^2 p_o}{r_o^2 - r_i^2} + \frac{(p_i - p_o) r^2 r_o^2}{r^2 (r_o^2 - r_i^2)} \qquad (15\text{-}12)$$

$$\sigma_r = \frac{r_i^2 p_i - r_o^2 p_o}{r_o^2 - r_i^2} - \frac{(p_i - p_o) r_i^2 r_o^2}{r^2 (r_o^2 - r_i^2)} \qquad (15\text{-}13)$$

15.4 RELIABILITY CALCULATIONS

The structural aspects of accumulator or pressure vessel reliability depend on the stress/strength relationships of the materials. The standard definition of reliability includes the probability that the strength random variable will exceed the stress random variable as shown in Figure 15.3.

$$R = P(S > s) = P(S-s) > 0 \qquad (15\text{-}14)$$

Where:
- R = Reliability
- S = Strength random variable
- s = Stress random variable

The stress is used to indicate any agency that tends to induce "failure" while strength indicates any agency resisting "failure"; "failure" meaning failure to function as intended. Failure is defined to have occurred when actual stress exceeds actual strength for the first time.

$$n = \frac{\mu_S}{\mu_s} \qquad (15\text{-}15)$$

Where:
- n = Factor of safety
- μ_S = Mean value for the strength
- μ_s = Mean value for the stress

The designer/analyst must estimate the tail probabilities for stress and strength variables based on previous experience and intimate knowledge of the design and operating environment. The lower and upper limits on these probabilities quantify the uncertainty of the estimates. The probability distributions of ultimate tensile, yield, and endurance strengths of steels are found to be normally distributed.

The standard normal variable of (S - s) will be equal to:

$$z = \frac{\mu_S - \mu_s}{\sqrt{\sigma_S^2 + \sigma_s^2}} \qquad (15\text{-}16)$$

Where:
- σ_S = standard deviation of strength
- σ_s = standard deviation of stress

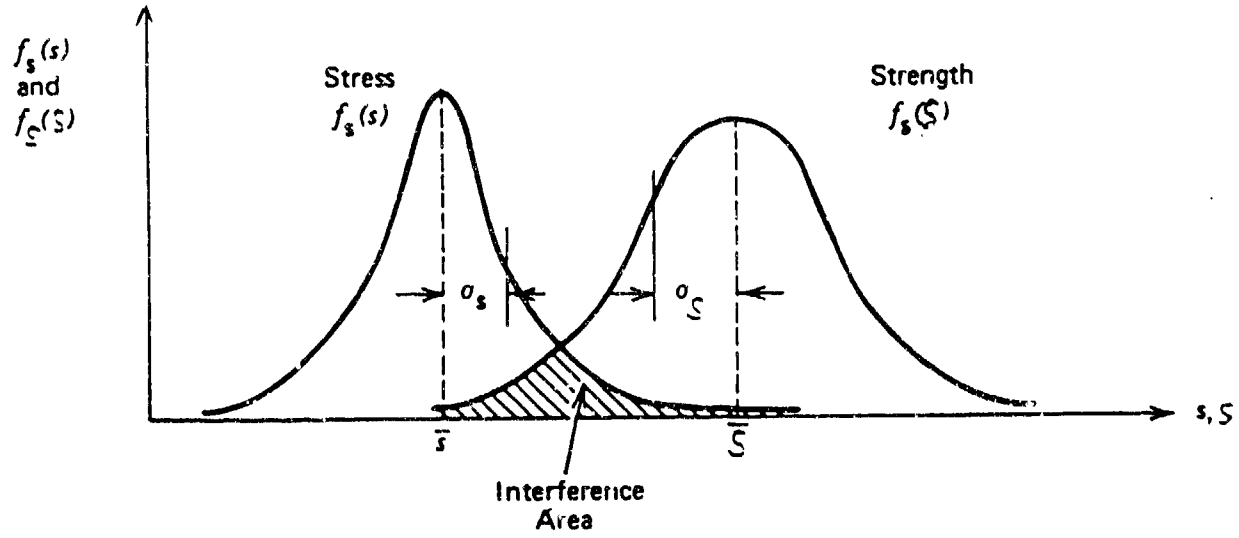

Figure 15.3 Stress Strength Relationship

The relationship between reliability and z is shown in Figure (15-4). The value of z and reliability can be determined mathematically using published tables of the normal distribution.

15.5 PRESSURE VESSELS

If a cylinder fitted with a piston encloses a quantity of gas, the maximum possible energy given to the piston by the expansion of gas is:

$$E_E = PV/k - 1 = (nRT/k - 1) \qquad (15\text{-}17)$$

Where:
- E_E = energy, in-lbs
- P = Initial pressure in cylinder, lb/in^2
- V = Initial volume in the cylinder, in^3
- k = ratio of specific heat

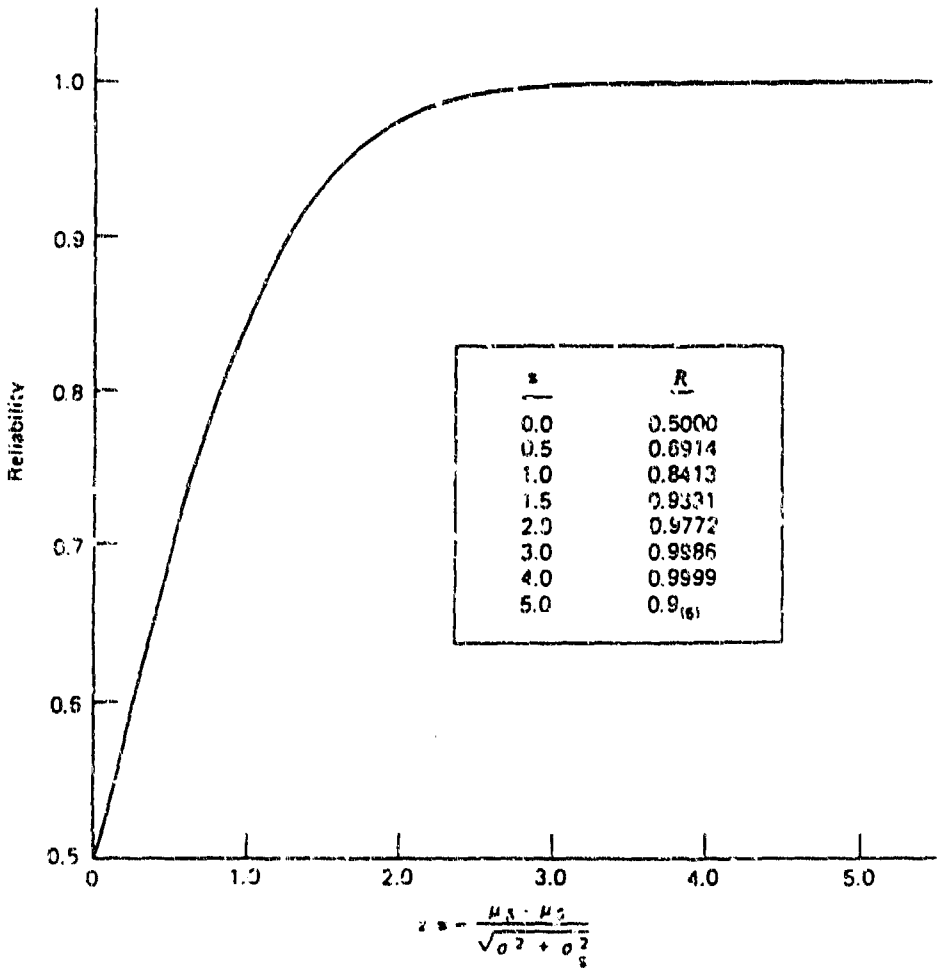

Figure 15.4 Reliability as a Function of z

THIS PAGE INTENTIONALLY LEFT BLANK

CHAPTER 16

THREADED FASTENERS

16.1 INTRODUCTION

Methods of fastening or joining components include threaded fasteners, welding, brazing, soldering, and various adhesive bonding systems. One advantage of threaded fasteners is that they permit disassembly of the equipment for maintenance and repair. Threaded fasteners also allow the use of automated as well as standard manual tools for assembly and installation procedures even under restricted conditions. And significantly, the multitude of available sizes, materials, finishes, and strength levels of mechanical fasteners provides a strong design support system for optimum structural compatibility, even under wide environmental extremes. The reliability of threaded fasteners in a given operating environment depends on the strength of materials, methods of fabrication and assembly, and the stress levels created by fatigue loads and environmental conditions. This chapter considers the reliability performance of externally and internally threaded fasteners.

16.1.1 Externally Threaded Fasteners

Bolts and screws are fasteners with a formed head on one end and an external thread on the other end. Studs are fasteners that incorporate external threads at each end. Structural bolts and screws are installed through prepared holes in the material to be joined. Various lengths of bolts and screws are produced to accommodate the thickness of the material to be fastened and the additional length of thread needed for proper engagement with the nut or with the internal tapped thread. These fasteners are subjected to tensile, shear, bending, and fatigue loads sensed by the joint. They also respond to the environment imposed on the joint, which may include temperature extremes or exposure to various corrosive conditions.

Studs represent a special class of externally threaded fasteners, and a number of configurations have found wide use in design. Double-end studs are threaded at both ends; they can be mated with two nuts, or one end of the stud can be installed in a tapped hole and a nut employed on the other end to tighten or

secure the joint. Another configuration is the continuous-threaded stud, which has been utilized both in general-purpose joining and in special classes for high-temperature and/or high-pressure bolting.

16.1.2 Internally Threaded Fasteners

Specific fastening devices which incorporate internal (female) threads include nuts and inserts. They are intended to engage with the external threads of bolts, screws, and studs, and should be compatible to develop the full rated strength of the external thread.

One aspect of threaded fastener performance that is of concern is the fastener's susceptibility to loosening as a result of severe vibration or dynamic loadings acting on the joint. Since vibratory stresses cannot be totally eliminated, several methods have been developed which have proven effective in maintaining fastener integrity.

- **Self-locking nuts** are integral fasteners which incorporate in the nut element a controlled high-torque feature which is designed to prevent rotation off the external threads, even if the initial tightening torque is completely relaxed. The same principle of an inherent self-locking feature is often extended to screws used in tapped holes.
- **Chemical thread-locking systems** include anaerobic and epoxy adhesives which are applied to the fastener threads before installation, and which cure and effect a permanent bond after assembly.
- **Cotter pins** are a supplemental locking device used with a slotted or castellated nut. They are installed through a drilled hole in the bolt threads to prevent rotation or movement of the nut after installation.
- **Safety lock wiring** is also a supplemental locking system. Usually two or more fasteners in series must be wired to prevent rotation in the "off" direction. The nut end can be wired using slotted or castellated nuts and bolts with drilled holes. However, the predominant use of safety wiring is to secure screw heads which have been drilled to accommodate the wire where the screws have been installed in tapped or blind holes.
- **Lockwashers** are used to resist the loosening effects of vibration, and come in a wide variety of designs for various applications. Conical spring washers are typically made of hardened and tempered steel that is slightly concaved. These washers deform when the bolt is tightened, acting as a spring that

compensates for small losses in bolt tension due to thermal expansion or compression set of the gaskets. Helical spring washers employ a single-coil helical spring that flattens under load. The spring action assists in maintaining the bolt load, while the split edges provide a locking action by biting into the bearing surfaces. Toothed lockwashers provide a gripping action resulting from the teeth biting into the material of the bolt head or nut, and being deformed axially, with the application of tension from bolt torquing.

All locking systems should be compatible. For example, using an elastic stop nut (a nut with a deformable plastic insert) on a male thread drilled for use with a cotter pin, may destroy the holding capability of the nut because of damage to the insert.

16.1.3 Threads

Inch-series thread forms were developed and used by countries employing the English system of measurement. In the United States, standards have been predicated on a 60^0 screw thread angle, originally standardized as the American National thread. Since 1948, the accepted standard has been the Unified thread form, which also specifies a 60^0 angle.

The relationship between nominal diameter and the number of threads per inch is referred to as the "diameter-pitch combination." There are several prominent thread forms which cover the majority of standards intended for general engineering use.

- **Coarse-thread series.** This is perhaps the most widely used series of commercial and industrial fasteners. The thread form is particularly advantageous for applications requiring rapid assembly or disassembly, or for threading into lower-strength materials, such as castings, soft metals, and plastics.
- **Fine-thread series.** For the same nominal diameter, this series incorporates more threads per inch. The result is a larger tensile stress area than that of the same size coarse thread, contributing to the greater strength capability of fine-thread fasteners. These fasteners are normally used where the length of thread engagement is short, or where a smaller lead angle is desired. Fine-thread-series fasteners are used extensively in aerospace and in applications where coarse threads would not be suitable.
- Other series include the extra-fine-thread, 8-thread, 12-thread, and 16-thread series.

In addition to establishing diameter-pitch combinations, the Unified screw-thread system also defines the distinct profile and

identification requirements for several screw-thread forms. The basic thread for the bulk of commercial and industrial fasteners is the Unified form, identified as "UNC" for the coarse-thread series and "UNF" for the fine-thread series.

16.2 FAILURE MODES

16.2.1 Hydrogen Embrittlement

The phenomenon of hydrogen embrittlement in threaded fasteners has been mostly associated with high-strength (over 160 ksi) steel parts which have been furnished with either zinc or cadmium electroplating. During the plating process, atomic hydrogen can be trapped in or under the plating. Other sources of hydrogen can be traced to material pickling or alkaline or acid cleaning. Unless the free hydrogen is removed, when the fastener is used and stressed, as in a structural application, the hydrogen can attack the grain boundaries. The result is rapid crack propagation and often catastrophic failure of the steel fastener.

Two major ways to avoid the problems of hydrogen embrittlement are to (1) bake the fasteners in a subsequent operation after plating to remove the excess hydrogen and (2) use mechanical plating processes in lieu of electroplating. Mechanical plating is the process of using glass beads to cold-weld a ductile metal (e.g., cadmium, zinc, etc.) onto a metal substrate by mechanical energy. Coating thicknesses are more uniform than when the 'hot dip' process is used. However, hot-dip fasteners have more corrosion protection built-in, due to the greater coating thickness. Usually, it is necessary to chase the hot-dip coated threads with a die, since the coating is not uniform.

16.2.2 Fatigue

The importance of fatigue strength properties is associated with the fact that when failure is encountered, it is invariably catastrophic in nature, and often occurs without warning. Research has established that rolled threads exhibit higher fatigue life than machined or ground threads. Further, threads rolled after heat treatment show better fatigue performance than comparable threads rolled before heat treatment. In addition, factors such as proper bolt head design, cold work of the head-to-shank fillet, quality control of the basic material used, and minimization of possible metallurgical defects all contribute significantly to improved fatigue life.

With respect to fatigue performance, it has been observed that

failures normally develop at stress levels well below the static strength of the fastener. The two main types of joint fatigue loading are shear fatigue and tension fatigue. For shear-loaded joints, fatigue failure normally occurs in the plate or sheet material. The applied fatigue or dynamic stresses, hole preparation, hole clearance, amount of induced bending, and fastener preload are some of the factors which influence shear joint fatigue life.

16.2.3 Temperature

Both high-temperature and low-temperature (cryogenic) service exposures are experienced in practice in nuclear systems, aerospace, electronics, transportation, energy systems, construction, and similar applications.

Characteristically, materials used at cryogenic temperatures will show an increase in tensile strength, but may sacrifice ductility. Conversely, at elevated temperatures, tensile strength properties are usually reduced, and above critical service temperature limits they may drop off dramatically.

16.2.4 Load and Torque

For every fastener system, there is an optimum torque range to develop the design clamp load. This is normally referred to as the "torque-tension relationship". Over torquing can result in excessive bolt yielding and possible subsequent relaxation, or even thread stripping and failure on installation. Too low an initial torque can contribute to potential fatigue and/or joint loosening with extended service life.

There are a number of factors which affect and influence the nominal torque-tension relationship, including condition of the threads, condition and squareness of the joint, method and equipment for torquing, installation from the nut or bolt head end, and lubrication. Possibly the most influential factor is the lubrication (plating and/or supplemental lubricant) on the fastener system, since the effective coefficient of friction can alter the installation torque requirements by as much as 50 to 100 percent.

16.2.5 Bolt and Nut Compatibility

Particularly where high-strength bolts are used, critical attention must be given to specifying the correct mating nut. Inadvertent specification of a lower-strength (grade) nut invites the possibility of nut thread stripping under high tensile loading. But more significantly, a weaker nut will not adequately develop

the full clamp load capability of a high-strength bolt when subjected to the necessary installation torque.

As a rule of thumb, the thickness (height) of a nut should approximate the diameter of the equivalent mating bolt to develop the full tensile strength properties of the bolt, if the bolt and nut materials have the same strength.

16.2.6 Vibration

Whereas fatigue loading is presumed to be relatively high with respect to the strength of the threaded fastener or the joint, vibration loads are relatively low, but may be associated with various ranges of cyclic frequencies. Critical combinations of frequency, loading, and amplitude can force a structure into resonance, often with catastrophic results. While the overwhelming majority of operating structures are not subjected to conditions of resonance, the vibration forces present (including random and steady-state vibration, shock, and impact) are sometimes serious enough to drastically affect the threaded fastener system.

Under repeated or extensive vibration, there is a tendency for the nut to rotate or loosen off the bolt threads. Continued vibration can actually result in the nut completely disengaging from the bolt, with subsequent loss of the bolt from the joint. Not as severe, but just as important, vibration loosening can reduce or completely relax the original preload in the bolt, causing the bolt to sense increased fatigue loads with continued exposure. What may have first started as vibration loosening may actually end as a fatigue failure because of the complex stress mechanisms involved.

16.3 STRESS-STRENGTH MODEL DEVELOPMENT

16.3.1 Static Preload

The most important factor that determines the preload induced in a bolt is the torque applied to tighten the bolt. There are several methods commonly used to apply a predetermined torque. The torque may be applied manually by means of a wrench which has a dial attachment that indicates the magnitude of torque being applied. Pneumatic air wrenches are also widely used. Another method is to tighten the nut by hand and then use a wrench to give the nut a predetermined number of turns.

An empirical equation can be used to show the relationship between induced preload and applied torque:

$$T = dF_i c \qquad (16\text{-}1)$$

Where:
- T = Applied torque, in.-lb
- d = Nominal bolt diameter, in.
- F_i = Initial preload, lb
- c = Torque coefficient, and is given by the relationship (Ref. 62):

$$c = \frac{d_m}{2d}\left(\frac{\mu_1 \sec\phi + \tan\psi}{1 - (\mu_1 \sec\phi \tan\psi)}\right) + \mu_c\left(\frac{d_c}{2d}\right) \qquad (16\text{-}2)$$

Where:
- d_m = Mean thread diameter, in.
- d = Nominal bolt diameter, in.
- d_c = Mean bearing face or collar diameter, in.
- μ_1 = Bolt thread coefficient of friction
- μ_c = Coefficient of friction at bearing face of bolt or nut
- ϕ = Thread half angle, degrees
- ψ = Thread helix angle, degrees

For most applications, the value for the torque coefficient can be approximated by the values listed in Table 16-3. The values presented are 'typical' because of the wide range of values reported from coating manufacturers. The user is cautioned to consult the noted reference in critical applications.

A simple bolted joint can also be dangerous unless it is properly designed for the loading and assembled by a trained mechanic. In any fastening situation, the basic aim is to determine as accurately as possible the least expensive fastener that, when properly tightened, will secure a joint during product life. Properly applied assembly torque produces the wedging action of the fastener threads that elongate the bolt to produce tension.

Tension (or preload) induced in a fastener at assembly should always be greater than any external load the joint will experience in service. A preload ensures optimum performance if it prevents the clamped parts from separating in service. Thus a preload should always exceed any external load or payload. The fastener generally remains unchanged until the external load exceeds the preload. Therefore, the higher the preload, the greater potential there is for withstanding larger external loads. This is applicable to perfectly rigid joints, which solid, metal-to-metal

joints approximate. A high preload also helps to retain friction at the joint interface, which is important when shear loads are present.

For the case of the fastener joint loaded statically, if the preload properly exceeds the external loading, a joint will remain in service. However, there are instances mentioned previously in Section 16.2, that can cause relaxation of the preload or an increase in the external loading, causing premature failure of the fastener joint.

16.3.2 Temperature Effects

Changes in temperature must be considered in fastener joint design, in that they can act to change the clamping force in joint and/or the tension (preload) in the fastener. If at any time during operation, the external loading exceeds the preload of the fastener at operating temperature, the fastener is considered to have failed. Therefore, the desired (room temperature) preload, with correction factors for temperature effects can be modeled as follows:

$$F_{i,ambient} = \left[F_{i,oper} \bullet \frac{E_1}{E_2} \bullet K_{SR}\right] - \frac{A_S E_1}{L_E} (\Delta L_J - \Delta L_B) \qquad (16\text{-}3)$$

Where:
- $F_{i,oper}$ = Fastener design preload at elevated operating temperature, lbs.
- E_1 = Modulus of elasticity at room temperature, psi
- E_2 = Modulus of elasticity at elevated operating temperature, psi
- A_S = Fastener tensile stress area, in^2 (See Table 16-2)
- ΔL_J = Change in length or thickness of the joint, in, i.e. (new thickness due to expansion) - (orig. thickness)
- ΔL_B = Change in grip length (L_G, See Fig 16.1) of the fastener, in, i.e. (new length due to expansion) - (orig. length)
- L_E = Effective length (as defined in Figure 16.1) of fastener, in
- K_{SR} = Correction factor accounting for stress relaxation in the fastener at elevated operating temperatures

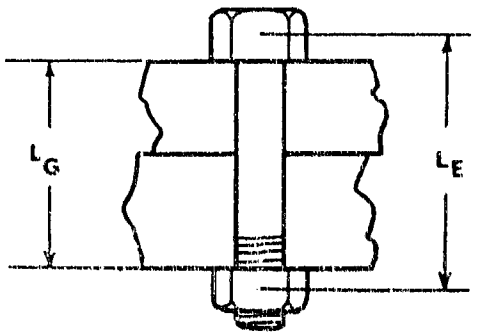

$L_E = L_G + 1/2$ [fastener head height + nut thickness] in inches

Figure 16.1 Determining Effective Fastener Length (L_E)

Table 16-1 presents values of material moduli of elasticity vs. various temperatures. It should be noted that the equation above will have lower preloads at room temperature assembly, if the fastener joint is designed to be operated at a lower temperature (lower temperatures increase the stiffness of a bolted assembly). Designers must also be aware that the strength of most bolts decreases with rising temperatures, as illustrated in Table 16-2.

Table 16-4 contains the values of coefficients of linear expansion for typical bolting material and joint material. These values are used in computing ΔL_J and ΔL_B of Equation (16-3). It is necessary to note that the coefficients themselves, are temperature dependent. The values in the table are based on room temperature. For evaluations of temperatures 400°F and above, the noted reference should be consulted. At elevated temperatures, with dissimilar joint/bolt materials, if the joint material expands more than the bolt material, the bolt will develop more stress or preload ($F_{i,oper}$) than it was designed to experience. To the contrary, if the bolt material expands more than the joint material at elevated operating temperatures, this will act to lessen the design bolt preload. The correction term in Equation (16-3) is therefore subtracted from the preload at assembly ($F_{i,ambient}$) to account for these situations.

It has been determined that at greatly elevated temperatures, many materials experience a slow increase in length under a heavy, constant load. This phenomenon is called creep. A bolted joint assembly may experience a slightly different phenomenon, under which a steady loss of stress in a heavily loaded part whose dimensions are fixed or constrained, called stress relaxation.

The second factor (K_{SR}) in Equation (16-3) accounts for this

time/temperature dependent "stress relieving" when the bolted assembly is to be operated at extreme temperatures. Figure 16.2 contains several plots of correction factors for various bolt materials, derived from stress relaxation data over an elevated temperature range after 1000 hours exposure at each temperature. From the fairly constant initial ranges of each curve in Figure 16.4, it is evident that the stress relaxation effect is of concern only at the higher temperatures (i.e., 600°F and above).

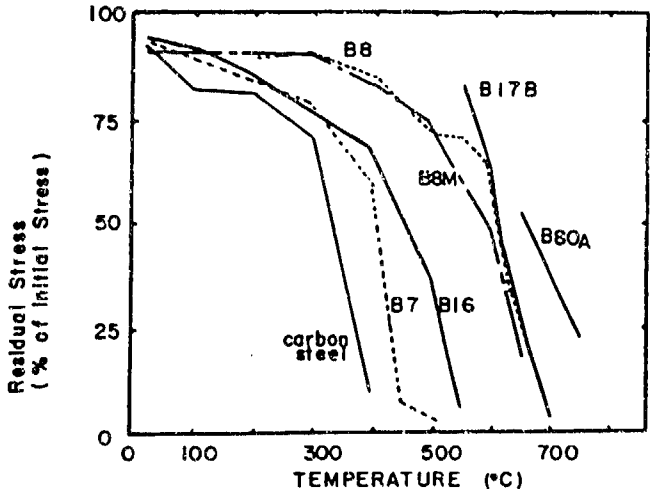

NOTES: (1) Equivalent Materials - ASTM A193 B7,B8,B8M,B16
NIMONIC 80A = B80A
AISI 660 = B17

(2) Residual Stress Reduction for other materials can be derived via Gieske's Correlation (Ref. 63) (Given creep data @ 1000 hrs & spec. temp); residual stress in a bolt = stress that produces 0.01% creep

Figure 16.2. Stress Relaxation Factor, K_{SR}, for Various Operating Temperatures & Materials (After 1000 Hours) (Ref. 63)

Stress relaxation losses are not repetitive in temperature cycling situations. The material stress value stabilizes at some lesser value after some period of time. This is because the tendency to relax decreases as the tensile stress (the driving force) in the bolt, decreases.

16.3.3 Corrosion Considerations

Corrosion is a problem often faced when dealing with bolted assemblies. Excessive corrosion can eventually lead to a reduction in preload, or to the total loss of clamping force through destruction of material. Several methods (Ref. 63) used to combat the onset of corrosion are as follows:

1. Select materials in the joint assembly (bolts, nuts, structure) that are identical, or as close together as possible in the galvanic series, minimizing electrical potential differences.

2. It is desirable, in a situation of dissimilar metals, to have the larger amount of material present to act as an anode, while the smaller amount of material behaves as the cathode.

3. Introduce a 'sacrificial' anode, that can be replaced from time to time. This can be a block of material placed in the vicinity of the bolted joint, where material is sacrificed in a galvanic reaction.

4. Minimize stresses and/or stress concentrations in fasteners and joints by providing generous fillets, polishing surfaces, preloading bolts uniformly, etc. Stress tends to make a material more anodic. Therefore, stress concentrations at the root of a crack will make that portion of the bolt body more anodic, with respect to the adjacent portion; this aids in the growth of fatigue cracks.

5. Various coatings can resist corrosion by -
   (a) providing a barrier by isolating the bolt from the corrosive environment. Cadmium is a common coating, which provides barrier protection.
   (b) inhibiting the process of corrosion.
   (c) provide galvanic/sacrificial protection of the anodic material. Zinc-coated, or 'galvanized' fasteners provide sacrificial protection, along with some barrier protection.

6. Periodic replacement of the bolts, prior to failure, can be a practical solution. This approach intensifies the need to be able to accurately predict the amount of life remaining in a fastener, so that the bolted assemblies are not dismantled prematurely.

Stress corrosion cracking is one of the more serious problems for bolting engineers. This is relatively common in many bolts, and may ultimately lead to sudden and unexpected failure (See Figure 16-3). Although every metallic bolting material is susceptible to stress corrosion cracking under certain conditions,

carbon steel and low alloy quenched and tempered fasteners with a hardness below about 35 HRC are generally immune (for environments such as humid air, aqueous chloride, etc.) (Ref. 63).

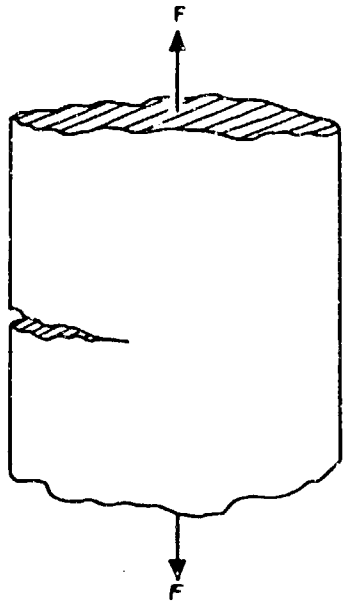

Figure 16.3 Stress Corrosion Cracking

A mathematical model can be developed to make an approximate assessment of the useable life remaining in a fastener through the manipulation of the empirical relationship (Ref. 63) for the determination of safe levels of applied stress to resist stress corrosion cracking:

$$\sigma = \frac{K_{ISCC}}{C_{thd}} (\pi a)^{-0.5} \qquad (16\text{-}4)$$

Where:
- σ = Nominal stress, psi
- K_{ISCC} = Threshold stress intensity factor for stress corrosion cracking, psi-in$^{0.5}$ (See Figure 16.4)
- C_{thd} = Material shape factor, considered 1.5 for fasteners with threads
- a = Material crack/flaw depth, in

Equation (16-4) can be re-written to generate an expression for the maximum preload, $F_{i,ambient}$, which can be safely applied at the time of joint assembly and prevent failure from stress corrosion cracking:

$$F_{i,ambient} = \frac{A_s K_{ISCC}}{C_{thd}} (\pi a)^{-0.5} \cdot C_{Dia} \qquad (16\text{-}5)$$

Where: A_S = Fastener tensile stress area, in^2 (See Table 16-1)

C_{Dia} = Correction factor for varying bolt diameters & thread pitch

A correction term has been added to Equation (16-5), since there is a relationship between the depth of the threads on a fastener and its sensitivity to stress corrosion cracking. Generally, the larger diameter fasteners of a given material will have a lower threshold stress level than small bolts. For the same reason, fasteners with fine pitch threads are less sensitive than those with coarse threads. Various correction factors for bolt sizes are given in Table 16-5.

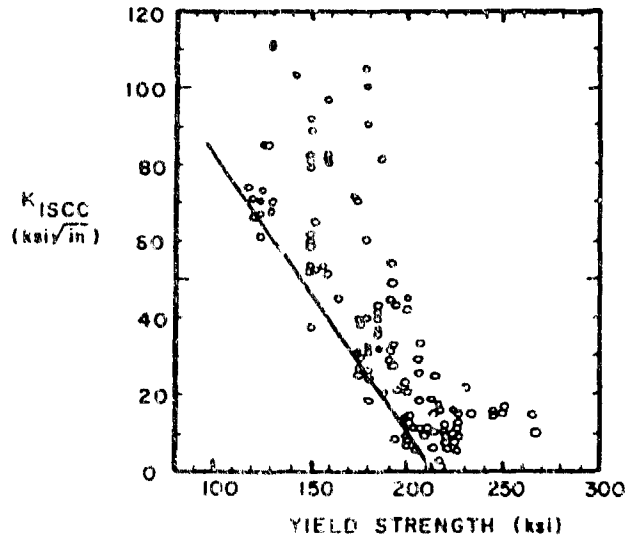

Figure 16.4 K_{ISCC} Factor vs. Material Yield Strength (low alloy, quenched & tempered material, in humid environment) (Ref.63)

16.3.3.1 Estimating the Remaining Life of a Fastener in a Corrosive Environment

The following paragraphs illustrate an approach to the estimation of useable life remaining in a fastener susceptible to the effects of corrosion (in the form of stress corrosion cracking).

A. Determine the desired design preload at ambient conditions to be developed by the fastener.
B. Using this value, solve Equation (16-5) for the maximum crack depth, a. This value should be between the limits, bolt surf. finish tolerance $\leq a \geq$ twice thread depth.

Once the value, a, has been solved for, and it has been checked to exist between proper boundaries, it can be correlated to a plot of corrosion data. This corrosion data should include samples of the same material, exposed to the same type of atmosphere used to compute the K_{ISCC} factor. The weight loss per area of specimen exposure can be computed using the following equation:

$$W = 0.03\ \gamma\ a \qquad \textbf{(16-6)}$$

Where: W = Weight per unit surface area, g/100 cm^2
γ = Bolt material density, g/cm^3
a = Bolt material crack/flaw depth, in

After solving Equation (16-6) for W, the user may enter the graph in Figure 16.5 to estimate a useful bolt life.

Much work has yet to be done in determining characteristics of the many fastener materials that aid in the prediction of the onset of failure due to stress corrosion cracking. The estimation is, however, subject to the following constraints, due to the limited experimental data available:

1. Susceptibility to stress corrosion cracking can increase significantly with elevated temperatures; model estimation is limited to room temperature applications.
2. K_{ISCC} values shown in Figure 16.4 are limited to low alloy, quenched & tempered fastener materials, such as:
   - ASTM A193 B7, B16
   - ASTM A490, A307, A540
   - SAE J 429 GR.8
   - AISI 4340
3. The corrosive environment used to derive the experimental data was based upon humid air.

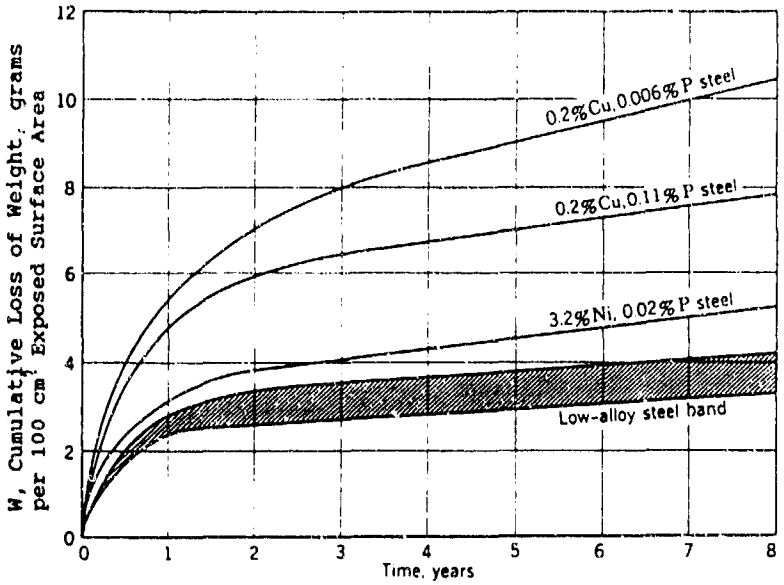

Figure 16.5 Typical Coupon Corrosion Penetration Test Results, (Low alloy steel in humid air) (Ref. 64)

16.3.4 Dynamic Loading

Machinery in operation is a dynamic situation. For the most part then, fasteners used in many applications have a small dynamic load superimposed on a much larger static prelcad. These dynamic or 'fluctuating' loads are augmented by stress concentrations and bending.

16.3.5 Determination of Base Failure Rate

Data available from fastener manufacturers that have performed extensive testing, can be used to determine the base failure rate, $\lambda_{F,B}$. However, since this data is somewhat specific to the conditions or environment of the test, it is often difficult to locate data that will yield the base failure rate of a specific type of fastener, under a particular set of loading conditions. This necessitates the development of a procedure to estimate the base failure rate of a generic fastener, with various characteristics and loading conditions.

Fatigue, as discussed in Section 16.2, can limit the useable life of a fastener in a dynamic loading condition. Fatigue limit testing can be valuable in developing a model for fastener failure rates. A large number of tests are necessary to establish the fatigue strength of a material due to the statistical nature of

fatigue. One of the most widely used fatigue testing devices is the R.R. Moore high speed rotating beam machine (Ref. 62). Figure 16.6 illustrates the specimen and method. A motor spins a slender, round, solid, polished test specimen, supported at each end but loaded in pure bending. The majority of published fatigue strength data was obtained using this method (Ref. 61). The generated bending stress and the number of stress reversal revolutions of the beam, required for failure, is recorded and graphed.

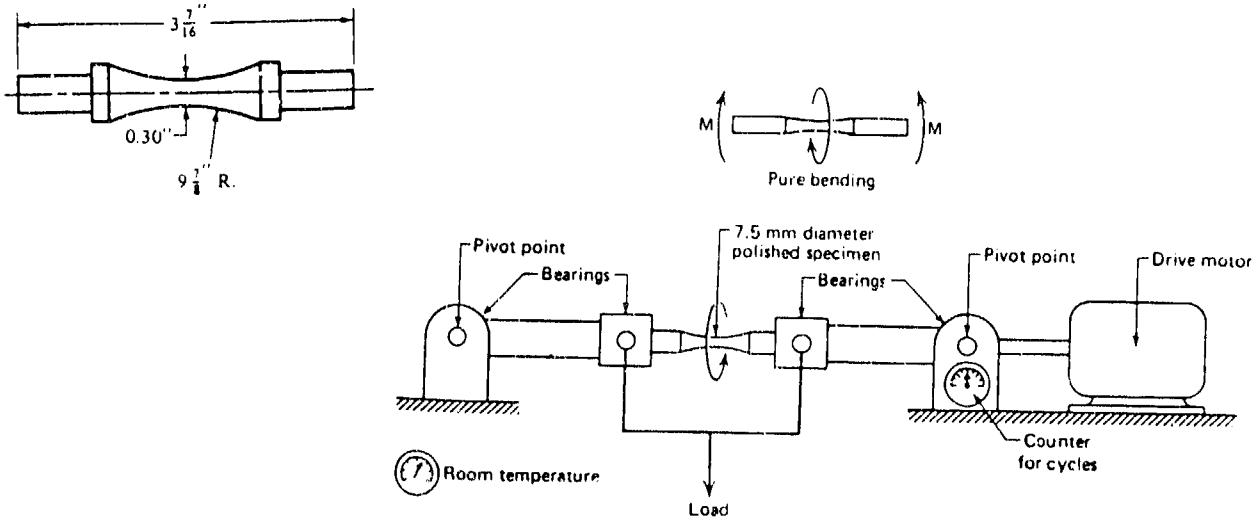

Figure 16.6 Diagram of Rotating Beam Machine, with Detail of Specimen (Ref. 61,62)

The stress values become less as the data is plotted against an increasing number of stress cycles. The graph becomes horizontal in the case of ferrous metals and alloys after the material has been stressed for a certain number of cycles. This is referred to as the 'endurance' or fatigue limit. Table 16-6 presents endurance limit properties for several bolting materials. Aluminum, or other nonferrous materials do not have a horizontal asymptote, hence limit. To develop a model to predict fastener failures under dynamic loading, it is necessary to correlate the results of standard material fatigue tests to the geometry and loading conditions of the fastener to be used. It must be noted that even when the material of the test specimen and that of the mechanical

fastener are identical, there will be significant differences between the fatigue curves for the two. Therefore, although correction factors will be presented in an effort to compensate for this, the user is cautioned that the analytical model developed will not yield absolutely precise results.

If the shape of a fatigue curve is known, the statistical number of cycles to failure, N, or ultimately the expected failure rate, $\lambda_{F,B}$, can be found. If the S-N diagram is not available, there exists a means to analytically determine it (Ref. 62). If the equation of the S-N curve is given by:

$$\sigma_f = a N^b \qquad (16\text{-}7)$$

Where: σ_f = Fatigue stress at failure, psi
N = Number of stress reversal cycles at failure, cycles
a,b = See Equations (16-9) & (16-10)

By taking the log of both sides of Equation (16-7), and using the following definitions from Ref. 39, the following are noted:

- the endurance limit occurs at $N=10^6$,
- low cycle fatigue terminates at $N=10^3$,
- S-N curves terminate low cycle fatigue at σ_f = 90% of material ultimate tensile strength ($\sigma_{T,ult}$)

Then:

$$\log \sigma_f = \log a + b(\log N) \qquad (16\text{-}8)$$

and solving for a,b:

$$a = \frac{(0.9\,\sigma_{T,ult})^2}{\sigma_e} \qquad (16\text{-}9)$$

and:

$$b = -\frac{1}{3}\left(\frac{\log\left(0.9\,\sigma_{T,ult}\right)}{\sigma_e}\right) \qquad (16\text{-}10)$$

Where: σ_e = endurance or fatigue limit, psi

The actual known fastener endurance limit value (Table 16-6) can be substituted for (σ_e) in Equations (16-9) and (16-10) above. If the specific endurance limit is not known (which is generally the case) an endurance limit for an S-N test specimen (of the same material) can be used. If this data is not readily available, an approximation can be made using the relationships in Table 16-7.

16.3.6 Correction Factors for the S-N Test Specimen Data

The S-N test specimen must be corrected for the specific conditions and geometry of the fastener under consideration. Correction factors have been established to account for the individual contributions by surface finish, size differential, loading, temperature, etc. The following equation should be employed when utilizing S-N data for fasteners based on rotating beam test specimen results:

$$\sigma_{e,corr} = \sigma_{e,S\text{-}N} \bullet C_{SZ} \bullet C_L \bullet C_T \bullet C_I \bullet \frac{1}{C_K} \qquad (16\text{-}11)$$

Where:
- $\sigma_{e,corr}$ = Endurance or fatigue limit, corrected to reflect fastener, psi
- $\sigma_{e,S\text{-}N}$ = Endurance or fatigue limit of S-N test specimen, psi
- C_{SZ} = Factor for the effects of size deviation from the S-N test specimen
- C_L = Factor to include the effects of different loading applications
- C_T = Factor for the effects of elevated temperatures
- C_I = Factor accounting for severity of in-service cyclic shock (impact) loading
- C_{SC} = Factor for the effects of surface coatings
- C_K = Stress concentration factor for fastener threads

It should be noted that rotating beam data generally carries with it, a great deal of scatter. Therefore, any life determinations based on the data will be statistical at best. No attempt has been made in Equation (16-11) to account for the statistical uncertainty. It has been suggested that rotating beam data reflects a reliability in actual survival of only 50% confidence. A factor of 0.814, applied to Equation (16-12) is encouraged by Reference 61, in order to introduce a 99% reliability confidence level in S-N endurance test data and estimates.

16.3.7 Size Factor, (C_{SZ})

Smaller machine parts tend to exhibit greater fatigue strength than larger ones, all other configurations and material properties being equal. Since larger surfaces have more defects overall, the probability of failure is greater in larger parts. A correction factor is established to account for this, as well as the bending of a solid circular material, without constant rotation (Ref 62):

For bending or torsional loading:

$$C_{SZ} = \left(\frac{0.370\ D}{0.3}\right)^{-0.1133} \qquad \textbf{(16-13)}$$

Where: D = Basic major diameter of fastener, 2 inches or less

For axial loading:

$$C_{SZ} = 1$$

16.3.8 Alternate Loading, (C_L)

Appropriate load factors are presented in Table 16-8.

16.3.9 Temperature Factor, (C_T)

Typical rotating beam data is acquired at room temperature. However, fasteners are often called upon to clamp equipment at higher temperatures. Since a decline in static and dynamic strengths, creep, and thermal expansion must all be taken into account at higher temperatures, the following factor should be applied to the S-N test specimen data to achieve correction:

For steel operating above 160°F:

$$C_T = \frac{620}{(460 + T_{oper})} \qquad (16\text{-}14)$$

Where: T_{oper} = operating temperature of fastener, °F

16.3.10 Cyclic Shock/Impact Loading, (C_I)

A correction factor must be applied when shock loads are present. In general, cyclic loads are less severe than applied shock loading. The factors are presented in Table 16-9.

16.3.11 Surface Coatings, (C_{SC})

Surface treatments such as electroplating and spraying act to reduce the endurance limit. If any of these operations are to be used, Table 16-10 provides the correction factors.

16.3.12 Thread Correction Factor, (C_K)

Observations of typical bolt failure pattern data from Ref. 62 have revealed that only about 15% of failures occur under the head, due to the stress riser caused by the fillet. The risers found in the thread area accounted for the other 85%. Therefore, Table 16-11 presents the correction factor for stress risers caused by the introduction of threads. The effects of notch sensitivity and surface finish have been incorporated.

Table 16-1. Elasticity Modulus (10^6 psi) as a Function of Temperature (Ref. 63)

SPECIFICATION	GRADE	TEMPERATURE, degrees F					
		-325	-200	70	400	600	800
ASTM A193	B5	32.9	32.3	30.9	29.0	28.0	26.1
	B6	31.2	30.7	29.2	27.3	26.1	24.7
	B7	31.6	31.0	29.7	27.9	26.9	25.6
	B8-CL 1	30.3	29.7	28.3	26.5	25.3	24.1
	B16	31.6	31.0	29.7	27.9	26.9	25.5
ASTM A307		31.4	30.8	29.5	27.7	26.7	24.2
ASTM A320	L7	31.6	31.0	29.7	27.9	26.9	25.5
	L43	31.6	31.0	29.7	27.9	26.9	25.5
	B8	30.3	29.7	28.3	26.5	25.3	24.1
ASTM A325	Type 1,2,3	31.4	30.8	29.5	27.7	26.7	24.2
ASTM A354		31.2	30.8	29.3	27.5	26.5	24.0
ASTM A449		31.2	30.6	29.3	27.5	26.5	24.0
ASTM A453		30.3	29.7	28.3	26.5	25.3	24.1
ASTM A490		31.2	30.6	29.3	27.5	26.5	24.0
ASTM A540	B21,B22	31.6	31.0	29.7	27.9	26.9	25.5
	B23,B24	29.6	29.1	27.6	26.1	25.2	23.0
SAE J429	GR 1,2,4	31.4	30.8	29.5	27.7	26.7	24.2
	GR 5,7,8	31.2	30.6	29.3	27.5	26.5	24.0

Table 16-2 Bolt Yield Strength (ksi) as a Function of Temperature (Ref. 63)

SPECIFICATION	GRADE	TEMPERATURE, degrees F 70	400	600	800	1000
ASTM A193	B8-C1 1	30	21	18	17	
ASTM A307	GR B	36	31	27		
ASTM A320	L7,L43,L7A	105	92	84	73	
Stainless Steel	420	80	71	66		93

Table 16-3. Typical Torque Coefficients (Ref. 63)

FASTENER MATERIAL/COATING	TORQUE COEFFICIENT
Aluminum on AISI 8740 alloy steel	0.52
Mild or alloy steel on steel	0.20
Stainless steel on mild/alloy steel	0.30
1" dia. A490	0.18
1" dia. A490 (rusty)*	0.39
Black Oxide	0.18
Cadmium plate (dry)	0.20
Cadmium plate (waxed)	0.19
Galvanized A325	0.46
Galvanized, hot-dip A325	0.09 - 0.37
Gold on stainless steel or beryllium copper	0.40
Graphitic coatings	0.09 - 0.28
Machine Oil	0.21
Moly paste or grease	0.13
Solid film PTFE	0.12
Zinc plate (waxed)	0.29
Zinc plate (dry)	0.30

* Exposed outdoors for two weeks

Table 16-4. Thermal Coefficients of Linear Expansion (10^{-6} in/in/°F) evaluated at 70°F (Ref. 63)

SPECIFI-CATION	GRADE	TEMPERATURE, degrees F 70	400	600	800
ASTM A193	B5	6.5	7.0	7.2	7.3
	B6	5.9	6.4	6.5	6.7
	B7	5.6	6.7	7.3	7.7
	B8	8.5	9.2	9.5	9.8
	B16	5.4	6.6	7.2	7.6
ASTM A307		6.4	7.1	7.4	7.8
ASTM A320	L7	5.6	6.7	7.3	7.7
	L43	6.2	7.0	7.3	7.6
	L7M	6.2	7.0	7.3	7.6
	B8 CL 1	8.5	9.2	9.5	9.8
ASTM A325		6.2	7.0	7.3	7.6
ASTM A354		6.2	7.0	7.3	7.6
ASTM A449		6.2	7.0	7.3	7.6
ASTM A453	651	9.1	9.7	10.0	10.2
ASTM A490		6.2	7.0	7.3	7.6

Table 16-5. Correction Factors for UNC Thread Bolt Sizes, (C_{Dia}) Derived from Data (Ref. 63)

BOLT DIAMETER (inches)	BOLT MATERIAL HARDNESS* 22 HRC	31 HRC	38 HRC
1.0 and below	1.0	1.0	1.0
1.5	0.93	0.92	0.95
2.0	0.87	0.87	0.88
2.5	0.84	0.82	0.85
3.0	0.84	0.82	0.85
4.0	0.84	0.82	0.85

* Data based on max initial crack depth (a) equal to thread depth

Table 16-6. Endurance Limit Properties for Various Bolting Materials (Ref.63)

MATERIAL GRADE OR CLASS	SIZE RANGE	ENDURANCE LIMIT
SAE 5	1/4 - 1 in	18.6 kpsi
	1 1/8 - 1 1/2 in	16.3 kpsi
SAE 7	1/4 - 1 1/2 in	20.6 kpsi
SAE 8	1/4 - 1 1/2 in	23.2 kpsi
ISO 8.8	M16 - M36	129 MPa
ISO 9.8	M1.6 - M16	140 MPa
ISO 10.9	M5 - M36	162 MPa
ISO 12.9	M1.6 - M36	190 MPa
Metric M16, CL 8.8	M16	10.2 ksi
Metric M14 x 1.5	M14 x 1.5	7.1 - 11.4 ksi
SAE J429, GR 8		18 ksi
Metric CL 10.9	M12 x 1.25	8 ksi
M10, grade 12.9		6.9 - 10.7 ksi

Table 16-7. Formulas for Estimating the Endurance Limit ($\sigma_{e,S\text{-}N}$) of S-N Test Specimens (Ref. 61)

For Steels, where $\sigma_{T,ult} \leq 200{,}000$ psi:

$$\sigma_{e,S\text{-}N} = 0.5\ \sigma_{T,ult}$$

For Steels, where $\sigma_{T,ult} > 200{,}000$ psi:

$$\sigma_{e,S\text{-}N} = 100{,}000 \text{ psi}$$

For Aluminum Alloys (wrought):*

$$\sigma_{e,S\text{-}N} = 0.4\ \sigma_{T,ult}$$

For Aluminum Alloys (cast):*

$$\sigma_{e,S\text{-}N} = 0.3\ \sigma_{T,ult}$$

*NOTE: The endurance limit for nonferrous alloys is taken to occur at approximately 10^8 cycles.

Table 16-8. Load Factors (Ref. 62)

TYPE OF LOAD APPLIED	C_L
Axial ($\sigma_{T,ult} \leq 220$ kpsi)	0.923
Axial ($\sigma_{T,ult} > 220$ kpsi)	1.0
Bending	1.0
Torsion & shear	0.577

Table 16-9. Correction Factor for Impact Loading (Ref. 61)

IMPACT CATEGORY	C_I
LIGHT (rotating machinery - motors, turbines, centrifugal pumps)	1.0
MEDIUM (rotary & reciprocating motion machines - compressors, pumps)	0.8
HEAVY (presses for tools & dies, shears	0.6
VERY HEAVY (hammers, rolling mills, crushers	0.4

Table 16-10. Correction Factor for Surface Coatings (Ref. 61 & 62)

SURFACE TREATMENT	C_{SC}
Electroplating (chromium, nickel, cadmium)	0.65
Electroplating (zinc)	1.00
Metal spraying	0.86

Table 16-11. Endurance Limit Reduction Factor for Threaded Elements, C_K (Ref. 62)

SAE GRADE BOLT	ROLLED THREADS	MACHINED THREADS
0 - 2	2.2	2.8
4 - 8	3.0	3.8

THIS PAGE INTENTIONALLY LEFT BLANK

CHAPTER 17

MECHANICAL COUPLINGS

17.1 INTRODUCTION

A coupling, typically, is a device which makes a semi-permanent connection between two shafts. Various types of couplings have been developed, and can be classed according to the relative position's of the coupled shafts. Fig. 17.1 illustrates common types of couplings. This chapter will examine the collinear shaft coupling and the intersecting shaft centerline coupling, or "universal joint", to which it is often referred.

Of the three basic designs of collinear shaft couplings shown in Figure 17.1, the most widely used employ mechanical connections. These mechanically connected couplings can be further grouped into either flexible or rigid types.

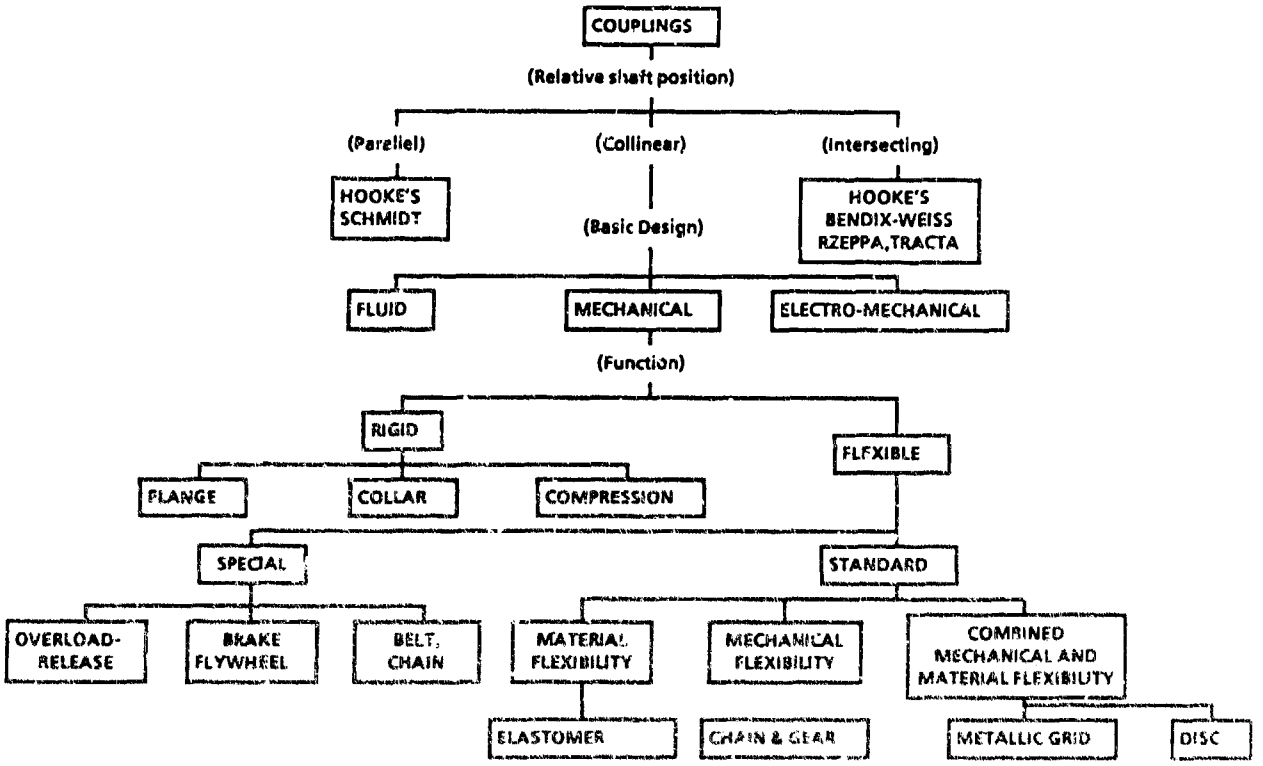

Figure 17.1 Common Classifications for Shaft Couplings (Ref. 75)

17.1.1 Rigid Collinear Shaft Couplings

Rigid couplings are used when shafts have good collinear alignment. Although simple in design, rigid couplings are usually restricted to relatively low speed applications where good shaft alignment or shaft flexibility can be expected. Three major types of rigid couplings are shown in Fig. 17.2.

-The clamp/compression type coupling relies on the clamping force developed from the fasteners to connect the two shafts. Torsional forces are normally transmitted via shaft keys.

-The sleeve type coupling is generally a single piece housing that transmits torque via shaft keys or tapered bushings. Axial positioning of the coupling is maintained by retaining rings or threaded shaft collars.

-The flange coupling mates two coupling halves together in a plane that is perpendicular to the shaft centerline. Torque can be transmitted between shafts either via the bolted fasteners in the flange, or the frictional contact between flange faces.

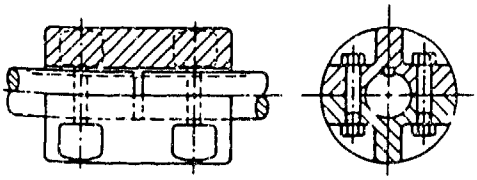

CLAMP/COMPRESSION TYPE

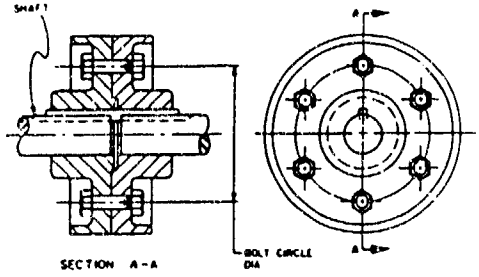

FLANGE TYPE

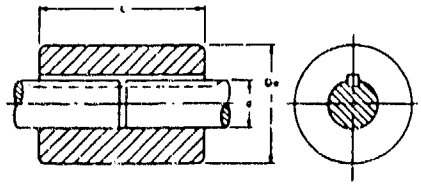

SLEEVE/COLLAR TYPE

Figure 17.2 Rigid Couplings
Ref. 76)

17.1.2 Flexible Collinear Shaft Couplings

Flexible couplings are used to connect collinear shafts subject to one or more kinds of misalignment, while reducing the effect of shock and impact loads that may be transferred between shafts. Figure 17.1 indicates that these types of couplings can be further classified into tree groups: couplings employing material flexibility, couplings employing mechanical flexibility, and couplings utilizing both types of flexibility.

Figure 17.3 shows examples of flexible couplings. Flexible couplings employing rigid parts (mechanical flexibility) transmit torque without backlash or angular play other than that due to manufacturing tolerances and wear. These types of couplings are generally incapable of dampening the transmittal of shock and impact loads. The bellows type coupling is used in applications involving large amounts of shaft misalignment, combined with low radial loading. The disc-type coupling can accommodate a smaller amount of angular misalignment than the bellows type, but by adding additional metallic "disks", radial load (torsional) carrying capacity can be greatly increased.

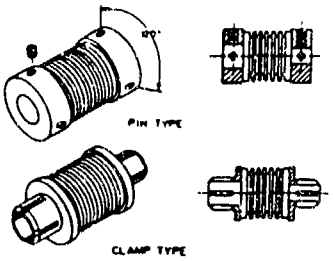

BELLOWS TYPE

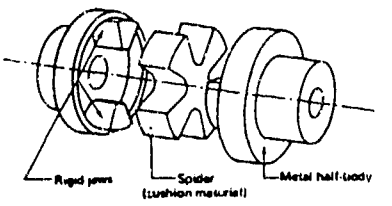

FLEXIBLE INSERT TYPE

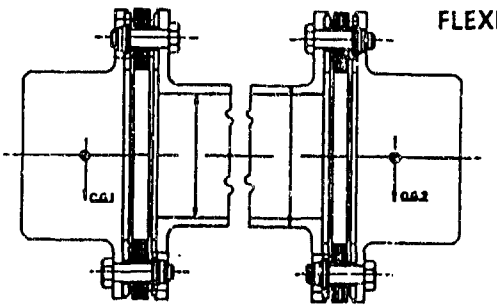

DISC-TYPE

Figure 17.3 Flexible Couplings
(References 66,75,76)

Flexible couplings containing resilient components (material flexibility) can accommodate shaft misalignment, as well as dampen shock and impact loads. This type of coupling possesses torsional flexibility, often acting as "detuning" devices by altering the vibration properties of the connected system. The flexible insert type coupling shown in Figure 17.3 transmits torque through an oil resistant rubber spider assembled between two pairs of axially overlapping rigid jaws.

Examples of the third type of flexible coupling type (material and mechanical flexibility) are the metallic grid and the diaphragm coupling. The metallic grid coupling consists of two metal half-bodies with slots cut into the peripheries to seat a serpent like spring steel alloy grid. The deflection of the springs under load help to reduce shock loading, thereby utilizing the best characteristics of material and mechanical coupling flexibilities.

Table 17-1 indicates the range of performance characteristics possible with flexible couplings. Due to the varying ranges of performance, it is easy to see why some caution must be taken in selecting the correct coupling for the operating conditions to be encountered. Diaphragm couplings are rated for high speed operation, but accept only a small amount of misalignment. Although elastomeric and gear type couplings can accommodate a fair amount of angular misalignment, in general, the gear coupling is rated to accept heavier duty (horsepower). Again, a tradeoff must made, since gear couplings require periodic maintenance in the replenishment of lubrication and seals.

A representative graphic comparison of flexible coupling types is shown in Figure 17.4. Figure 17.4(a) shows the clear superiority of an elastomeric material flexible coupling over the other two types when angular and parallel shaft misalignments are excessive. However, the mechanical flexibility of the disk-type or metallic grid can carry a much greater load at smaller degrees of shaft misalignment. This is illustrated in Figure 17.4(b).

17.2 FAILURE MODES OF FLEXIBLE COUPLINGS

Table 17.2 lists various failure modes encountered when using flexible couplings. Many of these failures can be avoided by properly selecting the correct type, size and rating for the intended operational environment.

Coupling reliability is affected by the method used to mount the coupling hub on the shafts of connected equipment. The preferred procedure is to use an interference fit between hub and shaft of approximately 0.005 inches per inch of shaft diameter. Although

clearance fit connections work satisfactorily for certain types of machinery, this practice should be avoided on any critical piece of equipment, because the reliability of the system can be affected. The most common cause of failure in this instance would be fretting of the coupling bore and of the shaft, and rolling of the key within the keyway due to looseness in the connection.

Table 17-1. Typical Flexible Coupling Performance Characteristics (Ref. 77)

COUPLING TYPE	TOLERABLE MISALIGNMENT ANGULAR (°)	PARALLEL (in)	AXIAL (in)	MAXIMUM SPEED (rpm)	HP PER 100 RPM	TORSIONAL RIGIDITY (lb-in/deg)
Bellows	5-10	0.008-0.010	0.035-0.055	----	----	2,618-35,989
Diaphragm	.17-.33	0.166	0.127	34,300-12,300	14-4,270	----
Disc	.5/disc pac	----	0.06-0.2	21,250-7,000	1.2-170	----
Elastomeric	3.0	0.031	0.031	5,800-1,900	10-476.7	28-1,348
Gear	3.0	0.034-0.145	-----	5,400-1,830	40-2,507	25,000-1.58M
Metallic Grid	.06-.25	.002-.02	.012-.05	10,000-540	0.67-11,900	----

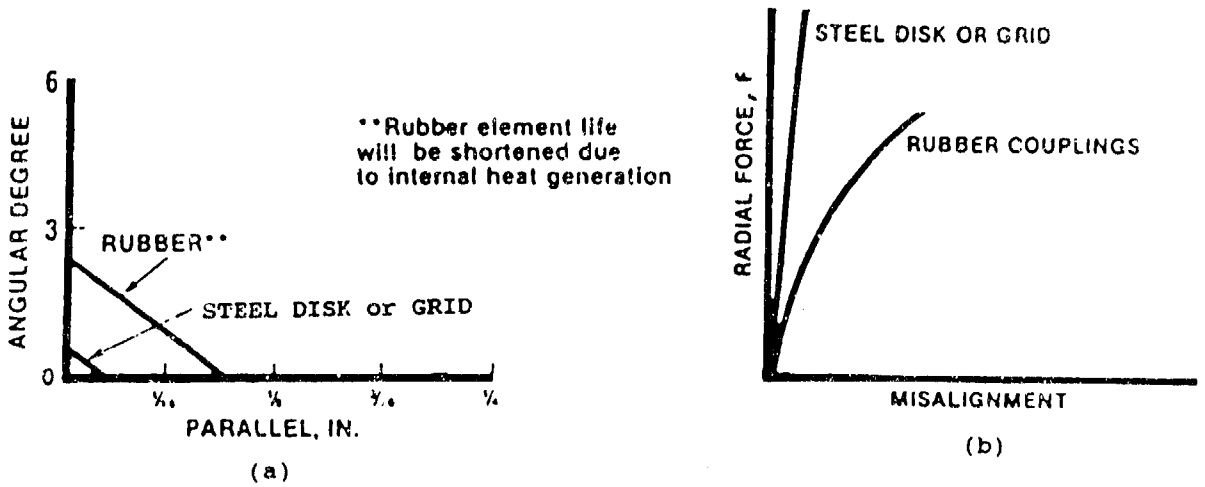

Figure 17.4 Coupling Characteristics

Table 17-2. Failure Modes for Flexible Couplings (Ref 78)

FAILURE MODE	PROBABLE CAUSE	CORRECTIVE ACTION
• WORN FLEXING ELEMENT OR SHAFT BUSHINGS • SHAFT BEARING FAILURE • HIGH-PITCHED OR STACCATO NOISE	• EXCESSIVE SHAFT MISALIGNMENT	• REALIGN COUPLING AND SHAFTS TO MEET SPECIFIED TOLERANCES
• RUPTURED ELASTOMERIC FLEXING ELEMENT • SHEARED HUB PINS OR TEETH • LOOSE HUBS ON SHAFT, SHEARED KEYS	• TORSIONAL SHOCK OVERLOAD	• FIND AND ELIMINATE CAUSE OF OVERLOAD • USE LARGER COUPLING
• FATIGUE OF FLEXING ELEMENT • OVERHEATED ELASTOMERIC TIRE OR SLEEVE • FATIGUE OF HUB PINS OR DISCS • WORN GEAR TEETH • STACCATO OR CLACKING NOISE • LOOSE HUBS ON SHAFT, KEYSEAT WALLOW	• TORSIONAL VIBRATION • EXCESSIVE STARTS AND STOPS • HIGH PEAK-TO-PEAK TORSIONAL OVERLOAD	• USE LARGER COUPLING FOR VIBRATION AND START/STOP OPERATION • ADD FLYWHEEL TO HUB FOR TORSIONAL OVERLOAD
• SHAFT BEARING FAILURES • HIGH-PITCHED WHINE • MOTOR THRUST BEARING FAILURE	• LUBRICANT FAILURE	• REPLACE OR REBUILD COUPLING
• SWOLLEN OR CRACKED ELASTOMERIC FLEXING MEMBER • LUBRICANT FAILURE • SEVERE HUB CORROSION	• CHEMICAL ATTACK	• USE MORE CHEMICALLY RESISTANT FLEXING MEMBER OR HUB • COAT HUBS
• DISTROTED OR DETERIORATED ELASTOMERIC FLEXING MEMBER • LUBRICANT FAILURE	• EXCESSIVE HEAT	• USE MORE HEAT-RESISTANT FLEXING MEMBER OR LUBRICANT
• SHATTERED FLEXING MEMBER • LUBRICANT FAILURE	• LOW TEMPERATURE (BELOW 0°F)	• USE SPECIAL LOW-TEMPERATURE RUBBER COMPOUNDS AND LUBRICANTS

Initial alignment of machinery is one of the most critical factors affecting coupling performance and reliability; this is true regardless of the type of coupling employed. It should be remembered that flexible couplings are basically in-line devices which are intended to compensate for small amounts of shaft misalignment caused by bearing wear, foundation settling, thermal growth, etc. The more attention paid to initial alignment, the larger the reserve margin that will exist for accomplishing the intended purpose of the coupling. There are definite advantages to be gained from aligning equipment to more precise values than those recommended by the manufacturer. The primary advantage, of course, is that the reserve margin for accepting misalignment during the life of the machinery is thereby increased.

Another factor to be considered, and one which is most important to satisfactory performance, is adherence to the manufacturer's bolt torquing recommendations. Loose bolts can induce fretting corrosion, as well as hammering and pounding which will eventually destroy the bolts and coupling discs.

Equipment maintenance is probably the most important factor affecting the life of the operating experience of gear couplings in the petroleum refining industry. Indications from the field show that at least 75% of all coupling failures are due to lack of lubrication. It should be kept in mind that even a well aligned gear type coupling requires periodic replenishment of the lubricant due to heat, oxidation, etc.

Some failure modes can be experienced with the accumulation of operating time. Specifically, shaft misalignment can develop after many cycles of operation as a result of:

-Settling Foundations. Once a coupled system's bed plate is grouted, it may experience settling due to foundation conditions. During welding operations of the bedplate, residual stresses may warp the base, causing difficulty during initial alignment.

-Thermal Growth. Due to differences between component material thermal expansion coefficients, at elevated operating temperatures, shaft centerlines may "grow" to be farther apart than at room temperature. In situations where a system will normally operate at elevated temperatures (i.e. steam turbine driven equipment, etc.), the zero misalignment condition should be set at these elevated temperatures. In addition, total operational scenarios must be considered. If the system has a substantial cool-down or warm-up period of operation, then consideration must be given as to whether or not operations can be sustained during these periods of misalignment.

-Connecting Piping Reactions. If, during extended operation, piping braces loosen or fail, the coupled components may have to support excessive reaction loads from connecting pipes. This can put a severe strain on bearings and coupling alignment.

-Vibration. Excessive vibration can act to bring about material fatigue, fastener loosening, or stress corrosion cracking. After extended operation, component wear can open clearances and augment vibration amplitudes. Increased vibration can act to worsen shaft misalignment.

-Bearing Wear. Lack of lubrication, contamination of the bearings, and wear can deteriorate a bearings performance over a period of time. Bearing failure can increase vibration, which can in turn, add to shaft operational misalignment.

17.3 CHARACTERISTIC COUPLING EQUATION

In machine design, it often becomes necessary to fasten or join the ends of two shafts axially so that they will act as a single unit to transmit power. This transmission is characteristically described in Equation 17-1:

$$\sigma_c = \frac{396{,}000\, H_{IH}\, d}{4\pi N I} \qquad (17\text{-}1)$$

Where: σ_c = Yield strength of the coupling in shear, psi
d = Outside diameter of coupling, in
H_{IH} = Input shaft horsepower
N = Shaft speed, RPM
I = Polar moment of inertia of coupling, in^4

Calculated stress from Equation (17-1) can be converted to an expected coupling life through various empirical data developed by various manufacturers for different types of couplings.

An example of the type of data that coupling manufacturer's develop when testing their coupling designs is shown is Figure 17.5. This type of data is often difficult to obtain, in that it is company proprietary. The data is also design specific and carries speed and load limitations. The stress calculated from Equation (17-1), can be converted to a base failure rate using relationships such as those pictured in Figure 17.5.

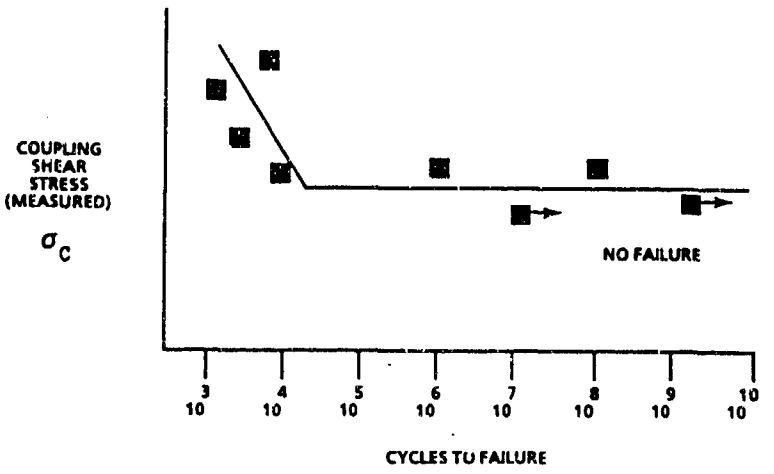

Figure 17.5 Stress as a Function of Cycles to Failure for a Disc-type Flexible Coupling (Ref. 71)

17.4 FAILURE RATE MODEL FOR COUPLING

In the event that manufacturer's data is not readily available, a base failure rate for a coupling can sometimes be derived from the sum of its component parts. In the case of a gear coupling, the base failure rate is given by:

$$\lambda_{CP} = \lambda_{GE} + \lambda_{SE} + \lambda_{H} \qquad (17\text{-}2)$$

Where:
- λ_{CP} = Failure rate of coupling, failures/million cycles
- λ_{GE} = Failure rate of gears, failures/million cycles
- λ_{SE} = Failure rate of seals, failures/million cycles
- λ_{H} = Failure rate of coupling housing including hubs, failures/million cycles

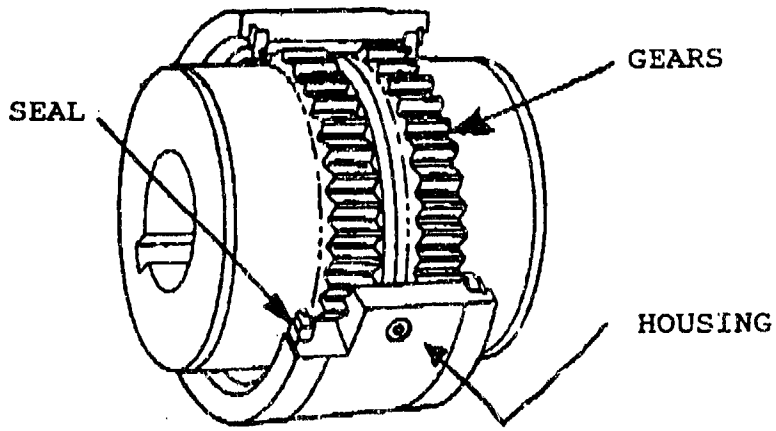

Figure 17.6 Gear Coupling (Ref. 65)

Each of the failure rate terms contained on the right side of Equation (17-2) have been developed under different chapters contained within this handbook. The user is referred to them for a complete evaluation.

17.5 UNIVERSAL JOINT (INTERSECTING SHAFT CENTERLINE COUPLING)

The universal joint, also known as the Cardan or Hooke Coupling consist of two yokes, connected by a cross through four bearings. The universal joint can be used in place of couplings where the

only misalignment between shafts is angular and permanent. It cannot be used to compensate for parallel misalignment of axial play. When this device, pictured in Figure 17.7, is operated at an angle, δ, nonuniform motion is developed. When the driving yoke of the joint is operating at a uniform rotational velocity, the driven yoke rotates non-uniformly with respect to angular displacement, velocity, and acceleration.

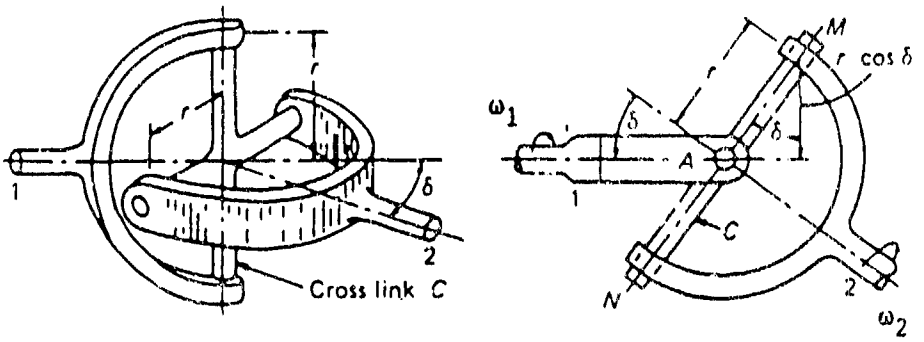

Figure 17.7 Typical Universal Joint (Ref 74)

17.6 CHARACTERISTIC EQUATION FOR UNIVERSAL JOINT

A relationship for the output shaft velocity (ω_2) as a function of the input velocity (ω_1), the angle between shafts (δ), and the angular displacement of the input shaft (θ) is given by (Ref. 74):

$$\omega_2 = \frac{\omega_1 \cos\delta}{1 - \sin^2\delta \sin^2\theta} \qquad (17\text{-}3)$$

The characteristics of Equation (17-3) are plotted in Figure 17.8. The motion of the joint has the following characteristics (Ref. 79):

1. The average angular displacement and velocity is uniform. That is, if the driving yoke rotates one revolution, the driven yoke also rotates one revolution. However, during this one revolution, the incremental angular displacement (θ) and instantaneous angular velocity (ω_2) and acceleration are not transmitted uniformly through the joint.
2. The angular displacement of the driven yoke (θ_2) during one

revolution lags and leads the driving yoke twice.

3. Assuming constant input motion of the driving yoke, the driven yoke has a maximum difference of output angular velocity (ω_2) with respect to the driving yoke when the driving yoke lies in the plane described by the joint angle (δ), and also, when the driving yoke is normal or perpendicular to this plane. The driven yoke has the same instantaneous angular velocity ($\omega_1 = \omega_2$) as the driving yoke at approximately 45 degrees from the joint angle plane for small joint angles.

4. The maximum instantaneous angular acceleration and deceleration of the driven yoke occurs when the angular velocity of the driven yoke is the same as the driving yoke ($\omega_1 = \omega_2$). Also, the maximum acceleration and deceleration coincide with maximum lag and lead respectively.

5. The incremental angular displacement, velocity, and acceleration increase as the joint angle (δ) increases, but at an increasing rate.

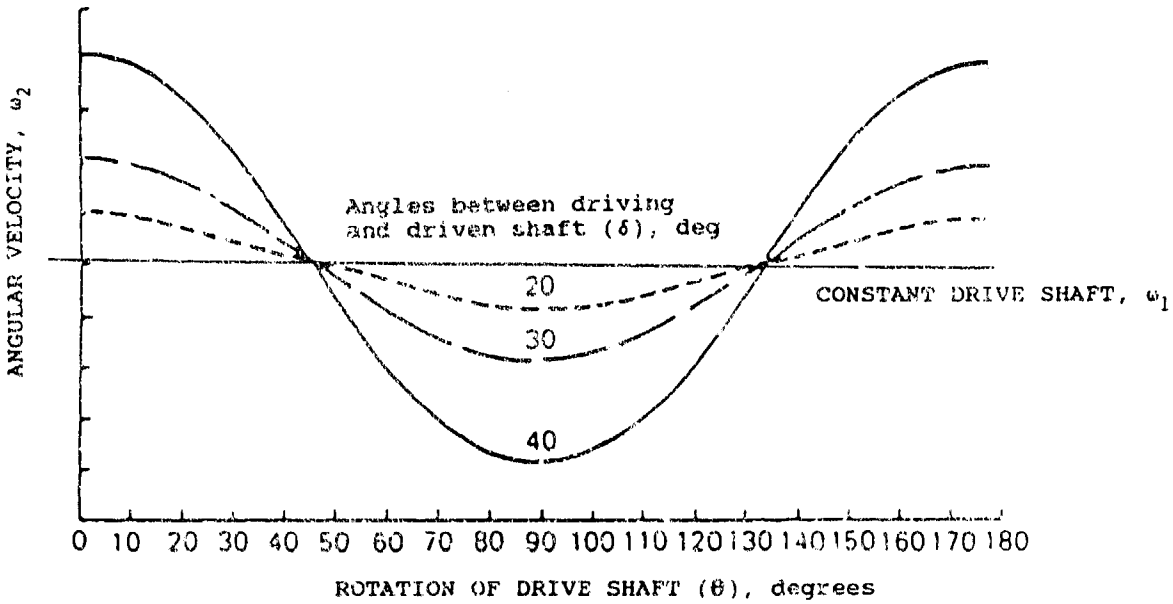

Figure 17.8 Velocity Characteristics of a Universal Joint

The principal advantages of the universal joint are its relatively low cost to manufacture as well as simple and rugged construction, combined with long life and ease of serviceability. In addition to providing the necessary torque capacity in a limited operating space, the joint has the thrust capability to withstand relatively high, externally imposed axial forces which may be produced, for example, by a sliding spline when shaft length changes are required during vehicle suspension movements .

The universal joint becomes a much more useful coupling device when it is used in tandem with another universal joint. In such applications, a constant velocity ratio between input drive shaft and output drive shaft is established. The restrictions for this to occur include:

- the input and output shaft yokes must lie in the same plane
- the angles between driver, driven, and connecting shafts must be equal (Refer to Figure 17.9).

Through the years. the universal joint has found the most widespread usage in the passenger car, truck, and various other on- and off-highway vehicle driveline, axle driveshaft, power take-off, and steering shaft systems. Other applications have been in aircraft, railway, marine, agricultural, industrial and stationary drive system installations.

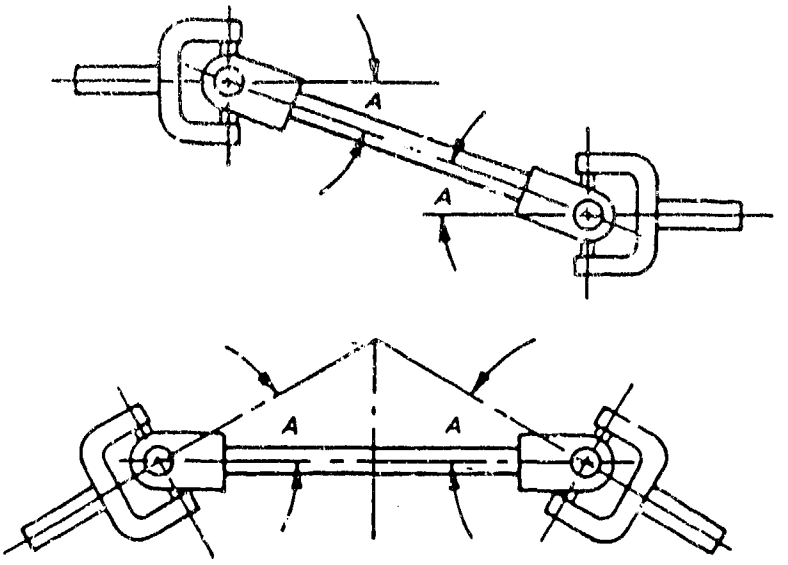

Figure 17.9 Universal Joints Used in Tandem for Constant Speed Ratios

17.7 FAILURE RATE MODEL FOR UNIVERSAL JOINT

The failure rate of a universal joint can be presented as a sum of the failure rates of its individual component parts:

$$\lambda_{UJ} = \lambda_{BE} + \lambda_{SE} + \lambda_{H} + \lambda_{P} \qquad (17\text{-}4)$$

Where: λ_{UJ} = Failure Rate of Universal joint, failures/million cycles

λ_{BE} = Failure Rate of Bearings,

failures/million cycles

λ_{SE} = Failure Rare of Seals, failures/million cycles

λ_{H} = Failure Rate of Structural Components, failures/million cycles

λ_{F} = Failure Rate of Coupling Fasteners, failures/million cycles

The life expectancy of a joint is a function of the application requirements such as torque, speed, and joint angle, as well as other factors. Therefore, the basic load-speed-life-stress relationships applicable to rolling element bearings are useful in life computations for universal joints employing similar rolling elements. These relationships have been established in the Bearing chapter of this Handbook. Although the contribution from terms other than in Equation (17-4) must be examined, in many cases λ_{BE} can drive the relationship. For speed and load variation, base failure rate is proportional to:

$$C_L = \left(\frac{L_A}{L_S}\right)^Y \qquad (17\text{-}5)$$

and:

$$C_N = \frac{N_A}{N_S} \qquad (17\text{-}6)$$

Where: L_A = Actual radial load

L_S = Specification radial load

Y = 3.33 for roller bearings

Y = 3.00 for ball bearings

N_A = Actual speed

N_S = Specification speed

For more detailed component failure rate development, the user is referred to the individual part chapters in this Handbook.

THIS PAGE INTENTIONALLY LEFT BLANK

CHAPTER 18

SLIDER CRANK MECHANISMS

18.1 INTRODUCTION

The slider crank mechanism is usually not thought of as an independent mechanical component but rather as an integral part of a more complex piece of equipment such as the piston rod/piston components of an internal combustion engine. Figure 18.1 shows a typical slider crank mechanism, the normal function of this particular device being the conversion of rotational force into a linear force or vice versa.

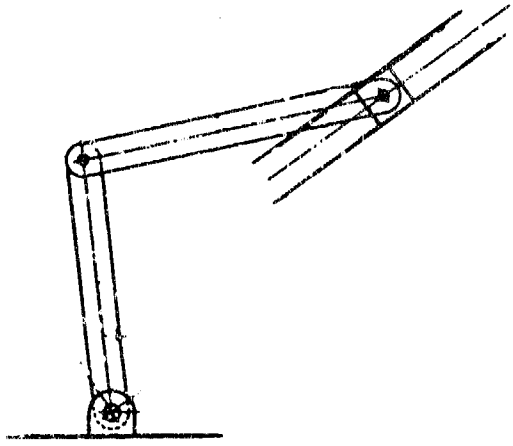

Figure 18.1 Typical Slider Crank Mechanism

The typical slider crank mechanism includes bearings, rods, linkages, seals and a sliding surface such as a cylinder wall. Wear of these parts becomes the primary failure mechanism, the failure modes and effects being dependent upon the application. The geometry of the design plays an important part of the reliability analysis since the mechanical advantage and the wear pattern are greatly influenced by the positioning of parts.

18.2 FAILURE MODES OF SLIDER CRANK MECHANISMS

The more predominant failure modes of a slider crank mechanism can be readily identified with frictional action on like or dissimilar materials. The component parts of a slider crank mechanism are subject to wear in varying degrees and the normal approach to reliability analysis is to establish the expected life of the individual parts in the projected operating environment.

Bearing wear will usually be influenced by the lubrication film thickness maintained, the side load on the bearing, the contamination level, and corrosion. Chapter 7 presents an approach to evaluating bearing life for theses considerations.

Slider crank wear will manifest itself in several ways to cause the degradation of the slider crank to the point of failure. This threshold of failure must be defined in terms of jamming friction, side movement, limit of travel, alignment of parts, etc. Some of the failure modes to be considered are included in the following table.

TABLE 18-1

TYPICAL FAILURE MODES OF SLIDER CRANK MECHANISMS

FAILURE MODE	FAILURE CAUSE
Linkage does not move in intended direction	Bearing parts separate causing jam
Restricted travel limited of linkage	Excess load combined with loss of bearing material
Broken linkage	Fatigue of linkage member
Linkage alignment out of tolerance	Bearing deformed

The function of a mechanical seal is to provide a barrier between the moving or rotating surfaces and prevent the trapped fluid from migrating into undesired areas. For example, in the case of an engine cylinder the rings on the piston prevent the combustion gases from going into a lubricant and also prevent loss of energy due to combustion gas by-pass. The O-ring and flat seals are designed to prevent the lubricant from contaminating other part

areas and also, the loss of the lubricant. Seals and gaskets are described in Chapter 3 and the models contained therein should be used for the analysis of seal and gasket reliability.

Rods and linkages within the slider crank mechanism are subject to fatigue and may crack although this failure mode is rare.

18.3 MODEL DEVELOPMENT

The failure rate model for the slider crank mechanism can be expressed by the following equation:

$$\lambda_{SC} = \lambda_{BE} + \lambda_{RD} \quad \lambda_{SE} + \lambda_{RI} + \lambda_{PC} \qquad (18\text{-}1)$$

Where: λ_{SC} = Total failure rate for slider crank, failures/million operations

λ_{BE} = Failure rate for bearings, failures/million operations

λ_{RD} = Failure rate for rods/shafts, failures/million operations

λ_{SE} = Failure rate for seals/gaskets, failures/million operations

λ_{RI} = Failure rate for rings/dynamic seals, failures/million operations

λ_{PC} = Failure rate for sliding surface areas, failures/million operations

Reliability models can be developed for each specific part or parts and the combination of failure rates in accordance with the slider crank reliability model will provide the projected design life.

18.3.1 BEARINGS

One of the predominant failure modes of a slider crank mechanism is caused by a malfunctioning bearing surface. Both roller and sliding bearings can be included in a slider crank design. Failure rate equations for roller/ball bearings are included in Chapter 7.

Typical sliding bearings are shown in Figure 18.2. The sliding bearing is usually comprised of three elements including the inner surface member, the outer surface member, and the lubricant film separating the inner and outer members. The sliding bearing is characterized as a shaft rotating within a sleeve. Sliding bearings can be classified by material, load direction, lubrication method, and configuration. Sliding bearings are well suited for large loads encountered in slider crank mechanisms. Although

sliding bearings may have less running friction than rolling bearings, their starting friction is much higher. Rolling bearings are also easier to lubricate during service life. Sliding bearings are well suited to low speed applications where shock and vibration occur such as punch presses and steam hoists. And for many applications such as hoists, sliding bearings need only minimal lubrication.

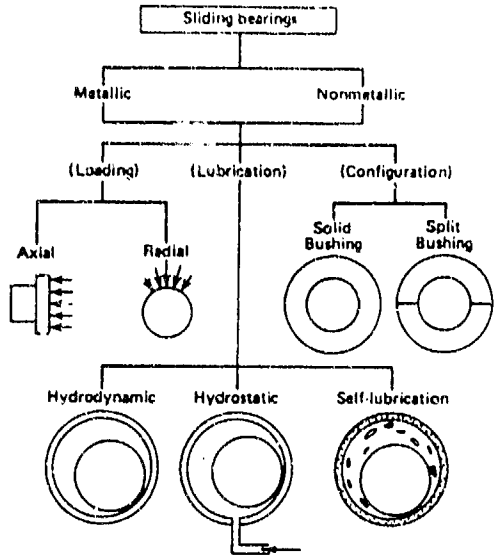

Figure 18.2 Sliding Bearing Classifications (Ref. 19)

Hydrodynamic sliding bearings are characterized by the load being carried by a film of oil generated by rotation and suitable oil grooves. The friction at start-up is large due to direct contact between the journal and sleeve while the friction during operation is moderate, the bearing acting like a low efficiency pump. The life of the bearing then is limited due to wear at start-up and stopping.

The reliability of the sliding crank mechanism will, of course, be affected by the lubricant being used. All liquids provide lubrication but some do better jobs in particular applications. Dry lubricants, for example, will adhere very well to the bearing surfaces but tend to wear quite rapidly as petroleum oils. Their capacity to minimize friction, however, is only fair.

The concept of lubricant viscosity is illustrated in Figure 18.3. A film of lubricant adheres to the stationary plate and supports a moving plate. In order to move the upper plate to the right at a constant velocity V, it is necessary to exert some constant force F. Thus a shear stress is applied at the wetted

surface of the moving plate. This shear stress is equal to (Ref. 19):

$$\tau = \frac{F}{A} \qquad (18\text{-}2)$$

Where: A = Area of plate surface in contact with lubricant

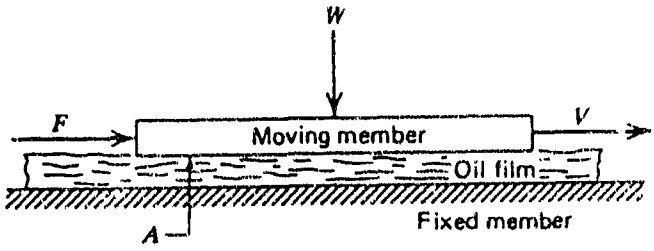

Figure 18.3 Lubricant Viscosity
(Ref. 19)

The rate of shearing strain R′ is defined as the ratio of the velocity V to the thickness h of the lubricant film (Ref. 19):

$$R' = \frac{V}{h} \qquad (18\text{-}3)$$

The ratio of shearing stress to rate of shearing strain is called the dynamic viscosity μ (Ref 19):

$$\mu = \frac{\tau}{R'} = \frac{Fh}{AV} \qquad (18\text{-}4)$$

Three types, or regimes, of lubrication occur in practice. They differ in the degree to which the lubrication is carrying the load. A full film lubrication physically separates the shaft and bearing surfaces by a relatively thick lubricant film of about 15 μm. This film prevents any metal-to-metal contact at the operating conditions. The coefficient of friction will be low, usually not above about 0.005. Full film operation implies minimum power losses and maximum life expectancy of the parts.

Complete boundary lubrication means that the bearing and shaft surfaces are being rubbed together with only a very thin lubricant film adhering to each surface and preventing direct contact. The coefficient of friction is high, in the range of 0.1.

Mixed film lubrication means that there is both boundary and hydrodynamic lubrication. Part of the load is carried by small pools of self-pressurized lubricant. Other areas of the surfaces are rubbing with only a thin film of lubricant separating the peaks. A typical friction coefficient for this regime is 0.02.

Figure 17-4 shows the coefficient of friction plotted against a bearing characteristic number $\mu n/P$. The three operating variables in this bearing characteristic number are the lubricant's viscosity μ(mPa·s or μreyn), the shaft speed n(rps), and the unit bearing load P, the last defined as (Ref. 19):

$$P = \frac{W}{LD} \qquad (18\text{-}5)$$

Where: W = Bearing load, lb
D = Bearing Diameter, in
L = Bearing length, in

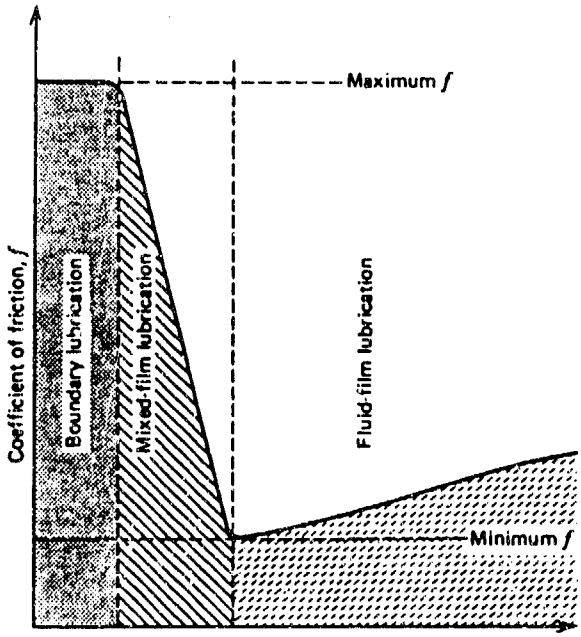

Figure 18.4 Variation of Friction Coefficient with the $\mu n/P$ factor (Ref. 19)

This bearing characteristic number provides a method of determining any potential problem with lubricant film. Any low viscosity, low shaft speed, or high unit bearing load implies a low value for $\mu n/P$. Conversely, the higher $\mu n/P$, the easier it is to establish a full-load-supporting film.

For the largest values of $\mu n/P$, there is full-fluid-film, or hydrodynamic, lubrication. In this regime of operation the coefficient of friction attains a minimum of about 0.001. A greater $\mu n/P$ value will assure an adequately thick film and a margin of safety with a somewhat greater power loss.

The lowest values of $\mu n/P$ correspond to the regime of complete boundary lubrication. The friction coefficient remains constant throughout this regime; its actual value depends on the character of the surfaces and the lubricant.

The midregime is that of mixed-film lubrication. In this regime a decrease in $\mu n/P$ is accompanied by a sharp increase in friction coefficient.

Most of the bearings utilized in mechanical devices are considered light service and operate in the mixed-film or boundary lubrication regimes. Typical office equipment and appliances with latching mechanisms contain bearings with little or even no lubrication and without the proper operating conditions to develop a full-lubricant film. Yet they survive and they provide a low-cost solution to the problem of supporting and controlling machine members in relative motion.

Manufacturers of bearings for light service usually base bearing selection on the PV factor, the product of unit bearing load P and rubbing velocity V. This factor indicates what bearing temperature will be reached and what rate of wear can be expected. Temperature rise and wear rate are maintained within reasonable limits by controlling the PV factor.

The unit bearing load P, already defined by Equation (18-5) is the ratio of the bearing's load to its projected area. The rubbing velocity V must be calculated differently for oscillating shaft motion than for continuous rotation. For continuous rotation the rubbing speed is (Ref. 19),

$$V = 5 \pi D n \qquad \textbf{(18-6)}$$

Where: V = rubbing velocity, fpm
D = bearing diameter, in
n = shaft speed; rps

However, if the shaft is oscillating relative to the bearing, the design value for V is based on the average rubbing speed (Ref 19).

$$V = \frac{\pi D \theta f}{72} \qquad (18\text{-}7)$$

Where: θ = Total angle traveled per cycle, deg
f = Frequency of oscillation, cps

The use of sleeve or journal bearings in severe service requires a full bearing or a thick lubrication film to support the load. While an external pump may be used to supply a lubricant under pressure to the bearing's feed hole, within the bearing itself it is the shaft that acts as a pump and pumps the oil adhering to it into the wedge-shaped oil film that supports the load. With the shaft stationary, the shaft simply rests on the bottom of the bearing. But at start-up the shaft begins to roll up the bearing wall. As it climbs, it also begins to pump oil between itself and the bearing. As this oil is pumped, the shaft lifts off the bearing surface and moves in the direction of rotation. At operating speed, the shaft has developed a wedge-shaped film between itself and the bearing that supports the shaft and its load. The radial displacement of the shaft's center from the bearing's center is the eccentricity, e. The pressure distribution in the oil film achieved depends on factors such as shaft speed, load, lubricant viscosity, bearing clearance, and length-to-diameter ratio.

18.3.2 Rods/Shafts

The reliability of the rod or shaft is generally very high when compared to the components in the sliding-action system. Generally, the life expectancy will be at least three times that of the bearing. The possibility that the rod or shaft will fracture can best be determined using finite element techniques. The effects of the rod or shaft breakage on adjacent components is of greater importance than the reliability of the rod or shaft itself. From Chapter 10 the following equation for rod or shaft failure rate is derived:

$$\lambda_{SH} = \lambda_{SH,B} \cdot C_{ASF} \cdot C_{DSF} \cdot C_{SE} \cdot C_{CON} \qquad (18\text{-}8)$$

Where: $\lambda_{SH,B}$ = Rod or shaft base failure rate

C_{ASF} = Surface finish factor
C_{DSF} = Material temperature factor
C_{SE} = Material endurance factor
C_{CON} = Contamination factor

Procedures for determining the base failure rate and the multiplying factors can be found in Chapter 10.

18.3.3 Seals/Gaskets

The failure rate of a seal or gasket is determined by ability of the seal to restrict the flow of fluid from one region to another for the intended life is prescribed operating environment. From Section 3.2 of Chapter 3 the following equation is derived for determining the failure rate.

$$\lambda_{SE} = \lambda_{SE,B} \cdot C_p \cdot C_Q \cdot C_{DL} \cdot C_H \cdot C_f \cdot C_v \cdot C_t \cdot C_M \qquad (18\text{-}9)$$

Where: $\lambda_{SE,B}$ = Base failure rate of seal, 0.85 failures/million operations
C_p = Multiplying factor which considers the effect of fluid pressure on $\lambda_{SE,B}$
C_Q = Multiplying factor which considers the effect of allowable leakage on $\lambda_{SE,B}$
C_{DL} = Multiplying factor which considers the effect of seal size on $\lambda_{SE,B}$
C_H = Multiplying factor which considers the effect of seal hardness and tightness on $\lambda_{SE,B}$
C_f = Multiplying factor which considers the effect of seat smoothness on $\lambda_{SE,B}$
C_v = Multiplying factor which considers the effect of fluid viscosity on $\lambda_{SE,B}$
C_t = Multiplying factor which considers the effect of temperature on $\lambda_{SE,B}$
C_M = Multiplying factor which considers the effect of contaminants on $\lambda_{SE,B}$

The procedures contained in Chapter 3 can be used to determine the base failure rate and multiplying factors.

18.3.4 Dynamic Seals

The sealing surface of rings and other dynamic seals are perpendicular to the shaft with contact between primary and

rings to achieve a dynamic seal at various speeds, pressures and temperatures. From section 3.3 of Chapter 3 the following equation is derived for determining the failure rate of a dynamic seal.

$$\lambda_{SE} = \lambda_{SE,B} \cdot C_Q \cdot C_H \cdot C_f \cdot C_v \cdot C_t \cdot C_N \cdot C_{PV} \qquad (18\text{-}10)$$

Where: C_{PV} = Multiplying factor which considers the effect of the seal PV value on $\lambda_{SE,B}$

The procedures contained in Chapter 3 can be used to determine the base failure rate and multiplying section for rings.

18.3.5 Sliding Surface Area

The wear life of the sliding surface area depends on the correlation of wear of the two surfaces involved with the material strength and the stress imposed on the sliding action mechanism. From a time standpoint, wear of the two surfaces will occur in two phases. The first or constant wear phase is characterized by the shearing of asperities due to sliding action. During this period the wear rate is practically linear as a function of the number of mechanical cycles and the wear depth at the end of the constant wear phase is one half the original surface finish. During the second or severe wear phase, wear debris becomes trapped between the two sliding surfaces and gouging of the surfaces takes place. The wear rate begins to increase very rapidly and failure of the sliding action mechanism is imminent. From Chapter 9, Section 9.3.1:

$$\lambda_{AC} = \lambda_{AC,B} \bullet C_{CP} \bullet C_T \qquad (18\text{-}11)$$

Where:
λ_{AC} = Failure rate of actuator, failures/million cycles
C_{CP} = Contaminant particle coefficient
C_T = Temperature factor

Section 9.3.1 of Chapter 9 describes a procedure to determine the number of cycles in Phase 1 wear and the number of cycles in Phase 2 wear at which point the slider crank mechanism is determined to have failed.

CHAPTER 19

REFERENCES

1. Abadzheva, R.N. et al., "Effects of Brake Fluid Components on Rubber," Khimiya i Tekhnologiya Topliv i Masel, No. 8, pp. 18-19 (Aug 1982).

2. Aleker, I.G et al., "Procedure for Calculating the Working Characteristics of Clutches for Motor Cars, Tractors, and Other Machines During the Design Stage," Vestnik Mashinostroeniya, Vol. 63, No. 3 (1983).

3. Anderson, A.E., "Wear of Brake Materials," in: Wear Control Handbook, M.B. Peterson and W.O. Winer, Eds., pp. 843-857, Am. Soc. Mech. Eng., New York (1980).

4. Armstrong, E.L., W.R. Murphy and P.S. Wooding, "Evaluation of Water Accelerated Bearing Fatigue in Oil-Lubricated Ball Bearings," Lubrication Engineering, Vol. 34, No. 1, pp. 15-21 (1 Nov 1977).

5. Bauer, P., M. Glickmon, and F. Iwatsuki, "Analytical Techniques for the Design of Seals for Use in Rocket Propulsion Systems," Volume 1, ITT Research Institute, Technical Report AFRPL-TR-65-61 (May 1965).

6. Bayer R.G., A.T. Shalhey and A.R. Watson, "Designing for Zero Wear," Machine Design (9 January 1970).

7. Bishop, F.E. and William M. Needleman, "The Effects of Fluid Contamination on Component Wear," Pall Corporation.

8. Block, H. and D. Johnson, "Downtime Prompts Upgrading of Centrifugal Pumps," Chemical Engineering Magazine, pp. 35-38 (25 Nov 1985).

9. Boone, Tony D., "Reliability Prediction Analysis for Mechanical Brake Systems," NAVAIR-SYSCOM Report (Aug 1981).

10. "Boston Gear Catalog" Catalog 100, INCOM International Inc., Quincy, Massachusetts 02171.

11. Canterbury, Jack, and James D. Lowther, "Application of Dimensional Analysis to the Prediction of Mechanical Reliability," Naval Weapons Support Activity, Washington Navy Yard, Wash., D.C., Report ADAD35295 (September 1976).

12. Carson, Harold, Springs: Troubleshooting and Failure Analysis, Marcel Dekker, Inc., New York. (1983).

13. Cormier, K.R., "Helicopter Drive System R&M Design Guide," Division of United Technologies Corp., Stanford, CT 06602, Report ADAD69835 (April 1979).

14. "Engineering Guide to Spring Design" Associated Spring, Barnes Group INc., Form No. 515 (1981).

15. "Fabrication and Testing of Lightweight Hydraulic System Simulator Hardware - Phase II," Report NADC-79024-60, prepared by Rockwell International, Columbus, Ohio, for Naval Air Systems Command, Washington, D.C.

16. Ferodo Limited, Friction Materials for Engineers, Stockport, England (1969).

17. Field, G.J., "Seals That Survive Heat," Machine Design (1 May 1975).

18. Hauser, D.L. et al., "Hardness Tester for Polyur," NASA Tech Briefs, Vol. 11, No. 6, p. 57 (1987).

19. Hindhede et al., Machine Design Fundamentals (1983).

20. Ho, T.I., F.E. Kennedy and M.B. Peterson, "Evaluation of Materials and Design Modifications for Aircraft Brakes," NASA Report CR134896 (Jan 1975).

21. Houston, John, "Getting to Grips with Clutches and Brakes," in: Engineering Materials and Design, Vol. 26, No. 4 (April 1982).

22. Howell, Glen W. and Terry M. Weathers, Aerospace Fluid Component Designers' Handbook, Volumes I and II, TRW Systems Group, Redondo Beach, CA prepared for Air Force Rocket Propulsion Laboratory, Edwards, CA, Report AD 874 542 and

Report AD 874 543 (February 1970).

23. Hubert, Christopher J., John W. Beck and John H. Johnson, "A Model and the Methodology for Determining Wear Particle Generation Rate and Filter Efficiency in a Diesel Engine Using Ferrography," Society of Automotive Engineers Paper No. 821195 (1982).

24. Hudgens, R.D. and L.B. Feldhaus, "Diesel Engine Lube Filter Life Related to Oil Chemistry," Society of Automotive Engineers Paper No. 780974 (1978).

25. Johnson, R.L. and K. Schoenherr, "Seal Wear," in: Wear Control Handbook, M.B. Peterson and W.O. Winer, Eds., Sect. 5, pp 727-754, American Society of Mechanical Engineers, New York, (1980).

26. Krutzsch, W.C., Pump Handbook, McGraw-Hill Book Company, New York (1968).

27. May, K.D., "Advanced Valve Technology," National Aeronautics and Space Administration, NASA Report SP-5019 (February 1965).

28. MIL-HDBK-217D, "Reliability Prediction of Electronic Equipment" (January 1982).

29. Minegishi, H. et al., "Prediction of Brake Pad Wear/Life by Means of Brake Severity Factor as Measured on a Data Logging System," SAE Paper 840358 (1984).

30. Mordkowitz, A., "Predicting Service Life for Zero Wear," Machine Design (10 January 1974).

31. Nagel, W.B., "Designing with Rubber," Machine Design (June 23, July 7, July 21, Aug 11, 1977).

32. Neale, M.J., Tribology Handbook, Butterworths, London.

33 Needleman, William M., "Filtration for Wear Control," in: Wear Control Handbook, M.B. Peterson and W.O. Winer, Eds., Sect. 4, pp 507-582, Americna Society of Mechanical Engineers, New York, (1980).

34. Newcomb, T.P., "Thermal Aspects of Vehicle Braking," Automobile Engineering (Aug 1960).

35. "Optimum Design of Helical Springs," Machine Design, (6 November 1980).

36. Orthwein, William C., Clutches and Brakes: Design and Selection, Marcel Dekker, Inc., New York (1986).

37. Rhee, S.K. and P.A. Thesier, "Effects of Surface Roughness of Brake Drums on Coefficient of Friction and Lining Wear," SAE Paper 720449 (1972).

38. Roack and Young, Formulas for Stress and Strain, McGraw-Hill Book Company, New York (1975).

39. Shigley, Joseph E., Mechanical Engineering Design, McGraw-Hill, Inc., New York, NY (1977).

40. Spokas, R.B., "Clutch Friction Material Evaluation Procedures," SAE Paper 841066 (1984).

41. "Standard Product Catalog," Catalog SPC 82, The Falk Corporation, Milwaukee, Wisconsin.

42. Weintraub, M.H. et al., "Wear of Resin Asbestos Friction Materials," in: Advances in Polymer Friction and Wear, pp. 623-647.

43. Wilhelm, James P. and Andrew V. Loomis, "Brake Friction Materials: A Market Survey," NASA Report (Aug 1975).

44. Sibley, L.B., "Rolling Bearings," in: Wear Control Handbook, M.B. Peterson and W.O. Winer, Eds., Sect. 5, pp 699-726, American Society of Mechanical Engineers, New York (1980).

45. Barron, Randall F., Revision of Wear Model for Stock Actuators, Engineering Model for Mechanical Wear (July 1987).

46. Fox, R.W., and A.T. McDonald, Introduction to Fluid Mechanics, John Wiley and Sons, New York (1978).

47. Machine Design, 1985 Fluid Power Reference Issue, Penton/IPC, Inc., (Sept. 19, 1985).

48. Bayer, R.G., A.T. Shalkey, and A.R. Watson, "Designing for Zero Wear," Machine Design, Vol. 41, pp. 142-151 (1969).

49. Kragelsky, I.V. and V.V. Alisin, Friction, Wear, and Lubrication, Vol. 2, pg. 30, Pergamon Press, London (1981).

50. Kuhlmann-Wildorf, D., "Parametric Theory of Adhesive Wear in Uni-Directional Sliding," Wear of Materials, pp. 402-413, American Society of Mechanical Engineers, New York (1983).

51. Bentley, R.M. and D.J. Duquette, "Environmental Considerations in Wear Processes," Fundamentals of Friction and Wear of Materials, pp. 291-329, American Society For Metals, Metals Park, Ohio (1981).

52. Sarkar, A.D., Wear of Metals, pp. 62-68, Pergamon Press, London (1976).

53. Lundberg, G. and A. Palmgren, "Dynamic Capacity of Rolling Bearings," Acta Polytechnica, No. 7 (1974).

54. Rumbarger, John H., "A Fatigue Life and Reliability Model for Gears," American Gear Manufacturers Association Report 229.16 (January 1972).

55. AGMA Standard for Surface Durability Formulas for Spiral Bevel Gear Teeth, American Gear Manufacturers Association Report 216.01 (January 1964).

56. AGMA Standard Nomenclature of Gear Tooth Failure Modes, American Gear Manufacturers Association Report 110.04 (August 1980).

57. Haviland, G.S., "Designing with Threaded Fasteners", MECHANICAL ENGINEERING, Vol 105, No. 10, Oct 83.

58. Deutschman, A.D., et al, Machine Design: Theory and Practice, MacMillan Publishing Co, NY, 1975

59. Parmley, R.O., Mechanical Components Handbook, McGraw-Hill Book Co., NY, 1985.

60. Handbook H28, Nat'l Bureau of Stds, Govt Printing Office, Washington, DC, 1957.

61. Hindhede, U., et al, Machine Design Fundamentals, John Wiley & Sons, NY, 1983.

62. Shigley, J.E., Mischke, C.R., Mechanical Engineering Design, McGraw-Hill Book Co., NY, 1989.

63. Bickford, J.H., An Introduction to the Design and Behavior of Bolted Joints, Marcel Dekker, Inc., NY, 1990.

64. Handbook of Corrosion Data, ASM International, Metals Park, OH, 1990

65. Baumeister, T, et al, Mark's Standard Handbook for Mechanical Engineers

66. Thomas Couplings Applications Manual

67. Bolam, J.R., "Coupling Alignment: The Reverse Indicator Method Simplified", P/PM Technology, July/Aug 90

68. Deutschman, A.D., et al, Machine Design: Theory & Practice, Macmillan Publishing Co,Inc. NY,NY.

69. Parmley, R.O., Mechanical Components Handbook, McGraw-Hill Book Co. NY,NY, 1985.

70. Dvorak, P., "Sorting Out Flexible Couplings", Machine Design, 11 Aug 88

71. Robertson, R., and Smith, B., "Why Flexible Couplings Fail", Plant Engineering and Maintenance, Jun 89

72. Universal Joint & Driveshaft Design Manual, Series No. 7, Society of Automotive Engineers, Inc, Warrendale, Pa.

73. Anderson, Edwin P., Electric Motors Handbook, Bobbs-Merrill Co., Inc., NY, NY 1983

INITIAL DISTRIBUTION

Copies			
3	ONT		
	3	ONT 226	CDR D. Bennett
6	NAVAIR		
	4	AIR-5115	R. Trakas
	1	AIR-411	D. Stacey
	1	AIR-411	J. McKendrew
5	Robins AFB		
	5	WR-ALC/LVRS	C. Perrazola
5	Picatinny Arsenal		
	5	SMCAR-QAH-P	S. Markowitz
2	NAVSEA		
	1	SEA-04	C. Geiger
	1	SEA-5121	M. Buckberg
2	NAVSUP		
	1	SUP-642C	J. Mays
	1	SUP-4233	R. Whitfield
2	Belvoir RD&E Center		
	1	SRRBE-TQR	C. Meese
	1	STRBE-TQR	L. Jackson
2	OP-403		
	1	OP-403R	CDR R. Thomas
	1	OP-403R	K. Stabenau
1	Wright-Patterson AFB		
	1	AFHRL/LRL	W. Cambell
1	Rome Air Development Center		
	1	RL/ERSR	M. McCallum
26	CARDEROCKDIV, NSWC		
	1	Code 00	CAPT D. Kruse
	1	Code 01	R. Metry
	1	Code 011	H. Chaplin
	5	Code 0116	R. Brengs
	1	Code 12	G. Kerr
	1	Code 125	R. Schaffran
	1	Code 129	R. Pice
	10	Code 1290	J. Chesley
	5	Code 2432	Reports Control